

Dynamics of the Structural Connectome in Traumatic Brain Injury

Phoebe Imms
Bachelor of Science (Honours)

~

Submitted in total fulfilment of requirements for the degree of
Doctor of Philosophy

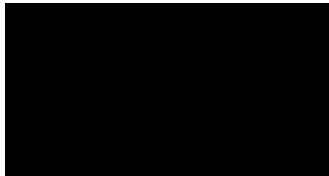
Mary MacKillop Institute for Health Research,
Faculty of Health Sciences,
Australian Catholic University

27th May 2021

Declaration of Authorship and Sources

This thesis contains no material that has been extracted in whole or in part from a thesis that I have submitted towards the award of any other degree or diploma in any other tertiary institution. No other person's work has been used without due acknowledgment in the main text of the thesis. All figures and illustrations in this thesis are original unless otherwise cited. All research procedures reported in the thesis received the approval of the relevant Ethics Committees (where required).

Signed:



Date: 27th May 2021

Abstract

Traumatic Brain Injury (TBI) is a leading cause of death and disability globally, with survivors often experiencing ongoing and debilitating cognitive impairments (e.g., slowed processing speed, poor attention, and executive functioning deficits). These impairments are often linked to focal lesions in regions of the cerebral cortex thought to uphold each cognitive function. However, the spectrum of impairments experienced by individual patients are not fully explained by focal lesions of the grey matter; instead, emerging theories suggest that many cognitive burdens result from disconnections in the white matter of the brain. With the advent of diffusion MRI (dMRI), new techniques are available to study how TBI disrupts the white matter pathways that connect brain regions (structural connectomics). Structural connectomics allows the quantification of network disruption in TBI patients using graph theoretical analyses, with studies reporting alterations in brain network integration and segregation. These studies suggest that graph metrics may be used as a ‘biomarker’ for TBI patients’ cognitive impairments, by linking changes in brain derived graph metrics to cognitive symptoms. However, challenges remain in ascribing behavioural relevance to graph metrics in this newly emerging field.

This thesis critically evaluates the use of graph theoretical measures of the structural connectome in moderate-severe TBI, and their use at a single-subject level. First, a meta-analysis of studies comparing healthy controls and TBI patients using graph metrics is used to demonstrate that communication metrics are most robustly linked to brain injury. This review also highlights issues with the over-interpretation of the relationship between graph metrics such as path-length and the efficiency of cognitive processes. Second, a study in

healthy adults shows that communication metrics are related to processing speed. This relationship between cognitive performance and measures of network alteration is underpinned by biologically plausible models of cognition and brain structure. Third, a profile of graph theoretical properties and alterations in six TBI patients is explored using a personalised connectomics approach. Spiderplots are used to represent graph metric alterations in each patient compared to healthy controls. Profiling individual patients in this way provides new insights into how graph metrics relate to lesion characteristics and TBI subtypes. Taken together, this thesis explores 1) how structural network topology is altered in patients with TBI, 2) how graph metrics can be interpreted, 3) how a personalised connectomics approach to TBI can be implemented, and 4) the methodological considerations for studying TBI using graph theory. The collective results of thesis indicate that graph metrics display potential for characterising network alterations in patients with brain injury; specifically, a profiling approach can account for heterogeneity in the TBI population, informing clinical decision making.

Acknowledgements

First and foremost, I wish to acknowledge the generosity, perseverance, and kindness of my supervisors. I want to express my immense gratitude to the incredible Karen Caeyenberghs, for four years of daily mentorship (and friendship); Govinda Poudel, for his brilliant ideas and for never turning me away when I showed up with my laptop and a question; and Peter Wilson, for his constant support. I also wish to thank Juan Dominguez for being a supervisor in everything but title. I learned so much and continue to learn from him.

I also would like to recognise the numerous collaborators who have made this research project possible, including the team at Monash Biomedical Imaging; the Murdoch Children's Research Centre and Royal Children's Hospital Medical Imaging team; Hamed Akhlaghi at St Vincent's Hospital Emergency Department; Derek Jones and the team in Cardiff; Thijs Dhollander for his insights on tractography and processing; Caio Seguin for being so patient with me; Paul Beech at the Alfred; Wendyl D'Souza and Mark Cook at St Vincent's Hospital; and the ENIGMA team for being the future of TBI research. Also, a big thank you to the staff and students of Mary MacKillop Institute for Health Research, the School of Psychology at ACU, and the Cognitive Neuroscience Unit at Deakin for their support during my candidature.

I would like to sincerely thank my work colleagues: Alex Burmester, for being a legend (don't ever change); Nick, Annalee, Jake, Liz, Ellen, Jordan, and Honey, for providing weekly doses of support and insight; Han and Tay, for countless bottles of vino and laughs; Amy for being incredibly hard-working and generous; and Evelyn, for inspiring

me every day and for showing me who I want to be when I grow up. Finally, Adam: From the day I first started to the day I submitted Adam has been there for me, (quite literally) by my side. He is a golden human being, and I am so lucky to have had his partnership for the last 4 years.

I am lucky enough to have had the support of two families, both here and in the U.S., who I wish to thank for their never-ending care. First, my Mum and Dad, who gave me the three best things parents could ever give to their child – imagination, independence, and a safe place to always come back to. They also gave me two brothers, but I forgive them for that. Just joking Tys (and Lali) and Lock, thank you for always loving me (even when I don't make it easy). Finally, to Rhonda and Richard and Laura, who welcomed me into their beautiful family, supported me from afar, and who I miss very much.

To my incredible friends – especially Caitie, Moni, Nupi, Annie, Viv, Beth & Lewis, Pat & Adrian, Toni & Malcolm, Elysia, Julia, Marco, and Alice – thank you for being my rocks, and keeping me sane. Shout out to the 'Backrow Bandits', 'the Tea Room', 'Meme Queens', 'Monday Funday', 'Staycation all I ever wanted', 'Bloody Good Route', 'The Corner Office Gang', and 'The Fellowship of the Clipboard' for the quality content. Finally, to my partner John: the strongest, kindest, funniest, and smartest person I've ever met. John got our little family through the last four years with tenacity and a smile. Some might even call him a hero.

Finally, I wish to thank our participants, the most important collaborators of any scientific endeavour. Their bravery and selflessness inspire me every day.

Table of Contents

Declaration of Authorship and Sources	1
Abstract	3
Acknowledgements	5
Table of Contents	7
List of Publications.....	11
Journal Articles Included in Thesis.....	11
Journal Articles Not Included in Thesis.....	11
Conference Proceedings	12
List of Tables.....	15
List of Figures	17
List of Commonly Used Abbreviations	19
Overview of Thesis	1
Chapter 1: Introduction.....	7
1.1 Traumatic Brain Injury.....	8
1.1.1 Causes, incidence, and impact	8
1.1.2 Diagnosis and classification.....	9
1.1.3 Pathophysiology over the phases of TBI	11
1.1.4 Chronic cognitive impairments.....	14
1.1.5 Heterogeneity in the TBI population	15
1.1.6 Mapping cognitive functions following brain damage.....	17
1.2 Neuroimaging.....	18
1.2.1 Magnetic Resonance Imaging	18
1.2.2 Diffusion Weighted Magnetic Resonance Imaging	21
1.2.3 Tensors and tractography in TBI	25
1.2.4 Advances in tractography	27
1.3 Connectomics and Network Analysis.....	29
1.3.1 Introduction to connectomics.....	29
1.3.2 Graph theoretical analysis	33
1.3.3 Graph metrics and cognition.....	36
1.3.4 Graph metrics: A biomarker of brain injury?.....	37
1.3.5 Use of graph metrics in individual patients.....	38
1.4 Aims and Research Questions	39
Chapter 2: Study 1 - The structural connectome in Traumatic Brain Injury: A meta-analysis of graph metrics	43
2.1 Published Article	45
2.1.1 Title Page	45
2.1.2 Abstract.....	47
2.1.3 Introduction.....	48
2.1.4 Method.....	51
2.1.5 Results.....	56
2.1.6 Discussion.....	66
2.1.7 Supplementary Materials	75
Chapter 3: General Methods for Data Collection	83
3.1 Participants	84
3.1.1 Participants for Study 2 (Monash Biomedical Imaging).....	84
3.1.2 Participants for Study 3 (Royal Children's Hospital)	85
3.1.2.1 Recruitment.....	85

3.2	Cognitive and Self-Report Measures.....	87
3.2.1	Demographics	87
3.2.2	IQ.....	87
3.2.2.1	Vocabulary.....	88
3.2.2.2	Matrix Reasoning.....	88
3.2.3	Subjective Cognitive Ability.....	88
3.2.3.1	Neurobehavioural Functioning Inventory	89
3.2.4	Objective Cognition	89
3.2.4.1	The Psychological Experiment Building Language.....	89
3.3	Magnetic Resonance Imaging of the Brain	91
3.3.1	MRI for Study 2 (Monash Biomedical Imaging).....	91
3.3.1.1	Anatomical scan.....	91
3.3.1.2	Diffusion Weighted Imaging	92
3.3.2	MRI for Study 3 (Royal Children’s Hospital).....	93
3.3.2.1	Anatomical scan.....	93
3.3.2.2	Diffusion Weighted Imaging	94
3.4	Procedure.....	95
3.4.1	Overview of the Testing Session	95
3.4.2	Details of the Data Collection Process.....	96
3.4.2.1	Computerised cognitive testing.....	96
3.4.2.2	MRI scan.....	97
3.4.3	Confidentiality	98
3.4.4	Data Entry and Security	98
3.4.5	General approach to data analysis.....	99
Chapter 4: Study 2 - Navigating the link between processing speed and network communication in the human brain.....		101
4.1	Preface.....	102
4.1.1	Advances in measuring processing speed	103
4.1.2	Advances in measuring communication	103
4.1.3	Advances in connectome reconstruction.....	104
4.1.4	Summary	105
4.2	Published Article	107
4.2.1	Title Page.....	107
4.2.2	Abstract.....	110
4.2.3	Introduction.....	111
4.2.4	Materials and Methods.....	115
4.2.5	Results.....	131
4.2.6	Discussion.....	141
4.2.7	Conclusion	149
Chapter 5: Study 3 - Personalised structural connectome mapping in Traumatic Brain Injury.....		151
5.1	Preface.....	152
5.1.1	How should heterogeneity in TBI patients be addressed?	152
5.1.2	Which graph metrics should be examined in TBI?	153
5.1.3	What methods should be used to create the connectome?	155
5.1.4	Summary	155
5.2	Prepared Article.....	161
5.2.1	Title Page.....	161
5.2.2	Abstract.....	164
5.2.3	Introduction.....	165
5.2.4	Methods	168
5.2.5	Results.....	182

5.2.6	Discussion.....	196
5.2.7	Supplementary Materials	203
Chapter 6: General Discussion and Conclusions.....		206
6.1	Restatement of the Research Aims and Main Findings.....	207
6.1.1	Summary by chapter	207
6.1.2	Collective summary of results.....	209
6.2	Discussion	210
6.2.1	Implications for the structural network topology of patients with TBI.....	210
6.2.2	Implications for the interpretive value of graph metrics	213
6.2.3	What can be gained from the use of Personalised Connectomics?	215
6.2.4	Methodological considerations of diffusion-based graph analysis in TBI.....	218
6.3	Strengths, Limitations and Future Directions.....	225
6.3.1	Limitations and future directions	225
6.3.2	Strengths	227
6.4	Conclusions.....	228
Reference List.....		230
Appendices		266
Appendix A. Proof of Publication and Publishing Rights for Study 1		266
Appendix B. Statement of Contribution for Study 1		267
Appendix C. Statement of Contribution for Study 2 and Proof of Acceptance		269
Appendix D. Statement of Contribution for Study 3		272
Appendix E. Flyer for recruitment of healthy adults (MBI)		274
Appendix F. Screening form for healthy adults (MBI).....		275
Appendix G. MRI screening form (MBI).....		277
Appendix H. Outline of what to expect on the testing day (MBI)		279
Appendix I. Explanatory statement provided to healthy adults (MBI)		284
Appendix J. Consent form provided to healthy adults (MBI).....		288
Appendix K. Letter of invitation to TBI participants (RCH).....		289
Appendix L. Participant information form for TBI participants (RCH)		290
Appendix M. Phone recruitment script for TBI participants (RCH).....		299
Appendix N. Screening form for TBI participants (Royal Children’s Hospital)		303
Appendix O. Participant information form for Healthy Controls (Royal Children’s Hospital).....		306
Appendix P. Screening checklist for Healthy Controls (RCH).....		314
Appendix Q. Consent form for TBI participants (RCH).....		316
Appendix R. Consent form for Healthy Controls (RCH)		318
Appendix S. Survey of demographic information		320
Appendix T. The Neurobehavioural Functioning Inventory.....		321
Appendix U. MRI scan running sheet.....		325
Appendix V. MatLab script for Graph Theoretical Analysis.....		327

List of Publications

Journal Articles Included in Thesis

- **Imms, P.**, Clemente, A., Cook, M., D'Souza, W., Wilson, P. H., Jones, D. K., & Caeyenberghs, K. (2019). The structural connectome in traumatic brain injury: A meta-analysis of graph metrics. *Neuroscience & Biobehavioral Reviews*, 99, 128-137.
- **Imms, P.**, Domínguez D, J.F., Burmester, A., Seguin, C., Clemente, A., Dhollander, T., Wilson, P.H., Govinda Poudel, G., & Caeyenberghs, K. (2021). Navigating the link between processing speed and network communication in the human brain. *Brain Structure & Function*, 226(4), 1281-1302.
- **Imms, P.**, Clemente, A., Deutscher, E., Radwan, A.M., Akhlaghi, H., Beech, P., Wilson, P., Poudel, G., Dominguez D., J.F., Caeyenberghs, K. (prepared).
Personalised structural connectome mapping in traumatic brain injury.

Journal Articles Not Included in Thesis

- Caeyenberghs, K., Clemente, A., **Imms, P.**, Egan, G., Hocking, D. R., Leemans, A., ... & Wilson, P. H. (2018). Evidence for training-dependent structural neuroplasticity in brain-injured patients: a critical review. *Neurorehabilitation and neural repair*, 32(2), 99-114.
- Dhollander, T., Clemente, A., Singh, M., Boonstra, F., Civier, O., Egorova, N., ... **Imms, P.**, ... & Gottlieb, E. (under review). Fixel-based Analysis of Diffusion MRI: Methods, Applications, Challenges and Opportunities. *NeuroImage*.

- Clemente, A., Dominguez D, J.F., **Imms, P.**, Burmester, A., Dhollander, T., Wilson, P., Poudel, G., Caeyenberghs, K. (accepted). Individual differences in attentional lapses are associated with fibre specific white matter microstructure in healthy adults. *Psychophysiology*.

Conference Proceedings

- **Imms, P.** & Clemente, A. (August 2020). *White matter alterations following traumatic brain injury*. (Invited speakers). The Florey Institute of Neuroscience and Mental Health Research symposium.
- **Imms, P.** (December 2019). *Linking cognition and graph metrics: Investigating the structural connectome after brain injury*. (Invited speaker). International Society for Magnetic Resonance in Medicine, Melbourne.
- Clemente, A., **Imms, P.**, Dominguez D. JF., Poudel G., & Caeyenberghs K. (June 2020). *White matter alterations with multimodal training in patients with traumatic brain injury: A case series*. (Poster). Frontiers in Traumatic Brain Injury, London.
- **Imms, P.**, Clemente, A., Dominguez D. JF., Poudel G., & Caeyenberghs K. (November 2019). *Morphological changes associated with multimodal training in patients with traumatic brain injury: Preliminary findings*. (Poster). Students of Brain Research symposium, Melbourne.
- Caeyenberghs, K., **Imms, P.**, Clemente, A., Poudel, G., Dominguez D. JF. (November 2019). *Morphological changes associated with multimodal training in patients with TBI: Case studies*. (Oral Presentation). Australasian Cognitive Neurosciences Society conference, Launceston.
- Clemente, A., **Imms, P.**, Caeyenberghs, K. (August 2019). *Combined cognitive and motor training for patients with traumatic brain injury: Preliminary findings of a pilot feasibility study*. (Poster). Presented at St Vincent's Hospital Research Week, Melbourne.
- **Imms, P.**, Clemente, A., Jones, D.K., Dominguez D. JF., Poudel G., & Caeyenberghs K. (June 2019). *Executive function and structural connectivity in*

healthy adults: Using SIFT2 as edge weights. (Poster). Organisation for Human Brain Mapping, Rome.

- **Imms, P.**, Clemente, A., Cook, M., D'Souza, W., Wilson, P.H., Jones, D.K., & Caeyenberghs K. (November 2018). *Insights into traumatic brain injury from graph theory.* (Poster). Organisation for Human Brain Mapping Australian Chapter, Melbourne.
- Clemente, A. & **Imms, P.** (November 2018). *Novel training for traumatic brain injury patients: Towards neuroplasticity.* (Oral presentation). Longitudinal Magnetic Resonance Imaging Workshop, Melbourne.
- Clemente, A. & **Imms, P.** (July 2017). *Multimodal training in patients with traumatic brain injury: A study protocol.* (Oral presentation). Longitudinal Magnetic Resonance Imaging Workshop, Melbourne.

List of Tables

Severity Ratings for Traumatic Brain Injury	10
Definitions of Basic Graph Metrics.....	34
Demographics and Processing Methods for Graph Theoretical Studies of Traumatic Brain Injury	57
Quality Assessment Results for Graph Theoretical Studies of Traumatic Brain Injury	59
Graph Metrics in Patients with Traumatic Brain Injury compared to Healthy Controls.....	61
Results of the Subgroup Analysis.....	63
Definition of Graph Metrics	75
Overall Effect Sizes for Graph Metrics	82
Example of PEBL Battery Tasks Assessing Objective Cognition	90
Scanning Protocol and Measures from Monash Biomedical Imaging (MBI)	92
Scanning Protocol from Royal Children’s Hospital (RCH)	94
Definitions and Interpretations of Parameters from the Drift Diffusion Model.....	118
List of Regions Included in the Global-Local Task-Specific Subnetwork.....	125
Definition of Communication Measures used in the Current Study	128
Correlations Between Communication Measures and Incongruent and Congruent Drift Rate	134
Correlations Between Whole Brain Communication Measures, and Incongruent and Congruent Drift Rate with Alternative Parcellation Scheme	138
Correlations Between Whole Brain and Fronto-Parietal Subnetwork Communication Measures, and Incongruent and Congruent Drift Rate with Alternative Streamline Weight	138
Correlations Between Whole Brain and Fronto-Parietal Subnetwork Communication Measures, and Incongruent and Congruent Drift Rate with Alternative Weight-Length Remapping.....	139
Correlations Between Whole Brain and Fronto-Parietal Subnetwork Communication Measures, and Incongruent and Congruent Drift Rate, Controlling for the Effect of Brain Size and Head Movement.....	140

Demographics and Processing Methods for Traumatic Brain Injury Studies Using Graph Theory.....	157
Summary of Literature Comparing TBI Patients to Healthy Controls Using Global Graph Metrics	159
Summary of Demographics and Clinical Characteristics of the Participants.....	169
Graph Metric Descriptions, Interpretations, and Evidence from Previous TBI Studies	178
Detailed Description of the PEBL Test Battery	203

List of Figures

Overview of the Chapters Included in the Thesis.....	5
Examples of Focal Lesions Caused by Traumatic Brain Injury	11
Magnetisation and Relaxation of Hydrogen Protons in Magnetic Resonance Imaging	20
Diffusion Properties and Models of the White Matter and the Cerebral Spinal Fluid	22
The Diffusion Tensor Model and Constrained Spherical Deconvolution	23
The Basics of Connectome Construction	30
PRISMA flow diagram of the systematic literature search	52
Inverted Forest Plot of the Overall Effect Sizes for Each Graph Metric.....	62
Global-Local Task Stimuli	117
Overview of the Processing Pipeline for Connectome Construction	122
The Group Average Whole-Brain Connectome	127
Drift Rate for Incongruent, Congruent, and Neutral Conditions of the Global-Local Task	133
Results of the Whole Brain Analysis.....	135
Results of the Subnetwork Analysis.....	137
Overview of the Processing Pipeline for Connectome Construction	174
Head Motion Summary for Six TBI Patients	175
Healthy Control Hub Regions	181
Personalised Connectome Profile for TBI1	185
Personalised Cognitive Profile for TBI2.	187
Personalised Connectome Profile for TBI3.....	189
Personalised Connectome Profile for TBI4.....	191
Personalised Connectome Profile for TBI5.....	193
Personalised Connectome Profile for TBI6.....	195

List of Commonly Used Abbreviations

ACT	Anatomically Constrained Tractography
BC	Betweenness Centrality
CSD	Constrained Spherical Deconvolution
CSF	Cerebral Spinal Fluid
CT	Computed Tomography
DAI	Diffuse Axonal Injury
dMRI	Diffusion Weighted Magnetic Resonance Imaging
FA	Fractional Anisotropy
FLAIR	Fluid-Attenuated Inversion Recovery
FOD	Fibre Orientation Distribution
FSL	Functional Magnetic Resonance Imaging of the Brain Software Library
MRI	Magnetic Resonance Imaging
NFI	Neurobehavioural Functioning Inventory
PEBL	Psychological Experiment Building Language
SIFT2	Spherically Informed Filtering of Tractograms
T1	Longitudinal Relaxation Time
TBI	Traumatic Brain Injury

VBG	Virtual Brain Grafting
WASI	Weschler Abbreviated Scale of Intelligence
WMH	White Mater Hypointensity

Overview of Thesis

The human brain is a dynamic network of ~100 billion neurons, comprising ~100 trillion connections. Signals travel between neuronal cell bodies which manifest as the grey matter, via bundles of axons that form white matter pathways. This complex structure can be damaged in many ways, the most common being stroke, Alzheimer's disease, multiple sclerosis, dementia, or trauma. Each method of injury has its own characteristics, aetiology and prognosis. While other brain injuries have been relatively well characterised due to their more homogenous causes and symptomatology, the mechanisms of Traumatic Brain Injury (TBI) are complex and therefore less coherently represented in scientific research. It is therefore the goal of this thesis to improve our understanding of the neurological and cognitive impacts of TBI.

Moderate-severe TBI is caused by a large force to the head, resulting in damage to brain tissue. TBI has a high incidence rate worldwide and causes widespread, persistent, and debilitating cognitive impairment. Patients more than 6 months post injury show a plateau in improvements and face a lifetime of disability (Rabinowitz & Levin, 2014). The long-term cognitive deficits following TBI are often due to injury in the frontal and temporal brain regions and shearing and degradation of the white matter pathways (Bigler, 2013). Diffusion MRI (dMRI) is a method that characterises organisation of the white matter pathways *in vivo* and has been used to study how damage to white matter tracts impacts cognitive outcome following TBI. However, individual tracts alone do not support brain activity, but instead are essential for synchronous integration of activity across brain regions (Bullmore & Sporns, 2012). As such, recent work has employed a novel framework *connectomics* to understand how TBI impacts the brain network as a whole (e.g., Caeyenberghs, Leemans, De Decker, et al., 2012). Connectome studies of traumatic brain injury (TBI) utilise graph theory to evaluate

network alterations in comparison to healthy controls, by calculating graph metrics – summary statistics of the brain network that represent integration, segregation, and centrality. Results suggest that the TBI brain network is altered in comparison to healthy controls; however, there is a lack of converging evidence between studies, likely due to the heterogeneous nature of TBI patients. Also, the nature of the relationship between graph metrics and cognitive performance remains unclear. This thesis aims to address these gaps by 1) systematically characterising the available literature, 2) identifying relationships between brain network measures and cognition, and 3) formulating a new approach to using connectomics in individual TBI patients.

In Study 1, a meta-analysis examines the robust patterns of change in graph metrics across the available literature. Ten studies are included in a random-effects meta-analysis of global graph metrics (N=429 TBI patients; N=306 healthy controls), and subgroup analyses (age, time since injury, severity of injury) to examine confounding effects. The meta-analysis reveals significantly higher values of normalised clustering coefficient and characteristic path length in TBI patients compared with healthy controls. Longer characteristic path length (less efficient network communication) is robust across studies. It is concluded that the pattern of change revealed, including increased communication measures (path length) and clustering, can be used in the next stages to guide our hypothesis-driven research into the role of graph metrics as diagnostic biomarkers of TBI.

Study 2 examines the relationship between communication measures such as characteristic path length and cognitive performance. Processing speed on cognitive tasks (which is often affected following brain injury) relies upon efficient communication between widespread regions of the brain such as the fronto-parietal attention network. What remains unclear is whether there is a direct link between these communication measures and processing speed. This relationship is tested in forty-five healthy adults (27 female, $M_{age} =$

30.9 years), where processing speed is defined as decision-making time on a Global-Local task and measured using drift rate from the hierarchical drift diffusion model.

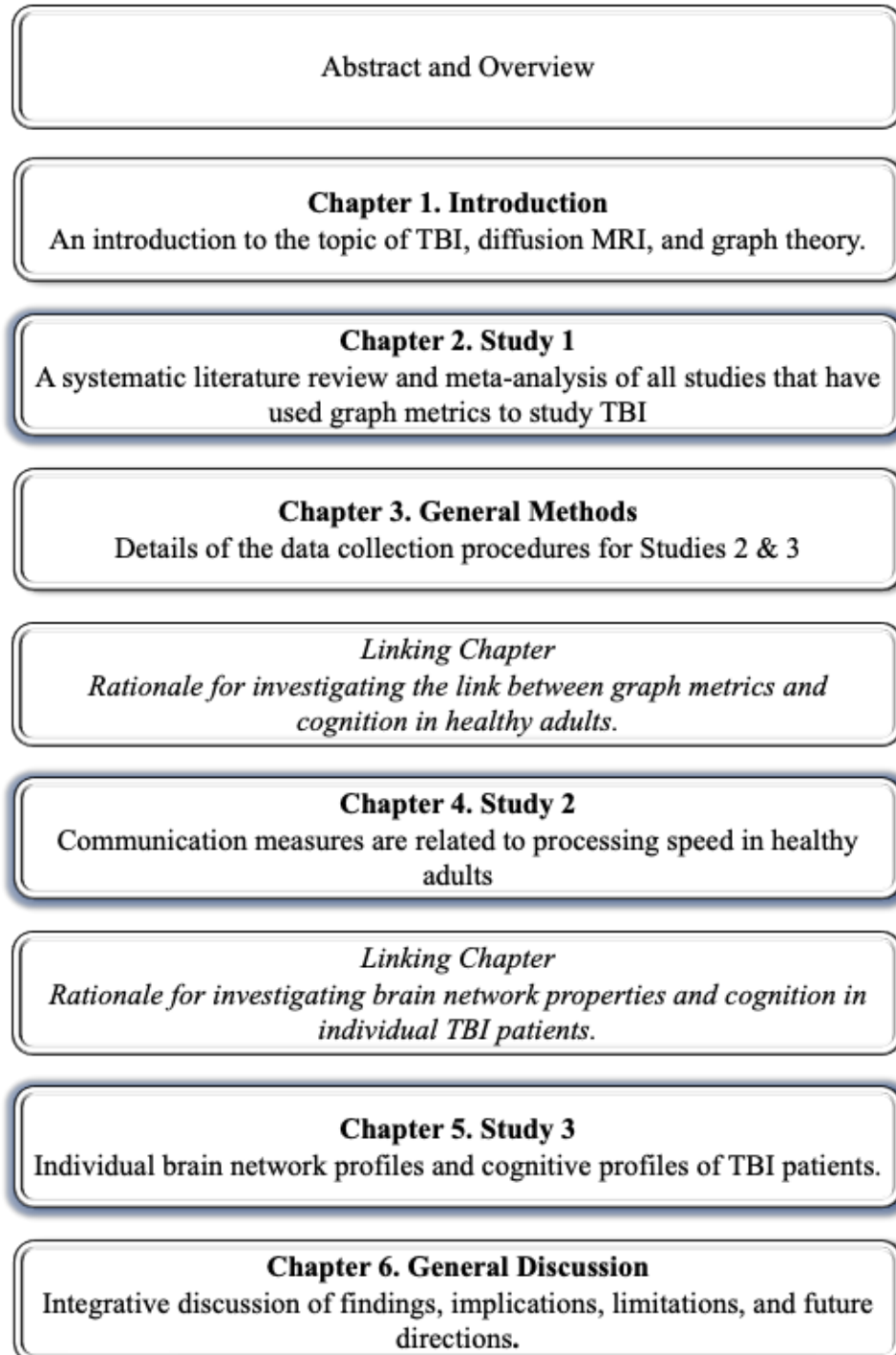
Communication measures are calculated for the whole brain structural connectome and for a task-relevant fronto-parietal structural subnetwork. A novel and more biologically plausible method of quantifying network communication is also included – called *navigation efficiency*. Faster processing speed is found to be correlated with higher navigation efficiency (of both the whole-brain and the task-relevant subnetwork). In the task-relevant subnetwork only, faster processing speed on trials that require more automatic processing is correlated with longer path-length. Overall, findings suggest that there is a relationship between the speed of cognitive processing and the structural constraints of the human brain network – though, this relationship depends on the specificity of the measures used.

In Study 3, a novel single-subject profiling approach is used to characterise the graph theoretical properties of individual TBI patients. In the search for graph metric ‘biomarkers’, group level analyses of TBI patients often average neuroimaging and cognitive data across patients regardless of lesion and patient characteristics. Instead, personalised connectomics (individual-level analysis of the structural connectome) may allow for an individual’s brain network to be used as a ‘fingerprint’, to examine the profile of graph metric alterations in one patient compared to healthy controls. In this study, a personalised structural connectome analysis is performed using high angular resolution dMRI data from five TBI patients, to facilitate interpretation of unique disconnectivity profiles. A large amount of variability is observed in the profile of graph metric alterations between patients. Where group analyses wipe out variability, individual normative comparisons allow researchers to capture the range of network alteration patterns. This renewed emphasis on profiling individual patients based on their unique injury presentation provides new insights into how graph metrics relate to lesion characteristics and TBI subtypes.

Overall, this thesis explores how graph analysis of the structural brain connectome adds to our understanding of TBI; whether graph metrics are related to cognitive performance in healthy adults and thus have potential as biomarkers of cognitive dysfunction; the benefits and limitations of single-subject profiling to study TBI; and the methodological considerations of diffusion-based graph analysis in brain injured patients (see Figure 1). The role of graph metrics as biomarkers of TBI is critically evaluated by examining the current state of the literature (Study 1), the relationship between metrics and measures of cognition (Study 2), and the ability of graph metrics to represent an individual patient (Study 3). In the review and meta-analysis, communication measures such as path length are longer in TBI patients than healthy controls, a finding which was robust across studies and TBI subtypes. In the second empirical chapter, these communication measures were related to processing speed, albeit when using specific measures of brain structure and cognition. In the third empirical chapter a large amount of variability is observed in the graph metric profiles of TBI patients. Thus, instead of a singular graph metric biomarker, it is argued that visualising a profile of graph metric alterations is a better method for characterising this heterogeneous patient group. In conclusion, this thesis represents a critical assessment of the role of graph metrics in the comparison of adults with chronic moderate-severe TBI to healthy controls.

Figure 1.

Overview of the Chapters Included in the Thesis



Chapter 1: Introduction

1.1 Traumatic Brain Injury

1.1.1 Causes, incidence, and impact

Traumatic Brain Injury is caused by an external force to the head resulting in damage to brain tissue (Kay & Lezak, 1990), often following a traffic accident (61.4%), fall (24.9%), or assault (non-gunshot; 7.2%) (Myburgh et al., 2008). In their epidemiological study of TBI, Majdan et al. (2011) found that while young men are most likely to experience TBI from motor vehicle accidents, older people are also more vulnerable to brain injury from falls. Unsurprisingly, the most severe injuries occur from traffic related incidents, such as motor vehicle and bicycle accidents – these patients spend on average the longest time in intensive care and on ventilation. However, fall related TBIs have the highest percentage of patients requiring cranial surgery due to bleeds in brain tissues, and show the poorest expected outcomes especially for older patients. Assault related TBI, while less common than falls and traffic accidents, is strongly related to being male, especially for men with substance abuse and/or financial problems (Schopp et al., 2006; Wagner et al., 2000). In truth, while some groups are more at risk than others, what separates TBI from other forms of brain injury is that sudden trauma can occur indiscriminately, and with devastating consequences.

TBI has a high prevalence internationally. The World Health Organisation estimates that traffic accidents will be the 3rd leading cause of premature death across all ages by the year 2020 (Murray et al., 1996) – a speculation which appears to have merit based on recent numbers (James et al., 2019). In 2016 there were 27.08 million new cases of TBI globally, with an incidence rate of 369 per 100,000 population (James et al., 2019) – in Australia, the incidence of TBI is approximately 100 in a 100,000 (Tate et al., 1998). In the western world TBI accounts for half of the trauma that leads to death and long-term disability (Baxter & Wilson, 2012). TBI case numbers are growing, due to increasing use of motor vehicles (Maas

et al., 2008) and sport injuries (Dashnaw et al., 2012). Fortunately, life support technologies have improved meaning survival is more likely than ever following serious trauma – though this does increase the prevalence of people living with debilitating disability for years after an injury.

Living with the consequences of a head injury requires medical, emotional, and financial support from workplaces, community support services, family, and friends. Consequently, in Australia it is estimated that the total cost of TBI in 2008 was \$8.6 billion, including both financial costs and burden of disease costs (including medical costs, carer salaries, loss of taxable income, etc.; Access Economics Pty Limited, 2009). The psychosocial costs of TBI are also high – most TBI survivors live with their family and are no longer employed or attending school (for review, see Humphreys et al., 2013). Therefore, family members also face social and financial hardship as they rise to the challenge of demanding medical costs and long-term caregiving (Kreutzer et al., 2002). In summary, TBI has a high incidence rate, a large human cost to both the patient and carer, as well as an enormous financial cost to society.

1.1.2 Diagnosis and classification

There are three widely accepted categories of TBI diagnosis – mild, moderate, or severe (see Table 1). Categorisation is performed based on the severity of the symptoms at the time of injury, and neuroimaging to identify the extent of the lesions (Hannawi & Stevens, 2016; Maas et al., 2008). The latter is accomplished using Computed Tomography (CT), or in more serious cases Magnetic Resonance Imaging (MRI), to check for intracranial pathologies. The former, the severity of the symptoms, is often assessed using three criteria; 1) the patient's level of responsiveness (Teasdale & Jennett, 1974), 2) the amount of time

with post traumatic amnesia (PTA; memory loss and confusion) (Russell & Smith, 1961), and 3) the duration of loss of consciousness (time period in coma/unaware).

Table 1.

Severity Ratings for Traumatic Brain Injury

Rating	Glasgow Coma Scale	Post-Traumatic Amnesia	Loss of Consciousness
Mild	13-15	< 24 hours	0 – 30 minutes
Moderate	9-12	1 – 7 days	30 minutes – 24 hours
Severe	3-8	> 7 days	> 1 day

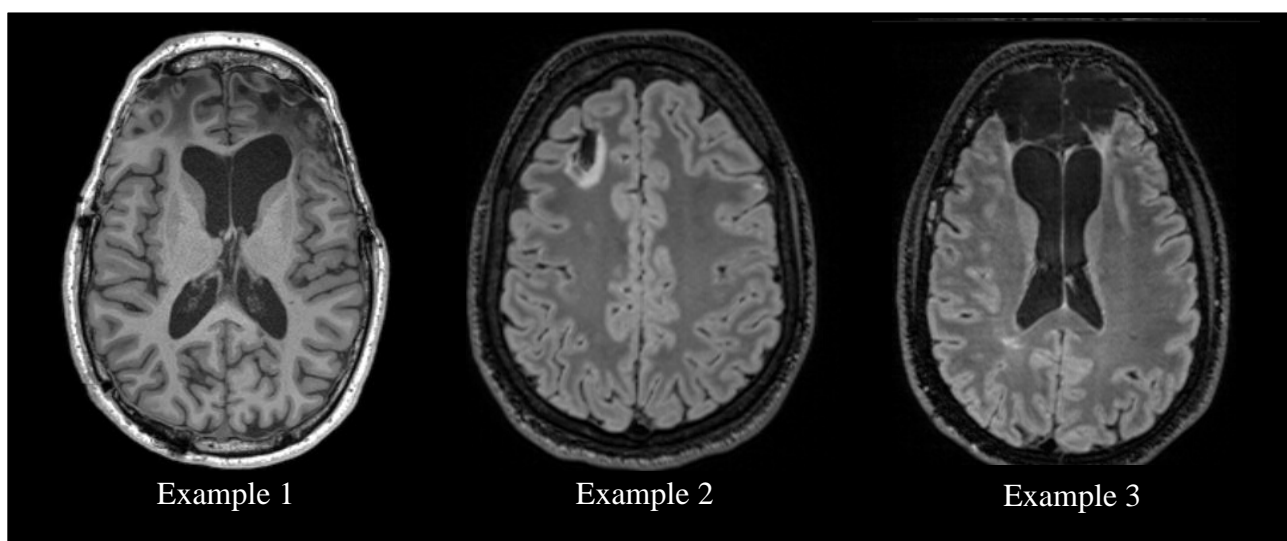
Mild TBI is identified by post traumatic amnesia for less than 24 hours, loss of consciousness for less than 30 minutes (Rabinowitz & Levin, 2014), and less severe cognitive impairments. Neuroimaging, especially CT, often does not demonstrate any injury-related abnormalities. Mild TBI is more common than moderate-severe TBI, representing 61.5% of cases (Tate et al., 1998). Following mild TBI, improvements in cognitive or motor impairments mostly occur within 3-6 months post injury (Belanger & Vanderploeg, 2005; Carroll et al., 2004). Conversely, moderate-severe TBI patients immediately suffer loss of consciousness for more than half an hour and post traumatic amnesia for longer than a day (see Table 1; Rabinowitz & Levin, 2014). For moderate-severe TBI, an MRI or CT scan may alert neurologists to a range of findings including (but not limited to) focal lesions, swelling, and damage to the grey-white matter boundaries of the brain. Moderate-severe TBI patients are less common and less often represented in the literature. However, these are the patients that tend to exhibit longer lasting or even permanent disabilities.

1.1.3 Pathophysiology over the phases of TBI

The pathophysiology of TBI is multifaceted and can continue to evolve for months or even years following the injury. To characterise the stages of injury progression, researchers and clinicians often refer to the acute (<1 month), subacute (1month - 6months), and chronic (>6 months) phases of TBI (Rabinowitz & Levin, 2014). At the time of injury and during the acute phase, the primary injuries that occurred directly from the external force are treated in hospital (Maas et al., 2008). Most often, primary injuries (e.g., hematoma, haemorrhage, and oedema) affect the frontal and temporal lobes where bony protuberances of the skull are prominent (Bigler, 2013). As the head hits the external surface inertia causes the brain to continue its trajectory and hit the inside of the skull at the site of impact (*coup*), which in turn forces the brain to ricochet back to hit the opposite side to the impact (*contre coup*) (Drew & Drew, 2004). At the cellular level, lesions involve the rupturing and necrotic death of neurons and glial cells (Kurland et al., 2012). These types of injuries cause tissue loss and are collectively referred to as focal lesions (see Figure 2).

Figure 2

Examples of Focal Lesions Caused by Traumatic Brain Injury



Primary injuries are not confined to the grey matter where physical impact occurred. Besides these focal lesions, it is estimated that approximately half of TBI patients also present with diffuse injuries in white matter pathways (Hammoud & Wasserman, 2002). When the brain experiences rapid acceleration-deceleration forces, the interface between tissues of different densities is vulnerable to shearing effects (Meythaler et al., 2001). These injuries are particularly evident in high-speed car crashes (Li & Feng, 2009), and are generally referred to as Diffuse Axonal Injury (DAI). DAI is evidenced by microlesions in the white matter tracts (Currie et al., 2016; Maas et al., 2008), apparent in deep brain white matter structures, the corpus callosum, periventricular and hippocampal regions, and the brainstem (Hammoud & Wasserman, 2002; Kou et al., 2015). Despite being well-described in the scientific literature, DAI is still often missed in clinical settings, due to the fact that the CT scans used for diagnosis at the time of injury are inadequate for visualizing microbleeds (Currie et al., 2016; Maas et al., 2008).

Secondary injuries may also occur, evolving over the acute and subacute phases of the injury. Secondary injuries are pathophysiological mechanisms triggered by the primary injury, as the intracellular substances released by dying neurons and the breakdown products of blood are toxic to the nearby cells (Kurland et al., 2012). Secondary injuries can be caused by excess neurotransmitter release and inflammation that causes oedema (swelling), ischemia (reduced blood flow), hypoxia (reduced oxygen), raising of intracranial pressure, and gliotic scarring (Maas et al., 2008). Often TBI leads to chronic excitotoxicity, where neurons and oligodendrocytes become vulnerable to glutamate stimulation as the neurotransmitter accumulates in brain tissues (Bramlett & Dietrich, 2015; Pekna & Pekny, 2012; Pekna et al., 2012). Overall, this secondary cascade of injuries leads to inflammation, glial and mitochondrial dysfunction, and destruction of vasculature (Maas et al., 2008; Park et al., 2008). The biochemical cascade can continue for months after the initial injury, causing

further damage to axonal pathways (Bramlett & Dietrich, 2015). Treatment of any secondary injuries may therefore continue into the subacute phase of TBI, when the patient begins to recover lost cognitive and motor functions.

The subacute phase is also when the patient's brain will begin the recovery and healing processes. Unlike other organs, brain tissue is limited in its ability to regenerate; instead, neurons can alter their interconnectivity in response to functional loss to circumvent damaged brain tissue – termed neuroplasticity. Upregulation of synaptic markers and axonal sprouting occurs during this time (Carmichael, 2003), leading to an increase in the density of synapses perilesional or contralateral to the damaged tissue (Pekna & Pekny, 2012). This neuroplasticity peaks one to three months post injury (Pekna & Pekny, 2012). In addition, during this subacute phase TBI patients begin to experience secondary pathologies that may continue well into the chronic phase of their injuries: these pathologies may include seizures, sleep disorders, neurodegeneration, neuroendocrine and psychiatric problems (Bramlett & Dietrich, 2015).

Typically, the chronic phase is characterized by a plateau in behavioural and physical improvements (Schretlen & Shapiro, 2003), due to the limits of intrinsic neurological repair processes. However, there is also evidence from rat and mouse studies that accelerated atrophy of grey and white matter occurs months and years after a TBI (Smith et al., 1997), potentially due to chronic excitotoxicity (Bramlett & Dietrich, 2015). TBI patients may also continue to show reductions in white matter, inflammation, and volume loss even years after the injury (e.g., Green, 2016). TBI can be a compounding issue for an individual already experiencing neurodegeneration (e.g., older adults) and is a risk factor for the onset of Alzheimer's Disease (e.g., Sivanandam & Thakur, 2012). However, not all outcomes are adverse. Recent work in the field of training-induced neuroplasticity shows that behavioural and neurological changes are still possible even years after an acquired brain injury (e.g.,

Caeyenberghs et al., 2018) providing evidence to support continued research into chronic TBI.

1.1.4 Chronic cognitive impairments

Cognitive impairments are the major cause long-term disability in patients with moderate-severe TBI. Around 25% of TBI patients cannot return to work for a year post-injury (Whiteneck et al., 2004), and almost half experience cognitive disability for a period of 6 months or more (Selassie et al., 2008). Cognitive impairment caused by TBI can impact participation in all aspects of life, from housework and hygiene, to schooling and employment. Simple tasks such as planning a trip on public transport might become impossible or frustratingly slow. The exact symptoms that a person may experience long-term following a TBI can depend on the severity of the injury, the affected areas of the brain, and the type of secondary pathologies that were triggered by the injury. Accurately predicting the outcome of an individual is complicated and doing so with precision and confidence is beyond the capacity of current medical practices. However, the ability to predict cognitive symptoms could enable a patient with TBI to understand what their future might look like.

One of the major domains of cognitive impairment following moderate to severe TBI is executive dysfunction, which occurs in 65% of the chronic TBI population (Rabinowitz & Levin, 2014). Executive functioning includes mental control and self-regulation – the set of processes by which the brain ‘manages’ itself. Till et al. (2008) found that in 27.3% of their TBI cases there was a decline in measures of executive functioning even 5 years after injury. Moderate-severe TBI patients often exhibit 1) processing speed, 2) memory, 3) attention, and 4) planning deficits for years after the injury (Ruff et al., 1989; Ruff et al., 1993). These cognitive functions are integral for daily life (Rabinowitz & Levin, 2014). TBI patients may experience delay when inhibiting responses, updating, and switching tasks, which are all

attributable to poor processing speed (Caeyenberghs et al., 2014). They may also show poor prospective and retrospective memory (Shum et al., 2011), and have difficulty organising information in a manner that facilitates encoding and retrieval of new memories (Dikmen et al., 2009). Sustained attention can be affected when insult occurs to frontoparietal areas, meaning the patient may be unable to maintain consistent performance on tasks over time (Bonnelle et al., 2011). Planning is also poorer in TBI patients than in healthy adults, with TBI patients more likely to take unnecessary extra steps when working towards a goal (Shum et al., 2009).

In particular, slowed processing speed is arguably one of the more persistent and influential cognitive complaints following TBI (Battistone et al., 2008). There is strong evidence for the relationship between moderate-severe TBI and slower performance on cognitive tasks (e.g., Madigan et al., 2000). Evidence suggests that slowed processing speed is not specific to one cognitive task, but a global slowing of the capacity for processing information and transmitting neural impulses (e.g., Ponsford & Kinsella, 1992), linked to diffuse axonal shearing and white matter damage. Furthermore, there is evidence that TBI patients can show the same accuracy as healthy counterparts on cognitive tasks when under no time constraint (e.g., Capruso & Levin, 1992); however, when asked to respond at a faster pace their accuracy decreases (Gronwall & Sampson, 1974). Battistone et al. (2008) found that TBI patients showed a slower rate of information accrual, as well as a hesitation to respond early. However, the exact mechanism of this slowed rate of information accrual is not well understood.

1.1.5 Heterogeneity in the TBI population

Studying TBI as a group is problematic as there is no ‘average’ TBI patient (Maas, 2016). Patients with TBI are diverse, and several clinical and demographic factors (such as

severity, age, IQ, race, and time since injury) will impact patient outcome (Roozenbeek et al., 2012). For example, longer PTA duration (severity) is widely acknowledged to be associated with more persistent and extensive cognitive impairment (Donders & Stout, 2019; Novack et al., 2001; Rapoport et al., 2002; Rassovsky et al., 2015). In the United States, people of colour are less likely to be referred for further care and therefore display worse outcomes following moderate-severe TBI, suggesting that race and ethnicity can impact cognitive outcome (Brenner et al., 2020). There is also a significant association between older age/longer PTA and larger lesion volumes, indicating that older age at injury can worsen the impact of TBI on the brain (Schönberger et al., 2009). In terms of cognitive recovery, higher IQ and younger age in moderate-severe TBI patients is associated with greater improvements in attention, memory, and executive function up to 5 years post injury (Fraser et al., 2019). Time since injury is an important factor to consider when comparing patients, as TBI is a continuing process involving a cascade of neurotoxic events and the full extent of the lesion may not be immediately apparent (Nortje & Menon, 2004).

Lesion characteristics are another source of heterogeneity that is important to consider. Intuitively, there is evidence that larger frontal, parietal, and occipital lesion volumes are associated with poorer memory and processing speed impairment (Spitz, Bigler, et al., 2013). The location of the injury can also have a large impact on patient outcome. Focal frontal and temporal lesions are particularly common in TBI patients and are thought to cause a range of impairments in executive functioning, attention, memory, social cognition, and processing speed (e.g., Fujiwara et al., 2008; Levine et al., 2008; Spikman et al., 2012). However, white matter lesions located in the anterior thalamic radiation and superior longitudinal fasciculus have also been associated with poorer executive functioning in a lesion-symptom mapping study of brain injury (Biesbroek et al., 2017). The exact link

between lesion size and location and cognitive outcome in TBI remains unclear (Lipton et al., 2008).

Group-level analyses, which constitute most publications investigating TBI patients, involve averaging across patients. Often, patients are grouped according to severity (mild or moderate-severe), age (paediatric, adolescent, or adult), and injury type (penetrating, focal, diffuse). While large cohort studies are necessary for driving statistical comparisons between large scale groups, methods that do not assume an individual patient will fit neatly into a group-average estimation of TBI are also needed (Mant, 1999). Instead, case series and individual-level analyses may be used to formulate hypotheses about TBI patient recovery and cognitive functioning according to lesion characteristics (e.g., Jelcic et al., 2013). Case series are essential for trend analysis, health-care planning, and hypothesis generation (Grimes & Schulz, 2002). While no cause-effect inferences can be drawn from single-subject observations, they do provide a more holistic understanding of the patient and their outcome. Pathological profiling of individual cases based on advanced neuroimaging approaches may also help with clinical rehabilitation planning (Irimia, Wang, et al., 2012).

1.1.6 Mapping cognitive functions following brain damage

Localisation of function is the guiding principle of modern lesion studies – where cognitive symptoms are matched to specific sites of brain damage following a brain injury or insult (notably, Phineas Gage; Henry Molaison and work by Scoville and Milner in 1957; “The Man Who Mistook His Wife for a Hat” case study by Oliver Sacks). For instance, damage to the left posterior temporal lobe can cause a speech deficit characterised by fluent yet meaningless speech (i.e., Wernicke’s aphasia) – and similar damage in the left inferior frontal lobe produces an expressive aphasia where the patient can only utter a few words or phrases, despite retaining full cognitive faculties (i.e., Broca’s aphasia) (Binder, 2015;

Fridriksson et al., 2015). The pursuit of ‘mapping’ cognitive functions such as language, memory, even personality to distinct regions of the brain has been the basis of neuropsychological research for decades.

However, it has recently become apparent that the profile of persistent cognitive impairments does not always match the location of a focal lesion following TBI (Lipton et al., 2008). This is because cognitive and motor functions use broadly distributed networks of brain regions to co-ordinate complex patterns of activity (Bressler & Menon, 2010). These networks are reliant on the density, myelination, and organisation of white matter pathways that connect grey matter areas. DAI can cause disconnection of the pathways between cortical and subcortical areas of the brain and may underlie the neurodisabilities following TBI (Adams et al., 1982; Kraus et al., 2007). As white matter damage increases so does the severity of cognitive and motor deficits (Kraus et al., 2007). As such, TBI is described as a disconnection syndrome (Catani & Ffytche, 2005; Griffa et al., 2013). Therefore, while it is necessary to look at the location of a grey matter lesion when examining the symptoms of a TBI patient, it is not always sufficient. Based on the disconnection concept of TBI, it is essential to unpack how white matter damage impacts the brain network in brain injured patients.

1.2 Neuroimaging

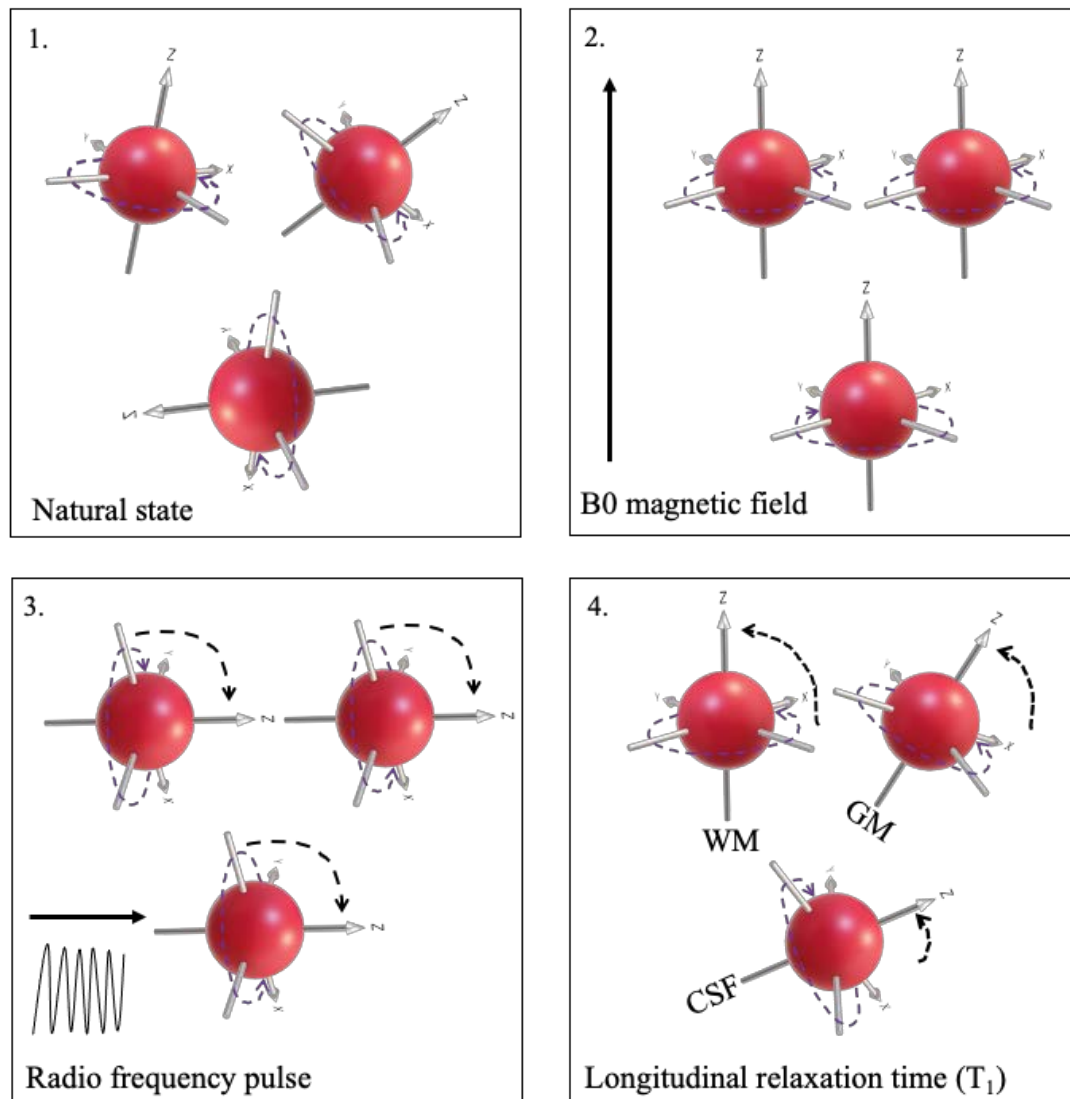
1.2.1 Magnetic Resonance Imaging

Magnetic Resonance Imaging (MRI) is a diagnostic medical imaging technique that leverages magnetic fields and radio frequency pulses to excite the protons of hydrogen atoms contained in water molecules. The hydrogen protons rotate on their own axes around a magnetic field (see Figure 3, panel 1). When they are placed in a homogenous magnetic field

such as in an MRI, their rotational axes align, and they begin to precess together (Figure 3, panel 2). A radio frequency pulse forces the precessing protons to flip transverse to their aligned position (Figure 3, panel 3). Once the pulse ends, the protons naturally return to alignment within the homogenous magnetic field – this is called the longitudinal relaxation time (T_1 ; Figure 3, panel 4). When the gradient coils localise the magnetic field on the brain, protons in fatty tissue such as myelin relax much faster than protons in free water such as cerebral spinal fluid (CSF). The contrast between the longitudinal relaxation time in the CSF and trapped water of the fatty tissues provides images of the anatomy brain *in vivo*.

Figure 3

Magnetisation and Relaxation of Hydrogen Protons in Magnetic Resonance Imaging



Note: WM = white matter; GM = grey matter; CSF = cerebral spinal fluid.

The current thesis examines the impact of moderate-severe TBI in adults who are experiencing ongoing cognitive impairments in the chronic phase of their injury. Of particular interest is the white matter of these individuals, which is often damaged following TBI. The imaging techniques clinically used to diagnose and manage TBI before diffusion imaging was made available 15 years ago (e.g., CT, T1-weighted MRI, FLAIR) were unable

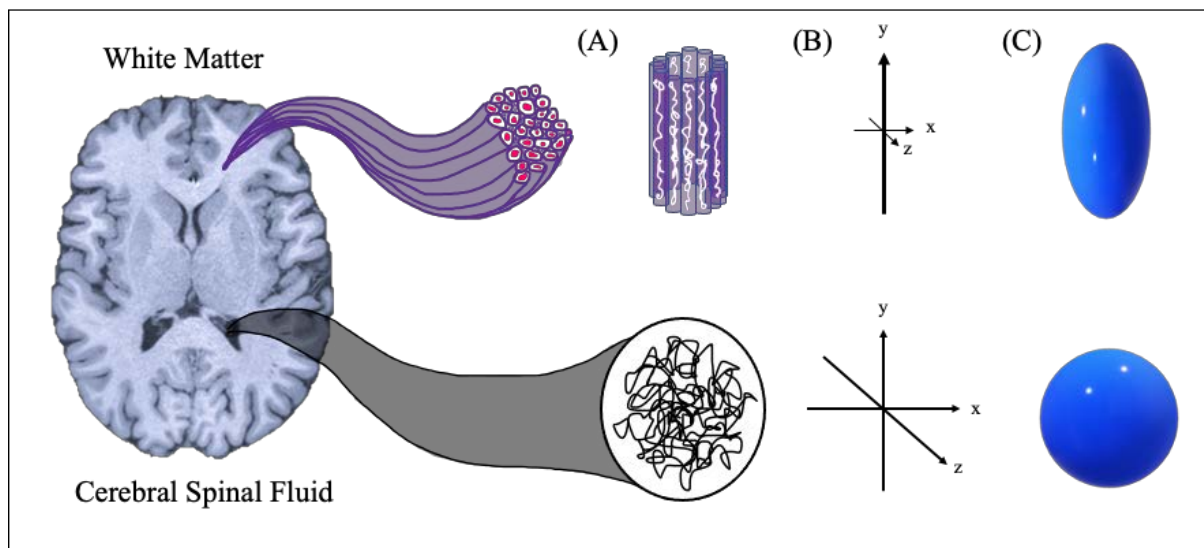
to visualise the white matter in a quantifiable way. These traditional neuroimaging techniques are tailored to measuring contrasts in signal intensity between fat and water in the brain, essential in the diagnosis of focal lesions but insufficient for investigating microstructural axonal injuries. Instead, diffusion MRI (dMRI) enables examination of the microstructural properties of the white matter (Hulkower et al., 2013).

1.2.2 Diffusion Weighted Magnetic Resonance Imaging

Recently, dMRI has been used to investigate the microstructural properties and architecture of the white matter by characterising the direction of water molecule diffusion in the brain (see Figure 4). MRI is sensitive to the magnetic properties of the hydrogen protons contained within water molecules (section 1.2.1). According to the properties of Brownian motion, water molecules are constantly in motion due to thermal energies and will move isotropically – randomly and equally in any direction – if not restricted, such as in the cerebrospinal fluid. However, water molecules in the white matter can only move anisotropically (longitudinally along the axonal pathway) as the fatty cell walls and myelin sheaths of the axonal bundles hinder diffusion in other directions. Thus, the boundaries created by the axon bundles restrict the movement of water molecules in the white matter. Following injury, the barriers that maintain the direction of water flow can be broken, and the differences in water molecule diffusion can be used as evidence of white matter damage following TBI.

Figure 4.

Diffusion Properties and Models of the White Matter and the Cerebral Spinal Fluid



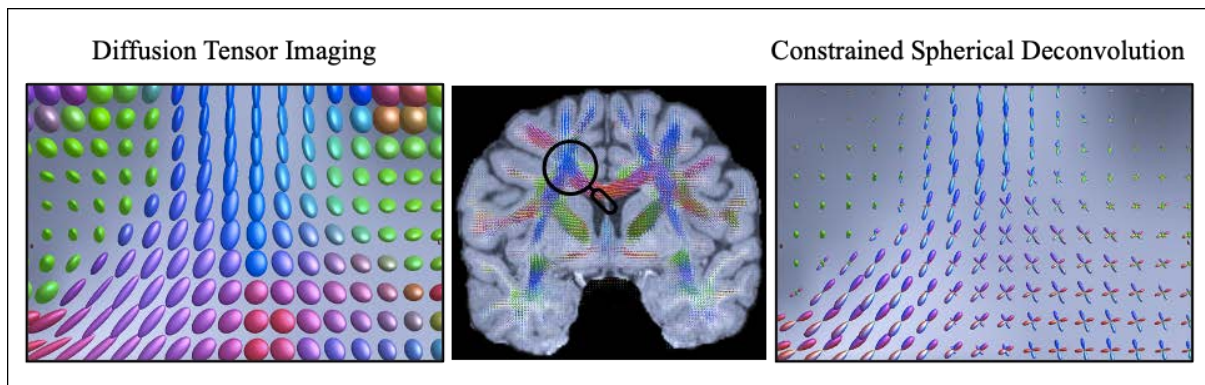
Note: (A) Diffusion is anisotropic in the white matter (i.e., movement is restricted along the white matter tract), but isotropic in the cerebral spinal fluid; (B) measurement of the primary direction of diffusion in the x, y, and z planes gives rise to; (C) models of brain tissue structure within a given voxel.

The dMRI signal is the T_2 signal, or the transverse decay time – the time taken for the hydrogen proton spin to return to the low energy state. This T_2 signal attenuates differently depending on how easily water can diffuse in each tissue type. Thus, dMRI uses the properties of water diffusion by applying multiple gradient fields (at least 6, often up to 60) alongside the strong b_0 magnetic field. Gradient fields are sensitive to the different directions of water movement, such that the water molecules that moved during one diffusion gradient will have a different magnetisation to those that did not move, forming an image contrast. These diffusion sensitising gradients can be applied in x, y, and z axes, or a combination of all – the more gradient directions are applied, the more contrast images are attained depicting differences in water movement in a particular direction. As water movement is hindered by the microstructural tissue geometries in the brain, these images can be used to provide information about the physical properties of the white matter bundles, including direction and magnitude (for a full description of the principles of diffusion MRI, see Jones, 2010b).

Once the diffusion-weighted signal is measured across the whole brain in multiple directions, a model can be used to estimate the primary direction and magnitude of water diffusion in each voxel (see Figure 5). There are different methods of doing this, including the diffusion tensor model (DTI) (for review, see Bassler & Jones, 2002) and the fibre orientation distribution (FOD) model (Tournier et al., 2004), through the use of constrained spherical deconvolution (CSD). The tensor model simply characterises the diffusion-weighted signal in each voxel using 6 parameters: three representing the magnitude of the diffusion, and three representing the direction. Geometrically, this portrays the diffusion signal in each voxel as an ellipsoid (Basser et al., 1994), with the longest axis of the tensor indicating the direction of the maximum diffusion and thus the primary fibre direction of that voxel.

Figure 5.

The Diffusion Tensor Model and Constrained Spherical Deconvolution



Note: This cross-section was chosen to highlight the crossing of the corona radiata, superior longitudinal fasciculus, corpus callosum, and cingulum bundle.

On the other hand, CSD (Tournier et al., 2007) allows the estimation of multiple fibre directions in one voxel, by measuring all fibre orientations and their respective uncertainty values within each voxel and representing this as an FOD. Given that 90% of voxels within the white matter contain crossing axonal projections (Jeurissen et al., 2013), the FOD model

is generally thought to be a more sensitive representation of white matter microstructure than the tensor model. It should be noted, other approaches have been proposed that are also capable of estimating multiple fibre directions in one voxel, including Q-ball imaging (Tuch, 2004); diffusion spectrum imaging (DSI; Hsu et al., 2015); composite hindered and restricted model of diffusion (CHARMED; Assaf et al., 2004). However, these approaches are less feasible for clinical imaging as they require large and multiple b -values, leading to long scan times.

Subsequently, there are divergent methods for analysing the dMRI signal. Traditionally diffusion metrics were calculated for each voxel and compared between subjects or groups in an area of interest (e.g., Caeyenberghs, Leemans, Geurts, et al., 2011), across the whole brain (e.g., Caeyenberghs et al., 2010), or using tractography approaches (e.g., Caeyenberghs, Leemans, Coxon, et al., 2011). These diffusion metrics are used to quantify the directionality of water movement as a proxy for measuring the integrity of the white matter within that voxel, or along a specific tract. The most common diffusion metrics are derived from the tensor model, including fractional anisotropy (FA), mean diffusivity (MD), axial diffusivity (AD), and radial diffusivity (RD) (Basser et al., 1994). FA represents the overall directional coherence of the water molecules within neuronal tissue. On the other hand, MD, AD, and RD can be used to represent the direction and magnitude of water diffusion more specifically – MD is the total diffusion within a voxel, regardless of the direction; AD measures diffusion along only the principal direction of diffusion; and RD is the average diffusion across the two minor axes.

Metrics such as these are often interpreted as a direct measure of axonal integrity, with low FA thought to represent alterations in white matter that are consistent with DAI (Shenton et al., 2012). However, this is not without pitfalls and challenges (e.g., Jones, 2010a; Jones & Cercignani, 2010; Le Bihan et al., 2006). FA values can change based on

myelination, axon density, or the layout of axons within the voxel (Jones et al., 2013). As such is it not a specific marker of any one property of the white matter (Caeyenberghs et al., 2018; Jones et al., 2013). Increases in FA are sometimes observed when decreases would be expected (e.g., Bazarian et al., 2007; Mayer et al., 2010) – while this is hypothesised to be caused by cytotoxic oedema (Mayer et al., 2010), the true mechanism remains unclear.

Recently, algorithms have been created that can estimate and reconstruct the white matter tracts of the brain using a technique called tractography. Unlike scalar metrics (e.g., voxel-wise FA), tractography is used to measure structural connectivity – how well regions of the brain are connected. Tractography uses the diffusion signal described above as the basis for an algorithm that reconstructs the white matter tracts, providing estimates of the axon pathway orientation and density in living brain tissue (Tournier et al., 2011). In other words, tractography is essentially a very complex game of connect-the-dots. The direction and magnitude of the tensor or FOD derived from the diffusion signal in each voxel is used by the tractography algorithm to generate streamlines. Of course, there are many algorithms available to choose from, and selection of the appropriate technique will depend on the acquisition parameters of the dMRI data (Jones et al., 2013). Numerous reviews and methodological comparisons have been published in this field, debating the appropriateness of each tractography technique from data acquisition through to statistical analyses (for example, Hutchinson et al., 2018).

1.2.3 Tensors and tractography in TBI

Diffusion imaging, whether analysed using voxel-wise metrics, region of interest, or whole brain tractography, has opened avenues for exploring the properties of the white matter in healthy and damaged brain tissue. There is mounting evidence supporting dMRI as a

sensitive diagnostic tool in the care of patients with TBI (for reviews, see Delouche et al., 2016; Hulkower et al., 2013; Hutchinson et al., 2018; Levin et al., 2008; Xiong et al., 2014). The relevance of dMRI techniques in the care of patients with TBI has long been acknowledged (e.g., Kraus et al., 2007; Rutgers et al., 2008). The first study to examine TBI in humans using diffusion imaging was published 18 years ago (Arfanakis et al., 2002) – since then, there have been hundreds of publications examining regional and whole brain alterations in anisotropy in patients with brain injuries.

In their seminal review, Hulkower et al. (2013) acknowledge the power of diffusion imaging for visualising white matter, which can quantify pathology not detected by other imaging modalities such as CT. They show that diffusion imaging can be leveraged to distinguish between TBI patients and healthy controls, regardless of time since injury, severity of injury, analytical or imaging discrepancies, and sampling characteristics. In particular, across the 100 articles included in the review, the most common regions where FA was significantly lower (or in some cases, higher) than healthy controls were the corpus callosum (e.g., Aoki & Inokuchi, 2016; Caeyenberghs et al., 2010; Mayer et al., 2010; Niogi et al., 2008) the posterior limb of the internal capsule (e.g., Caeyenberghs, Leemans, Coxon, et al., 2011), the frontal lobe (e.g., Oni et al., 2010), corona radiata (e.g., Bonnelle et al., 2011), cingulum (e.g., Benson et al., 2007), superior longitudinal fasciculus (e.g., Farbota et al., 2012; Spitz, Maller, et al., 2013), and the centrum semiovale (e.g., Huisman et al., 2004; Inglese et al., 2005).

Decreased white matter organization has also been shown to predict poorer outcomes in chronic TBI patients of all severity types (Kinnunen et al., 2011; Kraus et al., 2007), and in acute mild TBI patients with persistent symptoms (Niogi et al., 2008). Lower FA in the subregions of the corpus callosum is associated with poorer bimanual coordination (Caeyenberghs, Leemans, Coxon, et al., 2011) and with slower processing speed (e.g., Levin

et al., 2008; Wilde et al., 2006), while lower FA in the cerebellum is associated with poorer manual dexterity (Caeyenberghs, Leemans, Geurts, et al., 2011) in moderate-severe TBI patients. D'souza et al. (2015) found that reduced FA and MD in the corpus callosum, fornix, uncinate fasciculus and thalamic radiations are correlated with post-concussion symptom scores. Working memory deficits in children with TBI are associated with lower RD of the corpus callosum (Treble et al., 2013). Poorer visual motor tracking performance is associated with lower FA of tracts important for transmission of information for motor responses to visual stimuli, i.e., the cortico-spinal tract, posterior thalamic radiation, and optic radiation, in adolescents with TBI (Caeyenberghs et al., 2010). The list goes on – for reviews, see Delouche et al. (2016), Hulkower et al. (2013), Hutchinson et al. (2018), and Xiong et al. (2014). Importantly, the overwhelming majority of these studies have employed tensor-based metrics such as FA or have used tractography to look at tracts of interest.

1.2.4 Advances in tractography

It is well-known that tractography techniques suffer from several limitations and biases, impacting the reliability of findings (Jeurissen et al., 2013; Jones, 2010a). Both deterministic and probabilistic tractography algorithms are commonly used to reconstruct streamlines, and both have problems with accurately reconstructing voxels with crossing or kissing fibres (Jones et al., 2013). After all, tractography is not a direct replication of the anatomy of white matter pathways, but a reconstruction based on finite diffusion signals, voxel by voxel. Therefore, in order to obtain measures of structural connectivity that are robust and interpretable, reconstruction techniques that are as biologically accurate as possible must be used (Sporns et al., 2005). In the present research program, a state-of-the art diffusion MRI sequence and processing pipeline is employed to avoid biases that may result

in false pathways. Many of the studies described in section 1.2.3 that used tractography to examine white matter tracts in TBI patients were performed before these techniques became available. Three major avenues were explored in this thesis for improving the robustness of tractography: minimising false positives, generating streamlines from the grey-white matter boundary, and avoiding reconstruction biases.

First, to minimise false positives by avoiding overestimation of the volume of white matter in voxels containing both signal types, a single-shell 3 tissue CSD model with fibre orientation distributions estimated in the grey matter, white matter, and CSF is used (Jeurissen et al., 2014). To the best of our knowledge, this will be one of the first projects using this new multi-tissue method of CSD to estimate white matter tracts in TBI patients. Second, when generating tracts, certain termination criteria are required that tell the algorithm to discontinue the streamline. However, Smith et al. (2012) showed that these criteria allowed streamlines to terminate in the white matter or CSF, which is anatomically implausible. This precipitated their development of Anatomically Constrained Tractography (ACT) to accurately determine where streamlines should be generated and terminated based on grey matter segmentation from structural T1 images. ACT has also been shown to reduce the number of biologically implausible streamlines by restricting streamline initiation and termination to the grey-white matter boundaries (e.g., Horbruegger et al., 2019).

Finally, streamline density is often over-estimated in longer fibre pathways – referred to as the reconstruction bias. According to Jones et al. (2013), the density of the streamlines that are reconstructed are not equivalent to the density of the actual fibre pathways. The number of streamlines is an important measure often used to quantify the strength of the connection between any two regions of the brain – however, if the tractography is biased towards longer streamlines, this measure may not be reliable. To use a measure of streamline

density as a proxy for white matter organisation, it is important to use the most biologically accurate measure.

Using the FOD amplitude representing the density of fibres in each voxel, the advanced tractography reconstruction technique ‘SIFT’ (Spherical-deconvolution Informed Filtering of Tractograms) provides a more accurate representation of streamline count (Smith et al., 2013, 2015b; Yeh et al., 2016). SIFT filters the density of the streamlines to match the density implied by the FOD from the diffusion signal, by deleting streamlines. However, this has the unwanted effect of increasing the computation time, as ~90% of the reconstructed streamlines must be discarded. SIFT2 was designed shortly after in response to this concern (Smith et al., 2015a). Instead of eliminating streamlines to match the underlying fibre density, the FODs are used to determine an appropriate cross-sectional area that is then multiplied by the number of streamlines. The resulting streamlines are therefore proportionate to the density of the underlying FODs without the need for wasteful deletion processes – and therefore should be a closer estimation of the actual underlying white matter density (Smith, Raffelt, et al., 2020). Because it is more related to the actual diffusion signal than unfiltered structural connectivity measures, using SIFT2 has been shown to have the potential for stronger clinical relationships (McColgan et al., 2018), but has not yet been utilised to quantify structural connectivity in TBI patients.

1.3 Connectomics and Network Analysis

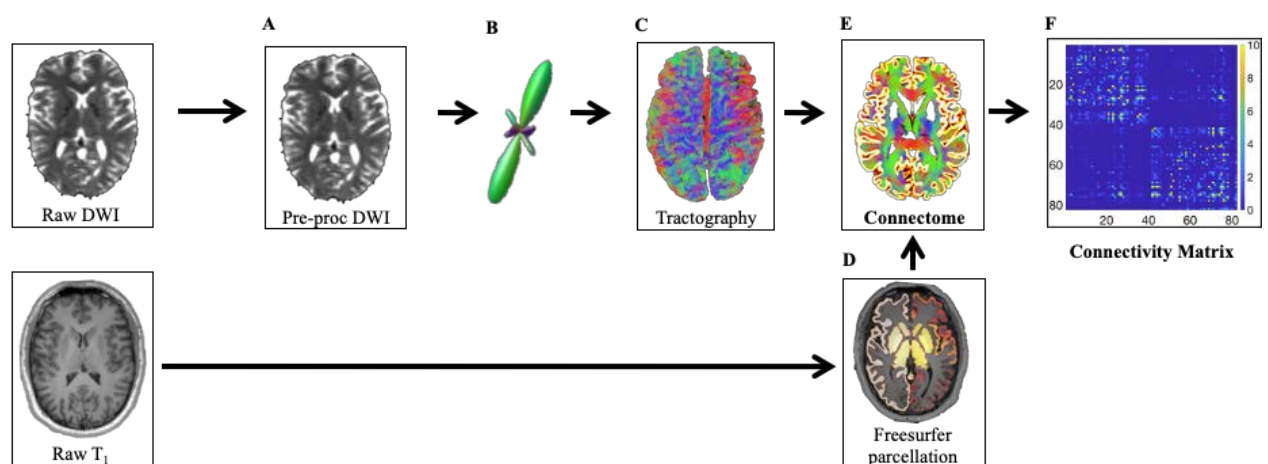
1.3.1 Introduction to connectomics

It is widely acknowledged that cognitive functions rely on broadly distributed cognitive networks, and so tract-based approaches such as those described in sections 1.2.2 and 1.2.3 may form an incomplete perspective of brain connectivity. Rather, the brain

operates as a set of interconnected networks in complex arrangements, disseminating information across distributed areas (Bressler & Menon, 2010). Connectome analyses have provided a novel way to understand communication in brain networks (Bassett & Sporns, 2017). The connectome is the entire collection of all white matter connections within the brain (Sporns et al., 2005) (see Figure 6 for an overview of connectome construction). Based on the disconnection concept of TBI, network analysis is highly suited to this topic as it can be used to consider the complex, integrated nature of the brain and the impact of both large focal lesions and small white matter lesions.

Figure 6

The Basics of Connectome Construction



Note: (A) Raw diffusion MRI images are pre-processed to remove noise; (B) FODs are estimated for each voxel; (C) tractography is performed to generate the streamlines (edges); (D) anatomical T₁ scans are used to segment brain regions (nodes); (E) the connectome is created by assigning the streamlines from tractography to the brain regions from Freesurfer, resulting in; (F) a connectivity matrix where each cell represents the connectivity strength between two brain regions.

To generate the structural connectome, the brain is mathematically described as a series of ‘nodes’ or regions of grey matter, connected by ‘edges’ that represent the white matter connections (Hagmann et al., 2008). The nodes of the graph are delineated from

structural T₁ images and segmented using ‘atlases’ that describe functionally specialised modules of grey matter tissue (e.g., Desikan-Killiany atlas; Desikan et al., 2006). The edges are the connections between these brain regions, quantified using either functional (fMRI) or tractography (see section 1.2.4). It is important to note that functional and structural imaging modalities summarise brain networks differently. In simple terms, the functional network summarises how likely two regions of the brain are to be active at the same time; the correlations between blood-oxygen-level-dependent (BOLD) signals of two regions indicate the likelihood that if one region is active then the other is as well. On the other hand, the structural network is an estimation of the microstructural properties of the white matter fibre bundles connecting two brain regions. Given white matter damage is a key element of TBI (Hulkower et al., 2013), and the questions that remain around whether DAI is an underlying cause of ongoing cognitive deficits in chronic patients, the focus of this thesis is on structural connectivity (dMRI). However, it should be noted that functional connectivity (fMRI) is another (enormous) field entirely and has its own relationship with brain injury. The link between the structural connectivity findings of this thesis and how these may relate to relevant functional theories is examined in the General Discussion (Chapter 6).

For the purposes of investigating structural connectivity, nodes and edges can be defined in different ways depending on the scale at which one wishes to analyse the network (Zalesky et al., 2010). A macroscopic view is normally preferred when studying the human connectome *in vivo*, where nodes are the major cortical and subcortical regions of the brain and the edges represent the white matter bundles that connect them (Bassett & Bullmore, 2009). The simplest way to define edges is using a binary measure of streamline connectivity (connection present = 1; connection absent = 0), which avoids problems with diverse streamline densities. In cases such as this, a certain threshold is applied to the connectivity matrix such that only the top 10% (or so) strongest connections remain. As such, binary

connectomes are oversimplified and are dependent on arbitrary density thresholds (Yeh et al., 2020). Instead, it is argued that the weight of the connection between two regions is important to factor in brain network representation. While dMRI cannot provide exact measures of the microstructural vasculature that underly information transmission (e.g., axon diameter, myelination, or density), it does allow indirect approximations of these biophysical properties (for review, see Sotiropoulos & Zalesky, 2019).

As such, the edges of the brain graph are often represented using weights derived from the tractography techniques and diffusion metrics described above (section 1.2.2). Most often, the number of streamlines (NOS) – the number of reconstructed streamlines between two regions – is used to quantify connectivity between two brain regions. NOS, however, is not an indication of the actual number of axons within that bundle, although it can be misinterpreted as such (Lazaridou et al., 2013; Schlaug et al., 2009). Instead, NOS can be heavily biased by processing of the tractography algorithms as described in section 1.2.4 (also see Jones & Cercignani, 2010), and it is therefore hard to make biologically meaningful interpretations following a change in NOS. Another common method of quantifying edge weights in a connectome analysis is using the average FA of all voxels traversed by a particular streamline. Again, as described above, FA is a measure of white matter organisation that is not specific to any one type of microstructural alteration and is heavily influenced by the presence of crossing fibres (Jeurissen et al., 2013). The utility of the advanced methods detailed in section 1.2.4 such as SIFT2 to quantify the edge weights in a connectome analysis has only just begun to be explored (Civier et al., 2019; Frigo et al., 2020).

1.3.2 Graph theoretical analysis

In modern-day neuroimaging, graph theoretical analysis is a mathematical tool used for summarising network properties of the human connectome. However, graph theory itself emerged in 1735, when the Swiss mathematician Leonard Euler answered the question of whether it was possible to completely traverse his hometown with seven bridges and four land masses using each bridge only once. To solve this geographical problem, Euler summarised the information into nodes (landmasses) and edges (bridges) and proved that it was not possible. In this instance, the topography (spatial distances between landmasses) was unimportant – it was the topology (the layout of the bridges that connected each landmass) that allowed Euler to solve the riddle. Since then, graph analysis has become a branch of mathematics devoted to describing and quantifying network structures by their topology. In the modern world, graph theory is used extensively to understand network properties in social sciences, epidemiology, website page rankings and data tracking. In the 1980's, graph theory was first applied to the study of the human brain (Watts & Strogatz, 1998).

The connectivity matrix (see Figure 6) represents the entire set of nodes and edges of the brain in a two-dimensional format, upon which mathematical applications can be performed. Each of the axes of the connectivity matrix represents the brain regions, while the squares of the matrix represent the connections between those regions. Matrix operations can be used to summarise connectivity strength between brain regions in terms of integration and segregation, or how central certain nodes are to the graph (Rubinov & Sporns, 2010). These summary measures are called graph metrics – Table 2 provides working definitions of the most common graph metrics, which are built from four basic matrix properties. These are degree (the number of connections for node i), strength (the sum of edge weights for node i), shortest path length (the shortest distance or fewest hops between node i and j), and clustering

coefficient (the probability that two nodes i and j each connected to a third node k are also connected to each other).

Table 2

Definitions of Basic Graph Metrics

Graph Metric	Description	Higher values mean...
<i>Integration</i>		
<i>Characteristic Path Length</i>	The shortest path is the fastest and most direct communication pathway between two network nodes. Characteristic path length is defined as the average shortest path length between all node pairs in a network (Watts & Strogatz, 1998).	A higher characteristic path length indicates that the fastest communication pathways between regions are, on average, longer and less efficient.
<i>Global Efficiency</i>	The inverse average shortest path efficiency between all possible pairs of nodes in a network, where efficiency is computed as the inverse of shortest the path length (Latora & Marchiori, 2001).	A higher global efficiency will indicate a greater capacity for efficient integration of information (in parallel) across the network.
<i>Segregation</i>		
<i>Clustering Coefficient</i>	The number of existing connections between the neighbours of a node, divided by all the possible connections, calculated for each node individually and averaged across the entire network (Watts & Strogatz, 1998).	A higher average clustering coefficient means that a greater proportion of connections are made between nodes neighbours, compared to the connections possible, and indicates more clustered connectivity around individual nodes.
<i>Local Efficiency</i>	The local efficiency is the average of inverse shortest path length in a local area. Mean local efficiency is taken as the efficiency of each node in the network averaged over the total number of nodes (Latora & Marchiori, 2001).	A higher local efficiency means greater capacity for integration between the immediate neighbours of a given node.
<i>Centrality</i>		

Graph Metric	Description	Higher values mean...
<i>Strength</i>	The strength of a node is the sum of the weights of its edges. Mean strength is the average of all the normalised strength values across each node of the network.	A higher strength indicates a greater average edge weight for each node.
<i>Betweenness Centrality</i>	The proportion of shortest paths that pass-through node <i>i</i> between its neighboring nodes, calculated for each node and averaged across the network (Freeman, 1978).	Higher betweenness centrality means that node lies on more shortest paths in the network pass through it, and this that node is more central and important to the network. A high network/average betweenness centrality indicates a high number of nodes that are central to shortest paths.
<i>Summary Measures</i>		
<i>Small-worldness</i>	The capacity of a network for an energy-efficient balance between clustering and short paths, relative to an appropriate random network (e.g., Maslov & Sneppen, 2002). A small-world network has normalised clustering higher than a random network ($\gamma > 1$), and normalised characteristic path length akin to a random network ($\lambda \sim 1$) (Humphreys & Gurney, 2008).	If $\sigma > 1$, the network is demonstrating small-world properties.

The connections in the human brain are predominantly short and weak, connecting proximal neighbours very tightly. This means that information can be shared very easily between neuronal columns that share similar functions. However, higher order cognition relies on signalling between broadly distributed regions to engage attention and execute complex actions (Bressler & Menon, 2010). Therefore, the human brain, both functionally and structurally, optimises performance by balancing functional segregation and network integration (Bullmore & Sporns, 2009).

Measures of integration are based on path length (e.g., characteristic path length and global efficiency) and are also known as communication measures, as they represent how

well brain regions can communicate with each other. Segregation is based on clustering and measures the decomposition of brain regions into functional modules. This modular structure is interspersed with some long-distance connections, via ‘hubs’ such as the thalamus and cingulate regions, allowing for information to integrate between modules (Watts & Strogatz, 1998). Hubs are measured using betweenness centrality, which determines the number of ‘shortest paths’ that traverse each brain region. This balance between segregation and integration, and the presence of hubs, is what is thought to give rise to higher order cognitive functions – and what is potentially damaged following brain injury.

1.3.3 Graph metrics and cognition

It is often assumed that higher order cognitive functions rely on efficient integration properties of the structural network (Bullmore & Sporns, 2012). As such, communication measures have been suggested to be important measures in graph theoretical analyses (Rubinov & Sporns, 2010). Several graph theoretical studies have revealed that communication efficiency can predict individual variation in processing speed in older adults (e.g., Wen et al., 2011) and clinical populations (e.g., Caeyenberghs et al., 2014; Reijmer, Leemans, Caeyenberghs, et al., 2013). For example, Caeyenberghs et al. (2014) revealed that slower processing speeds corresponded with lower global efficiency in adults with TBI. While these early results are promising, advances in the way we measure brain network communication, process diffusion weighted imaging data, and model information processing could lend further weight to the link between network efficiency and information processing speed.

Most connectome studies have computed communication metrics based on shortest path length – including characteristic path length and global efficiency (based on the seminal

article by Rubinov & Sporns, 2010) – to tap into information transfer (for review, see Betzel, 2020). A network with short path lengths is often interpreted as having efficient information transfer between brain regions (Latora & Marchiori, 2001). Similarly, longer path lengths in brain networks of brain-injured populations are interpreted in terms of poorer efficiency of information transfer (Imms et al., 2019). However, several connectome studies failed to show significant associations between processing speed and communication metrics (e.g., Kim et al., 2014a; van der Horn et al., 2017). For example, Kim et al. (2014a) found that path length was longer in people who had suffered brain injuries – but this increase wasn't associated with slower processing speed. The reason for this may lie in the sensitivity of the communication metrics used. Recently, a more biologically realistic routing model for brain network communication has been suggested, i.e., navigation efficiency (Seguin et al., 2018). Navigation metrics assume that information moves from one node to the next based on the distance between that node and the target node – and have been shown to be a plausible way of characterising communication in the human brain network (Seguin et al., 2020). The relationship between this communication measure and processing speed has yet to be examined. Furthermore, this communication measure has never been calculated in TBI patients.

1.3.4 Graph metrics: A biomarker of brain injury?

Graph theoretical analysis has previously been used to compare the connectivity of damaged brain networks to healthy connectomes (Griffa et al., 2013), but understanding of the brain network of patients with TBI is still emerging (Caeyenberghs & Leemans, 2014; Caeyenberghs, Leemans, De Decker, et al., 2012; Caeyenberghs, Leemans, Heitger, et al., 2012; Yuan, Treble-Barna, et al., 2017). In their seminal review paper, Griffa et al. (2013) describe how graph metrics can be used to represent network disruption in ADHD (Cao et al.,

2013), neurodegenerative diseases like Alzheimer's disease (Lo et al., 2010) and multiple sclerosis (Shu et al., 2011), and psychiatric disorders such as schizophrenia (Fornito et al., 2012). Griffa et al. state that graph theory provides a unique insight into how damaged neural tissue in one local area of the brain can impact the entire network structure – and that graph metrics therefore have the potential to be useful biomarkers of brain injury.

In one of the first structural graph theory studies of TBI, Caeyenberghs, Leemans, De Decker, et al. (2012) revealed that young TBI patients have decreased connectivity degree within the brain, which correlated significantly with poor balance. Similarly, Kim et al. (2014a) found that longer path length in moderate-severe adults with TBI correlated with poorer higher-order cognitive processes like executive function and verbal learning. Since then, more research has suggested that graph metrics could be 'biomarkers' of TBI (Hellyer et al., 2015; Yuan et al., 2015; Yuan, Wade, et al., 2017). In TBI, to date, 18 studies have been performed comparing graph metrics in TBI patients to healthy controls. The first empirical chapter of this thesis is a systematic literature review and meta-analysis of 13 of these studies (the remaining 5 studies published after this paper was accepted in January 2019 are described in linking Chapter 5.1).

1.3.5 Use of graph metrics in individual patients

TBI patients are heterogeneous (see section 1.1.5) and group-level comparisons disregard individual variability (Mant, 1999). Thus, there is a mounting call for the use of individual-level approaches to enable the analysis of clinically heterogeneous groups such as TBI (Irimia, Chambers, et al., 2012; Jolly et al., 2021) and Schizophrenia (Lv et al., 2020). For example, Lv et al. (2020) examined alterations in FA and CT in Schizophrenia patients compared to a normative range. They found overall reductions in both measures for the

Schizophrenia patients – however, the anatomical location of individual decreases was highly inconsistent, and as such group-level maps were not representative of individuals. Another study by Jolly et al. (2021) has used individual examination of FA in TBI patients in the chronic (>6 months) and subacute (10 days – 6weeks) phases to develop a structural connectivity pipeline for diagnosing diffuse axonal injury (DAI). These recent studies, however, do not utilise connectomics to represent individual patients.

The idea of personalised structural connectomics for improving the care of TBI patients was introduced by Irimia, Wang, et al. (2012). They produced a visualisation method that allows clinicians to rapidly identify white matter atrophy over time, in order to create personalised rehabilitation programs (Irimia, Chambers, et al., 2012). There is other evidence that individual network- and connectivity-based profiles are promising for patient characterisation. For example, individual measures of connectivity (dynamic resting-state of the default mode network) predict changes in symptoms in patients with Schizophrenia better than grey matter volume/cortical thickness and clinical observations (Kottaram et al., 2020); and individual variations in connectome topography have been shown to predict surgical outcome in patients with temporal lobe epilepsy (Bonilha et al., 2015). Thus, personalised connectomics holds promise as a means for characterising individual patients' topological profiles. To date, however, no study has examined the profile of graph metric alterations in individual TBI patients.

1.4 Aims and Research Questions

The overarching aim of this research program is to interrogate the use of graph metrics to study TBI. While there is great interest in the use of graph metrics as a diagnostic 'biomarker' of TBI, there is currently no systematic examination of which graph metric/s are specific enough to be given this label (section 1.3.4). In addition, the relationship between

graph metrics and measures of cognitive performance is not well understood (section 1.3.3), making interpretation of graph metric biomarkers difficult. Finally, the issue of heterogeneity in the TBI population (section 1.2.5) is not addressed by current group-level graph theoretical approaches. Therefore, this research project constitutes a substantive critical assessment of the use of graph metrics as biomarkers of TBI.

The first aim of this research program is therefore to systematically evaluate the current status of structural graph analysis findings in TBI patients. In the first empirical study (Study 1), a narrative review of diffusion MRI papers comparing healthy controls using global graph metrics – and the first meta-analysis of graph metrics in TBI – is conducted. The aim is to identify whether there are systematic differences in graph metric findings between TBI subtypes, and to provide a framework for hypotheses in future graph theoretical studies, which is currently lacking. The research questions were:

1. Which graph metrics are consistently different between TBI patients and healthy controls across all the currently available literature?
2. Do alterations in graph metrics vary according to time since injury; severity of injury; and age at injury?
3. What are the major methodological challenges associated with investigating graph metrics in TBI patients?

The second aim of this research program is to examine whether graph metrics are related to measures of cognition. The findings of the meta-analysis were used to decide which graph metric to focus on. The second empirical study (Study 2) therefore investigates how inter-individual differences in processing speed relates to *communication metrics* – i.e., characteristic path length, navigation, and global efficiency. This analysis is performed in a

healthy cohort, as a proof-of-concept for future studies. This study also demonstrates the methodology used to overcome the connectome reconstruction challenges raised in the first empirical study and in section 1.2.4; and a more specific measure of processing speed called *drift rate*. The research questions were:

1. Can communication metrics be used as a biological marker of inter-individual variability in processing speed?
2. Which communication metrics are the most specific to processing speed?

Finally, the third aim is to develop and implement a personalised structural connectome analysis and visualisation approach for a case-series of moderate-severe TBI patients. Thus, the third empirical study (Study 3) provides a demonstration of how graph metric biomarkers might be used in the care and treatment of heterogeneous TBI patients. This includes a profile of graph metrics that are shown to be altered in TBI patients compared to healthy controls from Study 1, including a new graph metric navigation efficiency which is emerging as a more biologically grounded representation of global network communication in Study 2. An extensive cognitive testing battery is also employed, including measures of core cognitive domains affected following TBI: processing speed, attention, and working memory (section 1.1.4; Rabinowitz & Levin, 2014). Finally, the advanced connectome construction pipeline from Study 2 is once again used to overcome known limitations of connectome reconstruction in TBI patients (section 1.2.4). The research questions were:

1. How can visual comparisons between TBI patients and healthy controls be facilitated using graph metrics?

2. What observations can be made regarding the variability in graph metrics and cognitive performance across individuals?
3. Do personalised connectomics have a role in the care and treatment of TBI patients – i.e., is using graph metrics as biomarkers of brain injury feasible?

The following three empirical chapters address each of these aims in turn. The first empirical chapter (Study 1) consists of a literature review and meta-analysis of all available TBI studies that use graph metrics to compare patients to healthy controls. This study investigates which graph metrics are consistently different between TBI patients and healthy controls, how these alterations change according to injury factors, and the methodological challenges that remain to improve connectome construction (Aim 1, Research Questions 1, 2, and 3).

**Chapter 2: Study 1 - The structural connectome in Traumatic Brain
Injury: A meta-analysis of graph metrics**

2.1 Published Article¹

2.1.1 Title Page

The structural connectome in traumatic brain injury: A meta-analysis of graph metrics

Phoebe Imms^{a,1}, Adam Clemente^a, Mark Cook^c, Wendyl D'Souza^c, Peter H Wilson^a, Derek K Jones^{a,b}, Karen Caeyenberghs^a

^a School of Behavioural, Health and Human Sciences, Faculty of Health Sciences, Australian Catholic University. 115 Victoria Parade, Melbourne VIC 3065 AUSTRALIA.

^b Cardiff University Brain Research Imaging Institute, School of Psychology, and Neuroscience and Mental Health Research Institute, Cardiff University. Maindy Rd, Cardiff CF24 4HQ, UNITED KINGDOM.

^c Department of Medicine, St. Vincent's Hospital, University of Melbourne. 41 Victoria Parade, Melbourne, VIC 3065, AUSTRALIA.

¹ Corresponding author; phoebe.imms@myacu.edu.au

Funding: Karen Caeyenberghs is supported by a National Health and Medical Research Council Career Development Fellowship and an ACURF Program Grant. Derek K Jones is supported by a Wellcome Trust Investigator Award (096646/Z/11/Z) and a Wellcome Trust Strategic Award

¹ Article published in *Neuroscience and Biobehavioral Reviews*.

Reference: Imms, P., Clemente, A., Cook, M., D'Souza, W., Wilson, P. H., Jones, D. K., & Caeyenberghs, K. (2019). The structural connectome in traumatic brain injury: A meta-analysis of graph metrics. *Neuroscience & Biobehavioral Reviews*, 99, 128-137.

(104943/Z/14/Z). Phoebe Imms and Adam Clemente are both supported by the Australian Postgraduate Award under the Australian Research Training Program.

Financial Disclosures: The authors report no biomedical financial interests or potential conflicts of interest.

Declarations of interest: None

Highlights: Higher clustering and longer path length in brain-injured patients; Graph metrics can be used to diagnose and differentiate TBI patients; TBI patients show a shift away from balanced small-world structure; We reveal a pattern of change to be used to guide hypothesis-driven research.

Key words: Traumatic Brain Injury; graph theory; graph metrics; structural connectomics; network analysis; diffusion MRI; biomarkers; meta-analysis; systematic search; narrative review.

2.1.2 Abstract

Although recent structural connectivity studies of traumatic brain injury (TBI) have used graph theory to evaluate alterations in global integration and functional segregation, pooled analysis is needed to examine the robust patterns of change in graph metrics across studies. Following a systematic search, 15 studies met the inclusion criteria for review. Of these, ten studies were included in a random-effects meta-analysis of global graph metrics, and subgroup analyses examined the confounding effects of severity and time since injury. The meta-analysis revealed significantly higher values of normalised clustering coefficient ($g=1.445$, $CI=[0.512, 2.378]$, $p=0.002$) and longer characteristic path length ($g=0.514$, $CI=[0.190, 0.838]$, $p=0.002$) in TBI patients compared with healthy controls. Our findings suggest that the TBI structural network has shifted away from the balanced small-world network towards a regular lattice. Therefore, these graph metrics may be useful markers of neurocognitive dysfunction in TBI. We conclude that the pattern of change revealed by our analysis should be used to guide hypothesis-driven research into the role of graph metrics as diagnostic and prognostic biomarkers.

2.1.3 Introduction

Traumatic Brain Injury (TBI) is one of the leading causes of death and disability in young people, affecting 10 million people worldwide every year (Humphreys et al., 2013; Hyder et al., 2007). The severity of a brain injury is typically described as mild, moderate, or severe, based on time spent unconscious and/or coma rating score, the duration of post-traumatic amnesia, and neuroimaging results. Cognitive deficits (e.g., slow processing speed and poor concentration), motor control deficits (e.g., poor manual dexterity, balance deficits), and behavioural problems (e.g., impulsivity) are particularly common (Rabinowitz & Levin, 2014; Rossi & Sullivan, 1996). Approximately 15-30% of mild TBI cases (Shenton et al., 2012) and up to 65% of moderate-severe cases (Rabinowitz & Levin, 2014; Selassie et al., 2008) report long-term problems. These persistent deficits cause disability and interfere with a patient's ability to perform day-to-day tasks, for example getting dressed, planning ahead, and preparing food (Rabinowitz & Levin, 2014). Isolating neurological biomarkers holds promise as a means to identify which patients are at risk of long-term disability, which has implications for patient management and development of economically sustainable treatment options.

There is mounting evidence supporting diffusion MRI as a sensitive diagnostic tool in the care of patients with TBI (for reviews, see Delouche et al., 2016; Hulkower et al., 2013; Hutchinson et al., 2018; Xiong et al., 2014). First, changes in white matter organisation following TBI have been demonstrated in several important fibre bundles of the brain (Bendlin et al., 2008), including the superior longitudinal fasciculus (e.g., Farbota et al., 2012; Spitz, Maller, et al., 2013) and the corpus callosum (e.g., Levin et al., 2008; Mayer et al., 2010; Rutgers et al., 2008). For example, in a meta-analysis of 13 diffusion studies of TBI, significant increases in

fractional anisotropy (FA) and decreases in mean diffusivity (MD) were found in the posterior parts of the corpus callosum (Aoki & Inokuchi, 2016).

Second, decreased white matter organization has been shown to predict poorer outcome in chronic TBI patients of all severity types (Kinnunen et al., 2011; Kraus et al., 2007), and in acute mild TBI patients with persistent symptoms (Niogi et al., 2008). Lower FA in the subregions of the corpus callosum has been associated with poorer bimanual coordination (Caeyenberghs, Leemans, Coxon, et al., 2011) and slower processing speed (e.g., Levin et al., 2008; Wilde et al., 2006) in moderate-severe TBI patients. Similarly, lower FA in the cerebellum has been associated with poorer manual dexterity (Caeyenberghs, Leemans, Geurts, et al., 2011). Despite multiple reports of altered diffusion metrics, the regional analyses reported in these studies cannot identify how whole brain networks are affected by white matter damage following TBI.

Because TBI may be considered a ‘disconnection syndrome’, where symptoms are accounted for by altered connectivity between regions of the brain, it is important to take global network disruption into account (Catani & Ffytche, 2005; Griffa et al., 2013). Where traditional diffusion approaches such as those outlined above examine isolated brain regions, graph theoretical analysis (GTA) can characterise the global structure of the brain network (or ‘connectome’; Bullmore & Bassett, 2011; Hagmann et al., 2008; Sporns, 2013). Structural GTA represents the brain as a set of ‘edges’ (white matter pathways) that pass between ‘nodes’ (brain regions), using the reconstruction of white matter tracts as weights. This graph is then used to calculate *graph metrics*, which estimate network properties such as global integration and functional segregation (see Supplementary Material 1 for definitions, interpretations, and calculations for the graph metrics included in this review).

Connectome analyses have rapidly found applications in the clinical neurosciences because the balance between integration and segregation necessary to support complex function may be affected by disease or injury. In their seminal review, Griffa et al. (2013) propose that graph metrics show promise as biomarkers in neurodevelopmental disorders such as ADHD (e.g., Cao et al., 2013), neurodegenerative diseases like Alzheimer's disease (e.g., Lo et al., 2010), and psychiatric disorders such as schizophrenia (e.g., Fornito et al., 2012). In one of the first structural GTA studies of TBI, Caeyenberghs, Leemans, De Decker, et al. (2012) have revealed that young TBI patients have decreased connectivity degree within the brain, which correlated significantly with poor balance. Similarly, Kim et al. (2014a) found that longer path length in adults with moderate-severe TBI correlated with poorer higher-order cognitive processes like executive function and verbal learning. Since then, more research has suggested that graph metrics could be 'biomarkers' of TBI (e.g., Hellyer et al., 2015; Yuan et al., 2015; Yuan, Wade, et al., 2017).

With recent growth in the use of structural GTA in all types of TBI, there is a need to conduct a meta-analytical review to probe consistent patterns of change in graph metrics to see which hold promise as biomarkers. In the study presented here, we conduct a narrative review of diffusion MRI papers comparing healthy controls (HCs) using GTA, and the first meta-analysis to date of graph metrics in TBI. Heterogeneity in patient samples is addressed using subgroup analyses. This divides up an already small body of research, and as such the results are for hypothesis generation only. It was also our aim to draw inferences from this data about how graph metrics might be used as biomarkers in TBI, and to provide a framework for hypotheses in future GTA studies.

2.1.4 Method

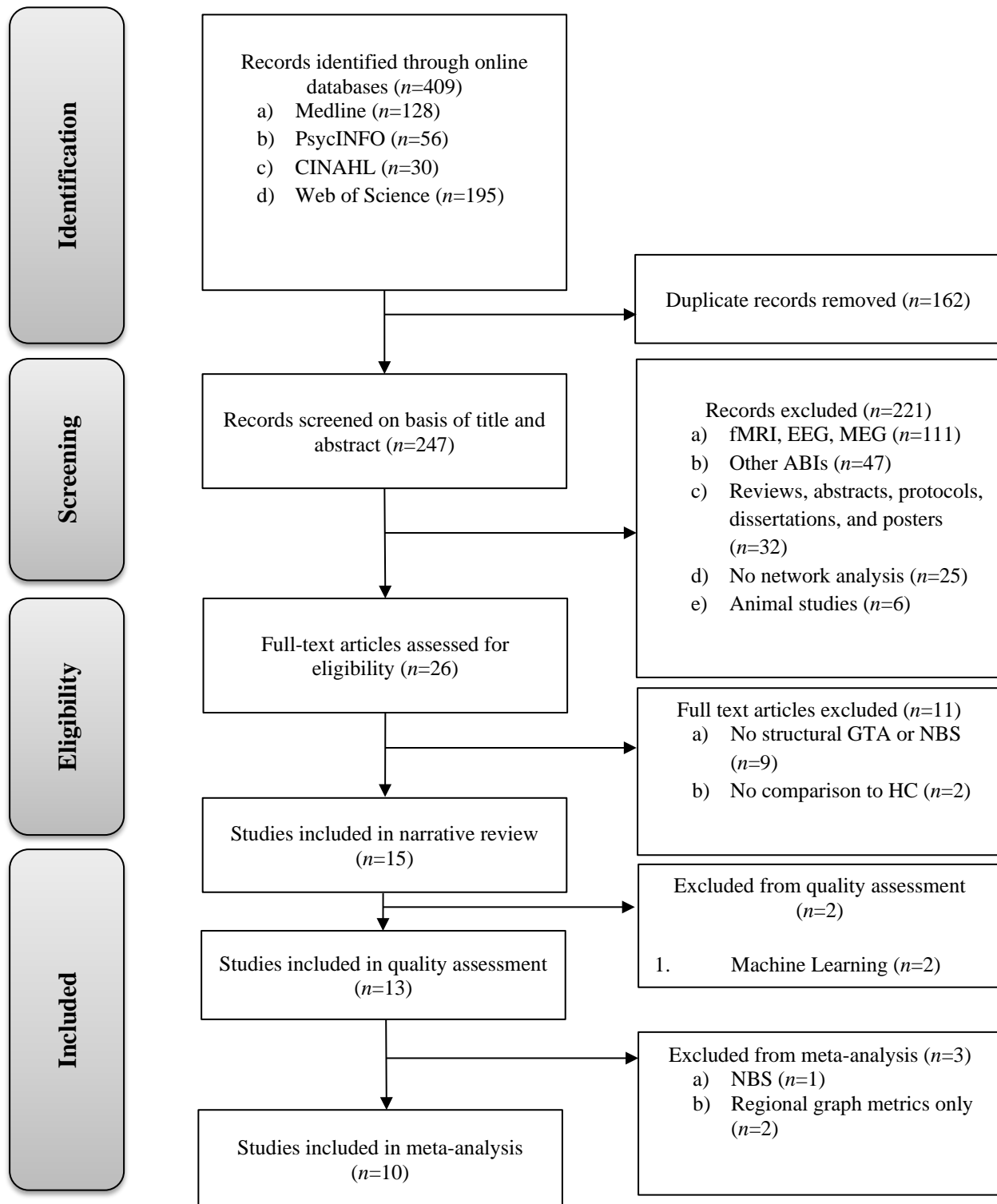
2.1.4.1 Search and Selection Strategy

A systematic literature search was conducted using Medline, CINAHL, PsycINFO, and Web of Science for all relevant articles published from 1999 until the last search date (4th of April 2018; see Figure 1 for PRISMA diagram). The search terms were [((TI OR AB) “traumatic brain injur*” OR TBI)) AND ((TI OR AB) connectom* OR “structural connect*” OR “graph theor*” OR “graph metric*” OR “graph analys*” OR “network analys*”)] (see Supplementary Material 2 for Mesh headings).

Abstracts and titles of 247 unique papers were returned from this search. The reference lists of review papers were searched for additional studies (but none were found). After screening titles and abstracts, we excluded studies of functional MRI, electro-encephalography (EEG) or magnetoencephalography (MEG), animal models of TBI, and other causes of acquired brain injury (such as brain tumours or stroke). Also excluded were studies that did not employ a network analysis (for example, tract-based comparisons of FA), any publications that were not peer-reviewed (e.g., conference abstracts), and review papers.

Figure 1.

PRISMA flow diagram of the systematic literature search



The remaining 26 articles were examined in full to assess eligibility. Studies that did not compare the structural connectomes between TBI patients and HCs, or that did not calculate graph metrics or run network-based statistics (NBS) were excluded, leaving 15 studies for inclusion in the narrative review. Of these, ten studies were included in the meta-analysis, addressing *global* graph metrics that directly compared the structural connectomes of TBI patients and HCs. The five studies not included in the meta-analysis were Fagerholm et al. (2015) and Mitra et al. (2016), both of which applied machine learning techniques; Dall'Acqua et al. (2016) which employed Network Based Statistics (NBS) for the group comparisons; and finally Solmaz et al. (2017) and Caeyenberghs et al. (2013), who only investigated group differences in *regional* graph metrics.

2.1.4.2 Quality Assessment

Two authors (PI, AC) assessed the methodological quality of each study independently, using a quality checklist for diffusion MRI studies adapted from Strakowski et al. (2000). This checklist has been used to measure methodological quality of papers in previous meta-analyses on schizophrenia (e.g., Baiano et al., 2007; Shepherd et al., 2012), major depressive disorder (e.g., Jiang et al., 2017), and bipolar disorder (Strakowski et al., 2000). As shown in Supplementary Material 3, the checklist included three categories: (i) subjects (items 1-4); (ii) image acquisition methodology and analysis (items 5-10); and (iii) results and conclusions (items 11-13). For each item, scores of 1, 0.5, and 0 were assigned (1 = criteria fully met; 0.5 = criteria partially met; 0 = not met). Total scores vary from 0 to 13. Currently, there are no established cut-off scores for high- and low-quality studies using this tool, however, it was decided by the research team that any study with less than half the total score would be excluded from the

analysis for poor methodological quality. Disagreements between reviewers were resolved by a third review from the senior author (KC).

2.1.4.3 Data Extraction for Quantitative Synthesis

Global graph metrics estimating global integration (global efficiency, normalised path length, and characteristic path length); functional segregation (normalised clustering coefficient, transitivity, mean local efficiency, modularity); centrality, resilience (betweenness centrality, small-worldness, assortativity); and basic measures (degree, density, and strength) were extracted across studies (see Supplementary Material 1 for comprehensive definitions of these graph metrics). To calculate effect sizes, means and standard deviations were extracted from published articles, supplementary materials, or via email correspondence with the authors (Caeyenberghs et al., 2014; Kim et al., 2014a; van der Horn et al., 2017). In one study, *p*-values and *t*-scores were used to estimate the effect size (Hellyer et al., 2015). For longitudinal GTA studies (Yuan, Treble-Barna, et al., 2017; Yuan, Wade, et al., 2017), only the baseline (‘pre-training’) comparisons between TBI and HCs were included. Two papers reported TBI connectivity data in separate subgroups, one according to severity level (Königs et al., 2017), and the other by post-traumatic complaints (van der Horn et al., 2017). The latter provided pooled data for the purpose of the overall synthesis via email. For Königs et al. (2017) the averages across the TBI group were pooled for the global synthesis in Microsoft Excel (using calculations included in Supplementary Material 4). Graph metrics that were calculated at the local or nodal level were excluded (i.e., local efficiency, eigenvector centrality, and betweenness centrality of singular nodes not averaged across the network) to constrain the scope of the analysis to network-level dysfunction.

2.1.4.4 Data Analysis for Quantitative Synthesis

Hedge's g , the standardised mean difference score between groups, was calculated for *each* outcome variable (i.e., graph metric) using the Comprehensive Meta-Analysis software, and analysed using a random-effects model (CMA; Biostat, USA, v2.2.064). In basic terms, a separate meta-analysis for each graph metric was run, as each metric should be treated as a separate outcome measure. To calculate the overall effect sizes, mean effects of each metric were pooled across studies and weighted by sample size and the 95% confidence intervals (CI). A positive effect size indicated that the TBI group had a higher mean value of the graph metric compared with the HC group, while a negative value indicated higher mean values in the HC group. Effect sizes were regarded as small if $g \geq 0.2$, medium if $g \geq 0.5$ and large if $g \geq 0.8$ (Cohen, 1988). Also, subgroup analyses on graph metrics were conducted for injury severity (mild, moderate-severe), chronicity (time since injury) (acute: <6 months post injury; chronic: >6 months post injury), and age at injury (paediatric: <18 years old; adult: 18-65 years old). The results of our meta-analysis should be considered as hypothesis generation only, as suggested by the Cochrane guidelines when the number of studies in the analysis is low (Sambunjak et al., 2017).

The I^2 statistic was used to index heterogeneity in the data, i.e., the percentage of observed variability that is greater than what would be expected by chance or sampling error alone. High scores ($I^2 > 75\%$) suggest heterogeneity due to differences in sample demographics (Higgins et al., 2003). Low I^2 scores ($I^2 < 50\%$) represent homogenous data, supporting a real effect between HC and TBI groups. Publication bias was assessed using Egger's test for asymmetry in a funnel plot (Egger et al., 1997).

Finally, *false discovery rate* (FDR) correction ($p < 0.002$) was conducted for all analyses in accordance with recommendations by Wang and Ware (2013). Interdependencies between outcomes were accounted for using the Benjamini-Yekutieli procedure on the Bioinformatics toolbox in MATLAB_R2018a (Benjamini & Yekutieli, 2001).

2.1.5 Results

2.1.5.1 Sample characteristics

The TBI patient pool included 429 participants, and the HC pool 306, with an age range of 8 – 65 years old. Four studies included mTBI patients only, six studies included moderate-severe TBI patients only, and two studies included both severity types (see Table 1). Chronicity varied widely between studies, with TBI groups ranging from acute (e.g., within 96 hours post injury; Yuan et al., 2015) to chronic (e.g., 5.91 years post injury, ± 3.1 years; Yuan, Treble-Barna, et al., 2017). Six studies recruited paediatric TBI patients, two studies included both children and young adults, and four studies recruited adult TBI patients.

Table 1

Demographics and Processing Methods for Graph Theoretical Studies of Traumatic Brain Injury

	PARTICIPANTS			DATA ACQUISITION			PROCESSING PIPELINE						
	Sample size (TBI) (HC)	Age range at scan (years) or <i>M(SD)</i>	Ave age at injury (years)	Severity	Time ^a since injury	Number of directions	b-value	Parcellation Scheme	Areas Removed	Number of ROIs	Orientation model	Tractography ^d	Weighted By ^c
Caeyenberghs et al., 2012	12(17)	8 - 20	10.5	Moderate-severe	42 (31.2)	45	800 (1 b0)	Automated Anatomical Labelling	-	116	Principle eigenvector	DT	SD
Caeyenberghs et al., 2013	17(16)	16 - 34	21.2	Moderate-severe	51 (29)	64	1000 (1 b0)	Switching Network	-	22	Principle eigenvector	DT	NOS FA
Caeyenberghs et al., 2014	21(17)	9 - 29	21.3	Moderate-severe	51 (29)	64	1000 (1 b0)	Automated Anatomical Labelling	-	116	Principle eigenvector	DT	%
Dall'Acqua et al., 2016	51(53)	18 - 61	34.5	Mild	0.2	64	1000 (1 b0)	Automated Anatomical Labelling	Cerebellar regions	90	Principle eigenvector	DT	NOS
Hellyer et al., 2015	63(26)	37.4 (12.4)	31.9	All ^b	5.5 (3.3)	64	1000 (4 b0)	Destreux (Freesurfer)	-	164	Principle eigenvector	PT	FA
Kim et al., 2014	22(18)	17 - 57	26.0	Moderate-severe	40.9 (75.6)	30	1000 (1 b0)	Desikan (Freesurfer)	Cerebellar regions	95	Principle eigenvector	PT	SCP
Königs et al., 2017	36(27)	8 - 14	7.3	All	33.6 (13.2)	30	750 (5 b0)	Automated Anatomical Labelling and FIRST	Cerebellar regions	84	Principle eigenvector	PT	SLD FA
Solmaz et al., 2017	40(35)	18 - 64	NA	Moderate-severe	3.45 (0.6)	30	1000 (7 b0)	Desikan (Freesurfer)	-	86	Principle eigenvector	PT	NOS
van der Horn et al., 2016	53(20)	18 - 65	33.4	Mild	1 (NA)	60	1000 (7 b0)	Desikan-Killianey and subcortical	Cerebellar and ventricle regions	85	CSD	PT	NOS
Verhelst et al., 2018	17(17)	11 - 17	13.4	Moderate-severe	28.3 (13)	64	1200 (1 b0)	Individual parcellation (Freesurfer)	Not known	82	CSD	PT (ACT)	NOS
Yuan et al., 2015	23(20)	11 - 16	13.7	Mild	0.1 (NA)	61	1000 (1 b0)	Automated Anatomical Labelling	Cerebellar regions	90	Principle eigenvector	DT	NOS
Yuan, Treble-Barna et al., 2017	17(11)	9 - 18	7.8	Moderate-severe	70.9 (37.2)	61	1000 (1 b0)	Automated Anatomical Labelling	Cerebellar regions	90	Principle eigenvector	DT	NOS
Yuan, Wade et al., 2017	22(20)	15.45 (1.72)	15.3	Mild	1 - 4	61	1000 (7 b0)	Automated Anatomical Labelling	Cerebellar regions	90	Principle eigenvector	DT	NOS

Note: ^a Time is from the injury/onset until MRI scan for TBI patients, described in months; M(SD)). NA = Not Applicable.

^b 55 of the 63 TBI patients were moderate-severe, and as such Hellyer et al. (2015) was included in the moderate-severe subgroup analyses.

^c NOS = number of streamlines; FA = fractional anisotropy; % = percentage of all streamlines that pass through the node; SD = streamline density (number of fibre connections per unit surface); SLD = the probability of a tract connecting two ROIs; SCP = scaled conditional probability (the number of streamlines from node i to node j, divided by the number of streamlines seeded in node i, scaled by the surface area of the ROI i).

^d CSD = constrained spherical deconvolution; DT = deterministic tractography; PT = probabilistic tractography; ACT = anatomically constrained probabilistic tractography

2.1.5.2 Quality Assessment

Table 2 summarises the quality of the 13 papers according to the diffusion MRI checklist categories, ranked according to overall score (maximum score 13). Most papers scored full points for describing parameters of the diffusion scanning sequences. Points were often deducted for poor description of graph metric calculations and failing to correct for multiple comparisons. The ‘subjects’ category of the checklist had the highest average score (3.6/4, 90.5%), followed by ‘methodology’ (5.4/6, 89.7%), and ‘results/conclusions’ (2.5/3, 83.3%). Overall, the total quality score was high, and varied from 9 to 12.5 points out of a possible 13 (average score: 11.5/13, 88.5%). The study of Verhelst et al. (2018) had the highest methodological quality. There was no significant effect of publication bias (Egger’s regression intercept=1.81, CI: [-1.94, 5.57], $p=0.34$), and all studies met the benchmark for inclusion in the meta-analysis, showing that the published studies are a good representation of available evidence.

Table 2

Quality Assessment Results for Graph Theoretical Studies of Traumatic Brain Injury

	SUBJECTS				METHODOLOGY								RESULTS/CONCLUSIONS				FINAL SCORE
	T1	T2	T3	T4	Overall (/4)	T5	T6	T7	T8	T9	T10	Overall (/6)	T11	T12	T13	Overall (/3)	
Verhelst et al. (2018)	1	1	1	1	4	1	1	1	0.5	1	1	5.5	1	1	1	3	12.5/13
Caeyenberghs et al. (2012)	1	1	1	0.5	3.5	1	1	1	1	1	0.5	5.5	1	1	1	3	12/13
Dall'Acqua et al. (2016)	1	1	1	1	4	1	0.5	0.5	1	1	1	5	1	1	1	3	12/13
van der Horn et al. (2017)	1	1	1	0.5	3.5	1	1	1	0.5	1	1	5.5	1	1	1	3	12/13
Yuan et al. (2015)	1	1	1	1	4	1	1	1	0.5	0.5	1	5	1	1	1	3	12/13
Caeyenberghs et al. (2013)	1	1	1	1	4	1	1	1	1	1	0.5	5.5	0	1	1	2	11.5/13
Caeyenberghs et al. (2014)	1	1	1	0.5	3.5	1	1	1	1	1	0.5	5.5	1	0.5	1	2.5	11.5/13
Konings et al. (2017)	1	1	1	1	3.5	1	1	1	0.5	1	1	5.5	0	1	1	2	11.5/13
Solmaz et al. (2017)	1	0.5	0.5	1	3	1	1	1	1	1	1	6	1	1	1	2.5	11.5/13
Yuan et al. (2017a)	1	1	1	1	3.5	1	1	1	0.5	1	0.5	5	0.5	1	1	2.5	11.5/13
Hellyer et al. (2015)	1	1	0.5	1	3.5	1	1	1	1	1	1	6	0	0.5	1	2.5	11/13
Kim et al. (2014)	1	1	0.5	1	3.5	1	1	1	0.5	1	1	5.5	0	1	1	2	11/13
Yuan et al. (2017b)	1	1	0.5	0.5	3	1	1	1	0.5	0.5	0.5	4.5	0	1	0.5	1.5	9/13

Note: * Fagerholm et al. (2015) and Mitra et al. (2016) were excluded from the quality assessment due to incompatibility with the questionnaire (machine learning experiments).

2.1.5.3 Meta-Analysis

Table 3 summarises the differences in global graph metrics between TBI and HC cohorts across studies. For each graph metric, the direction of significant group differences between TBI and HCs was the same across studies, with the exception of small-worldness and normalised path length. The overall effect sizes for normalised clustering coefficient, global efficiency, density, and characteristic path length were found to be significant ($p < 0.05$), with moderate to large Hedge's g effect sizes ($g > 0.5$) (see Figure 2, and Supplementary Material 5 for statistics). However, only normalised clustering coefficient and characteristic path length remained significant following FDR correction ($p < 0.002$). The subgroup analyses revealed longer normalised path length in acute/mild patients; higher small-worldness in chronic patients; higher small-worldness in paediatric TBI patients; and higher normalised clustering coefficient in paediatric TBI patients compared to HCs (FDR corrected, $p < 0.001$, see Table 4). In the next paragraphs, we will present the results of key overall effects and subgroup analyses for each graph metric that was significant after FDR correction.

Table 3

Graph Metrics in Patients with Traumatic Brain Injury compared to Healthy Controls

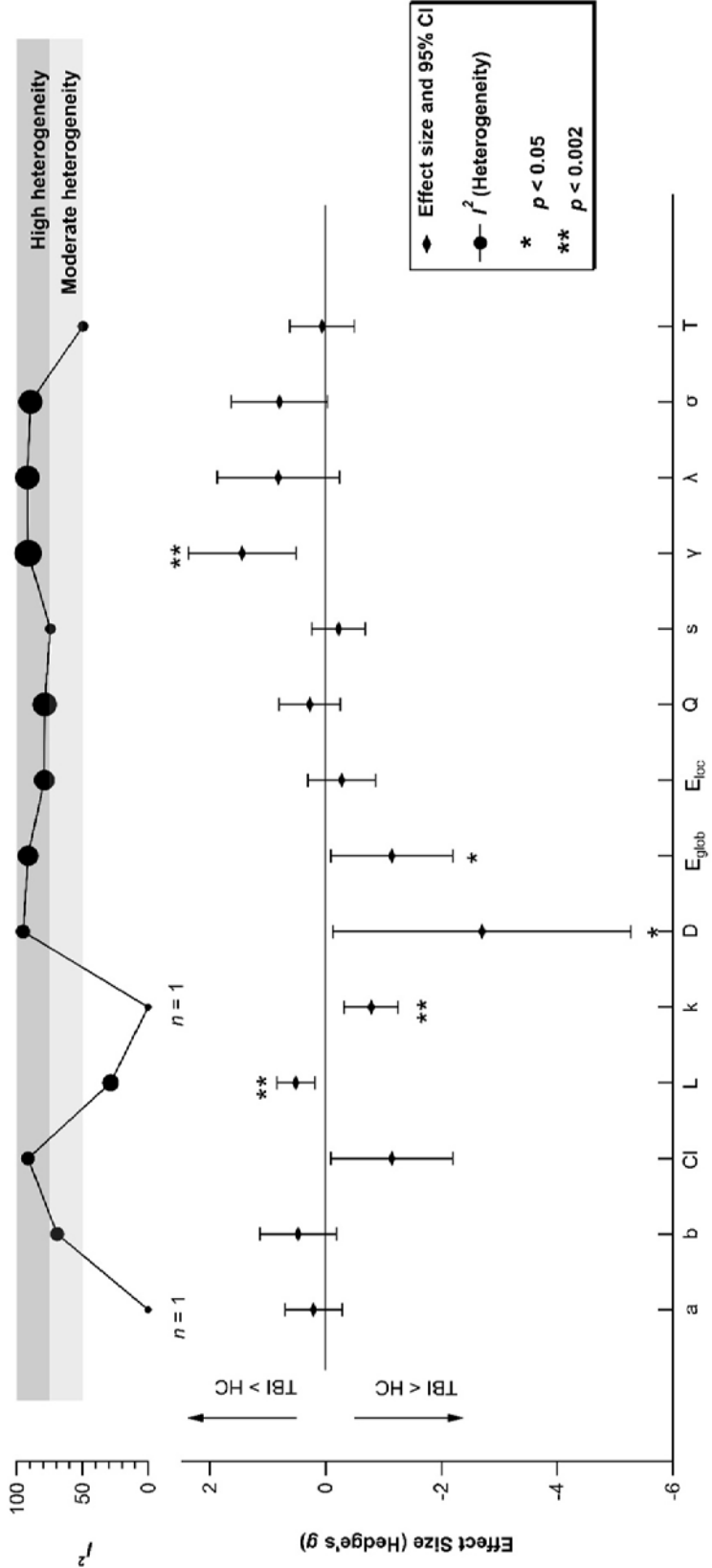
GRAPH METRICS																
	Segregation					Integration					Centrality/ General measures					
	Cl	γ	Q	E_{loc}	T	a	E_{glob}	L	λ	b	σ	k	D	s		
Caeyenberghs et al., 2012	•	↑	•	↓	•	•	•	•	↓	↑	↑	•	↓	•		
Caeyenberghs et al., 2014	-	-	•	•	•	•	↓	↑	-	•	-	•	•	-		
Hellyer et al., 2015	↓	•	•	•	•	•	•	↑	•	•	↓	↓	•	•		
Kim et al., 2014	•	•	-	•	-	•	•	↑	•	•	•	•	-	•		
Königs et al., 2017	•	•	-	•	-	-	•	-	•	•	•	•	•	•		
van der Horn et al., 2016	-	-	-	-	•	•	-	•	•	-	•	•	•	•		
Verhelst et al., 2018	•	↑	•	•	•	•	•	•	↑	•	•	•	↓	-		
Yuan et al., 2015	•	↑	↑	-	•	•	↓	•	↑	-	↑	•	•	•		
Yuan, Treble-Barna et al., 2017	•	-	-	-	•	•	-	•	-	•	↑	•	•	•		
Yuan, Wade et al., 2017	•	↑	-	-	•	•	↓	•	↑	•	↑	•	•	•		
	3	7	6	5	2	1	5	4	6	3	6	1	3	2		

Note: ↑/ ↓ higher/lower respectively in TBI patients than in HCs; - no significant difference between TBI and HC; • this metric wasn't measured
* the total number of times this metric was measured.

Cl	γ	Q	E_{loc}	T	a	E_{glob}	L	λ	b	σ	D	k	s
Clustering coefficient	Normalised clustering coefficient	Modularity	Local efficiency	Transitivity	Assortativity	Global efficiency	Characteristic path length	Normalised characteristic path length	Betweenness Centrality	Small-worldness	Density	Degree	Strength

Figure 2

Inverted Forest Plot of the Overall Effect Sizes for Each Graph Metric



Note: Inverted forest plot of the overall effect sizes and 95% confidence intervals for each graph metric, including heterogeneity values (I^2). The size of the markers on the I^2 graph represent the number of studies in each pooled analysis (range: $n=1$ to $n=7$), with larger circles indicating a larger n .

Table 4

Results of the Subgroup Analysis

OUTCOME	SUBGROUP	VARIABLE	N	HEDGES G	LOWER LIMIT	UPPER LIMIT	Z-VALUE	P-VALUE	I-SQUARED (%)
Global Efficiency (E_{glob})	Chronicity/Severity	Acute/mild	3	-1.610	-3.402	0.181	-1.762	0.078	95.109
		Chronic/modsev	2	-0.485	-1.408	0.437	-1.031	0.302	71.268
	Age at injury	Adult	2	-0.446	-1.368	0.475	-0.949	0.343	79.580
		Pediatric	3	-1.625	-3.298	0.047	-1.905	0.057	92.912
Local Efficiency (E_{loc})	Chronicity/Severity	Acute/mild	3	0.031	-0.292	0.354	0.188	0.851	0.000
		Chronic/modsev	2	-0.677	-2.067	0.713	-0.995	0.340	89.863
Modularity (Q)	Chronicity	Acute/mild	3	0.602	-0.479	1.683	1.091	0.275	89.877
		Chronic/modsev/both	3	-0.038	-0.379	0.302	-0.221	0.825	0.000
	Age at injury	Adult	2	-0.233	-0.625	0.159	-1.163	0.245	0.000
		Pediatric	4	0.532	-0.182	1.247	1.460	0.144	81.165
Normalised Clustering Coefficient (γ)	Chronicity/Severity	Acute/mild	3	0.915	-0.379	2.209	1.386	0.166	92.389
		Chronic/modsev	4	1.924	0.382	3.465	2.446	0.014	92.440
	Age at injury	Adult	2	0.150	-0.571	0.871	0.408	0.683	68.072
		Pediatric	5	2.000	0.857	3.143	3.430	0.001	89.822
Normalised Path Length (λ)	Chronicity/Severity	Acute/mild	2	0.965	0.523	1.408	4.274	*<0.001	0.000
		Chronic/modsev	4	0.789	-0.903	2.482	0.914	0.361	94.501
Small Worldness (σ)	Chronicity	Acute	3	0.625	-0.892	2.142	0.808	0.419	94.950
		Chronic	3	0.950	0.402	1.499	3.396	*0.001	39.536
	Severity	Mild	2	1.309	0.203	2.414	2.320	0.020	81.922
		Modsev	4	0.533	-0.491	1.558	1.021	0.307	89.792
	Age at injury	Adult	2	-0.087	-1.358	1.185	-0.133	0.894	90.342
		Pediatric	4	1.246	0.694	1.798	4.423	*<0.001	56.949

significant at $p < .05$ *significant at $p < .001$

2.1.5.4 Global Integration

Four of the ten studies investigated characteristic path length (Caeyenberghs et al., 2014; Hellyer et al., 2015; Kim et al., 2014b; Königs et al., 2017). Of the 142 patients in this analysis, 114 were moderate to severe; 63 acute patients were on average 5.5 months post-injury, while 79 chronic patients were on average 3.5 years post-injury; and 101 were adults (average age: ~26.9 years) and 41 were paediatric (average age: ~10.5 years) at injury. Across this entire cohort, characteristic path length was longer in the TBI patients compared with HCs ($g = 0.514$, $p = 0.002$, $I^2 = 28.601\%$). The heterogeneity value of this graph metric was low, indicating that the dataset was homogenous.

Six studies investigated normalized path length (Caeyenberghs, Leemans, De Decker, et al., 2012; Caeyenberghs et al., 2014; Verhelst et al., 2018; Yuan, Treble-Barna, et al., 2017; Yuan et al., 2015; Yuan, Wade, et al., 2017) with no overall group effect ($g = 0.815$, $p = 0.129$, $I^2 = 92.1\%$). Of the 112 patients in this analysis, 67 were moderate to severe; 45 acute patients were between 96 hours and 4 months post-injury, while 67 chronic patients were on average 4 years post-injury; and 21 were adults (average age: ~21.3 years) and 91 were paediatric (average age: ~12.1 years) at injury. Subgroup analysis revealed that the acute/mild TBI group showed significantly increased normalised path length compared with HCs ($g = 0.965$, $p < 0.001$, $I^2 = 0.0\%$), with a decreased heterogeneity value. The effect size for the chronic/moderate-severe group was not significant.

2.1.5.5 Functional segregation

Seven studies calculated normalized clustering coefficient (Caeyenberghs, Leemans, De Decker, et al., 2012; Caeyenberghs et al., 2014; van der Horn et al., 2017; Verhelst et al., 2018;

Yuan, Treble-Barna, et al., 2017; Yuan et al., 2015; Yuan, Wade, et al., 2017). Of the 165 patients in this analysis, 67 were moderate to severe; 98 acute patients were between 96 hours and 4 months post-injury, while 67 chronic patients were on average 4 years post-injury; and 74 were adults (average age: ~27.4 years) and 91 were paediatric (average age: ~12.1 years) at injury. Normalised clustering coefficient was higher in TBI patients in the overall meta-analysis ($g = 1.445$, $p = 0.002$, $I^2 = 91.484$). In the chronicity and severity subgroup-analysis, the effect remained significant in the chronic/moderate-severe patients only (chronic/moderate-severe: $g = 1.924$, $p = .014$, $I^2 = 92.440\%$). However, this effect retained a high heterogeneity value. Similarly, in the age at injury subgroup analysis, normalised clustering coefficient was significantly higher in the paediatric TBI patients than HCs ($g = 2.00$, $p = 0.001$, $I^2 = 89.82$). This effect was not observed for adult TBI patients. However, grouping by age at injury only lowered the observed heterogeneity in normalised clustering coefficient by ~2%.

2.1.5.6 Small-Worldness

Six studies reported on small-worldness differences between TBI and HCs (Caeyenberghs, Leemans, De Decker, et al., 2012; Caeyenberghs et al., 2014; Hellyer et al., 2015; Yuan, Treble-Barna, et al., 2017; Yuan et al., 2015; Yuan, Wade, et al., 2017), with no significant effect size overall; however, a trend was evident for larger values in TBI patients ($g = 0.794$, $p = 0.06$, $I^2 = 89.736\%$). Of the 158 patients in this analysis, 105 were moderate to severe; 108 acute patients were between 96 hours and 5.5 months post-injury, while 50 chronic patients were on average 4.6 years post-injury; and 84 were adults (average age: ~26.6 years) and 74 were paediatric (average age: ~11.8 years) at injury. Subgroup analysis showed a significant effect size for chronic patients only, with increased small-worldness in chronic TBI patients

compared with HCs ($g = 0.950$, $p = .001$, $I^2 = 39.536\%$). Grouping by chronicity also greatly reduced heterogeneity in the chronic group. Subgroup analysis by severity revealed larger small worldness values for the mild group ($g = 1.309$, $p = .020$, $I^2 = 81.922\%$); however, heterogeneity remained high and did not survive FDR correction. Finally, small-worldness was significantly higher in the paediatric TBI patients (but not adult TBI patients) compared to HCs ($g = 1.25$, $p < 0.001$, $I^2 = 56.949$). Grouping by age at injury reduced the heterogeneity observed in small-worldness, meaning that age at injury could be explaining some of the differences in small-worldness between TBI patients and HCs.

2.1.6 Discussion

Our study is the first meta-analysis to assess the consistency of recent graph theoretical studies of TBI. The overall quality of the papers was high, and all met the benchmark for inclusion in the review. Findings suggest that *normalized clustering coefficient* and *characteristic path length* may be sensitive diagnostic biomarkers to distinguish TBI patients from HCs, with the former particularly high in chronic/moderate-severe and paediatric TBI patients after subgroup analyses. Furthermore, we suggest that values of normalised path length may be increased in acute/mild patients, and small worldness may be higher in chronic and paediatric TBI patients. In the following sections we will examine the use of graph metrics from a critical view. Specifically, we will discuss the following topics: (4.1) evidence that the TBI network is closer to a regular lattice structure than HCs, and (4.2) the use of graph metrics as diagnostic and prognostic biomarkers in longitudinal studies. In (4.3) we will also point out several methodological issues and provide recommendations for the future study of structural

connectomics in TBI. Finally, in (4.4) we will address any limitations of this pooled analysis, including heterogeneity in patient samples and parcellation schemes.

2.1.6.1 Towards a regular network structure in TBI patients

The hypotheses presented in the research papers reflect the exploratory nature of GTA in TBI studies. Clear rationales and *a priori* hypotheses regarding the specific choice of graph metrics (together with the expected direction of effect) were omitted in many of the studies analysed. For example, Yuan, Wade, et al. (2017) ambiguously predicted that metrics would be “*abnormal* at baseline but would *normalise* after training”. Only Yuan et al. (2015) and Königs et al. (2017) justified their choice of each graph metric. While exploratory research is necessary, a clear rationale concerning the selection of graph metrics will advance theoretical reasoning in the field. Furthermore, having *a priori* hypotheses about the expected direction of effect will minimise multiple comparisons, thereby reducing chance findings that inflate the false positive rate. The findings from our meta-analysis, outlined in the following paragraphs, can serve as a guide in the development of hypotheses for the next generation of GTA studies in TBI.

Small-worldness is the ratio of normalised clustering coefficient to normalised path length, and represents the balance between segregation for local specialization and global integration (Watts & Strogatz, 1998). While all studies found that the TBI connectome is still a small-world network, there was evidence of a shift towards a regular lattice structure. Small-worldness values were significantly higher for TBI patients greater than 6 months post injury, and for children with TBI. These results suggest a shift in network structure, which is probably due to a secondary process of neurodegeneration and/or is specific to those patients injured during childhood. However, further research is needed to evaluate the neurobiological

mechanisms underlying increases in small-worldness. Yuan et al. (2015) and Yuan, Treble-Barna, et al. (2017) suggested that higher small-worldness is primarily driven by an increase in local clustering. Still, changes in small-worldness alone do not provide insight into the nature of the group differences. Instead, researchers could focus on more specific metrics that can differentiate between alterations in segregation and integration (Fornito et al., 2013; Papo et al., 2016), including measures of clustering and path length as described next.

In line with the observed shift towards a regular network, our review revealed that *normalised clustering coefficient* was significantly higher in the TBI group compared to HCs. This result indicates that TBI patients have more ‘closed triangles’ in their network graph compared to the controls, denoting greater functional specialisation. We also observed that this effect remained significant in the paediatric group but not the adult group. Yuan et al. (2015) suggested that this finding in paediatric TBI patients reflected an adaptive response to the injury, whereby local connections are increased because they are less vulnerable to damage than long-range connections. However, we argue that this is a costly adaptation, as it would increase the number of steps needed for information to travel between any two regions (Fornito et al., 2016; Sporns, 2011). In fact, our meta-analysis also showed that *characteristic path length* was significantly longer in the TBI population compared to the HCs, meaning there are a greater number of steps between any two nodes on average in the TBI network than in the HC network. Furthermore, the subgroup analysis demonstrated that *normalised path length* in the acute mild TBI group (but not the chronic moderate-severe group) was significantly higher than HCs. However due to the paucity of data available, it was impossible to determine whether this effect was driven by chronicity or severity. Despite the lack of data, our findings support the idea that the TBI network topology departs from the economical random-graph (Sporns, 2011).

2.1.6.2 Use of graph metrics as diagnostic and prognostic biomarkers

The effects described in section 4.1 support the use of normalised clustering coefficient and characteristic path length as *diagnostic biomarkers* to identify group differences between TBI patients and HCs. Graph metrics can also be used to detect the presence or absence of diffuse axonal injuries (DAI) within TBI patients. Two papers included in the review (Fagerholm et al., 2015; Mitra et al., 2016) employed machine learning methods on graph metrics to classify patients. Fagerholm and colleagues were able to classify the presence of DAI in TBI patients with a high accuracy rate of 93.4% and found that betweenness centrality had the highest ‘feature importance’ when differentiating between patients with microbleeds and HCs. Using a similar machine learning technique, Mitra et al. found that connectivity strength could differentiate mild TBI patients with DAI from HCs with an accuracy rate of 68.16%. These are very promising techniques that clearly demonstrate the use of graph metrics as diagnostic biomarkers.

Another important aspect of evaluating a diagnostic biomarker is the association of the metric with behavioural/clinical outcomes, which was done in all studies apart from one (Hellyer et al., 2015). For example, longer characteristic path length correlated with worse performance on verbal learning task as well as executive dysfunction in moderate-severe TBI patients (Kim et al., 2014a). Longer characteristic path length also coincided with lower intelligence scores and shorter working memory span in moderate-severe TBI patients (Königs et al., 2017). Lower normalised clustering coefficient was found to be associated with slower processing speed in mild TBI patients (van der Horn et al., 2017). These significant correlations highlight the potential of normalised clustering coefficient and characteristic path length as biomarkers of behavioural deficits following TBI. However, reminding us of the preliminary nature of this work, several studies did not correct for multiple comparisons when running correlations

between graph metrics and behavioural tests (Kim et al., 2014a; Yuan, Treble-Barna, et al., 2017). While uncorrected thresholds can be useful for exploratory research, correction for multiple comparisons would strengthen the validity of these findings. Finally, comparison between studies is problematic because different outcome measures were used across studies. We recommend the use of a core set of behavioural tests in the future (e.g., Wefel et al., 2011).

Finally, we wanted to explore whether graph metrics can be used as *prognostic* biomarkers to predict treatment response. Longitudinal studies are necessary to investigate which graph metrics change in response to training. Only two GTA studies (by the same group, Yuan, Treble-Barna, et al., 2017; Yuan, Wade, et al., 2017) so far have conducted longitudinal training studies. Yuan, Treble-Barna, et al. (2017) found that normalised clustering-coefficient and small-worldness values decreased following 10 weeks of attention and executive function training in TBI patients but remained the same in the HCs. In an aerobic training study, Yuan, Wade, et al. (2017) found that improved Post-Concussion Symptom Inventory scores following 4 – 16 weeks of training correlated with increased global efficiency and lower normalised path length. However, this study did not investigate the interaction effect between group and time directly. Overall, there is some evidence that network measures can be used as prognostic biomarkers, but further longitudinal analyses are needed to investigate the predictive value of graph metrics.

2.1.6.3 Methodological considerations and further recommendations

As a tentative conclusion, our meta-analysis showed that normalized clustering coefficient and characteristic path length are potential diagnostic biomarkers that may be sensitive to group differences between TBI and controls. However, GTA is a mathematical framework that has only recently been applied in neuroscience (for a critical review, see Fornito

et al., 2013), and the underlying biological mechanism of change (e.g., increase in axon density, diameter, myelination, sprouting of synapses) is so far unknown. Due to inherent limitations in tractography, we do not know yet whether graph metrics directly reflect white matter integrity (e.g., Jones, 2010a). Therefore, it is important to refrain from diagnosing ‘abnormal’ graph metrics, when comparing TBI patients to HCs (e.g., Yuan, Wade, et al., 2017), until we know the biological mechanisms underpinning graph metrics. Validated neuro-psychometric testing could couple structural connectome measures such as graph metrics (and other diffusion-based measures) to multimodal data with known information processing properties. Until then, structural graph metrics represent the necessary but insufficient properties of the network to function (Sporns, 2012). However, we can get a better understanding if we first obtain reliable patterns of brain connectivity.

There are methodological challenges associated with investigating graph metrics in patients with TBI. These include applying appropriate MRI acquisition and preprocessing techniques, connectome construction, and specifying edge weights (see Table 1 for a summary of the methods used in the studies in this review). Future research should (a) utilise advanced diffusion sequences (e.g., multishell, not used by any studies in the review) with accelerated acquisition speed to accommodate for non-compliance due to poor concentration (e.g., multiband/compressive sensing); (b) employ robust estimation approaches for diffusion MRI metrics (e.g., Slicewise OutLier Detection 'SOLID'; Sairanen et al., 2018); and (c) apply a model that can resolve crossing fibre orientations (e.g., constrained spherical deconvolution, only used by two papers in the current review). Furthermore, although connection density has a noticeable impact on graph metrics (van Wijk et al., 2010), only six of the thirteen studies in the quality assessment accounted for differences in network density (as suggested by Bullmore & Bassett,

2011) when comparing structural networks of TBI and HCs (Caeyenberghs, Leemans, De Decker, et al., 2012; Hellyer et al., 2015; Königs et al., 2017; Solmaz et al., 2017; van der Horn et al., 2017; Yuan et al., 2015). Similarly, researchers should consider using multiple edge weighting and parcellation schemes to examine the robustness of data (Qi et al., 2015; Sotiropoulos & Zalesky, 2019), as was done by Caeyenberghs, Leemans, De Decker, et al. (2012), Caeyenberghs et al. (2014), Caeyenberghs et al. (2013), Fagerholm et al. (2015), and Königs et al. (2017). Finally, future studies should employ advanced measures of white matter such as fibre density and cross section (Raffelt et al., 2017) as edge weights, because FA (used by three studies) and number of ‘streamlines’ (used by eight studies) lack the microstructural specificity to fully characterise the integrity of the structural network. In summary, by using more advanced MRI acquisition and pre-processing techniques we can get closer to an understanding of the biological underpinnings of the TBI structural connectome.

2.1.6.4 Limitations of the pooled analysis

Heterogeneity in parcellation schemes

One limitation of combining different graph analyses is that it inevitably requires pooling data obtained with different parcellation schemes. Differences in the way the cortex is parcellated can significantly impact the results of GTA (Zalesky et al., 2010). As shown in Table 1, five different parcellation schemes (e.g., the Desikan atlas from Freesurfer and the Automated Anatomical Labelling atlas) were used across the papers included in the meta-analysis, each with a different number of regions of interest or ‘nodes’ (range: 82-164). Parcellation schemes with higher resolution (i.e., more nodes) will demonstrate gradual increases in normalised path length and reductions in normalised clustering coefficient (Bassett et al., 2011), while measures of

network organisation (e.g., small-worldness) will remain largely the same (Qi et al., 2015). However, because whole brain node templates in this current study were of similar spatial scales, impact on pooled graph metrics should be negligible (Zalesky et al., 2010), and it is therefore likely that this effect is small and does not detract from the overall findings.

Heterogeneity in the TBI samples

Patients with TBI are diverse, and several clinical and demographic factors (such as severity, chronicity, and age at injury) will impact the comparability of patient cohorts across studies. In the present meta-analysis, we attempted to address the issue of heterogeneity in our pooled TBI population by conducting subgroup analyses. However, the heterogeneity values remained above 75% for the majority of the subgroup analyses, indicating that results may still have been driven by differences in sample demographics (Higgins et al., 2003). This is not surprising given the diversity present in the structure of an injured brain, which may include focal lesions, diffuse axonal injury, or both. There were also limited studies that could be included in this review, making some subgroup analyses hard to interpret. For example, there were no studies of moderate-severe TBI patients in the acute phase, or mild TBI patients in the chronic phase that could be included in the normalised path length subgroup analyses (see Table 4). Therefore, it is impossible to determine whether normalised path length was increased in the acute/mild group due to the time since injury, or the severity of the injury. Overall, this meta-analysis allows us to see universal trends that are present in the structural connectome of TBI patients; however more research is needed that span across all TBI subgroups, so that future pooled analyses can better distinguish between all TBI populations.

2.1.6.5 Conclusion

Despite the complexity of applying GTA to the heterogeneous TBI population, our meta-analysis of structural connectivity studies revealed that normalised clustering coefficient and characteristic path length can be regarded as diagnostic biomarkers of TBI. These findings provide an evidentiary framework for future research. The emerging evidence suggests that average path length and clustering is increased in TBI patients, with the overall network more closely resembling a regular lattice. Using graph metrics, we are able to differentiate between TBI population and healthy controls on the one hand, and the presence/absence of DAI on the other hand. Also, there is preliminary evidence that graph metrics predict future response to training. Despite the promising results, the biological mechanisms underlying alterations in graph metrics is unclear. Future research should employ advanced diffusion MRI tools and obtain biologically validated measures of structural connectivity in longitudinal studies.

2.1.7 Supplementary Materials

Supplementary Material 1

Definition of Graph Metrics

GRAPH METRIC	DEFINITION	HIGHER VALUE DENOTES	CALCULATION
BASIC MEASURES			
k Degree	Degree k_i is the number of connections that node i has to its neighbours. Degree can be calculated for weighted or binary networks and can also be measured separately in directed networks as out-degree, or in-degree (number of edges leading out/in from a node, respectively; for these calculations see Rubinov & Sporns, 2010 or Fornito, Zalesky, & Bullmore, 2016).	A high degree means a high level of interaction between node i and the rest of the network. A high number of connections on a particular node will identify that node as a 'hub'.	$k = \sum_{i \in N} A_{i \in N}$ <p>$A_{i \in N}$ = the connection status between i and all other nodes in the network</p>
D Density	Density is an estimate of the 'wiring cost' of the network. It is calculated as the number of existing connections divided by the total number of possible connections within the graph. Sometimes density is also calculated by summing all the edges in individual i 's graph, then averaging this sum across all individuals – perhaps more appropriately termed as the mean number of edges.	Higher density indicates that a greater percentage of all the possible connections have in fact been made between regions of the brain. Interpretation and comparison of density should be done with care, as calculation of density may differ between studies.	$D = \frac{2 E }{ N (N - 1)}$ <p>N = complete set of nodes in the network E = complete set of edges in the network</p>
s Strength	Strength is similar to degree, but for weighted networks. The strength of node i is the sum of the weights of its edges. The average of the edge weights connected to node i are the normalised strength s' . Mean strength can be the average of all	A higher strength indicates a greater average edge weight for each node. The interpretation of this will vary depending on the weighting variable (e.g., fractional anisotropy or number of	$s'_i = \frac{1}{N - 1} \sum_{j \neq i} w_{ij}$ <p>w_{ij} = weight of edges from nodes i to j</p>

		the normalised strength values across each node of the network. Strength can also be measured of direction or undirected networks and calculated separated for positive and negative connections (see Fornito et al., 2016).	streamlines) that was used.	
l_{ij}	Shortest path length	The number of edges or sum of weights of edges on the shortest possible path between any two nodes (i.e., the pathway between node i and node j with the least number of edges).	A higher value indicates a longer shortest path length – which means more connections must be passed through in order to transfer information from node i to node j .	$l_{ij} = \sum_{i \rightarrow j} w_{ij}$
GLOBAL INTEGRATION				
L	Characteristic path length	The average shortest path length between all possible pairs of nodes in a network (Watts & Strogatz, 1998). The harmonic characteristic path length (L') takes into account nodes with no possible path by summing the inverse of l_{ij} so that they equal 0 (Fornito et al, 2016). For weighted and directed calculations see Rubinov & Sporns (2010).	A higher average shortest path length indicates a greater number of steps is required to transmit information between any two regions.	$L = \frac{1}{N(N-1)} \sum_{i \neq j} l_{ij}$ $L' = N(N-1) \left[\sum_{i \neq j} \frac{1}{l_{ij}} \right]^{-1}$
λ	Normalized path length	Characteristic path length of the network, relative to a random network. Small world architecture indicates that path lengths will be similar to a random network, and shorter than a regular lattice.	If $\lambda > 1$ there is longer average path length than a random network, indicating worse global integration. If $\lambda \sim 1$, average path length is similar to that of a random network.	$\lambda = \frac{L}{\langle l_{rand} \rangle}$
E_{glob}	Global efficiency	Average inverse harmonic characteristic path length between all pairs of nodes in the network. The harmonic L' is normally used to calculate E_{glob} rather than L because the brain is thought to work as a massively parallel system, and the harmonic better represents a parallel (compared to a serial)	A higher global efficiency will indicate a greater capacity for efficient integration of information across the network.	$E_{glob} = \frac{1}{L'}$

system (Latora & Marchiori, 2001).

FUNCTIONAL SEGREGATION

CI	Clustering coefficient	<p>The number of existing connections between the neighbours of node i, divided by all the possible connections, calculated for each node individually and averaged across the entire network (Watts & Strogatz, 1998).</p>	<p>Globally, a higher CI means that a greater proportion of connections are made between nodes neighbours, compared to the connections possible, and indicates more clustered connectivity around individual nodes, with all nodes weighted equally.</p>	$Cl = \frac{1}{N} \sum_{i \in N} \frac{2t_i}{k_i(k_i - 1)}$ <p>$t_i = \text{number of closed triangles}$</p>
T	Transitivity	<p>An alternative to CI, which can be biased by inflation from nodes with small degree. Transitivity uses network-wide normalisation that weights nodes depending on their degree, to estimate the probability that any two nodes connected to a third node are also connected to each other (Newman, 2003).</p>	<p>A higher value of T indicates a greater probability that two nodes with a shared neighbour are also connected to each other, i.e., the probability of finding a closed triangle in an entire network.</p>	$T = \frac{\sum_{i \in N} 2t_i}{\sum_{i \in N} k_i(k_i - 1)}$
γ	Normalized clustering coefficient	<p>Clustering coefficient of the network normalized to a random network. Small world architecture indicates that the clustering will be greater than random, comparable to a regular lattice.</p>	<p>Higher local specialization. If $\gamma = 1$, the clustering is similar to that of a random network, and if $\gamma > 1$, the network has greater than random clustering.</p>	$\gamma = \frac{Cl}{\langle Cl_{rand} \rangle}$
E_{loc}	Local efficiency	<p>The local efficiency is the average of the normalised sum of the reciprocal of the shortest path length (e.g., global efficiency), in a local area. The immediate neighbours of node i become a 'subgraph' on which the efficiency is calculated, once i is removed. Mean E_{loc} is taken as the efficiency of each node in the network averaged over the total number of nodes</p>	<p>A higher local efficiency means greater capacity for integration between the immediate neighbours of a given node.</p>	$E_{loc}(i) = \frac{1}{N_{G_i}(N_{G_i} - 1)} \sum_{j, h \in G_i} \frac{1}{l_{jh}}$ <p>$G_i = \text{subgraph of } i\text{'s neighbours}$</p>

(Latora & Marchiori, 2001).			
Q	Modularity	<p>The subdivision of the network in groups of nodes with many connections to nodes within the group and few to nodes outside the group, based on the premise that some nodes preferentially network with one another (Newman, 2004). Modular networks will mostly show small-worldness, in that high within module connectivity results in high clustering, while just a few direct links between modules is sufficient to support short path length (Fornito et al., 2016).</p>	<p>A positive modularity value indicates greater density of connections within modules than expected by chance, a negative value means it lacks modular structure, and a zero-value means there is no difference from the null model.</p> $Q = \frac{1}{2E} \sum_{ij} (A_{ij} - e_{ij}) \delta(m_i, m_j)$ <p>$\delta(m_i, m_j)$ = the indicator of whether nodes i and j belong in the same module (1 if yes, 0 if no)</p>
CENTRALITY AND RESILIENCE			
b	Betweenness centrality	<p>The proportion of shortest paths that pass through node i between its neighboring nodes, calculated for each node and averaged across the network (Freeman, 1978).</p>	<p>A node that lies on many shortest paths in the network is central and important to the network. This can be used as a way to identify hubs. A high network betweenness centrality indicates a high number of nodes that are central to shortest paths.</p> $b_i = \frac{1}{(N-1)(N-2)} \sum_{h \neq i, h \neq j, j \neq i} \frac{\rho_{hj}(i)}{\rho_{hj}}$ <p>$\rho_{hj}(i)$ = the shortest paths from h to j that traverse i</p>
σ	Small-worldness	<p>The capacity of a network for an energy-efficient balance between clustering and short paths, relative to an appropriate random network (e.g., Maslov & Sneppen, 2002). A small world network will have high levels of clustering compared to a random network ($\gamma > 1$), combined with low average path length, similar to that of a random network ($\lambda \sim 1$) (Humphreys & Gurney, 2008).</p>	<p>If $\sigma > 1$, the network is demonstrating small-world properties.</p> $\sigma = \frac{\gamma}{\lambda}$ <p>for γ see normalised clustering coefficient for λ see normalised path length</p>

<i>a</i>	Assortativity	<p>The correlation between the k_i of connected nodes, in other words the tendency for nodes with similar degrees to be connected. Assortativity should not be confused with rich-club analysis – assortativity investigates the tendency for similar degree nodes to be connected, while rich-club analysis measures the density of connection between high degree nodes (Fornito et al., 2016).</p>	<p>A high Pearson correlation for a indicates that high degree nodes tend to be linked to each other and low degree nodes tend to be link with each other – this kind of network is termed an ‘assortative’ network. Low values mean that high degree nodes tend to link with low degree nodes and low degree nodes link with high.</p>	$a = \frac{E^{-1} \sum_i j_i k_i - \left[E^{-1} \sum_i \frac{1}{2} (j_i + k_i) \right]^2}{E^{-1} \sum_i \frac{1}{2} (j_i + k_i) - \left[E^{-1} \sum_i \frac{1}{2} (j_i + k_i) \right]^2}$ <p>j_i and k_i = degrees of nodes linked by i^{th} edge</p>
-----------------	----------------------	--	--	--

Note: Definitions are based on descriptions in Rubinov & Sporns, 2010; Fornito, Zalesky, & Bullmore, 2016. *Node* = brain region; *functional segregation* = functional specialization within densely interconnected groups of brain regions; *global integration* = the capacity of the network to rapidly combine information from distributed brain regions at a global level

Supplementary Material 2.

Mesh Headings:

Medline: [MH “Brain Injuries, Chronic” OR “Brain Injuries”] AND [MH “Connectome”]

PSYCinfo: [DE “Traumatic Brain Injury”] AND [DE “Brain Connectivity”]

CINAHL: [MH ”Brain Injuries”]

Supplementary Material 3.

Imaging Methodology Quality Assessment Checklist (adapted Strakowski et al., 2000)

Category 1: Subjects

1. Patients were evaluated prospectively, specific diagnostic criteria were applied, and demographic data was reported
2. Healthy comparison subjects were evaluated prospectively, psychiatric and medical illnesses were excluded, and demographic data was reported
3. Important variables (e.g., illness duration, severity of illness, injury type, drug status, handedness) were checked either by stratification or statistically
4. Sample size per group > 10, and no significant difference in age and sex existed
- 5.

Category 2: Methods for image acquisition and analysis

6. Magnet strength at least 1.5T.
7. DTI with at least 12 directions was used.
8. The imaging technique used was clearly described and is reproducible
9. Parcellation scheme clearly reported, reproducible, and no brain regions were excluded from the parcellation scheme (e.g., cerebellum)
10. Calculation of edge weights were clearly reported and are reproducible
11. Calculation of graph metrics were clearly described and are reproducible

Category 3: Results and conclusions

12. Corrections for multiple comparisons (if necessary)
13. Statistical parameters for significant and important non-significant differences were provided
14. Conclusions were consistent with the results obtained and the limitations were discussed

TOTAL /13

Supplementary Material 4

Calculations of pooled mean and standard deviation.

$$M_{pooled} = \sqrt{\frac{M_{mild}n_{mild} + M_{modsev}n_{modsev}}{n_{mild} + n_{modsev}}}$$

$$SD_{pooled} = \sqrt{\frac{(n_{mild} - 1)SD_{mild}^2 + (n_{modsev} - 1)SD_{modsev}^2}{n_{mild} + n_{modsev} - 2}}$$

Supplementary Material 5

Overall Effect Sizes for Graph Metrics

Graph Metric	Number of studies	Hedge's g	Lower limit*	Upper limit*	z -value	p -value	I^2 (%)
Assortativity (a)	1 ^a	0.207	-0.287	0.701	0.822	0.411	0
Betweenness Centrality (b)	3	0.475	-0.186	1.136	1.407	0.159	69.317
Clustering Coefficient (Cl)	3	-0.108	-0.556	0.34	-0.473	0.636	53.664
Characteristic Path Length (L)	4	0.514	0.190	0.838	3.109	*0.002	28.601
Degree (k)	1 ^a	-0.790	-1.258	-0.323	-3.313	*0.001	0
Density (D)	3	-2.706	-5.283	-0.128	-2.057	0.04	95.329
Global Efficiency (E_{glob})	5	-1.144	-2.195	-0.094	-2.136	0.033	91.587
Local Efficiency (E_{loc})	5	-0.453	-1.067	0.161	-1.445	0.148	77.961
Modularity (Q)	6	0.272	-0.257	0.801	1.007	0.314	78.876
Strength (s)	2	-0.223	-0.684	0.238	-0.949	0.343	74.466
Normalised Clustering Coefficient (γ)	7	1.445	0.512	2.378	3.034	*0.002	91.484
Normalised Path Length (λ)	6	0.815	-0.238	1.868	1.517	0.129	92.1
Small Worldness (σ)	6	0.794	-0.034	1.623	1.88	0.06	89.736
Transitivity (T)	2	0.059	-0.494	0.613	0.21	0.833	49.738

Note: * Significant at $p < 0.05$; significant at $p < *0.002$ (FDR corrected)

^a Effect sizes with less than 2 studies are not considered in the meta-analysis

Chapter 3: General Methods for Data Collection²

² This chapter provides a detailed account of the data collection protocol for Study 2 and Study 3. Information regarding specific study methods, data processing, and statistical analyses are included separately within each publication.

3.1 Participants

3.1.1 Participants for Study 2 (Monash Biomedical Imaging)

3.1.1.1 Recruitment

This project was approved by the Monash University Human Research Ethics Committee (MUHREC) (Project: #1181, Title: Cognitive Function and Brain Structure, Chief Investigator: Karen Caeyenberghs, Expiry: 27/10/2021) and lodged with the ACU Human Research Ethics Committee (ACU project #2017-222R). Recruitment of healthy adults occurred using flyers and by word of mouth – participants were not offered compensation. Flyers were used (Appendix E) to give interested participants an overview of the study. Effort was taken to ensure variety of background demographics and equality in gender, age, and education level. This was done by recruiting from the general public and targeting under-represented demographics later in the recruitment phase (e.g., older adults, lower education levels). Initial screening occurred via the phone (Appendix F). To be included in the study, participants had to be *(a)* aged between 18 to 65 years; *(b)* generally healthy with no history of head injury; *(c)* right-hand dominant; and *(d)* fluent in English. Exclusion criteria included *(a)* history of psychiatric illness (moderate levels of depression and anxiety not included); *(b)* pregnancy; and *(c)* any contra-indications for MRI as ascertained by the MRI screening and information form (Appendix G). Once recruited, participants were sent an outline of what to expect on the testing day (Appendix H).

3.1.1.2 Consent

A Plain Language Statement was given to each participant prior to testing that described the research project in full (Appendix I). Written informed consent was obtained from each subject prior to testing; consent was also given with regards to incidental and adverse findings (Appendix J). More precisely, participants could choose to be advised of *(a)*

any diagnostic findings (both incidental and adverse); (b) all incidental findings (any finding that may require treatment or have implications for future health); or (c) only those adverse findings that would usually lead directly to treatment. Communication of these findings could either be from their General Practitioner or another doctor, or from a member of the research team (at the participants discretion). Participants were informed that they could withdraw at any time during the experiment.

3.1.2 Participants for Study 3 (Royal Children's Hospital)

3.1.2.1 Recruitment

This project was approved by the St Vincent's Human Research Ethics Committee (SVHREC) (Project: #250/17, Title: The effects of tablet-based home interventions on brain structure, cognitive functioning, motor performance, and daily life participation in patients with Traumatic Brain Injury, Chief Investigator: Karen Caeyenberghs)³. Recruitment of patients with a TBI was conducted in association with Professor Mark Cook and Associate Professor Wendyl D'Souza of the Neurology department at St. Vincent's Hospital in Melbourne. Medical files of patients both past and present were examined to determine if they met the inclusion criteria. Once a patient was deemed to be a potential participant by Prof Cook or A/Prof D'Souza, they were contacted by one of the three principal investigators of the study (Prof Caeyenberghs, Prof Cook, or A/Prof D'Souza). Patients were provided with a letter of invitation to the study (Appendix K), along with the participant information form (Appendix L). Following this, if patients were interested in participating, they were contacted by researchers via phone using a phone script (Appendix M) and screening form (Appendix N). Recruitment also occurred via Dr. Hamed Akhlaghi in the Emergency

³ Recruitment occurred in conjunction with a training study. Only data from the baseline assessment was included in this thesis.

Department of St Vincent's Hospital Melbourne. Patient records from more than 6 months prior were used to source the contact information of TBI patients who fit the inclusion criteria for the study.

To be included in the study, participants were required to meet the following criteria: (a) aged between 18-65 years old; (b) more than 6 months post injury; (c) experienced a moderate-severe TBI (determined by Professor Cook and Associate Professor D'Souza); (d) speak fluent English; (e) ambulant or independently mobile (able to travel to and from the testing location; (f) no previous history of TBI (single TBI); and (g) able to give their own informed consent (i.e., able to describe back to the researcher the procedure of the experiment in their own words, and demonstrate a clear understanding of the true nature and purpose of the study). Professor Cook and Associate Professor D'Souza also gave their own professional opinion on whether or not a patient had the capacity to give informed consent. Participants were excluded if (a) they had a history of psychiatric illness that they take medication for; (b) they were pregnant; or (c) they had any contraindications for the MRI. If the participants were eligible after this process, they were invited to participate in the study at a mutually convenient time. Participants were offered \$50 as compensation for their time.

Recruitment of healthy adults from the general population occurred using flyers and by word of mouth – participants were sent the information letter upon expression of interest via email (Appendix O). Effort was taken to ensure equivalence in gender, age, and education level in comparison to the TBI participants. This was done by targeting recruitment of healthy controls that matched already recruited TBI participants based on age, gender, and education. Screening occurred via the phone (Appendix P). To be included in the study, control participants had to meet criteria for healthy adult functioning, as outlined in section 3.1.1.1. Participants were offered \$50 as compensation for their time.

3.1.2.2 Consent

A participant information letter was given to every participant prior to testing, which described the research project in full. Written informed consent was obtained from each subject prior to testing, and a declaration was signed by the study doctor or senior researcher verifying that the verbal explanation of the project was understood by the participant (TBI patients, Appendix Q; healthy controls, Appendix R). Participants were informed that they could withdraw at any time during the experiment.

3.2 Cognitive and Self-Report Measures

Study 2 and 3 both included computerised tests of cognitive performance; surveys of cognitive complaints, daily-life-participation, and IQ; and structural MRI scans. Measures were identical between the two testing sites, with the exception of the IQ test (only administered for Study 3).

3.2.1 Demographics

Demographic information was acquired via survey (Appendix S), including age, gender, education level, and handedness (Edinburgh Handedness Inventory; Oldfield, 1971).

3.2.2 IQ

The Weschler Abbreviated Scale of Intelligence (WASI-II) (Revised edition; Wechsler, 2011) was administered to TBI patients and healthy controls for Study 3 only. The WASI-II consists of four individually administered assessments of intelligence for participants aged between 6 and 90 years. Two of the four subtests of the WASI-II (vocabulary and matrix reasoning) were used to generate the Full-Scale Intelligence Quotient 2 (FSIQ-2). Higher scores in both subtests indicate higher IQ.

3.2.2.1 Vocabulary

The Vocabulary subtest consists of three picture items and 28 verbal items (or 31 items in total). The picture items are only used if the participant incorrectly describes the first verbal item ('shirt') – then, the participant is asked to name the object that is visually presented to them – otherwise only the verbal items are used. The participant must define words that are presented to them in written form (words are also verbalised out loud by the investigator). Answers are recorded verbatim by the investigator using the WASI-II scoring sheet and scored according to the standardised administration protocol. Correct responses are given a full score of '2'; otherwise, the participant is queried for more information, or given a score of '1' or '0'. Item administration stops if the participant receives three '0' scores in a row, or if they reach the end of the word list.

3.2.2.2 Matrix Reasoning

The Matrix Reasoning subtest requires the participant to view sequence of four patterns with the fifth missing and select the response option that completes the series. The subtest has 30 items that are used to assess fluid intelligence, broad visual intelligence, classification and spatial ability, knowledge of part-whole relationships, simultaneous processing, and perceptual organisation. The participant is shown the series and asked, "Which of these [here] belong [here]". Participants have four responses to choose from. Answers are recorded on the WASI-II scoring sheet. For the Matrix Reasoning task, correct responses are given '1', or '0' for incorrect. Testing ends if three '0's is received in a row or if the participant reaches the end of the test booklet. Combined, scores on the Vocabulary and Matrix Reasoning subtests provide a single measure of IQ.

3.2.3 Subjective Cognitive Ability

3.2.3.1 Neurobehavioural Functioning Inventory

The Neurobehavioural Functioning Inventory (NFI) was used to provide an indication of self-reported daily life cognitive function (Appendix T). The NFI (Kreutzer et al., 1999) contains 76-items that measure the frequency of symptoms that often occur following TBI (Sandberg, 2011) such as confusion, headaches, or forgetfulness. The NFI includes six subscales; depression (e.g., feeling worthless); somatic complaints (e.g., headaches); memory/attention (e.g., forgetting or missing appointments); communication (e.g., difficulty making conversation); aggression (e.g., hitting or pushing others); and motor problems (e.g., dropping things). In TBI patients, factor analysis found that the internal consistency for each individual scale was very high (ICC=0.86 – 0.95), as is that for the total scale (Cronbach's $\alpha = 0.97$). Convergent validity is also very good with each subscale of the NFI correlating significantly with other measures of memory, attention, learning, communication, motor and cognitive functioning, personality, and psychopathology (Kreutzer et al., 1996).

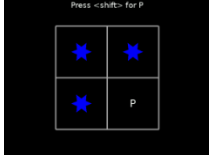
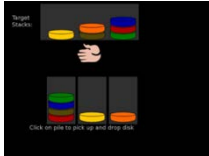
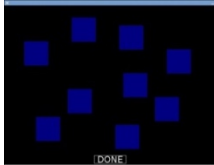
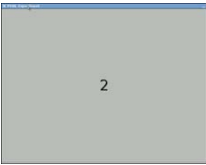

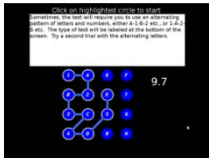

3.2.4 Objective Cognition

3.2.4.1 The Psychological Experiment Building Language

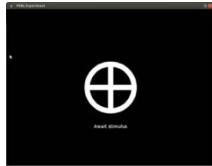
Objective cognitive ability was assessed using the computerised Psychology Experiment Building Language (PEBL) battery (Mueller & Piper, 2014; see Table 1). A Dell Inspiron 15" 3537 laptop (response latency=80ms; refresh rate=60Hz) was used to display and record responses to the PEBL, with the stimulus display synchronised to device refresh rate. A subset of eight tasks were used to measure core domains of cognitive functioning: processing speed, memory, attention, and planning.

Table 1.

Example of PEBL Battery Tasks Assessing Objective Cognition

Name	Task	Cognition	Variables
Go/No-Go 	For the first part of the test, the participant must respond to the letter “P” (Go trials), but not the letter, “R” (No-Go trials) by pressing the ‘shift’ key. There are more P’s than R’s. In the second section of trials, the participant must respond to the letter “R” (Go trials), but not the letter, “P” (No-Go trials). There are less R’s than P’s in this section.	Response inhibition	Number and average reaction time (RT) of correct and incorrect responses, for Go and No-Go trials.
Tower of London 	Participants must match the pattern of stacked discs in as few moves as possible, using the mouse to drag the tiles in the bottom row to match the tiles in the top row. The pattern must be matched on colour, location, and position of the disc within the stack.	Planning	Total number of movements and RT for all trials.
Corsi Blocks 	The participant must reproduce the sequence of blocks after they light up by clicking on the box using a mouse, in the correct order. After two correct trials of a particular length, sequence length increases by one box.	Visuospatial working memory span	Longest sequence correctly remembered
Digit Span 	The task is to reproduce the sequence of numbers heard and seen, in the correct order. The participant hears/sees the sequence, then has as long as they need to type out the sequence using the keyboard. After two correct trials of a particular length, sequence length increases by one digit.	Verbal working memory span	Longest sequence correctly remembered
Letter-Digit Substitution 	Participants are asked to match the letter that appears with its corresponding number, according to the code displayed at the top of the screen, by pressing the corresponding key on the keyboard.	Processing speed	Number of correct responses and RT of correct responses.
Connections 	In the non-switch trials (e.g., 1-2-3; or A-B-C), the participant has 20 seconds to create as large a trail as possible by clicking on letters/digits in sequence using a mouse. In the switch trials, the trials alternate between letters and digits (e.g., A-1-B-2-C-3; or 1-A-2-B-3-C).	Mental flexibility	Mean number of items per sequence (separately for non-switch and switch trials).
Global Local Task 	The participant must respond to either the large (global) or small (local) stimuli, an ‘S’ or ‘H’, as directed, by pressing either the left or right ‘shift’ key (respectively). Stimuli are both congruent (e.g., a large ‘S’ made of small ‘s’s) or incongruent (e.g., a large ‘S’ made of small ‘h’s).	Selective attention and task switching	Number of correct/incorrect stimuli, and RT difference between congruent and

Name	Task	Cognition	Variables
Vigilance	The participant must wait for an X to appear in the circle. A cross appears before each trial, to alert the participant that a response will be required soon. When the X appears in the circle, the participant must respond as fast as possible by pressing the space bar. If the letter is not an X, the participant must withhold a response.	Sustained attention, response inhibition	incongruent trials RT to X trials



3.3 Magnetic Resonance Imaging of the Brain

The imaging protocol for Study 2 and 3 were largely identical. At each site (MBI and RCH) a suite of six scans were acquired – though only the anatomical T₁, diffusion, and FLAIR scans are used in this thesis. The anatomical T₁ and diffusion scans were used to perform the structural connectome analyses, and the FLAIR scans of all healthy participants were used by neurologists at the respective scan sites to check for the presence of hyperintensities and other incidental findings. The T₁ and FLAIR scans of the TBI patients were sent to neurologist Paul Beech (Alfred Hospital Melbourne) for lesion description. Therefore, only these three scans are described in detail. For a full overview of all scans acquired (for use in other projects) see Tables 2 and 3.

3.3.1 MRI for Study 2 (Monash Biomedical Imaging)

Images were acquired on a Siemens 3T SKYRA, 32-channel head coil, whole-body scanner. The entire acquisition time was 53 minutes and 49 seconds (Table 2).

3.3.1.1 Anatomical scan

High resolution 3D T₁-weighted imaging was performed with magnetisation-prepared rapid gradient-echo acquisition (MPRAGE), ADNI protocol with 192 contiguous

slices (A>>P), FOV = 256mm, voxel size = 1.0mm isotropic, TR = 2300ms, TE = 2.07ms, flip angle = 9°, and a total acquisition time of 3:52min.

3.3.1.2 Diffusion Weighted Imaging

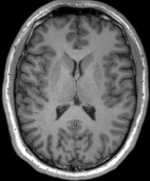
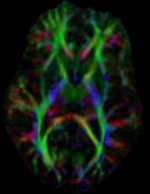
Diffusion MRI (dMRI) was performed using single-shot echo planar with twice-reinforced spin echo and was obtained with 60 contiguous sagittal slices (FOV = 220mm, voxel size = 2.5mm isotropic, TR = 10100ms, TE = 101.0ms. A high angular resolution diffusion imaging (HARDI) gradient scheme was applied in 66 non-collinear gradient directions, b-value of 3000s/mm², and seven interleaved b0 images. A pair of reverse phase encoded b0 images was also collected to correct for geometric distortions (TA = 42 seconds each). Total acquisition time was 13:26mins.

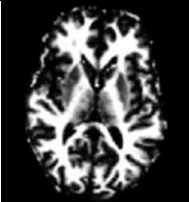
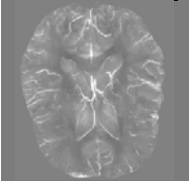
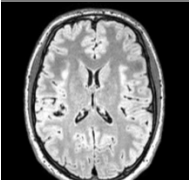
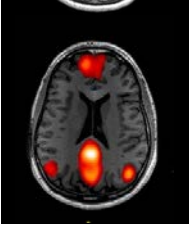
3.3.1.3 FLAIR

3D fluid-attenuated inversion recovery was performed to assess the presence of lesions (192 slices, FOV = 256mm, voxel size = 1mm isotropic, TR = 5000ms, TE = 397ms, TI = 1800 ms, TA = 4:52mins).

Table 2.

Scanning Protocol and Measures from Monash Biomedical Imaging (MBI)

Scan	Measures	Toolbox	Image	Scan Values	Time (min)
<i>3D MPRAGE</i>	Anatomy	Freesurfer/FSL		MPRAGE (ADNI protocol). 1mm isotropic, 192 slices. TR 2300.0ms, TE 2.07ms. FoV 256mm.	03:52
<i>HARDI</i>	Tractography	MRtrix3 ExploreDTI		66 directions, maximum b-value 3000. 2.5mm isotropic, 60 slices. Ten b0 images. Extra LR and RL image for dist. correction. Phase encoding L>>R. TR 10100ms, TE 101.0ms.	13:26

Scan	Measures	Toolbox	Image	Scan Values	Time (min)
<i>mcDESPOT</i>	Myelin Mapping	QUIT		Four subsequences: SSFP phase 0; SSFP phase 180; SPGR; and irSPGR. 8 flip angles.	15:00
<i>QSM</i>	Magnetic Susceptibility	Nipype (python)		4 Echo, monopolar, 0.7x0.7x1.3mm, TR 35.0ms, TE 14.80ms, FoV 256mm.	10:00
<i>T2 FLAIR</i>	Lesion identification	FSL		1mm isotropic, FoV 256mm. TR 5000ms, TE 397.0ms.	4:52
<i>fMRI</i>	Resting state Connectivity	REST/ICA (SPM)		BOLD. 3mm isotropic. FoV 190mm. TR 754ms, TE 21.00ms. Multi-band acceleration factor 3, 42 slices, 400 measurements.	5:16
					Total 53:49

3.3.2 MRI for Study 3 (Royal Children's Hospital)

Images were acquired on a Siemens 3T PRISMA, 32-channel head coil whole-body scanner. The entire acquisition time was 52 min (Table 3).

3.3.2.1 Anatomical scan

High resolution 3D T₁-weighted imaging was performed with magnetisation-prepared rapid gradient-echo acquisition (MPRAGE), ADNI protocol with 208 contiguous slices (A>>P), FOV = 256mm, voxel size = 0.8mm isotropic, TR = 2100ms, TE = 2.22ms, flip angle = 8°, and a total acquisition time of 5:48 min.

3.3.2.2 Diffusion Weighted Imaging

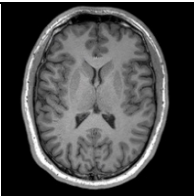
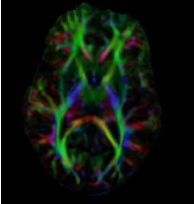
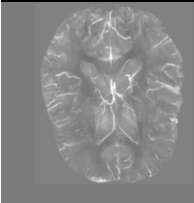
Diffusion weighted imaging was performed using single-shot echo planar with twice-reinforced spin echo, obtained with 70 contiguous transversal slices (FOV = 260mm, voxel size = 2.3mm isotropic, TR = 3500ms, TE = 67.0ms. A high angular resolution diffusion imaging (HARDI) gradient scheme was applied in 66 non-collinear gradient directions, b-value of 3000s/mm², and seven interleaved b0 images. A pair of reverse phase encoded b0 images (BU and BD) were also collected to correct for geometric distortions (TA = 50 s each). Total acquisition time was 6:17 min.

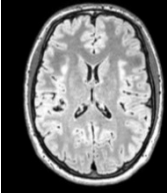
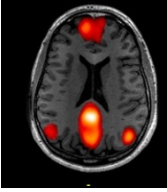
3.3.2.3 FLAIR

3D fluid-attenuated inversion recovery was performed to assess the presence of lesions (176 slices; FOV = 256mm; voxel size = 0.5x0.5x0.9mm; TR = 6000ms; TE = 437ms; TI = 2100ms). Total acquisition time was 7:20 min.

Table 3.

Scanning Protocol from Royal Children's Hospital (RCH)

Scan	Purpose	Toolbox	Image	Scan Values	Time (min)
<i>3D MPAGE</i>	Anatomy	Freesurfer/FSL		MPAGE 0.8mm isotropic, 208 slices, TR 2100.0ms, TE 2.22ms, FoV 256mm.	5:48
<i>HARDI</i>	Tractography	MRtrix3 ExploreDTI		66 directions, maximum b-value 3000, 2.3mm isotropic, 70 slices, 7 b0 images, phase encoding A>>P, TR 3500ms, TE 67ms, reverse encoded images for dist. correction	6:17
<i>QSM</i>	Magnetic Susceptibility	Nipype (python)		3 Echo, monopolar, 1mm isotropic. TR 35.0ms, TE 14.80ms. FoV 256mm. Readout mode bipolar.	8:43

Scan	Purpose	Toolbox	Image	Scan Values	Time (min)
<i>T2 FLAIR</i>	Lesion identification	FSL		0.5x0.5x0.9mm, FoV 256mm, TR 6000ms, TE 437.0ms.	7:20
<i>FWF</i>	Piloting	NA	NA	NA	6:40
<i>Resting state fMRI</i>	Resting state Connectivity	REST/ICA (SPM)		BOLD, 2.5mm isotropic, FoV 250mm, TR 1150ms, TE 37ms, multiband AF 4, 56 slices, X volumes.	7:48
					Total 42:36

3.4 Procedure

The testing session for each participant was three to four hours in total, including surveys, cognitive/motor/IQ testing, and MRI scan. The procedure for Study 2 and 3 was identical, and as such is described here together.

3.4.1 Overview of the Testing Session

The testing session took place in a quiet room with space for the participant and their carer or partner (if necessary for the TBI patients), and one investigator. Upon arrival, participants were given the plain language/explanatory statement and consent form to sign. After this, participants either went to the scanner for their MRI, or completed the surveys and cognitive testing. Effort was taken to ensure the participant's comfort during the testing process to minimise fatigue; for instance, breaks were offered after completion of cognitive testing, IQ testing, and MRI scanning. Participants were allowed to drink coffee or tea or water during the testing process, but food was only consumed during break times. As much or as little break time was given depending on the participants' needs. The length of the

testing session varied between participants, depending on their level of proficiency and length of their break time/s.

3.4.2 Details of the Data Collection Process

Surveys (demographic questionnaire and NFI⁴) were completed using pen and paper with the investigator present to answer any questions or clarify any ambiguities. In total, the surveys took approximately 30 min to complete. IQ (WASI-II⁵) testing took place using pen and paper with the investigator acting as scribe according to protocols described fully in the manual. The Vocabulary test was administered first with participants asked to describe the meaning of a word out loud. For the Matrix Reasoning task, the investigator showed the participant the flipbook of matrices and asked the participant to indicate which of five multiple choice options was correct. The participant gave their response verbally.

3.4.2.1 Computerised cognitive testing

Cognitive testing was completed in the same quiet room, with the investigator present to explain each of the eight computerised tasks to the participant if necessary. The Dell Inspiron 15" laptop was arranged next to a mouse and mousepad in front of the participant, who was seated in an ergonomic chair. The eight-task PEBL test battery was run consecutively, with no gap between tasks. The sequence of tasks is as follows: Go/No-Go, Tower of London, Corsi Blocks, Digit Span, Letter-Digit Substitution, Connections, Global-Local, and Vigilance. Tasks were not randomised but ordered so as minimise fatigue by interspersing longer more effortful tasks with shorter easier ones. Each task began with an instruction screen and a set of practice trials, during which the participant could ask the investigator any questions they might have or take a break if necessary. The duration of the

⁴ also performed were the MASQ, PART-O, and SPRS, though these were not used in this thesis.

⁵ NB: the WASI-II was only delivered at the RCH testing site

cognitive testing was approximately 50 mins. Raw data were stored directly on the Dell laptop once the PEBL was completed.

3.4.2.2 MRI scan

MRI data acquisition occurred variably either before or after the testing, depending on the convenience of the participant. At both sites, the MRI scans took approximately 1 hour and 15 min, including 5-10 min before the scan for the radiographer interview. All subsequent preparations were performed by the radiographer – the investigator remained in the radiographer’s office taking notes on the sequence of events on the Scan Running Sheet (Appendix U). The radiologist first double-checked for contra-indications to the MRI scan by going through the MRI screening form at length with the participant. Next, a fiducial marker was placed on the participant’s right temple. The participant was then positioned comfortably in the scanner using cushions and blankets – this also minimised any movement on the bed. Participants were asked not to move during the scans by reminding them that they would be given allocated times to move their arms and legs (but preferably not their head). Verbal instructions and check-ins were given via the intercom system. A movie was screened for them, if requested, during the structural MRI scans. The sequence of scans remained the same for all participants, with breaks offered between each scan to enhance comfort during the scan. Scans were checked visually by the radiographer and investigator for major movement artefacts and performed again if necessary (and if time allowed). Notes were taken of any movement or change to the scan protocol on the scan running sheet. Following the completion of the MRI scan the participants were extracted from the MRI and left the MRI suite with the investigator.

Once scans were acquired, the FLAIR images were sent to a neuroradiologist to check for abnormalities. In the case of abnormalities, the consent form was checked to indicate

whether they would like to be informed, and then either their general practitioner was contacted, or a senior member of the research team (Prof. Karen Caeyenberghs) contacted the participants.

3.4.3 Confidentiality

Once the pen and paper testing finished, the surveys and IQ testing forms were compiled into a folder labelled with the participants ID (HC##: Healthy Adults at MBI; CMT## or DTC##: TBI patients at RCH; CON##: Healthy Controls at RCH). The only paperwork that contained both the participants' name and their ID was the consent form. This paperwork was organised into folders depending on testing location and participant ID and stored in a locked cabinet at the Mary MacKillop Institute for Health Research, in Prof. Karen Caeyenberghs office.

3.4.4 Data Entry and Security

Raw data from the pen-and-paper surveys and IQ test were entered into a master spreadsheet in Excel (v16.43) which was then saved on a locked hard drive and stored in the same locked cabinet as the paperwork. Variables of interest from the cognitive testing were entered into the master spreadsheet, and all raw data files from the PEBL were backed up onto the same hard drive and removed from the testing computer. The MRI data for Study 2 (MBI) was downloaded directly from the project's DARIS (Nov 2016 – Sep 2017) or XNAT (Sep 2017 – Apr 2018) server and saved onto the same locked hard drive. The MRI data Study 3 was pushed to the DICOM node of Mark Seal, the institute director at the Murdoch Children's Research Institute, who then forwarded the downloadable files to the investigator via secure links using Cloudstor (Feb 2019 – Jan 2020). Also, the data was saved onto a DVD at the time of scanning and transferred onto the hard drive as a back-up while the XNAT data was being transferred. All DVDs were stored in the same locked cupboard as the hard drive

and paperwork. After January 2020 when the Australian Catholic University's XNAT server went live, data was transferred and downloaded directly from the project's XNAT. All data transfers occurred using secure links.

3.4.5 General approach to data analysis

Study 2 and 3 both utilise a graph theoretical analysis (Rubinov & Sporns, 2010) of brain imaging data. The details of these analyses are detailed in the empirical chapters. MRI data were analysed on MASSIVE using freely available image processing tools, including *mrtrix3* (v3.0_rc3; Tournier et al., 2019) *mrtrix3tissue* (v5.2.8; <https://3tissue.github.io>), *Freesurfer* (6.0; <http://surfer.nmr.mgh.harvard.edu/>) (Fischl, 2012), and *FSL* (6.0; Jenkinson et al., 2012). Once processing was performed, brain data was downloaded to Matlab in the form of connectivity matrices for further analysis. Connectome analyses were performed using the Brain Connectivity Toolbox (Rubinov & Sporns, 2010) and in-house built Matlab (R2019b) scripts (see Appendix V). Also, cognitive data (demographics, PEBL, NFI, and IQ) were stored in an Excel spreadsheet before being imported into Matlab for data analysis.

Chapter 4: Study 2 - Navigating the link between processing speed and network communication in the human brain

4.1 Preface

Connectome analyses have recently provided a novel way to understand the mechanisms of information transfer in brain networks (Bassett & Sporns, 2017). In Study 1, it is substantiated that graph metrics are useful for evaluating structural differences between TBI patients and healthy controls (Imms et al., 2019). However, what remains unclear is whether graph metrics have interpretive value as biomarkers of brain injury (Woo et al., 2017). In this regard, it is important to establish whether graph metrics are behaviourally relevant – in other words, do they relate to measures of cognition. Thus, the purpose of Study 2 is to investigate the relationship between graph metrics and cognitive performance in healthy adults.

Rather than investigating the cognitive correlates of all graph metrics, Study 2 focusses on one important sub-group – *communication measures*. The rationale for choosing communication measures was as such: the meta-analysis (Study 1) revealed that characteristic path length showed the most robust alterations in TBI patients. In particular, path length was longer on average in TBI patients than healthy controls in three of the four of studies where it was measured. Characteristic path length also had the lowest heterogeneity value ($I^2 = 28.60\%$), supporting the idea of a real effect between TBI patients and healthy controls. Finally, path length measures were found to correlate with some measures of cognition, such as processing speed and task switching (Caeyenberghs et al., 2014); and executive functioning and verbal learning (Kim et al., 2014a). These findings suggest that the behavioural relevance of communication within the brain network should be further investigated.

In the discussion of Study 1 it was noted that communication measures such as path length and global efficiency are often interpreted in terms of information transfer or

processing speed. This is due to an underlying assumption that the speed of executive processes relies on efficient integration properties of the structural network to facilitate communication within the brain (Bullmore & Sporns, 2012). Several graph theoretical studies outside the TBI literature have revealed that network communication is also related to individual variation in processing speed in older adults (e.g., Wen et al., 2011) and Alzheimer's Disease (e.g., Caeyenberghs et al., 2014; Reijmer, Leemans, Caeyenberghs, et al., 2013). While these early results are promising, advances in connectome reconstruction and cognitive modelling could lend further weight to the link between network communication and information processing speed. These advanced measures of processing speed and network communication should provide more specific estimates of brain structure and cognition and thus improve the strength of the observed relationships.

4.1.1 Advances in measuring processing speed

In the present study, we apply the hierarchical Bayesian drift diffusion model (HDDM; Wiecki et al., 2013) to estimate decision-making time from the overall reaction time for each trial. The drift-diffusion model has been successfully used to investigate processing speed in Autism (Powell et al., 2019), and neurodegenerative disorders (Zhang et al., 2016). By removing the confounding effect of non-decision times, we expect that this measure of processing speed should be more sensitive to individual differences in healthy adults (Voss et al., 2004).

4.1.2 Advances in measuring communication

Most connectome studies have computed communication measures based on shortest path length – including characteristic path length and global efficiency (for an overview of the definition of global integration metrics used in this study, the interested reader is referred to Appendix A). A network with short path lengths is often interpreted as having efficient

information transfer between brain regions (Latora & Marchiori, 2001). Similarly, longer path lengths in brain-injured populations are often interpreted in terms of poorer efficiency of information transfer (see Imms et al., 2019). However, the assumption of information transfer under global integration is problematic because it assumes that every node has a global ‘roadmap’ of the overall network – an assumption which may be biologically implausible. Therefore, Study 2 also investigates a new communication measure, called *navigation efficiency*, which has been shown to be a more plausible way of characterising communication in the human brain network (Seguin et al., 2018).

4.1.3 Advances in connectome reconstruction

It is well-known that diffusion imaging and processing techniques suffer from several limitations and biases, impacting the reliability of global integration findings (Jeurissen et al., 2013; Jones, 2010a). Previous structural connectome studies have used a deterministic tractography approach, which can result in false negatives and do not account for crossing fibres. Constrained Spherical Deconvolution (CSD) is often used to address these concerns, albeit at the expense of accumulating false positives (Thomas et al., 2014). In the present study a state-of-the art diffusion MRI sequence and processing pipeline is used to avoid biases that may result in false pathways. Specifically, we employ (i) single-shell 3 tissue CSD with fibre orientation distributions estimated in the grey matter, white matter, and CSF (to avoid overestimating the volume of white matter in voxels containing both signal types) (Jeurissen et al., 2014), (ii) Anatomically Constrained Tractography (ACT) to accurately determine where streamlines should be generated (Smith et al., 2012), and (iii) an advanced tractogram reconstruction SIFT2 technique to provide a more ‘biologically accurate’ representation of streamline count (Smith et al., 2015a) with the potential for stronger clinical relationships (McColgan et al., 2018).

4.1.4 Summary

In summary, Study 2 examines the relationship between structural brain networks and cognitive processing speed in healthy adults, as a proof of concept that communication measures are a biomarker of slowed processing speed (Aim 2, Research Questions 1 and 2). Innovative measures of network communication and decision-making time are used to improve the specificity of the findings. Processing speed is often chronically impaired in TBI patients (see section 1.1.4); as such, this proof-of-concept study in healthy adults constitutes an important step towards assessing the link between graph metrics and cognitive impairment after brain injury. Furthermore, this chapter provides a detailed description of the state-of-the-art connectome processing pipeline that is also used in Study 3.

4.2 Published Article⁶

4.2.1 Title Page

Navigating the link between processing speed and network communication in the human brain

Phoebe Imms^{a,1}, Juan F Domínguez D^b, Alex Burmester^b, Caio Seguin^c, Adam Clemente^a, Thijs Dhollander^d, Peter H Wilson^e, Govinda Poudel^{a,*} & Karen Caeyenberghs^{b,*}

^a Mary MacKillop Institute for Health Research, Australian Catholic University; 5/215 Spring Street, Melbourne VIC, Australia 3000

^b Cognitive Neuroscience Unit, School of Psychology, Faculty of Health, Deakin University; 221 Burwood Highway, Burwood VIC, Australia 3125

^c Melbourne Neuropsychiatry Centre, The University of Melbourne and Melbourne Health; 3/161 Barry Street, Carlton VIC, Australia 3053

^d Developmental Imaging, Murdoch Children's Research Institute; 50 Flemington Road, Parkville VIC, Australia 3052

^e Healthy Brain and Mind Research Centre, School of Behavioural, Health and Human Sciences, Faculty of Health Sciences, Australian Catholic University; 115 Victoria Parade, Fitzroy VIC, Australia 3065

¹ Corresponding author; phoebe.imms@myacu.edu.au

* Shared senior author

⁶ Article published in *Brain Structure and Function*.

Reference: Imms, P., Burmester, A., Seguin, C., Clemente, A., Dhollander, T., Wilson, P. H., Poudel, G. & Caeyenberghs, K. (2021). Navigating the link between processing speed and network communication in the human brain. *Brain Structure and Function*, 226(4), 1281-1302.

Keywords: Processing speed; structural connectomics; graph theory; communication measures; drift diffusion model; navigation efficiency

Declarations

Funding: This work was supported by an Australian Catholic University Research Fund [#902915]. Govinda Poudel is a Research Fellow on an ACURF Program grant by the Australian Catholic University (ACU). Karen Caeyenberghs is supported by a National Health and Medical Research Council Career Development Fellowship (APP1143816). Phoebe Imms and Adam Clemente are both supported by the Australian Postgraduate Award under the Australian Research Training Program. Caio Seguin is supported by a Melbourne Research Scholarship.

Conflicts of interest: The authors declare that they have no conflict of interest.

Ethics approval: Ethical approval for the study was obtained from Monash University HREC (1181) and Australian Catholic University (2017-222R).

Consent to participate: Written informed consent was obtained from each subject prior to testing.

Consent for publication: Participants provided written informed consent for the publication of any associated data.

Availability of data and material: Not applicable

Code availability: Not applicable

Electronic supplementary material: Not applicable.

Authors' contributions:

Conceptualisation: Phoebe Imms, Juan F Domínguez D, Caio Seguin, Adam Clemente, Peter H Wilson, Govinda Poudel, Karen Caeyenberghs; *Methodology:* Phoebe Imms, Juan F Domínguez D, Alex Burmester, Caio Seguin, Thijs Dhollander, Govinda Poudel, Karen Caeyenberghs; *Software:* Phoebe Imms, Juan F Domínguez D, Alex Burmester, Caio Seguin, Thijs Dhollander, Govinda Poudel; *Validation:* Juan F Domínguez D, Govinda Poudel, Karen Caeyenberghs; *Formal Analysis:* Phoebe Imms, Juan F Domínguez D, Alex Burmester, Caio Seguin, Govinda Poudel, Karen Caeyenberghs; *Investigation:* Phoebe Imms, Alex Burmester, Adam Clemente, Karen Caeyenberghs; *Resources:* Phoebe Imms, Juan F Domínguez D, Caio Seguin, Adam Clemente, Thijs Dhollander, Peter H Wilson, Govinda Poudel, Karen Caeyenberghs; *Data Curation:* Phoebe Imms, Juan F Domínguez D, Alex Burmester, Caio Seguin, Adam Clemente, Thijs Dhollander, Govinda Poudel; *Writing – Original Draft:* Phoebe Imms, Karen Caeyenberghs; *Writing – Review & Editing:* Phoebe Imms, Juan F Domínguez D, Alex Burmester, Caio Seguin, Adam Clemente, Thijs Dhollander, Peter H Wilson, Karen Caeyenberghs; *Supervision:* Juan F Domínguez D, Peter H Wilson, Govinda Poudel, Karen Caeyenberghs; *Funding Acquisition:* Peter H Wilson, Karen Caeyenberghs

4.2.2 Abstract

Processing speed on cognitive tasks relies upon efficient communication between widespread regions of the brain. Recently, novel methods of quantifying network communication like ‘navigation efficiency’ have emerged, which aim to be more biologically plausible compared to traditional shortest path-length based measures. However, it is still unclear whether there is a direct link between these communication measures and processing speed. We tested this relationship in forty-five healthy adults (27 females), where processing speed was defined as decision-making time and measured using *drift rate* from the hierarchical drift diffusion model. Communication measures were calculated from a graph theoretical analysis of the whole brain structural connectome and of a task-relevant fronto-parietal structural subnetwork. We found that faster processing speed on trials that require greater cognitive control are correlated with higher navigation efficiency (of both the whole-brain and the task-relevant subnetwork). In contrast, faster processing speed on trials that require more automatic processing are correlated with shorter path-length within the task-relevant subnetwork. Our findings reveal that differences in the way communication is modelled between shortest path-length and navigation may be sensitive to processing of automatic and controlled responses respectively. Further, our findings suggest that there is a relationship between the speed of cognitive processing and the structural constraints of the human brain network.

4.2.3 Introduction

Processing speed is the time it takes to perform a cognitive task, including identifying, manipulating, and responding to information (Holdnack et al., 2015). It plays a central role in a broad range of cognitive abilities, in particular top-down control of attention and executive functioning (Kail & Salthouse, 1994). Notably, inter-individual variability in processing speed is related to intelligence (Sheppard & Vernon, 2008) and is argued to be one of the most meaningful ways of measuring mental capacity (Kail & Salthouse, 1994). It is theorized that processing speed relies on the topological organisation of white matter pathways that connect regions of the brain, allowing for efficient communication between brain regions (Bullmore & Sporns, 2012). Consequently, slowed processing speed has been implicated in patients with brain injuries (Battistone et al., 2008) and neurodegenerative disorders that disrupt these connections (Soloveva et al., 2018). However, few studies have investigated whether inter-individual variability in processing speed is directly related to white matter connectivity measures, especially in healthy populations.

Processing speed is thought to be constrained by white matter network organisation, since cognitive processes rely on efficient communication along axonal pathways between brain regions (Bullmore & Sporns, 2012; Lynn & Bassett, 2019). Cognitive processing is slowed if signals must travel via more synaptic connections (Fornito et al., 2016) or via connections with poor myelination or low axon density (e.g., Tolhurst & Lewis, 1992). Neuroimaging studies have used diffusion MRI to examine the relationship between processing speed and properties of specific white matter tracts in healthy populations (e.g., Karahan et al., 2019; Turken et al., 2008). For instance, Turken et al. (2008) found that faster processing speed is associated with higher connectivity of fronto-parietal and fronto-temporal white matter pathways. While these studies suggest that processing speed relies on white

matter organisation, they used tract-based approaches that provide an incomplete picture of the link between processing speed and brain connectivity. Rather, the brain operates as a set of interconnected networks in complex arrangements, disseminating information across distributed areas (Bressler & Menon, 2010). Brain organization in terms of these complex networks will likely determine processing speed over and above the structure of individual brain regions or tracts.

Network analysis has been used to understand how ensembles of brain regions work together in a network, which is crucial for higher-order cognitive processing (Bullmore & Sporns, 2009; Sporns, 2010; Sporns et al., 2005). These analyses have rapidly found applications in the clinical neurosciences (for reviews, see Fornito et al., 2015; Griffa et al., 2013; Imms et al., 2019) and have provided several global graph measures to capture the different structural properties of the brain (Rubinov & Sporns, 2010). A particular class of graph measures is concerned with modelling how the structure of brain networks facilitates and constrains large-scale neural signalling (Avena-Koenigsberger et al., 2018; Seguin et al., 2020). Network communication measures take into account the organization of white matter networks to compute the efficiency of putative communication pathways between brain regions. Of particular interest are communication measures based on the shortest path between brain regions (i.e., characteristic path length and global efficiency; Rubinov & Sporns, 2010). There is emerging evidence from clinical populations that suggests slower processing speed is associated with longer path length and/or lower global efficiency in aging (e.g., Wen et al., 2011), brain injury (e.g., Caeyenberghs et al., 2014), and diabetes (e.g., Reijmer, Leemans, Brundel, et al., 2013). For example, Caeyenberghs et al. (2014) found that slower processing speed was associated with lower global efficiency in adults with traumatic brain injury. This relationship between processing speed and communication measures in clinical populations suggests that there may be similar patterns in healthy adults.

There has been no dedicated structural connectome analysis examining processing speed and graph communication measures in healthy adults, though communication models have recently been shown to improve prediction of behaviours, such as overall cognition and tobacco use (Seguin et al., 2020). Furthermore, previous clinical studies have only used shortest path-based algorithms to measure communication (e.g., Caeyenberghs et al., 2014; Reijmer, Leemans, Brundel, et al., 2013; Wen et al., 2011). This is potentially problematic because shortest path-based routing relies on the assumption that every brain region has a global ‘roadmap’ of the network, which may be biologically implausible (Avena-Koenigsberger et al., 2019; Goñi et al., 2014). Recently, a more realistic routing model for neural communication has been suggested, named “*navigation*” (Seguin et al., 2018). Navigation assumes that neural signalling unfolds based on local knowledge of the spatial positioning of brain regions. Therefore, navigation models neural communication as a decentralized process, which may be more robust with regards to the biological mechanisms of information transfer in the brain. The associated measure “*navigation efficiency*” has shown stronger correlations with resting-state brain activity compared with shortest path-based routing (Seguin et al., 2018), and is reported to track abnormalities in the functional synchronization of brain regions following stroke (Wang et al., 2019). Navigation efficiency may therefore represent a more specific marker of how communication is structurally facilitated by the brain network.

The present study aims to investigate how inter-individual differences in processing speed relates to communication measures in healthy adults. We employed measures that are as specific as possible to individual differences in (1) processing speed and, (2) white matter connectivity. First, processing speed is traditionally measured by means of overall reaction time on tasks such as the global-local task (which taps into processing speed by asking participants to identify either global or local elements of a stimulus while ignoring interfering

information) (Navon, 1977). However, theoretical models of cognition suggest that processing speed can be divided into three components, including the time taken to (a) visually perceive the stimulus, (b) ‘process’ the information and decide how to respond (decision-making), and (c) execute the motor response (e.g., Romo & Salinas, 1999). There is evidence that decision-making time (b) is relevant to cognitive performance (for review, see Forstmann et al., 2016), and is a more specific measure of processing speed (Poudel et al., 2017; Powell et al., 2019). As such it is useful for investigating the white matter substrates of processing speed in healthy adults (Schall, 2001). To extract decision-making time, we employ a drift diffusion model where processing speed is operationalised as the rate of information accumulation during the decision-making process—“*drift rate*”—with higher values denoting faster decision-making time (Ratcliff & McKoon, 2008; Voss et al., 2004; Wiecki et al., 2013). Second, we modelled network communication using both shortest path-based and navigation-based routing strategies, to examine whether navigation efficiency is more strongly correlated with decision-making speed than path-length. Furthermore, we computed each communication measure for the whole-brain *and* for a task-relevant subnetwork, as the specificity of these measures can be improved by examining connectivity in the subnetwork important for the task at hand (e.g., Román et al., 2017). The global-local task is known to elicit specific activation in fronto-parietal regions, the temporal-parietal junction, areas of the occipital cortex, and the thalamus (Gadgil et al., 2013; Han et al., 2004; Hedden & Gabrieli, 2010; Liddell et al., 2015; Weissman & Woldorff, 2005). These regions were therefore selected for the task-relevant subnetwork.

We hypothesised that drift rate on the global-local task would be lowest (i.e., slow processing speed) on incongruent trials where the large and small elements of the stimuli are different. On the basis of previous studies (Caeyenberghs et al., 2014; Reijmer, Leemans, Brundel, et al., 2013; Wen et al., 2011), we hypothesised that higher drift rate on the global-

local task would be (i) positively correlated with navigation efficiency, (ii) positively correlated with global efficiency, and (iii) negatively correlated with characteristic path length.

4.2.4 Materials and Methods

4.2.4.1 Participants

Forty-five healthy adults (27 female) aged 21 – 59 years (mean age=30.9 years, $SD=11.8$ years) participated in this study. All participants were right-handed (average Edinburgh Handedness Inventory score: 9.91/10; Oldfield, 1971) and reported no history of psychiatric illness or neurological disorders. The majority of participants (94.6%) were high school graduates or above (Less than high-school or equivalent = 5.41%; High-school or equivalent = 5.41%; Diploma/Vocational qualification = 8.11%; Bachelor's Degree = 29.72%; Postgraduate Diploma = 8.11%, Master's Degree = 32.34%; Doctoral Degree = 10.81%). Ethical approval for the study was obtained from Monash University HREC (No. 1181) and Australian Catholic University (project #2017-222R), and written informed consent was obtained from each subject prior to testing. All testing was carried out in accordance with The Code of Ethics of the World Medical Association (Declaration of Helsinki).

4.2.4.2 Processing Speed

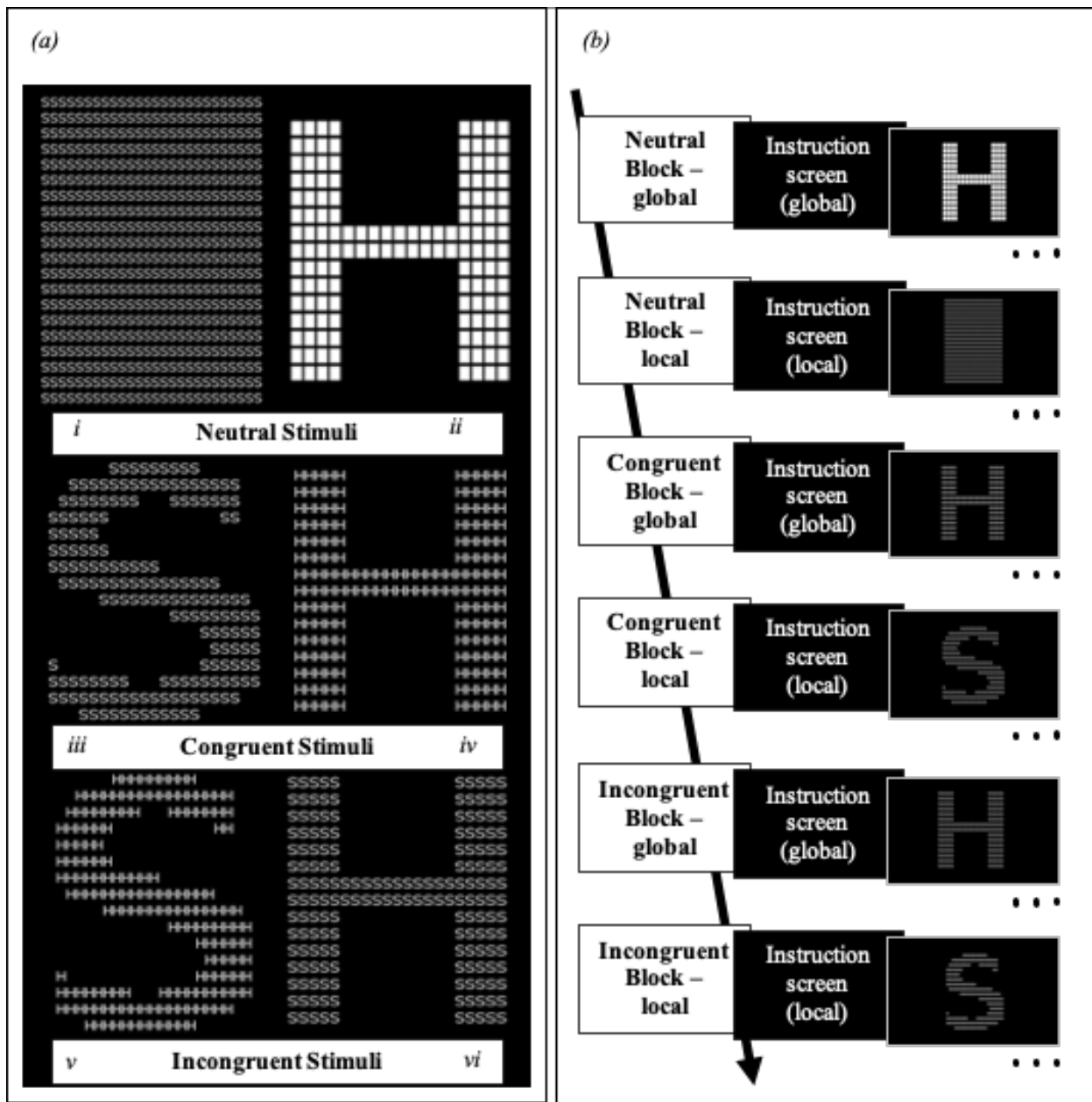
Global-Local Task

The global-local task (Navon, 1977) was performed using the computerized Psychological Experimental Building Language test battery (Mueller & Piper, 2014) on a Dell Inspiron 15-3537 laptop (response latency=80ms; refresh rate=60Hz; stimulus display was synchronised to device refresh rate). Participants were instructed to respond as quickly as possible to either the global (large) or local (small) level of the stimuli—either an “S” or “H”

as illustrated in Figure 1(a)—using the left or right shift keys of the laptop keyboard. The task consisted of neutral, congruent, and incongruent conditions to measure processing speed across different levels of interference. Neutral trials consisted of rectangular blocks made of local letters, or a global letter made of white rectangles (see panels *i* and *ii*). For congruent trials both levels of the stimuli matched (see panels *iii* and *iv*), and for the incongruent trials the global and local elements of the stimulus did not match (see panels *v* and *vi*). First, 60 practise trials were presented as a single local letter (30 trials of each letter). All subsequent trials ($N=240$) were grouped into 3 blocks (see Figure 1(b)); (1) neutral trials ($n=80$); (2) congruent trials ($n=80$); and (3) incongruent trials ($n=80$). Within each block, participants were instructed to respond to either the global or local level of the stimulus. Participants were to respond as quickly as possible, however there was no time limit on trials. Overall, the task took on average 9:20mins to complete (the mean reaction time for each trial was 545ms, intertrial interval was 775ms). Reaction times for incongruent, congruent, and neutral trials were recorded separately, in milliseconds. One subject failed to complete the task, and one subject was identified as an extreme outlier (average response time was >2.5 standard deviations slower than the mean); these two subjects were excluded from further analyses. All trials regardless of accuracy were included in the analysis (average accuracy rate for all participants was 95.89%).

Figure 1.

Global-Local Task Stimuli



Note: (a) Example stimuli from the global-local task executed in the Psychological Experimental Building Language (Mueller & Piper, 2014); (i) and (ii) are neutral stimuli; (iii) and (iv) are congruent stimuli; and (v) and (vi) are incongruent stimuli; (b) Block design was structured by condition (neutral, congruent, incongruent) and trial type (global or local).

Drift diffusion modelling of the Global-local data

The hierarchical Bayesian drift diffusion model was used to obtain a sensitive measure of decision-making time from the processing speed data of the global-local task (Wiecki et al., 2013; see Appendix Table 1 for definitions, interpretations, and a schematic of the general drift diffusion model). Reaction times and trial conditions (congruent, incongruent, and neutral) for each participant were entered into the model in python (v2.7) package ‘HDDM v0.6.0’ (Wiecki et al., 2013). Based on a comparison of drift diffusion models performed by Wiecki et al., we opted for the *hierarchical* drift diffusion model, which requires fewer data points (~50-60 trials per block) compared to other standard maximum-likelihood drift diffusion models (which require ~100 trials per block). Moreover, Wiecki et al. advocate the use of the *Bayesian* model, as it enables quantification of uncertainty around the estimate of each parameter. The drift rate (v) was estimated for each trial, resulting in a distribution of drift rates for each participant and for each condition. We excluded individual trials that were in the furthest 5% from the mean reaction time, according to recommendations from the authors (Wiecki et al., 2013). An optimal estimate of v (defined as the highest point on the drift rate posterior distribution) was calculated per individual for each condition. This estimate was used in the correlation analyses as an apparent measure of that individual’s processing speed.

Table 1

Definitions and Interpretations of Parameters from the Drift Diffusion Model

Name	Definition	Interpretation
<i>a</i> Threshold	The threshold is the distance between the upper and lower boundaries.	A large value can be interpreted as the process needing to accumulate more information before reaching a limit and initiating a response.

Name		Definition	Interpretation
t	Non-decision time	The non-decision time is the time not measured by the diffusion process (e.g., motor processing and encoding before coming to a decision).	A larger non-decision time means a longer amount of time needed to perform non-decision relating processing tasks.
z	Bias	The bias is the starting point of the diffusion process (i.e., closer to either the upper or lower threshold).	A larger bias towards the upper threshold indicates that less information is needed to initiate a response towards that threshold.
v	Drift rate	The drift rate is the change over time in the approach towards either the upper or lower threshold.	A higher drift rate indicates a faster decision-making speed.

4.2.4.3 Structural Connectome

MRI data

MRI data were acquired on a Siemens 3T Skyra scanner using a 32-channel head coil at the Monash Biomedical Imaging facilities in Clayton, Victoria, Australia. A 3D T1-weighted image was acquired for each subject with a magnetisation-prepared rapid gradient-echo (MPRAGE) sequence, 192 sagittal slices, FOV = 256mm, voxel size = 1.0mm isotropic, TR = 2300ms, TE = 2.07ms, flip angle = 9°, and a total acquisition time of 3:52min. Diffusion MRI (dMRI) data were acquired using a single-shot echo planar imaging sequence (twice-reinforced spin echo) and 60 contiguous sagittal slices, FOV = 220mm, voxel size = 2.5mm isotropic, TR = 10100ms, TE = 101ms, and right-to-left phase encoding direction. The data were acquired using a high angular resolution diffusion imaging (HARDI) gradient scheme with 66 non-collinear gradient directions, a b-value of 3000s/mm², and seven b=0 images interspersed throughout the HARDI scheme. A pair of reverse phase-encoded b=0 images was also collected to allow for correction of susceptibility induced echo planar imaging distortions. The total acquisition time of the entire dMRI data was 13:26mins.

Quality Assessment

Visual quality assessment for movement and radio frequency artefacts in the anatomical and diffusion scans was performed using the viewer in MRtrix (v3.0_rc3; Tournier et al., 2019). Two subjects were excluded from all subsequent analyses, one due to exceptional susceptibility artefacts and one due to incidental findings. The dMRI data of four subjects had incorrect phase encoding and were also removed from further analyses. The sample for all remaining analyses included 37 subjects.

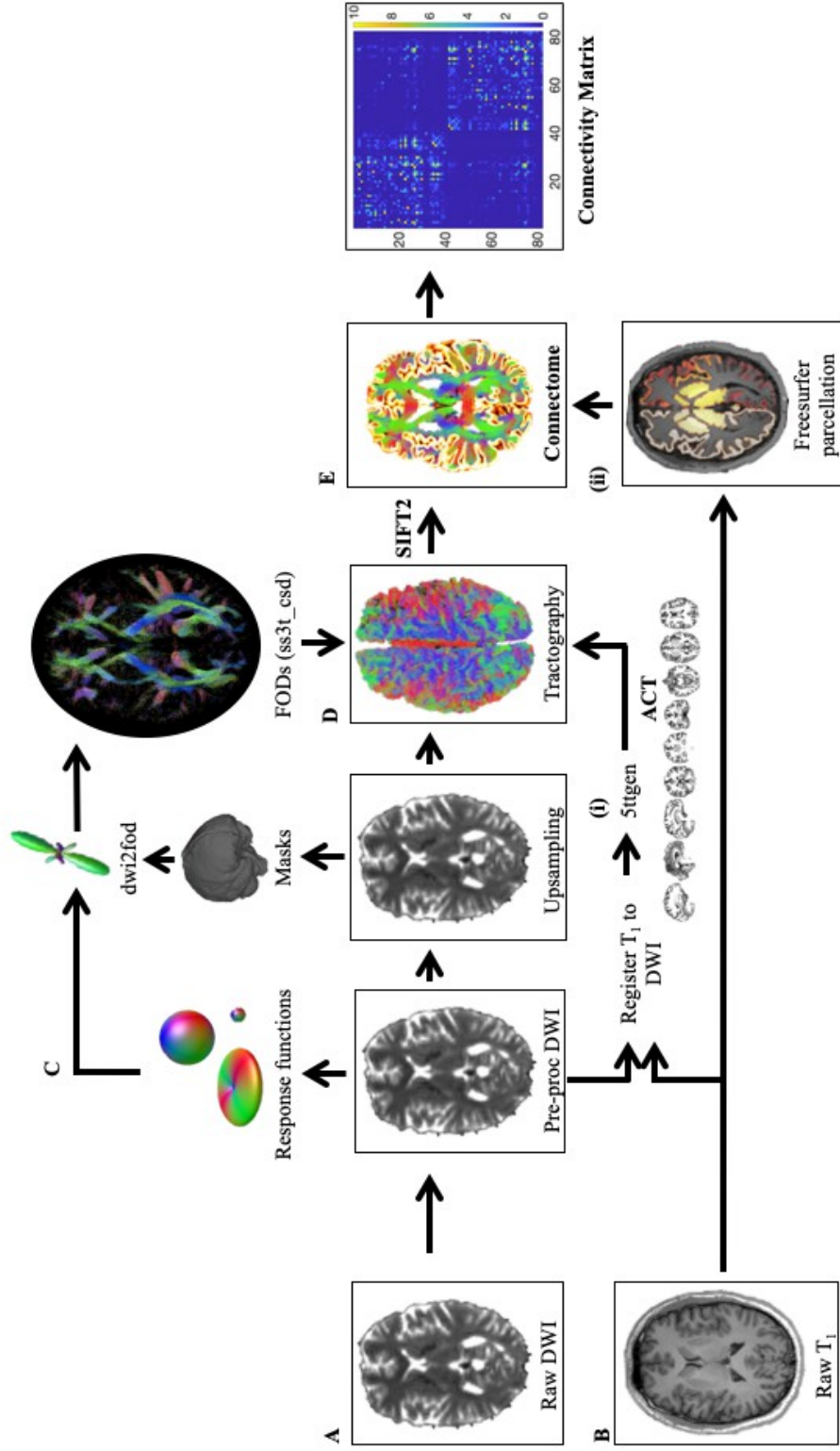
Pre-processing

Raw dMRI data were processed using MRtrix3Tissue (v5.2.8; <https://3tissue.github.io>), a fork of MRtrix3 (Tournier et al., 2019). A schematic overview of our tractography pipeline (Figure 2) can be seen below. First, noise (Cordero-Grande et al., 2019; Veraart et al., 2016), Gibbs ringing artefacts (Kellner et al., 2016), and motion, eddy current distortions and susceptibility induced (EPI) distortions were corrected (Andersson et al., 2003; Andersson & Sotiropoulos, 2016; Skare & Bammer, 2010). At this stage we also (1) removed outlier slices (mean=1.17%, maximum=2.46% of slices were removed across participants); and examined (2) motion across volumes (mean_{rms}=0.517, maximum_{rms}=1.068); and (3) translation (x=0.405mm, y=0.137mm, z=0.276mm) and rotation (x=0.286°, y=0.172°, z=0.177°) parameters across volumes. These values were below the voxel size of image acquisition for this sample (2.5mm³). Next, average response functions for white matter, grey matter, and cerebrospinal fluid were estimated from the dMRI data themselves using an automated unsupervised approach (Dhollander et al., 2019; Dhollander et al., 2016). Pre-processed data were up-sampled to a voxel size of 1.3mm isotropic to improve anatomical details and image registration before binary masks were created for the up-sampled images (Tournier et al., 2019). To estimate the white matter fibre

orientation distributions (FODs) in each voxel, single-shell 3-tissue constrained spherical deconvolution (SS3T-CSD) was performed (Dhollander & Connelly, 2016). Finally, the resulting FODs were corrected for intensity inhomogeneity and global intensity level differences (Raffelt et al., 2017). Quality checks were performed throughout the pre-processing pipeline: residuals were checked after denoising; the pre-processed image was checked for residual geometric distortions; and the brain masks were checked for holes. Hole filling was performed for five subjects by dilating the mask and filling in empty voxels that were surrounded by masked voxels.

Figure 2

Overview of the Processing Pipeline for Connectome Construction



Notes: (A) Raw diffusion images are preprocessed to remove imaging artefacts (noise, Gibbs-ringing, motion correction, distortion correction). (B) Concurrently, T_1 images are registered to diffusion images for (i) 5tgen, to create images for anatomically constrained tractography (ACT), and (ii) Freesurfer, to parcellate the nodes for the connectome analysis. (C) Fibre orientation distributions (FODs) are estimated from the group average response functions on upsampled images, and intensity normalised. (D) Anatomically Constrained Tractography (ACT) is performed using the FODs from (C) and the 5tgen images from (B(i)), before Spherically Informed Filtering of Tractograms (SIFT2) is applied to filter the streamlines and to make the weight of the streamlines proportional to the underlying fibre orientation distribution. (E) The connectome is created using the Freesurfer parcellation and the sifted tractogram.

The advanced normalization tools package (ANTS; Avants et al., 2009) was used to remove non-brain structures from the T1 weighted images for white matter extraction (Zhang et al., 2001). Next, FSL FLIRT (Jenkinson et al., 2002; Jenkinson & Smith, 2001) was used to perform the boundary-based registration between brain-extracted anatomical and diffusion images. For best results, the (upsampled) 1.3mm isotropic resolution diffusion b=0 images were registered to the 1.0mm isotropic resolution T1w images, and then were inverse transformed to bring the structural images back into the space of the dMRI data. MRtrix's 5 tissue-type segmentation script was then used on the T1w images in dMRI space to create the relevant masks for tractography.

Connectomics

Next, we implemented a series of steps as recommended by Yeh et al. (2020), to reconstruct structural connectomes for all subjects. To this end, whole brain anatomically constrained tractography was performed, guided by the FODs of each subject (Smith et al., 2012). The FOD cut-off threshold, step size, and angle were carefully determined to attain a reasonable trade-off between false negatives and false positives (seed points=dynamic; maximum length=250mm; minimum length=5mm; step size=1.25; angle=45°; FOD amplitude cut-off threshold = 0.08). Twenty-two million streamlines were generated to keep connectome variability low enough for SIFT2 to be relatively stable (Yeh et al., 2018). Next, the SIFT2 algorithm was applied to match the density of the reconstructed streamlines to that of the underlying white matter structures (Smith et al., 2015a). A proportionality coefficient μ was also calculated for each participant to be later applied to the connectome edge weights to ensure these are proportional to the apparent fibre density in each subject (Smith et al., 2015b). Anatomical images were parcellated using Freesurfer's 'recon-all' function (6.0; <http://surfer.nmr.mgh.harvard.edu/>), as described in previous publications (e.g., Fischl &

Dale, 2000). In brief, for all anatomical images subcortical grey-matter structures were segmented (Fischl et al., 2002); image intensity normalised (Sled et al., 1998); pial surfaces and the grey-white matter boundaries estimated (Dale et al., 1999); and the entire brain “inflated” to smooth the gyri and sulci (Fischl et al., 1999). On this surface model the automated cortical parcellation of 82 regions was generated using the Desikan-Killiany atlas (Desikan et al., 2006). While there is no consensus on the optimal choice of parcellation scheme (Sotiropoulos & Zalesky, 2019; Yeh et al., 2020; Zalesky et al., 2010), we utilized the Desikan-Killiany atlas for the following reasons: This atlas is (i) one of the most commonly used parcellation schemes and shows good test-retest reliability in structural connectome analysis (e.g., Buchanan et al., 2014); (ii) uses surface-based definition of gyri to register landmarks, indicating that the algorithms used to determine streamline termination are also compatible with brain parcellation (Yeh et al., 2018); and (iii) has previously shown functionally relevant links between brain and behaviour (e.g., Dhamala et al., 2020; Jolly et al., 2020) and includes subcortical structures, which facilitates the region of interest definition for the subnetwork analysis (e.g., Metzler-Baddeley et al., 2016). The robustness of results across multiple parcellation schemes was also examined by performing a control analysis utilizing the Destrieux atlas (164 regions; Destrieux et al., 2010), which is another commonly used atlas from the Freesurfer software (e.g., Buchanan et al., 2014). The Destrieux atlas has the same strengths as the Desikan-Killiany atlas listed above, albeit with a higher number of nodes. Quality checks were performed by inspecting output of the Freesurfer pipeline at each stage. In addition to a whole-brain network resulting from the parcellation, we also constructed a task-specific subnetwork by selecting 28 regions, forming a fronto-parietal subnetwork that are purported to be important for the global-local task (for a full list of these regions and their supporting citations, see Table 2). Connectivity matrices for whole-brain and fronto-parietal networks were generated using the summed streamline

weights and the cortical and subcortical regions from node parcellation. To explore the effect of area size normalisation on the main results, we conducted a control analysis utilizing streamline counts scaled to the inverse of the volumes of the two nodes they connect (Hagmann et al., 2008). We checked that the connectivity matrices for each individual were non-fragmented, to avoid problems with disconnected nodes that can confound calculation of communication measures. As a sanity check, group average whole-brain connectome (see Figure 3) demonstrated small-world properties when compared to the random connectome ($\sigma=1.0649$), and edge weights followed a power law distribution according to Bullmore and Sporns (2012).

Table 2

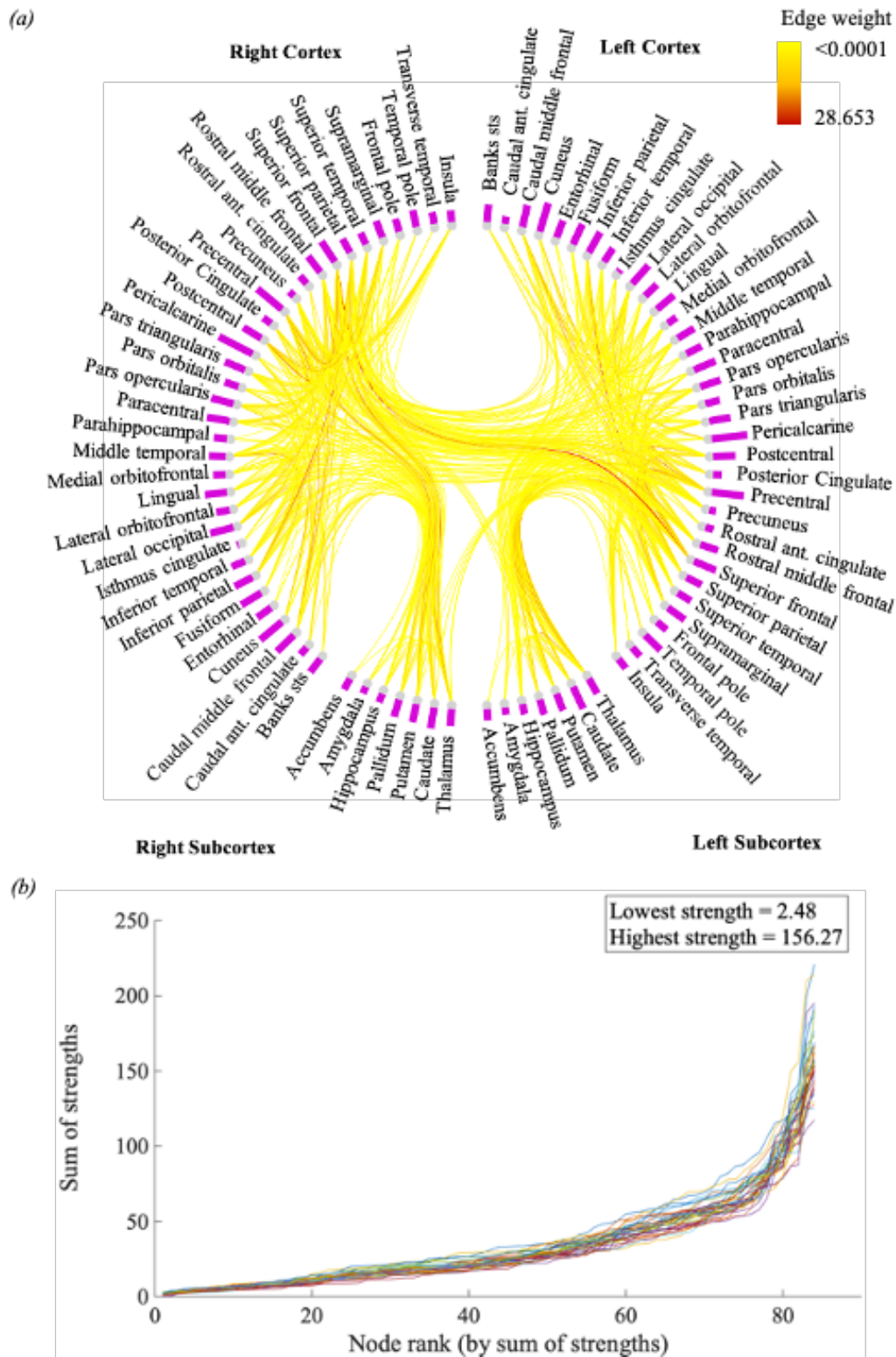
List of Regions Included in the Global-Local Task-Specific Subnetwork

Node	Region	Citation
7	L.inferiorparietal	Hedden & Gabrieli, 2010; salmon et al., 2010
10	L.lateraloccipital	Gadgil et al., 2013
14	L.middletemporal	Hedden & Gabrieli, 2010
18	L.parsorbitalis	Hedden & Gabrieli, 2010
19	L.parstriangularis	Hedden & Gabrieli, 2010
21	L.postcentral	Han et al., 2004
22	L.posteriorcingulate	Gadgil et al., 2013
23	L.precentral	Gadgil et al., 2013
24	L.precuneus	Han et al., 2004; Hedden & Gabrieli, 2011
27	L.superiorfrontal	Gadgil et al., 2013
28	L.superiorparietal	Gadgil et al., 2013; Liddell et al., 2015; Salmon et al., 2010
29	L.superiortemporal	Han et al., 2004
30	L.supramarginal	Han et al., 2004; Hedden & Gabrieli, 2010
35	L.thalamus	
42	R.thalamus	

Node	Region	Citation
55	R.inferiorparietal	Hedden & Gabrieli, 2010; Salmon et al., 2010
58	R.lateraloccipital	Gadgil et al., 2013
62	R.middletemporal	Hedden & Gabrieli, 2010
66	R.parsorbitalis	Hedden & Gabrieli, 2010
67	R.parstriangularis	Hedden & Gabrieli, 2010
69	R.postcentral	Han et al., 2004
70	R.posteriorcingulate	Gadgil et al., 2013
71	R.precentral	Gadgil et al., 2013
72	R.precuneus	Han et al., 2004; Hedden & Gabrieli, 2011
75	R.superiorfrontal	Gadgil et al., 2013
76	R.superiorparietal	Gadgil et al., 2013; Liddell et al., 2015; Salmon et al., 2010
77	R.superiortemporal	Han et al., 2004
78	R.supramarginal	Han et al., 2004; Hedden & Gabrieli, 2010

Figure 3

The Group Average Whole-Brain Connectome



Note: Whole brain connectome of the group average connectivity matrix (a) visualized using NeuroMARVL (<https://immersive.erc.monash.edu/neuromarvl/>); (b) and distribution of strengths for all 37 connectivity matrices across the whole-brain network (nodes sorted from lowest to highest strength per individual).

Graph Measures

The Brain Connectivity Toolbox (Rubinov & Sporns, 2010) was used to calculate network communication measures (for full definitions, see Table 3). Two communication measures were based on shortest-path routing: i.e., characteristic path length, defined as the average shortest path length between all node pairs in a network (Watts & Strogatz, 1998), and global efficiency, which is the average inverse of the shortest path length to characterise parallel network communication (Latora & Marchiori, 2001). Shortest path-based routing assumes that each node has a centralized knowledge of the network, in that information travels via the fastest possible route between any two nodes. The third measure, i.e., navigation efficiency, was calculated using the navigation-based routing and is defined as the average navigation path efficiency between all node pairs in a network (Seguin et al., 2018). Navigation-based routing strategies do not assume that each node has a centralized knowledge of the network – instead, navigation models information transfer using a decentralized, geometrically greedy heuristic (Boguna et al., 2009). Information travels from the starting node, to the next node in line that is geometrically closest to the target node – which may not necessarily be the fastest and most direct path. Greater capacity for efficient integration is indicated by higher values of navigation efficiency and global efficiency, and lower values of characteristic path length.

Table 3

Definition of Communication Measures used in the Current Study

Metric	Definition	Calculation	Interpretation
Characteristic path length (CPL)	The shortest path is the fastest and most direct communication pathway between two network nodes. The shortest path	More specifically, let $L \in \mathbb{R}^{N \times N}$ denote the matrix of connection lengths between N regions, where L measures the	A higher CPL indicates that the fastest communication pathways between regions are, on

Metric	Definition	Calculation	Interpretation
Global efficiency (E_{glob})	length denotes the length or signalling cost associated with the shortest path. CPL is defined as the average shortest path length between all node pairs in a network (Watts & Strogatz, 1998).	length of the connection between regions i and j . Region pairs that do not share a direct connection have $L_{ij} = \infty$. The shortest path length between regions i and j is defined as $\Lambda_{ij}^* = L_{iu} + \dots + L_{vj}$, where $\{u, \dots, v\}$ is the sequence of intermediate regions comprising the shortest path. The characteristic path length is defined as: $CPL = \frac{1}{N^2 - N} \sum_{i,j \in N} \Lambda_{ij}^*$	average, longer and less efficient.
	The average shortest path efficiency between all possible pairs of nodes in a network, where efficiency is computed as the inverse of shortest the path length (Latora & Marchiori, 2001). While CPL describes serial information transfer, global efficiency characterizes massively parallel network communication, which may better reflect neural signalling.	Formally, global efficiency is defined as: $E_{glob} = \frac{1}{N^2 - N} \sum_{i,j \in N} \frac{1}{\Lambda_{ij}^*}$	A higher global efficiency will indicate a greater capacity for efficient integration of information (in parallel) across the network.
	Navigation paths are use a decentralized and geometrically greedy heuristic (Bogunã et al., 2009). While navigation paths are not the fastest and most direct routes in a network, their computation does not mandate centralized knowledge of the network. Navigation efficiency is defined as the average navigation path efficiency between all possible pairs of nodes in a network (Seguin et al., 2018).	The navigation path from region i to region j is delineated as follows. Identify which of i 's neighbours is closest (shortest Euclidean distance) to j and progress to it. For each new visited region, repeat this process until j is reached (successful navigation) or a region is revisited (failed navigation). Let Λ denote the matrix of navigation path lengths. If the case of failed navigation from i to j , $\Lambda_{ij} = \infty$. Otherwise, $\Lambda_{ij} = L_{iu} + \dots + L_{vj}$, where $\{u, \dots, v\}$ is the sequence of nodes visited during navigation. Analogous the global efficiency of shortest paths, navigation efficiency is defined as: $E = \frac{1}{N^2 - N} \sum_{i,j \in N} \frac{1}{\Lambda_{ij}}$	Higher navigation efficiency indicates greater capacity for efficient integration of information across the network, without the assumption of centralized knowledge.

First, the weighted connectivity matrix (W) of each individual participant was normalised between 0 and 1, by dividing each weight by the sum of the maximum plus the minimum value ($W/W_{\max}+W_{\min}$). For characteristic path length and global efficiency, weight-to-length remapping was performed according to methods outlined in Rubinov and Sporns (2010) by calculating the inverse of the connectivity matrix ($1/W$; Floyd, 1962; Warshall, 1962). For navigation efficiency weights were remapped logarithmically ($-\log_{10}[W]$) according to procedures outlined in Seguin et al. (2018). The weight-length remapping procedures differed between the communication metrics so as to remain consistent with previous methods (path length: Caeyenberghs et al., 2014; Rubinov & Sporns, 2010; Wen et al., 2011) (navigation: Seguin et al., 2020; Seguin et al., 2018). Nevertheless, a control analysis was also performed to examine the sensitivity of results under the different normalisation procedures. In this analysis, navigation is calculated using the inverse method ($1/W$), and characteristic path length and global efficiency are calculated using the logarithm method ($-\log_{10}[W]$), and results are compared. All three communication measures were calculated for the whole-brain and the task-specific fronto-parietal subnetwork.

4.2.4.4 Statistical analyses

A one-way analysis of variance (ANOVA) was conducted to examine the effect of condition (neutral, congruent, incongruent) on drift rate. Partial correlation analyses were performed in Matlab (R2019b) to examine the relationships between the communication measures and processing speed. We performed these analyses separately for the whole brain and subnetwork levels, controlling for the effect of age (as a covariate). Moreover, correction for six comparisons (between the three communication measures and drift rates for each condition) was performed using the false discovery rate ($FDR < 0.05$, critical value $p < 0.016$) (Benjamini & Yekutieli, 2001). For each of the exploratory control analyses (parcellation

scheme, area size normalisation, and weight-length remapping alternatives), the critical FDR value was identical to the main analysis ($p < 0.016$). To explore the influence of brain size and movement in the scanner, a control analysis was performed whereby these two variables were also included as covariates in the model. Brain size (volume inside the skull) was measured using estimated Total Intracranial Volume (eITV), which is a fast automated procedure for head size correction provided by the Freesurfer software (Buckner et al., 2004). Movement in the scanner was measured as the square root of the displacement per voxel averaged across each volume, using output from FSL's motion correction algorithm (Andersson & Sotiropoulos, 2016).

To test for the specificity of our findings, we evaluated the model against a null model, similar to previous works (e.g., Poudel et al., 2020; Poudel et al., 2019). We randomly selected subnetworks of 28 regions each (to preserve the number of nodes) 10,000 times. Communication measures were calculated for each of these 10,000 random subnetworks, which were then correlated with drift rate to form a distribution of 10,000 correlation values. The frequency of each correlation value was fitted to a Gaussian distribution, and the *observed* correlation value from the task-specific subnetwork analysis was then plotted against this distribution. Using a standard z test, the likelihood of observing the task-specific subnetwork correlation from the distribution of randomly permuted subnetwork correlations was calculated as a p -value.

4.2.5 Results

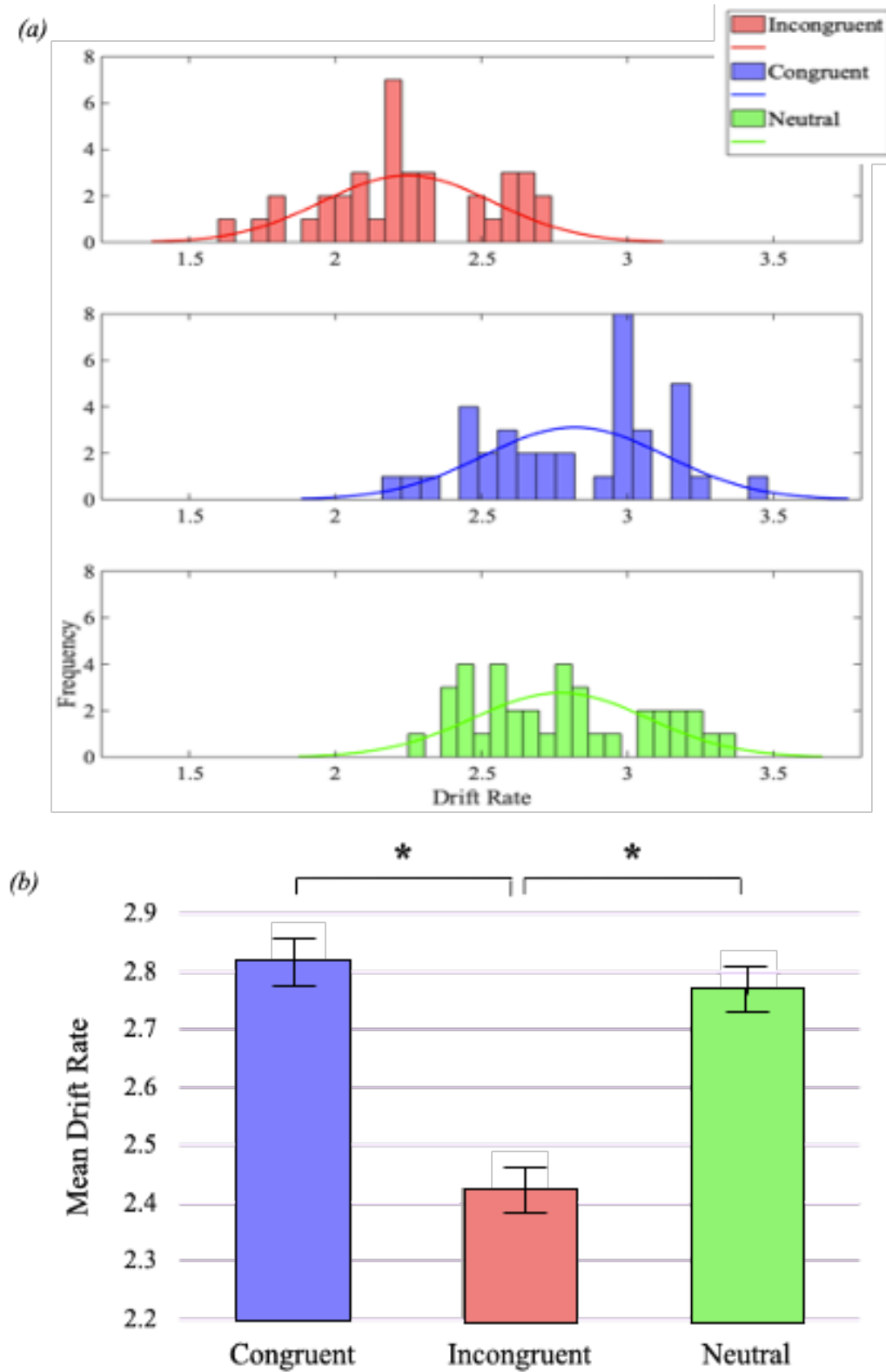
4.2.5.1 Global-local results and HDDM analysis

With respect to assumption testing, drift rates of the incongruent ($M=2.25$, $SD=0.29$, range=1.26), congruent ($M=2.82$, $SD=0.31$, range=1.08), and neutral conditions ($M=2.77$, $SD=0.30$, range=1.08) had similar ranges and equivalent variances (all $F > 0.87$, $p > 0.68$).

Sample skewness of the drift rates for each condition were between -0.5 and 0.5 and thus not significantly skewed ($g_{incongruent}=-0.04$; $g_{congruent}=-0.17$; and $g_{neutral}=0.33$) (Bulmer, 1979). The omnibus ANOVA comparing mean drift rate of incongruent, congruent, and neutral conditions was significant (mean sum of squares=3.74, $F=41.25$, $p<0.001$, see Figure 4). Post-hoc analyses revealed that drift rate was significantly lower in the incongruent trials compared to the congruent ($MD=0.57$, $p<0.001$, $g_{Hedges}=2.60$) (Hedges & Olkin, 2014) and neutral trials ($MD=0.52$, $p<0.001$, $g_{Hedges}=2.36$) with lower drift rate indicating slower processing speed. Because the congruent and neutral conditions did not differ significantly ($MD=0.05$, $p=0.48$, $g_{Hedges}=0.22$), only drift rates from congruent and incongruent trials were included in subsequent analyses to minimise the number of comparisons.

Figure 4

Drift Rate for Incongruent, Congruent, and Neutral Conditions of the Global-Local Task



Notes: (a) distribution of individual mean drift rates for each condition; and (b) average drift rate for each condition, including error bars (standard error of the mean, SEM). * indicates average drift rate was significantly different between conditions.

4.2.5.2 Whole-brain communication analysis

Partial correlation analysis revealed that navigation efficiency was positively correlated with faster processing speeds on incongruent trials ($r=0.427$, $p=0.009$; see Figure 5), but not on congruent trials ($r=0.213$, $p=0.213$), when controlling for the effect of age. This remained significant after correction for multiple comparisons (FDR critical p -value=0.016). We failed to observe significant correlations between drift rate and whole-brain communication based on shortest-path algorithms i.e., characteristic path length or global efficiency (see Table 4).

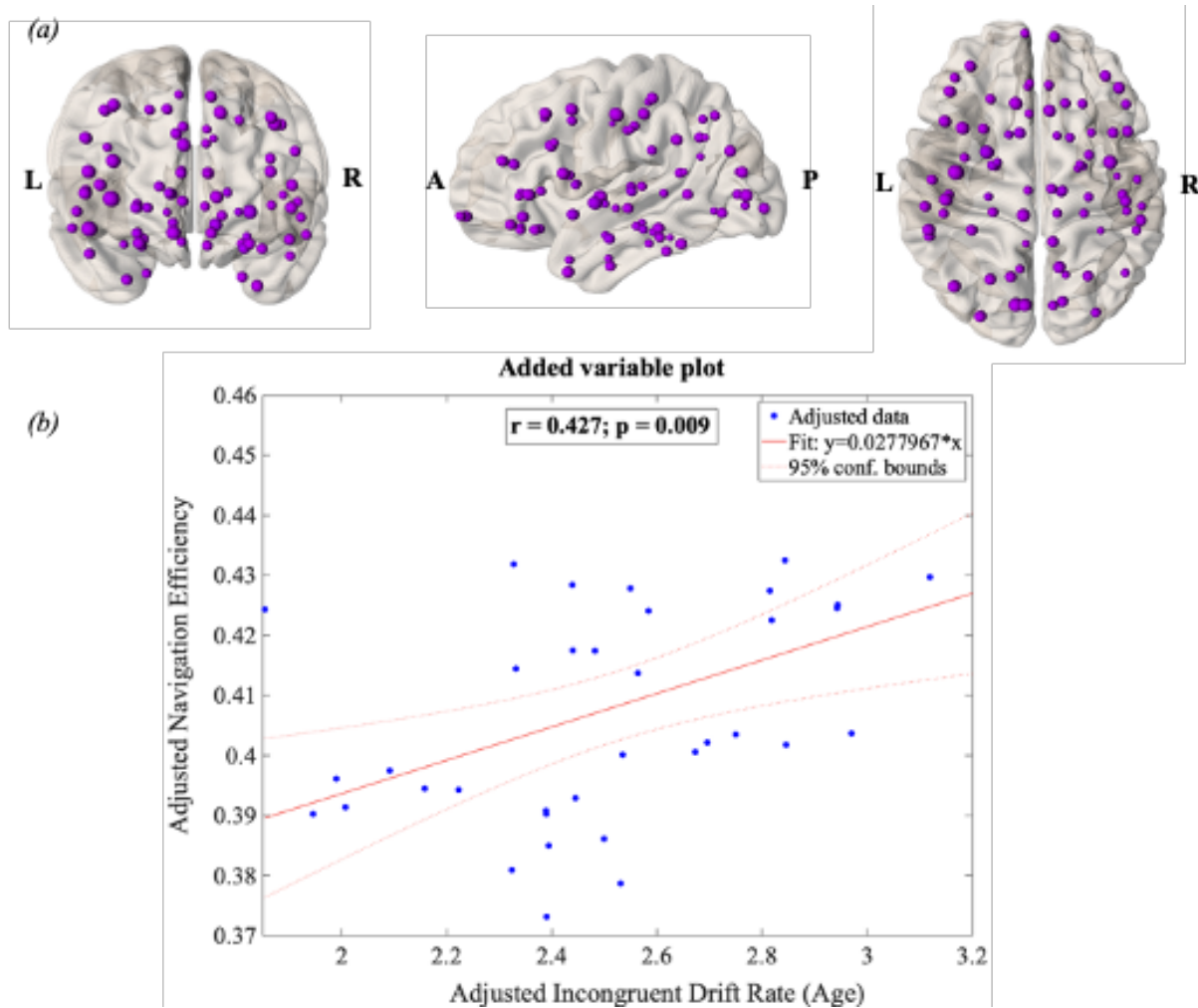
Table 4

Correlations Between Communication Measures and Incongruent and Congruent Drift Rate

<i>Communication measure</i>	<i>Incongruent drift rate</i>	<i>Congruent drift rate</i>
<i>(a) Whole brain analysis</i>		
Navigation efficiency	$r=0.427$; $p= 0.009$	$r=0.213$; $p=0.213$
Characteristic path length	$r=-0.158$; $p=0.358$	$r=-0.169$; $p=0.325$
Global efficiency	$r=0.110$; $p=0.522$	$r=0.212$; $p=0.215$
<i>(b) Subnetwork analysis</i>		
Navigation efficiency	$r=0.417$; $p= 0.011$	$r=0.274$; $p=0.105$
Characteristic path length	$r=-0.239$; $p=0.160$	$r=-0.399$; $p=0.016$
Global efficiency	$r=0.129$; $p=0.452$	$r=0.266$; $p=0.117$

Figure 5

Results of the Whole Brain Analysis



Notes: Results of the whole brain analysis, including a) the 82 regions of the whole brain network, and b) added variable plot of whole-brain navigation efficiency and incongruent drift rate including r - and p -values for the partial correlation (controlling for age)

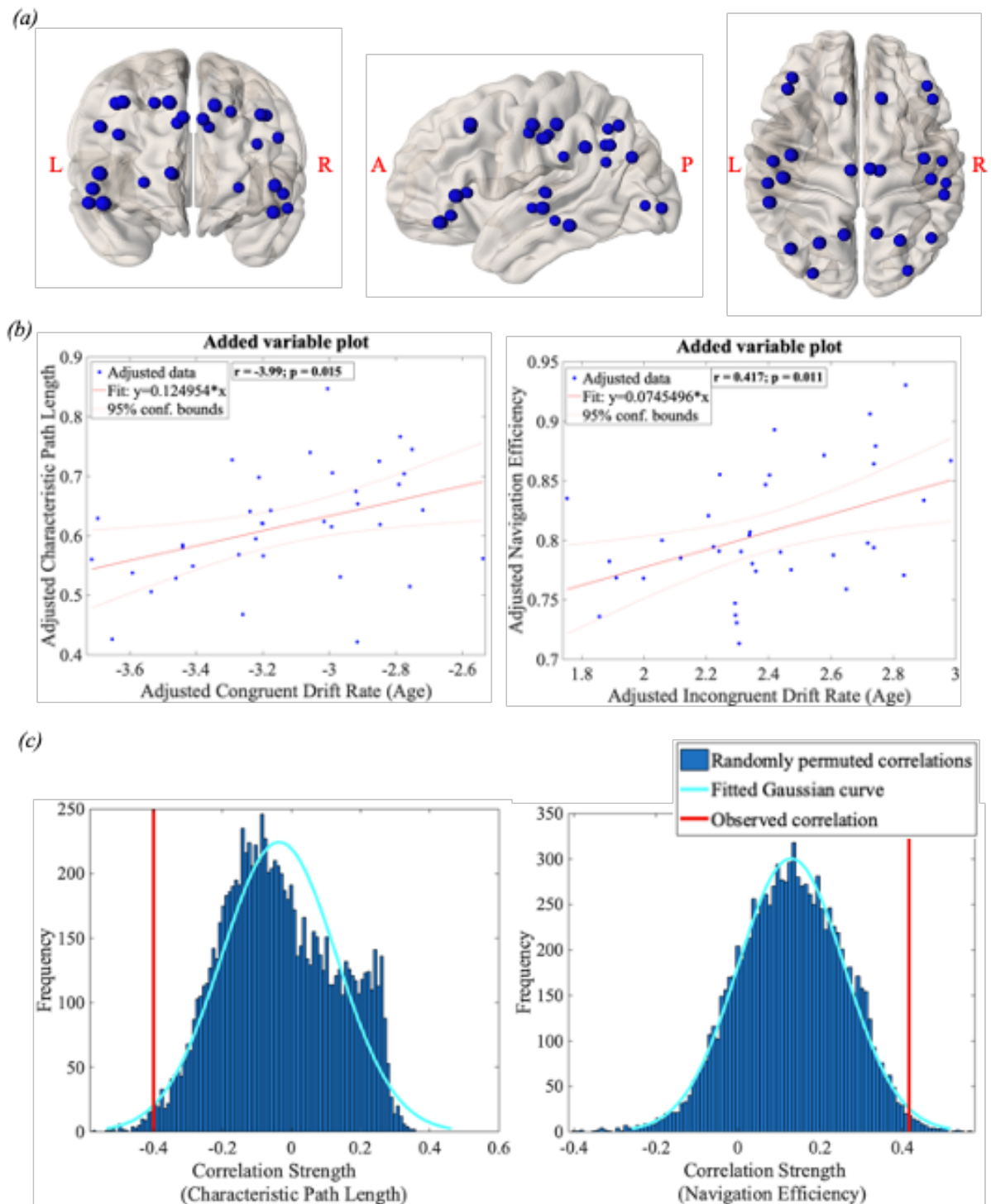
4.2.5.3 Task-relevant subnetwork analysis

Results of the subnetwork correlation analysis revealed that navigation efficiency was positively correlated with drift rate on the incongruent trials ($r=0.417$; $p=0.01$) when controlling for the effect of age, indicating that higher navigation efficiency in the fronto-parietal network was related to faster processing speed on the global-local task. In addition, characteristic path length of the subnetwork was negatively correlated with drift rate on the

congruent trials ($r=-0.399$; $p=0.016$) when controlling for the effect of age, indicating that longer, less efficient shortest paths in the fronto-parietal network coincided with slower processing speed (see Figure 6a and b). Both findings remained significant after FDR correction (FDR critical p -value=0.016). Global efficiency of the subnetwork was *not* related to drift rate of either condition of the global-local task (see Table 4).

Figure 6

Results of the Subnetwork Analysis



Notes: (a) the 28 regions of the Desikan-Killiany atlas (Desikan et al., 2006) that comprise the global-local task-relevant subnetwork, including fronto-parietal regions, the temporal-parietal junction, lateral occipital regions, and the thalamus; (b) added variable plots for the two significant correlations found, and (c) frequency histograms for the correlations between processing speed (congruent for characteristic path length, and incongruent for navigation efficiency) and the 10,000 randomly permuted subnetworks. The red vertical line indicates the observed correlation between the task-relevant subnetwork and processing speed

4.2.5.4 Control Analyses

Parcellation scheme

No significant (FDR corrected) results were obtained utilizing the Destrieux parcellation scheme (see Table 5a).

Table 5a

Correlations Between Whole Brain Communication Measures, and Incongruent and Congruent Drift Rate with Alternative Parcellation Scheme

<i>Communication measure</i>	<i>Incongruent drift rate</i>	<i>Congruent drift rate</i>
<i>(a) Whole brain analysis*</i>		
Navigation efficiency	$r=0.124; p=0.473$	$r=0.279; p=0.099$
Characteristic path length	$r=-0.076; p=0.664$	$r=-0.012; p=0.945$
Global efficiency	$r=0.091; p=0.596$	$r=0.183; p=0.286$

Note: Subnetwork analyses were not replicated for this control.

Area size normalisation

No significant (FDR corrected) results were obtained at the whole-brain or subnetwork level when area size normalisation was applied (see Table 5b).

Table 5b

Correlations Between Whole Brain and Fronto-Parietal Subnetwork Communication Measures, and Incongruent and Congruent Drift Rate with Alternative Streamline Weight

<i>Communication measure</i>	<i>Incongruent drift rate</i>	<i>Congruent drift rate</i>
<i>(a) Whole brain analysis</i>		

<i>Communication measure</i>	<i>Incongruent drift rate</i>	<i>Congruent drift rate</i>
<i>Navigation efficiency</i>	$r=0.357$; $p=0.033$	$r=0.174$; $p=0.311$
<i>Characteristic path length</i>	$r=-0.114$; $p=0.508$	$r=-0.064$; $p=0.710$
<i>Global efficiency</i>	$r=0.047$; $p=0.784$	$r=0.019$; $p=0.913$
<i>(b) Subnetwork analysis</i>		
<i>Navigation efficiency</i>	$r=0.277$; $p=0.102$	$r=0.176$; $p=0.305$
<i>Characteristic path length</i>	$r=-0.111$; $p=0.519$	$r=-0.124$; $p=0.472$
<i>Global efficiency</i>	$r=-0.01$; $p=0.953$	$r=0.050$; $p=0.770$

Weight-length remapping procedures

No correlations met the FDR threshold for significance at either the whole-brain or subnetwork level for the different weight-length remapping procedures (see Table 5c).

Table 5c

Correlations Between Whole Brain and Fronto-Parietal Subnetwork Communication Measures, and Incongruent and Congruent Drift Rate with Alternative Weight-Length Remapping

<i>Communication measure</i>	<i>Incongruent drift rate</i>	<i>Congruent drift rate</i>
<i>(a) Whole brain analysis</i>		
<i>Navigation efficiency</i>	$r=0.147$; $p=0.391$	$r=0.244$; $p=0.152$
<i>Characteristic path length</i>	$r=-0.331$; $p=0.049$	$r=-0.104$; $p=0.546$
<i>Global efficiency</i>	$r=0.355$; $p=0.033$	$r=0.157$; $p=0.362$
<i>(b) Subnetwork analysis</i>		
<i>Navigation efficiency</i>	$r=0.156$; $p=0.365$	$r=0.266$; $p=0.117$

Brain size and head motion

The results remained largely the same when brain size and head movement were included as covariates in the analysis (see Table 5d). A significant positive correlation was observed between incongruent processing speed and navigation efficiency at the whole-brain level ($r=0.449$; $p=0.007$), and at the subnetwork level ($r=0.420$; $p=0.012$) (FDR corrected). The negative correlation between congruent processing speed and characteristic path length of the task-relevant subnetwork did not remain significant at the FDR corrected level ($r=-0.337$; $p=0.048$).

Table 5d

Correlations Between Whole Brain and Fronto-Parietal Subnetwork Communication Measures, and Incongruent and Congruent Drift Rate, Controlling for the Effect of Brain Size and Head Movement

<i>Communication measure</i>	<i>Incongruent drift rate</i>	<i>Congruent drift rate</i>
<i>(a) Whole brain analysis</i>		
<i>Navigation efficiency</i>	$r=0.449$; $p=0.007$	$r=0.110$; $p=0.530$
<i>Characteristic path length</i>	$r=-0.043$; $p=0.808$	$r=-0.136$; $p=0.437$
<i>Global efficiency</i>	$r=0.036$; $p=0.836$	$r=0.178$; $p=0.306$
<i>(b) Subnetwork analysis</i>		
<i>Navigation efficiency</i>	$r=0.420$; $p=0.012$	$r=0.182$; $p=0.295$
<i>Characteristic path length</i>	$r=-0.209$; $p=0.229$	$r=-0.337$; $p=0.048$
<i>Global efficiency</i>	$r=0.090$; $p=0.608$	$r=0.212$; $p=0.222$

Comparison against null model subnetworks

The comparison against null models demonstrated that the findings of the task-specific subnetwork analysis are unlikely to be due to chance. The observed correlation between navigation efficiency of the fronto-parietal subnetwork and drift rate of the

incongruent trials ($r = 0.417$) was 2.2 standard deviations above the mean of the distribution of random subnetwork correlation values ($p=0.0077$; see Figure 6c). Similarly, the observed correlation between characteristic path length of the fronto-parietal subnetwork and drift rate of the congruent trials ($r = -0.399$) was 2.18 standard deviations below the mean ($p=0.0078$).

4.2.6 Discussion

In the present study, we examined whether individual differences in processing speed are related to measures of network communication in healthy adults. Communication efficiency was quantified using shortest path length-based metrics as well as a novel routing strategy, navigation efficiency (Seguin et al., 2018), across both whole-brain and subnetwork levels. We found that measuring processing speed as ‘drift rate’ provides estimates of decision-making time that are relevant to underlying white matter organisation. Our findings further reveal that navigation efficiency of the whole brain network is related to faster decision-making speeds. Finally, we also show that navigation efficiency *and* shorter characteristic path length of the fronto-parietal subnetwork are related to faster decision-making on the global-local task.

4.2.6.1 Drift rate is slower during incongruent trials

We observed normally distributed inter-individual variability in drift rate, with equivalent variances across the conditions of the global-local task, supporting our hypothesis that drift rate can effectively be used parametrically to examine individual differences in decision-making time. Decision-making requires top-down control of attention and necessitates longer processing times compared to visual perception and/or motor response time (Lamme, 2003; Posner & Boies, 1971). By examining the decision-making time separately from the overall reaction time, our results should arguably be more specific to

individual differences in global-local processing speed. This supports previous studies that also found drift rate to be more reliable than reaction time alone (Poudel et al., 2017; Powell et al., 2019).

We found that information accumulation is slower when stimuli are incongruent, compared with trials where stimuli have no distracting features. This observation is likely due to the effect of global interference (e.g., Gerlach & Poirel, 2018; Kimchi, 2015). According to Weissman et al. (2006), the response to the global letter in incongruent trials must be inhibited in order to give a correct answer, thereby slowing the rate of information accumulation. Our results are consistent with a previous study that used an accumulator model to examine global-local processing in healthy adults (Hübner, 2014). Furthermore, our findings support recent clinical research that has used drift rate to measure processing speed in autism and Parkinson's disease (e.g., Powell et al., 2019; Zhang et al., 2016). For instance, Powell et al. (2019) found lower drift rate in individuals with autism compared with healthy controls; and Zhang et al. (2016) identified slower drift rates in Parkinson's patients compared to controls, which they interpreted as a detrimental effect of the disease on the rate of information accumulation. Our findings highlight the utility of drift-diffusion model based decision-making time as a sensitive measure of cognitive processing.

4.2.6.2 Processing speed is associated with whole-brain navigation efficiency

Our whole-brain analysis revealed that higher navigation efficiency – a measure of network communication – was related to faster decision-making on incongruent trials of the global-local task. This finding supports the idea that more 'navigable' white matter topology increases the capacity to perform higher-order cognitive tasks more efficiently (Seguin et al., 2020; Wang et al., 2019). Incongruent trials of the global-local task require greater top-down

cognitive control to avoid interference from conflicting information (Posner & DiGirolamo, 1998). Top-down control of responses rely on a broad range of temporary neural pathways across the whole brain (not just the fronto-parietal attention network), including regions that are important for guiding controlled responses such as the cortico-basal ganglia structures (Hikosaka & Isoda, 2010; Leunissen et al., 2016) and fronto-striato-thalamic circuits (Leunissen et al., 2014). The results of the whole-brain analysis suggest a relationship between whole brain networks that are navigable with a shorter average Euclidean distance, and faster decision-making time when top-down cognitive control is required.

An individual with higher navigation efficiency tends to have stronger edge weights in the pathways characterised by the navigation heuristic (Seguin et al., 2018). Using the SIFT2 approach, this edge weight is roughly proportional to the apparent fibre density (Smith et al., 2015a). Thus, the tempting explanation for the correlation between network communication and processing speed is that there is higher axon density or cross-sectional area in the brain networks of people with faster processing speed, indicating faster signal transmission. However, it is still unclear whether graph metrics based on tractography alone can predict the speed of information transfer (for review, see Jones, 2010a; Lynn & Bassett, 2019), as conduction velocity has been shown to be more related more to axon diameter and *g*-ratio (Drakesmith et al., 2019). Additional measures of white matter organisation therefore may have stronger and more direct links to signal transmission speed, like *g*-ratio (Mancini, 2017) or myelination (Caeyenberghs et al., 2016). In the current work, we use the SIFT2 method to relate edge weights to apparent fibre density via the streamline tractogram (Smith et al., 2015a). It is still being explored how well the assumptions of the SIFT2 method assumptions hold in the presence of a large proportion of false positive streamlines, which are common for whole brain probabilistic tractograms (Maier-Hein et al., 2017): the SIFT2 approach optimises all connection weights globally, meaning in false positives may impact

directly on genuine connection weights and should be used with some degree of caution (Zalesky et al., 2020). Nevertheless, we do not argue that neural transmission speed can be directly inferred from communication measures. Instead, we suggest that navigation efficiency might quantify network topology in a way that reflects the capacity of a neural network to shift information around efficiently – in this capacity it may have value as a potential biomarker.

4.2.6.3 Processing speed and communication in the fronto-parietal subnetwork

The subnetwork analyses revealed that individual differences in decision-making time are also related to characteristic path length and navigation efficiency of fronto-parietal structures. In accordance with previous literature, the control analysis indicated that communication within this fronto-parietal subnetwork is more strongly correlated with global-local decision-making time than other subnetworks in the brain. This finding was expected as previous work suggests that processing speed on the global-local task relies on the fronto-parietal attention network to focus attention on the target stimuli (Gadgil et al., 2013; Han et al., 2004; Hedden & Gabrieli, 2010; Liddell et al., 2015; Weissman & Woldorff, 2005). For example, Han et al. (2004) found that attention to global elements of the stimuli elicited activation in temporal regions of the subnetwork, and local elements were related to parietal activation. Hedden and Gabrieli (2010) found that switching attention and inhibiting responses were reliant upon bilateral prefrontal, parietal, and basal ganglia structures. Our work further demonstrates that the structural constraints of this broad frontoparietal attention network are related to the speed of decision-making on the global-local task.

Interestingly, our study indicates that characteristic path length and navigation efficiency are related to decision-making time on different trial types—congruent and incongruent, respectively. This may be related to the dual processing theory of automatic and controlled processing (Schneider & Chein, 2003). Congruent trials require less attention than incongruent trials, as there is no distracting information; therefore, responses might occur more automatically via a relatively permanent set of neural connections (Banich, 2009; Banich et al., 2000; Schneider & Shiffrin, 1977). Given that characteristic path length represents an ‘optimal’ pathway between two regions, it would follow that this model of communication relates to automatic responses that have been performed many times before. By comparison, navigation efficiency correlated with decision-making time on incongruent trials, which require greater top-down cognitive control and attention (Posner & DiGirolamo, 1998). It may therefore be reliant on a more temporary set of neural pathways—perhaps those that show differential neural activation patterns in the parietal and occipito-temporal regions compared to controlled response activation patterns (Banich et al., 2000). Because navigation routing includes deviations from the optimum pathways, it may more closely model these temporary neural pathways. It is therefore logical that navigation efficiency is related to incongruent trials, and that responses to these stimuli require longer processing times to control attention. In other words, different behavioural contexts might be facilitated by special underlying patterns of neural signalling, which would in turn be better captured by different network measures of communication. To test this theory, future studies could investigate whether the correlation between navigation efficiency and processing speed on incongruent trials disappears with as the response becomes well-learned and automated.

We expected that examining communication within a task-specific subnetwork with strong links to performance on the global-local task would increase the specificity of our analyses, similar to previous graph theory studies (e.g., Román et al., 2017). This was the

case for characteristic path length, which negatively correlated with processing speed at the subnetwork level only. Surprisingly, however, navigation efficiency was sensitive to processing speed on both the subnetwork *and* whole-brain level. One possible explanation for this discrepancy again stems from the fact that characteristic path length and navigation efficiency were related to processing speed on different conditions. Given that characteristic path length represented communication for automatic tasks with predefined routes, it follows that only the subnetwork required for the task at hand was related to decision-making time. By comparison, navigation efficiency was related to trials that demanded greater top-down control of responses and might therefore be reliant on fronto-parietal topology *as well as* other distributed regions of the whole-brain network. Alternatively, navigation might be overall a more suitable model of neural signalling, which picks up on differences in processing speed even when not computed on the task-relevant subnetwork.

4.2.6.4 Strengths, Limitations and Future Directions

A causal link between brain structure and behaviour cannot be identified by correlation analyses alone (Woo et al., 2017). The main purpose of relating white matter organisation to individual variability in cognitive performance is ultimately to develop a ‘diagnostic biomarker’, a neuroimaging metric that is indicative of behaviour (e.g., Imms et al., 2019). To this end, the use of techniques such as multivariate pattern-recognition and machine learning in future investigations will better enable prediction of behavioural outcomes from graph metrics (e.g., Dhamala et al., 2020; Jolly et al., 2020). An important limitation of the present study is the relatively small sample size. Compared with previous network communication studies utilizing data from the Human Connectome Project (e.g., Seguin et al., 2020), conclusions drawn from the current study are limited by the moderate sample size and lack of a validation dataset. We observed significant results at an FDR-

corrected level, indicating sufficient power; nevertheless, larger samples would enable machine learning techniques to examine whether communication measures can be used to predict processing speed in individuals. Furthermore, the cause-effect relationship between brain structure and behaviour can be better understood by longitudinal studies that investigate changes in response to training. For example, Caeyenberghs et al. (2016) found that improved cognitive performance with adaptive working memory training was associated with increased global efficiency in healthy adults, indicating that graph metrics are sensitive to neuroplastic changes over time. A longitudinal examination could be the next step towards using communication measures to predict inter-individual variation in processing speed through healthy development (Kail & Salthouse, 1994) and aging (Kerchner et al., 2012).

Connectome analyses can be heavily influenced by methodological choices in the processing pipeline (for reviews, see Sotiropoulos & Zalesky, 2019; Yeh et al., 2020; Zalesky et al., 2010). Thus, the interpretation of results from the current study are mitigated by the specific graph construction parameters employed during analysis. These effects were explored in the present study using control analyses, whereby we examined the robustness of results across different methodological choices, including parcellation scheme and normalization procedures. For instance, we did not observe significant correlations using the higher-resolution Destrieux atlas (164 regions, Destrieux et al., 2010). Zalesky et al. (2010) found that network parameters such as path length vary as spatial scale of the parcellation scheme increases, and thus findings should be reported with reference to the scale of the parcellation used. The fact that significant relationships were observed only under the lower-resolution Desikan-Killiany parcellation scheme (82 regions, Desikan et al., 2006) reflects the idea that parcellation granularity does impact the sensitivity of communication measures to individual differences. In the case of processing speed on the global-local task, our results suggest a lower-resolution representation of brain regions seems to be important.

Also, both the Desikan-Killiany and the Destrieux atlases have differently sized parcels designed to reflect neuroanatomy (Desikan et al., 2006; Destrieux et al., 2010). While this makes these atlases potentially more neurobiologically relevant, differently sized parcels are a mathematical confound given larger regions are bound to have stronger weights due to the size of the nodes. In an effort to minimise the number of control analyses, the current study does not evaluate measures across a range of parcellation schemes of equally sized nodes as was done in a larger sample size (N=889) by Seguin et al. (2020). Instead, we conducted a control analysis utilizing the streamline weighting scaled to the volume of each node, which revealed no significant correlations at the FDR corrected level. This implies that communication is related to processing speed when node volume differences are not taken into account. While this is a confounding factor, it may also suggest that the variance in node size is an interesting feature of the human brain network when using edge weights based on SIFT2 (Smith, Raffelt, et al., 2020).

We also observed no significant correlations at the FDR corrected level when using different remapping procedures. We chose to use the standard remapping procedure for each communication measure according to key publications (e.g., Rubinov & Sporns, 2010; Seguin et al., 2018). However, this does introduce a limitation in that variance in the distribution of edge weights may be a confounding factor. Because there is no ‘best practice’ method for this step, there is a need for thorough investigation of performance of communication measures for predicting behaviour under these different remapping procedures (e.g., Avena-Koenigsberger et al., 2018). Finally, we observed that controlling for the effect of brain size and head movement had little impact on the results of the analysis (apart from characteristic path length) probably due to the nature of our sample (healthy cohort). However, these variables will play an important role in connectome studies in paediatric and/or clinical populations (Makowski et al., 2019).

With these limitations in mind, promising relationships are emerging between cognitive processing speed and macroscale brain network communication. A strength of the current analysis lies in the diffusion MRI modelling approaches that were used to overcome some known limitations of earlier tensor-based techniques (for reviews, see Jeurissen et al., 2013; Jones, 2010a). We used single-shell 3 tissue constrained spherical deconvolution to avoid overestimating the amount of diffusion signal attributed to white matter in the presence of partial voluming with other tissues (Dhollander et al., 2016); anatomically constrained tractography to generate streamlines from the grey-white matter boundary (Smith et al., 2012); and attempted to avoid reconstruction biases and make the streamline tractography measures proportional to the underlying apparent fibre density, using SIFT2 (Smith et al., 2015a). We also measured processing speed more specifically, using cognitive models that go beyond basic reaction time and that are sensitive to individual differences (Ratcliff & McKoon, 2008; Wiecki et al., 2013). Finally, we used a new measure of communication (navigation efficiency) that relies on more biologically realistic assumptions than shortest path length (Seguin et al., 2018).

4.2.7 Conclusion

Our analysis revealed a relationship between the white matter constraints of the macroscale healthy brain network and the speed of cognitive decision-making processes. Navigation is emerging as a more biologically grounded alternative to shortest path-based approaches at the whole-brain level, making it potentially useful as a marker of processing speed in healthy adults. Furthermore, by investigating the fronto-parietal subnetwork more specifically, we also found evidence that navigation efficiency and characteristic path length are differentially related to controlled and automatic processing speeds respectively. This opens up a new set of possible theories about how different communication models relate to

processing speed under different levels of cognitive demand. Overall, these results indicate that communication measures may have interpretive value in healthy adults, with higher communication efficiency (especially when calculated using the navigation heuristic) relating to faster processing speed on executive functioning tasks requiring cognitive control—bringing us closer to bridging the gap between graph theory and cognition.

**Chapter 5: Study 3 - Personalised structural connectome mapping in
Traumatic Brain Injury**

5.1 Preface

The purpose of Study 3 was to investigate alterations in brain network structure and cognition in a series of six moderate-severe TBI patients who are in the chronic phase post injury: thus, advancing the use of graph theory in the study of brain injury. Building on the insights of the Study 1, this study addresses three main issues in the use of graph theory: 1) representing heterogeneity in the TBI population (5.1.1), 2) the rationale behind choice of graph metrics to examine (5.1.2), and 3) methodological considerations for graph analysis in patients with lesions (5.1.3). As well, an updated review of the literature published since the final systematic literature search conducted in Study 1 is provided (i.e., post April 2018) (Imms et al., 2019).

A personalised connectomics approach uses the structural connectome as a ‘fingerprint’ of an individual’s brain network (e.g., Sanz Leon et al., 2013; Schirner et al., 2015). The vast majority of personalised connectomics research has focussed on the functional network profiles of healthy adults using fMRI (Finn et al., 2015; Gratton et al., 2018; Miranda-Dominguez et al., 2014; Satterthwaite et al., 2018). However, as argued by Irimia and colleagues (Irimia, Chambers, et al., 2012; Irimia, Wang, et al., 2012), there is a need for individual-level structural connectome analysis of TBI patients; where the structure that entails the function of the brain is studied to determine how network organisation is rewired following trauma. Nevertheless, structural network differences between groups of TBI patients and healthy controls remained the dominant method of evaluation (Imms et al., 2019) and the role of personalised structural connectomics is still undervalued, especially in chronic patients.

5.1.1 How should heterogeneity in TBI patients be addressed?

In Study 1 it was noted that patients with TBI are diverse and vary in severity, time since injury, age at injury, method of injury, type of lesion, and other characteristics. Most research examining the link between brain structure and cognition has adopted group-level analyses that average TBI patient data regardless of this undeniable variability. While group-level analysis is essential for statistical evaluation, the TBI population is notoriously heterogeneous in terms of their lesion characteristics and cognitive outcomes; as such, group-level results are not necessarily applicable to individual patients (Mant, 1999). Instead, there is impetus for the use of single-subject profiling approaches to investigate the cognitive and neurological consequences of brain injury (e.g., Irimia, Chambers, et al., 2012; Irimia, Wang, et al., 2012). Therefore, this study develops and implements a framework for evaluating a profile of graph metrics, including the communication metrics investigated in Study 2, enhancing the applicability of the approach to any patient with TBI.

Another important gap in the TBI field is methods to improve segmentation of patients with large lesions, so that they are not excluded from connectome analyses. It has been an unfortunate fact that, to increase the homogeneity of the TBI group, studies often discard patients with large lesions as ‘outliers’, meaning these patients are not being represented in the literature. This is often done because the altered signal intensity of the structural pathology causes failures in anatomical segmentation and streamline generation. However, newly available lesion filling techniques may allow for automated processing of these patients, allowing their inclusion in connectome analyses (i.e., 'Virtual Brain Grafting'; Radwan et al., 2021). Hence, Study 3 advances the use of a profile of graph metrics at the individual level, including new brain imaging tools to facilitate segmentation in the presence of large, bilateral lesions.

5.1.2 Which graph metrics should be examined in TBI?

The meta-analytic study (Study 1) was used to define which graph metrics were selected for Study 3, and to inform predictions about whether they were expected to be higher or lower in the TBI patients compared with healthy controls. This profiling approach is a major advance in the theoretical reasoning behind the use of graph theory to understand TBI. Previous graph theoretical studies of TBI patient groups were generally exploratory, with no clear rationale behind the selection of graph metrics for analysis, and no theoretically informed hypotheses about group differences. For example, (Yuan, Wade, et al., 2017) predicted that metrics would be *abnormal* in TBI patients compared with healthy controls, and that following training they would normalise. However, normality was not defined in reference to the graph metrics. This is, perhaps, understandable given the exploratory nature of the field and lack of available evidence upon which to base a hypothesis. The meta-analysis in Study 1 provides a comprehensive summary of the graph metric findings in TBI populations compared with healthy controls, providing a foundation for selecting graph metrics and predictions for profiling in Study 3.

Since publication of Study 1, a number of new studies have explored brain alterations in TBI patients using graph theory (see Table 1 for an updated summary of the demographics and processing techniques, and Table 2 for an updated summary of graph metric alterations in TBI). Overall, eight graph metrics were found to be frequently different between TBI patients and healthy controls: strength, global efficiency, characteristic path length, local efficiency, normalised clustering coefficient, clustering coefficient, betweenness centrality, and small-worldness. These same metrics were therefore selected in Study 3, with one exception; small-worldness was not selected because it is a summary statistic of normalised clustering coefficient and normalised path length and, therefore, redundant. Another metric, navigation efficiency (Study 2) (Seguin et al., 2018) was included because it is showing promise as a more specific measure of network communication.

5.1.3 What methods should be used to create the connectome?

As noted in Study 1, due to inherent limitations in tractography it is difficult to directly relate ‘edge’ properties to white matter organisation. The studies included in the meta-analysis were mostly conducted between 2012 and 2017, during which time tractography was largely deterministic and few options were available to address crossing fibres (with the exception of van der Horn et al., 2017; Verhelst et al., 2018). Furthermore, dMRI acquisition was slower and generally had lower b values (750-1200), which means the signal-to-noise ratio was poorer than is available currently. In Study 2 a state-of-the-art diffusion and connectome processing pipeline is described that includes advances in post processing and a short, 6-minute single-shell dMRI acquisition (b=3000) (Dhollander & Connelly, 2016; Dhollander et al., 2019; Dhollander et al., 2016; Smith et al., 2015a; Smith et al., 2012, 2015b). The length of the acquisition was important because it is often difficult for TBI patients to remain still in the scanner for long periods of time. This acquisition and processing pipeline follow very recent guidelines approved by experts in the field (Yeh et al., 2020). The benefits and rationale behind the pipeline are outlined in detail in Study 2 (and in section 6.2.4) and are carried forward in Study 3. While no imaging or processing technique is perfect or future-proof, the methods in this thesis (arguably) represent the best of the current connectome analysis techniques.

5.1.4 Summary

In summary, Study 3 addresses themes raised in the meta-analytic study (Study 1) and employs the methodological advances used in Study 2. Taken together, the findings from these previous two studies are used to inform a novel approach to single-subject profiling of moderate-severe TBI patients in the chronic phase of their injury. This study addresses Aim 3, Research Questions 1, 2, and 3: to facilitate visual comparison of graph metric alterations

in TBI patients compared to healthy controls; observe variability in graph metrics and cognitive performance; and establish the role of graph metrics as biomarkers of TBI. The technique implemented in Study 3 demonstrates a high level of heterogeneity in the six TBI patients included, regardless of their similarities in severity, lesion location and lesion size. Thus, single-subject profiling approaches may allow researchers to capture the range of network alteration patterns in TBI patients.

Table 1

Demographics and Processing Methods for Traumatic Brain Injury Studies Using Graph Theory

	PARTICIPANTS			DATA ACQUISITION		PROCESSING PIPELINE							
	Sample size <i>TBI (HC)</i>	Age range at scan (years) <i>or M(SD)</i>	Ave age at injury (years)	Severity	Time ^a since injury	Number of directions	b-value	Parcellation Scheme	Areas Removed	Number of ROIs	Orientation model	Tractography ^d	Weighted By ^c
Caeyenberghs et al., 2012	12(17)	8 - 20	10.5	Moderate-severe	42 (31.2)	45	800 (1 b0)	Automated Anatomical Labelling	-	116	Principle eigenvector	DT	SD
Caeyenberghs et al., 2013	17(16)	16 - 34	21.2	Moderate-severe	51 (29)	64	1000 (1 b0)	Switching Network	-	22	Principle eigenvector	DT	NOS FA
Caeyenberghs et al., 2014	21(17)	9 - 29	21.3	Moderate-severe	51 (29)	64	1000 (1 b0)	Automated Anatomical Labelling	-	116	Principle eigenvector	DT	%
Dall'Acqua et al., 2016	51(53)	18 - 61	34.5	Mild	0.2	64	1000 (1 b0)	Automated Anatomical Labelling	Cort., subcort. & cerebellar regions	90	Principle eigenvector	DT	NOS
Hellyer et al., 2015	63(26)	37.4 (12.4)	31.9	All ^b	5.5 (3.3)	64	1000 (4 b0)	Destreux (Freesurfer)	-	164	Principle eigenvector	PT	FA
Kim et al., 2014	22(18)	17 - 57	26.0	Moderate-severe	40.9 (75.6)	30	1000 (1 b0)	Desikan (Freesurfer)	Cerebellar regions	95	Principle eigenvector	PT	SCP
Königs et al., 2017	36(27)	8 - 14	7.3	All	33.6 (13.2)	30	750 (5 b0)	Automated Anatomical Labelling and FIRST	Cerebellar regions	84	Principle eigenvector	PT	SLD FA
Solmaz et al., 2017	40(35)	18 - 64	NA	Moderate-severe	3.45 (0.6)	30	1000 (7 b0)	Desikan (Freesurfer)	-	86	Principle eigenvector	PT	NOS
van der Horn et al., 2016	53(20)	18 - 65	33.4	Mild	1 (NA)	60	1000 (7 b0)	Desikan-Killianey and subcortical	Cerebellar and ventricle regions	85	CSD	PT	NOS
Verhelst et al., 2018	17(17)	11 - 17	13.4	Moderate-severe	28.3 (13)	64	1200 (1 b0)	Individual parcellation (Freesurfer)	Not known	82	CSD	PT (ACT)	NOS
Yuan et al., 2015	23(20)	11 - 16	13.7	Mild	0.1 (NA)	61	1000 (1 b0)	Automated Anatomical Labelling	Cort., subcort. & cerebellar	90	Principle eigenvector	DT	NOS
Yuan, Treble-Barna et al., 2017	17(11)	9 - 18	7.8	Moderate-severe	70.9 (37.2)	61	1000 (1 b0)	Automated Anatomical Labelling	Cort., subcort. & cerebellar	90	Principle eigenvector	DT	NOS
Yuan, Wade et al., 2017	22(20)	15.45 (1.72)	15.3	Mild	1 - 4	61	1000 (7 b0)	Automated Anatomical Labelling	Cort., subcort. & cerebellar	90	Principle eigenvector	DT	NOS

PARTICIPANTS				DATA ACQUISITION		PROCESSING PIPELINE						
Sample size <i>TBI</i> (<i>HC</i>)	Age range at scan (years) <i>or M(SD)</i>	Ave age at injury (years)	Severity	Time ^a since injury	Number of directions	b-value	Parcellation Scheme	Areas Removed	Number of ROIs	Orientation model	Tractography ^d	Weighted By ^c
Jolly et al., 2020	92(105)	20 - 80	Moderate-severe	130.4 (154)	64	1000 (4 b0)	Desikan-Killianey and subcortical Automated	-	90	Principle eigenvector	PT	FA
Raizman et al., 2020	22(24)	21 - 44	All	12	25	1000 (1 b0)	Anatomical Labelling	Cort., subcort. & cerebellar	90	Principle eigenvector	DT	NOS
Watson et al., 2019	44(57)	8 - 15	All	2	32	1000 (1 b0)	Desikan-Killianey Atlas	Cerebellar	82	Principal eigenvector	PT	WNOS FA
Mishra et al., 2019	69(70)	18 - 35	RHI	NA	71	1000 (8 b0)	Automated Anatomical Labelling	-	116	Principal eigenvector	DT	NOS x FA
Chung et al., 2019	8(8)	11-16	Mild	0/0.5/12	63	3000 (4 b0)	Desikan-Killianey	Cerebellar and ventricle regions	68	Principal eigenvector	DT (Runga-Kutta)	NOS

Note: ^a TSJ=Time since injury. Time is from the injury/onset until MRI scan for TBI patients, described in months; M(SD)). NA = Not Applicable.

^b 55 of the 63 TBI patients were moderate-severe, and as such Hellyer et al. (2015) was included in the moderate-severe subgroup analyses.

^c NOS = number of streamlines; FA = fractional anisotropy; % = percentage of all streamlines that pass through the node; SD = streamline density (number of fibre connections per unit surface); SLD = the probability of a tract connecting two ROIs; SCP = scaled conditional probability (the number of streamlines from node i to node j, divided by the number of streamlines seeded in node i, scaled by the surface area of the ROI i. WNOS = weighted number of streamlines (by pathway length, ROI size, or both).

^d CSD = constrained spherical deconvolution; DT = deterministic tractography; PT = probabilistic tractography; ACT = anatomically constrained probabilistic tractography

Table 2.

Summary of Literature Comparing TBI Patients to Healthy Controls Using Global Graph Metrics

GRAPH METRICS															
Segregation						Integration					Centrality/ General measures				
Cl	γ	Q	E _{loc}	T	a	E _{glob}	L	λ	b	deg_c	σ	k	D	s	
Caeyenberghs et al., 2012	•	•	•	•	•	•	•	•	•	•	•	•	•	•	•
Caeyenberghs et al., 2014	-	•	•	•	•	•	•	•	•	•	•	•	•	•	•
Helyer et al., 2015	•	•	•	•	•	•	•	•	•	•	•	•	•	•	•
Kim et al., 2014	•	-	•	-	•	•	•	•	•	•	•	•	•	•	•
Königs et al., 2017	•	-	•	-	-	•	-	•	•	•	•	•	•	•	•
van der Horn et al., 2016	-	-	-	•	•	-	•	•	-	•	•	•	•	•	•
Verhelst et al., 2018	•	•	•	•	•	•	•	•	•	•	•	•	•	•	•
Yuan et al., 2015	•	•	•	•	•	•	•	•	-	•	•	•	•	•	•
Yuan, Treble-Barna et al., 2017	•	-	-	•	•	-	•	-	•	•	•	•	•	•	•
Yuan, Wade et al., 2017	•	•	-	•	•	•	•	•	•	•	•	•	•	•	•
Jolly et al., 2020	•	•	•	•	•	•	•	•	•	•	•	•	•	•	•
Raizman et al., 2020	•	•	•	•	•	•	•	•	-	•	•	•	•	•	•
Watson et al., 2019	•	•	•	•	•	•	-	•	•	•	•	•	•	•	•
Mishra et al., 2019	-	-	•	-	•	-	-	-	•	•	•	•	•	•	•
Chung et al., 2019	-	•	-	-	•	•	-	•	-	•	-	•	-	•	•
NUMBER OF STUDIES	6	8	8	7	3	1	10	7	7	5	1	7	1	4	4

Note: ↑ / ↓ higher/lower respectively in TBI patients than in HCs; - no significant difference between TBI and HC; • this metric wasn't measured

Caeyenberghs et al., 2012	•	•	•	•	•	•	•	•	•	•	•	•	•	•	•
Caeyenberghs et al., 2014	-	•	•	•	•	•	•	•	•	•	•	•	•	•	•
Helyer et al., 2015	•	•	•	•	•	•	•	•	•	•	•	•	•	•	•
Kim et al., 2014	•	-	•	-	•	•	•	•	•	•	•	•	•	•	•
Königs et al., 2017	•	-	•	-	-	•	-	•	•	•	•	•	•	•	•
van der Horn et al., 2016	-	-	-	•	•	-	•	•	-	•	•	•	•	•	•
Verhelst et al., 2018	•	•	•	•	•	•	•	•	•	•	•	•	•	•	•
Yuan et al., 2015	•	•	•	•	•	•	•	•	-	•	•	•	•	•	•
Yuan, Treble-Barna et al., 2017	•	-	-	•	•	-	•	-	•	•	•	•	•	•	•
Yuan, Wade et al., 2017	•	•	-	•	•	•	•	•	•	•	•	•	•	•	•
Jolly et al., 2020	•	•	•	•	•	•	•	•	•	•	•	•	•	•	•
Raizman et al., 2020	•	•	•	•	•	•	•	•	-	•	•	•	•	•	•
Watson et al., 2019	•	•	•	•	•	•	-	•	•	•	•	•	•	•	•
Mishra et al., 2019	-	-	•	-	•	-	-	-	•	•	•	•	•	•	•
Chung et al., 2019	-	•	-	-	•	•	-	•	-	•	-	•	-	•	•

5.2 Prepared Article

5.2.1 Title Page

Personalised structural connectome mapping in traumatic brain injury

Phoebe Imms^{a,1}, Adam Clemente^a, Evelyn Deutscher^b, Ahmed M. Radwan^c, Hamed Akhlaghi^d, Paul Beech^e, Peter H Wilson^f, Govinda Poudel^a, Juan F Domínguez D^{b*} & Karen Caeyenberghs^{b*}

^a Mary MacKillop Institute for Health Research, Australian Catholic University; 5/215 Spring Street, Melbourne, VIC 3000, AUSTRALIA.

^b Cognitive Neuroscience Unit, School of Psychology, Faculty of Health, Deakin University; 221 Burwood Highway, Burwood, VIC 3125, AUSTRALIA.

^{cc} KU Leuven, Department of Imaging and Pathology, Translational MRI, Leuven, BELGIUM.

^d Department of Medicine, St. Vincent's Hospital, University of Melbourne. 41 Victoria Parade, Melbourne, VIC 3065, AUSTRALIA.

^e Department of Radiology and Nuclear Medicine, The Alfred Hospital. 55 Commercial Road, Melbourne, VIC 3004, AUSTRALIA.

^f Healthy Brain and Mind Research Centre, School of Behavioural, Health and Human Sciences, Faculty of Health Sciences, Australian Catholic University; 115 Victoria Parade, Fitzroy, VIC 3065, AUSTRALIA.

¹ Corresponding author: Phoebe Imms – phoebe.imms@myacu.edu.au. ORCID identification: 0000-0002-7205-4177

* Joint senior authors

Keywords: Traumatic Brain Injury; structural connectomics; graph theory; personalised medicine; personalised connectomics; lesion filling.

Acknowledgements: We would like to thank Alex Burmester for help with the Hierarchical Drift Diffusion Modelling; and Michael Kean and the radiographers at the Royal Children's Hospital.

Declarations

Funding: This work was supported by an Australian Catholic University Research Fund [#902915]. Govinda Poudel is a Research Fellow on an ACURF Program grant by the Australian Catholic University (ACU). Karen Caeyenberghs is supported by a National Health and Medical Research Council Career Development Fellowship (APP1143816). Phoebe Imms and Adam Clemente are both supported by the Australian Postgraduate Award under the Australian Research Training Program.

Conflicts of Interest: Not applicable.

Availability of data and material: Not applicable.

Code availability: Not applicable.

Authors' contributions:

Imms, P (corresponding): Conceptualisation; Methodology; Software; Formal Analysis; Investigation; Data Curation; Writing – Original Draft; Writing – Review & Editing; Visualisation. *Clemente, A:* Investigation; Resources; Data Curation; Writing – Review & Editing. *Deutscher, E:* Formal Analysis; Writing – Review & Editing. *Ahmed Radwan:* Software; Resources. *Hamed Akhlaghi:* Resources; Data curation. *Beech, P:* Formal

Analysis; Writing – Review & Editing. *Wilson, PH*: Conceptualisation; Resources; Writing – Review & Editing; Supervision; Funding acquisition. *Poudel, G*: Conceptualisation; Methodology; Software; Validation; Formal Analysis; Resources; Data Curation; Writing – Review & Editing; Visualisation; Supervision. *Domínguez D, JF (senior)*: Conceptualisation; Methodology; Software; Validation; Formal Analysis; Resources; Data Curation; Writing – Review & Editing; Supervision. *Caeyenberghs, K (senior)*: Conceptualisation; Methodology; Validation; Formal Analysis; Investigation; Resources; Writing – Original Draft; Writing – Review & Editing; Supervision; Project Administration; Funding Acquisition.

Ethics approval: Ethical approval for the study was obtained from St Vincent’s Hospital Melbourne HREC (250/17) and Australian Catholic University (2017-222R).

Consent to participate: Written informed consent was obtained from each subject prior to testing.

Consent for publication: Participants provided written informed consent for the publication of any associated data.

5.2.2 Abstract

Graph theoretical analyses of the structural connectome have successfully been used to characterise brain network alterations in Traumatic Brain Injury (TBI). However, the population of moderate-severe TBI patients is heterogeneous with regards to cognitive function and neurological outcome, and group-level analyses tend to cancel out variability between subjects. Single-subject profiling approaches can instead be utilised to better represent individual patients. The current study examines cognitive and neurological impairments in six chronic moderate-severe TBI patients who underwent an MRI scan and completed a cognitive test battery. We develop a single-subject graph metric and cognitive profile for each patient comprising their i) cognitive performance, ii) lesion characteristics, iii) personalised connectome, and iv) regional brain network alterations. The individual profiles are compared with a healthy reference group to facilitate interpretation of graph metrics and cognitive performance. We show that cognitive and brain network alterations are highly variable across patients. This customised profile based on clinical manifestations and injuries provides new insights into how a profile of graph metrics, rather than a single metric, can be used to represent structural network alterations in TBI; and devise neuroimaging-guided rehabilitation.

5.2.3 Introduction

Traumatic Brain Injury (TBI) is one of the leading causes of death and disability worldwide, with approximately 27 million new cases recorded every year (James et al., 2019). TBI severity (mild, moderate, or severe) is determined by a combination of factors, including the duration of loss of consciousness, length of post-traumatic amnesia, as well as lesions identified using neuroimaging techniques (Hannawi & Stevens, 2016; Maas et al., 2008; Poudel et al., 2020). Moderate-severe TBI can result in diverse and long-term cognitive impairments including slow processing speed, poor attention and memory, and difficulties with communication and visuospatial processing, leading to significant decline in overall intellectual ability (Rabinowitz & Levin, 2014; Wallace et al., 2018). These impairments can persist for years following injury, interfering with the performance of daily tasks that are essential for independent living.

White matter pathology is strongly considered to be a major cause of cognitive impairment following brain injury (Bressler & Menon, 2010). Executive functions that rely on broadly distributed regions of the brain are hindered due to disruptions to the axonal pathways (Catani & Ffytche, 2005; Hampshire et al., 2016). Numerous studies utilising structural connectomics using diffusion weighted MRI have linked cognitive deficits to different graph theoretical properties of brain networks in TBI patients (e.g., Caeyenberghs et al., 2014; Kim et al., 2014a; Raizman et al., 2020; van der Horn et al., 2017) supporting the *disconnectivity* theory of TBI-related impairment (e.g., Håberg et al., 2015; Hannawi & Stevens, 2016; Hulkower et al., 2013). For example, Kim et al. (2014a) found not only that the average path length was longer in TBI patients compared to controls but also that it was associated with poorer executive functioning and verbal learning. More recently, in a meta-analysis of studies that used graph theory to examine TBI, our group found that only few graph metrics were robustly identified to be altered in TBI across studies – namely,

characteristic path length and normalised clustering coefficient (for review, see Imms et al., 2019). We suggested that this finding reflects, at least in part, the heterogeneous nature of TBI (represented in individual variation in lesion location, severity of injury, time since injury, age, etc.). Because of degeneracy (the brain's ability to attain the same function with different structures; see Mason et al., 2015; Price & Friston, 2002) in response to injury, different graph metrics may be altered across different individuals. As such, examining a profile of graph metric alterations – a literature-driven selection of measures that represent integration, segregation, and centrality – holds promise for capturing the range of individual network alterations caused by brain injury.

As chronic TBI patients are heterogeneous, group-level comparisons do not represent intra-patient variance in brain network topography: thus, they cannot capture individual-specific features (Mant, 1999). There is impetus for the use of individual-level approaches to enable individual diagnosis and treatment planning (e.g., Icometrix: <https://icometrix.com/services/icobrain-tbi>) (Irimia, Chambers, et al., 2012; Irimia, Wang, et al., 2012; Jolly et al., 2021). Recent studies have exploited this heterogeneity with the aim of individualising tract-level comparisons of fractional anisotropy (FA), cortical thickness (CT), and streamline count (Attyé et al., 2020; Jolly et al., 2021; Lv et al., 2020). For example, in their study of Schizophrenia patients, Lv et al. (2020) examined alterations FA and CT in 48 white matter and 68 cortical regions. They found that overall, the Schizophrenia group demonstrated reductions in structural FA and CT. However, the anatomical locations of changes at the individual level were highly inconsistent, and as such group-level maps were not representative of individuals. In a separate study, Jolly et al. (2021) used individual examination of FA in TBI patients in the chronic (>6 months) and subacute (10 days – 6weeks) phases to develop a structural connectivity pipeline for diagnosing diffuse axonal injury (DAI). Patients who were deemed to have DAI were also significantly more likely to

show cognitive impairment or poorer functional outcome. Despite these promising findings, these studies failed to analyse individuals' brain networks, which is possible using *personalised connectomics* (Irimia, Wang, et al., 2012).

Personalised connectomics allow for an individual's brain network to be used as a 'fingerprint' – analogous to genotyping (e.g., The Virtual Brain; Sanz Leon et al., 2013; Schirner et al., 2015). Irimia, Wang, et al. (2012) introduced the idea of personalised structural connectomics for TBI patients as a way to visualise trauma-related white matter atrophy. In particular, they exemplify the need for techniques that allow clinicians to rapidly compare changes in structural connectivity profiles to create personalised rehabilitation programs (Irimia, Chambers, et al., 2012). They characterised white matter atrophy from the acute stage (1-day post-injury) to the chronic stage (7-months post injury) in moderate-severe TBI patients, using a circular graph which highlights the tracts that show evidence of degeneration based on decreases in white matter fibre density. This enabled clinicians to track the location of white matter atrophy over time for each TBI patient. To date, however, no approach has examined an individualised profile of network alterations using graph metrics in TBI patients – whereby a literature-driven selection of graph metrics that summarise segregation, integration, and centrality (Rubinov & Sporns, 2010) are represented for each individual patient. Not only do graph metrics summarise network properties that show relationships with cognitive outcome in TBI patients, but they are also potentially more reproducible than FA and CT across scanning protocols and subjects (Vaessen et al., 2010). This approach could provide valuable information to clinicians leading to neuroimaging guided strategies that help understand and improve outcomes for chronic TBI patients.

In the present study, we describe a novel framework to produce a detailed subject-specific characterisation of cognitive impairments and brain network metrics in moderate-severe TBI patients. Patients underwent an MRI scan and completed a cognitive test battery

that assesses the core domains affected in chronic moderate-severe TBI. Next, single-subject analyses of cognitive data and structural MRI scans were used to provide the following output: (i) a spider plot for the assessment of processing speed, attention, memory and planning (Rabinowitz & Levin, 2014; Ruff et al., 1993) – compared against reference scores in healthy controls to provide information about the magnitude of impairment; (ii) a lesion mask alongside the lesion load derived from the anatomical MRI scan, to identify the brain regions affected in the individual patient; (iii) color-coded segmentation of grey matter regions using the newly available *Virtual Brain Grafting* toolbox, which performs virtual repair of lesioned brains to improve segmentation and parcellation for structural connectome analyses (VBG; Radwan et al., 2021); (iv) graphical representation of the large-scale connectome, i.e. Graph Metrics profile (GraphMe) plot to elucidate subject-specific changes in global integration, functional segregation, and centrality (also compared with a reference sample); and finally v) regional assessment of the hub regions and edge alterations in each TBI patient. We test this single-subject profile in moderate-severe TBI patients with heterogeneous lesions loads, ages, and types of injuries to highlight the translational potential of our individual-level patient structural networks.

5.2.4 Methods

5.2.4.1 Traumatic Brain Injury Cases

Six patients with chronic, moderate-severe TBI were recruited from St Vincent's Hospital in Melbourne. The TBI patients had sustained closed head injuries due to sports or motor-vehicle accidents >6 months prior to testing. Participants were diagnosed with moderate-severe TBI, with clinical factors and initial presentations according to the following criteria: (i) Glasgow Coma Scale score between 3-12 (Teasdale & Jennett, 1974); (ii) loss of consciousness longer than 30 minutes; (iii) post traumatic amnesia longer than 24 hours

(Rabinowitz & Levin, 2014):and (iv) anatomical features of their brain injury including DAI and lesion extent and location (Table 1) as per evaluation by a neuroradiologist (PB).

Informed written consent was obtained from each subject in accordance with the Helsinki declaration, and ethical approval was granted by the St Vincent's Hospital Melbourne ethics committee for human research (project #250/17).

5.2.4.2 Reference population

The resulting individual profiles of cognitive impairments and brain networks need to be evaluated against a reference population of healthy controls. Without this contextual information, it is difficult to meaningfully assess and interpret cognitive impairment and network alterations in single subjects. We therefore also obtained data from 12 healthy controls to be used as a reference cohort in this study (see Table 1). Healthy controls were recruited from the general population using flyers and had to be (a) aged between 18 to 65 years; (b) generally healthy with no history of head injury; and (c) fluent in English, with (d) no history of psychiatric illness (moderate levels of depression and anxiety not included), and (e) no contra-indications for MRI.

Table 1

Summary of Demographics and Clinical Characteristics of the Participants.

ID	Age	Sex	TSI ¹	Cause	Pathology (at testing) ²	DAI ³	IQ ⁴	NFI ⁵
HC	35.7± 11.4	M=4 F=8	-	-	-	-	119± 9	134 ±5
TBII	45y, 3m	M	21y, 0m	Car accident	Small area of encephalomalacia in the (R) precentral gyrus	0	101	133

ID	Age	Sex	TSI ¹	Cause	Pathology (at testing) ²	DAI ³	IQ ⁴	NFI ⁵
<i>TBI2</i>	49y, 10m	M	15y, 6m	Motorbike accident	Large areas of encephalomalacia involving both ant. F and inf. F lobes, (R) T lobe and (R) parietotemporal region extending to the (R) post. F lobe. Focal T ₁ hypointensities in the anteromedial aspect of the (L) thalamus. Volume loss and T ₁ hypointensity on the ant. body and genu of the corpus callosum.	2	106	102
<i>TBI3</i>	49y, 8m	F	3y, 8m	Horse riding accident	Bilateral ant. and inf. F encephalomalacia, (R) greater than (L), and (R) ant. T encephalomalacia. Small deep white matter T ₂ hyperintensities med. (R) P lobe. Small focal T ₁ hypointensity in the ant. body of the corpus callosum.	2	95	234
<i>TBI4</i>	29y, 5m	F	15y, 6m	Horse riding accident	Bilateral inf. F and (L) ant. T encephalomalacia. Small area of encephalomalacia (L) sup. F gyrus. (R) F burr hole with underlying ventricular drain tract.	0/1	91	218
<i>TBI5</i>	50y, 2m	M	18y, 1m	Car accident	Two small nonspecific deep white matter T ₂ hyperintensities in the (R) P lobe (within normal limits for age).	0	104	123
<i>TBI6</i>	29y, 7m	F	5y, 10m	Horse riding accident	Small T ₁ hypointensity in splenium of corpus callosum. Scattered punctate T ₂ hyperintensities in both cerebral hemispheres (approx. 6).	2	120	120

Note: ¹TSI=Time since injury (years, months). ²Abbreviations: (R) = right, (L) = left, ant. = anterior, post. = posterior, inf. = inferior, mid. = middle, med. = medial, sup. = superior, F = frontal, P = parietal, O = occipital, T = temporal. ³Grading of diffuse axonal injury (DAI) occurred according to Adams et al. (1989); a grade of '0' indicates no confirmed DAI present, '1' indicates DAI present in white matter of cerebral hemispheres, corpus callosum, brainstem, cerebellum; '2' indicates there is also a focal lesion in corpus callosum; and '3' identifies an additional lesion in dorsolateral quadrants of brainstem. ⁴IQ was measured using the Weschler Abbreviated Scale of Intelligence Vocabulary and Matrix Reasoning subtests (Revised edition; WASI-II; Weschler, 1999; "Superior" = >130; "Very high" = 120-129; "Bright normal" = 110-119; "Average" = 90-109; "Low average" = 80-89; "Borderline mental functioning" = 70-79). ⁵The Neurobehavioural Functioning Index (NFI) is a measure of self-reported daily life cognitive function, where scores above 157 (in **bold**) indicate 'abnormal' cognitive function (Kreutzer, Seel, & Marwitz, 1999).

5.2.4.3 Cognitive testing

Eight cognitive tasks from the computerised Psychological Experimental Building Language test battery (Mueller & Piper, 2014) were used to evaluate core cognitive domains that are commonly affected in chronic moderate-severe TBI patients (Rabinowitz & Levin, 2014; Ruff et al., 1993), including The Go/No-Go task (response inhibition), Vigilance (sustained attention), the Corsi Blocks task (visuospatial working memory), the Digit Span task (verbal working memory span), Letter Digit Substitution (processing speed), Connections (mental flexibility), the Global-Local Task (decision making speed), and the Tower of London task (planning). These tasks have also been recommended by the ENIGMA-TBI consortium (Olsen et al., 2020). For full descriptions of the tasks, see Supplementary Table 2. Cognitive data were acquired using a Dell Inspiron 15-3537 laptop (response latency=80ms; refresh rate=60Hz; stimulus display was synchronised to device refresh rate).

5.2.4.4 MRI data acquisition

MRI scans were performed at the Royal Children's Hospital 3T Siemen's PRISMA 64-channel head coil scanner. Diffusion MRI (dMRI) data were acquired using a single-shot echo planar imaging sequence (twice-reinforced spin echo, multi-band acceleration factor of 2, 70 contiguous sagittal slices) and a high angular resolution diffusion imaging (HARDI) gradient scheme with 66 non-collinear gradient directions ($b=3000\text{s/mm}^2$, $R \gg L$, FOV = 260mm^2 , voxel size = 2.3mm isotropic, TR = 3500ms, TE = 67ms). Seven $b=0$ images were interspersed throughout the HARDI scheme, and two reverse phase-encoded $b=0$ images were also collected to allow for correction of susceptibility induced echo planar imaging distortions. The total acquisition time of the entire dMRI data was 6:17mins. T₁-weighted images were also acquired for each participant with magnetisation-prepared rapid gradient-

echo acquisition (208 contiguous slices, FOV = 256mm², voxel size = 0.8mm isotropic, TR = 2100ms, TE = 2.22ms, flip angle = 8°), with a total acquisition time of 5:48min.

5.2.4.5 Lesion masking

Manual lesion delineation for computation of lesion load and for improvement of anatomical segmentation was performed by a blinded assessor (ED), who was trained in lesion identification by neuroradiologist (PB). Lesions were drawn in the T1 native space using Fsleyes version 0.27.3 in FSL version 6.0.1 (<https://fsl.fmrib.ox.ac.uk/fsl/fslwiki>). An in-house systematic search method and lesion identification protocol was developed by JD, KC, ED, and PB to ensure accurate lesion delineation. Abnormalities resulting in tissue loss, such as regions of encephalomalacia or gliosis and damage as a result of surgical drainage tracts were included in binarised lesion masks. Enlarged ventricles and hyperintensities often occurring in proximity to the skull (e.g., as a result of surgical craniotomies) were not included in the lesion masks. Lesion load was computed (in cm³) as the total volume of the binary lesion masks in FSL.

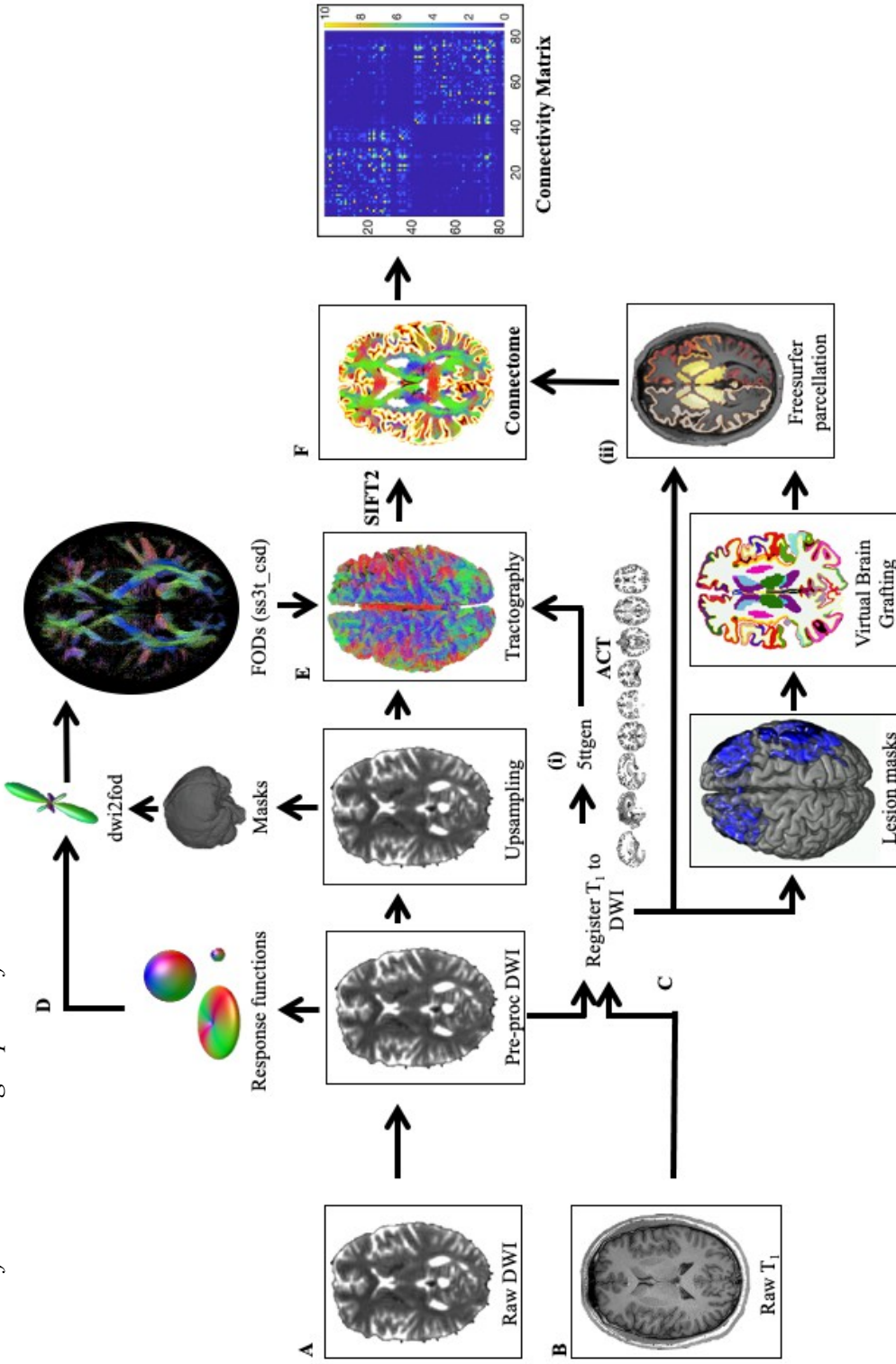
5.2.4.6 Personalised connectome construction

Preprocessing: An overview of our connectome processing pipeline can be seen in Figure 1. Raw dMRI data were processed using MRtrix3Tissue (v5.2.8; <https://3tissue.github.io>), a fork of MRtrix3 (Tournier et al., 2019). First, noise (Cordero-Grande et al., 2019; Veraart et al., 2016), Gibbs ringing artefacts (Kellner et al., 2016), and motion, eddy current distortions and susceptibility induced (EPI) distortions were detected and corrected (Andersson et al., 2003; Andersson & Sotiropoulos, 2016). Slices that were greater than two standard deviations from the average were replaced automatically by FSL's outlier correction (Andersson et al., 2016). After outlier correction, motion values were below the voxel size of image acquisition for each patient except TBI2 (TBI2_{rms}=5.41mm;

see Figure 2); this patient was excluded from subsequent diffusion imaging analyses. Next, average response functions for white matter, grey matter, and cerebrospinal fluid were estimated from the dMRI data using an automated unsupervised approach (Dhollander et al., 2019; Dhollander et al., 2016).

Figure 1

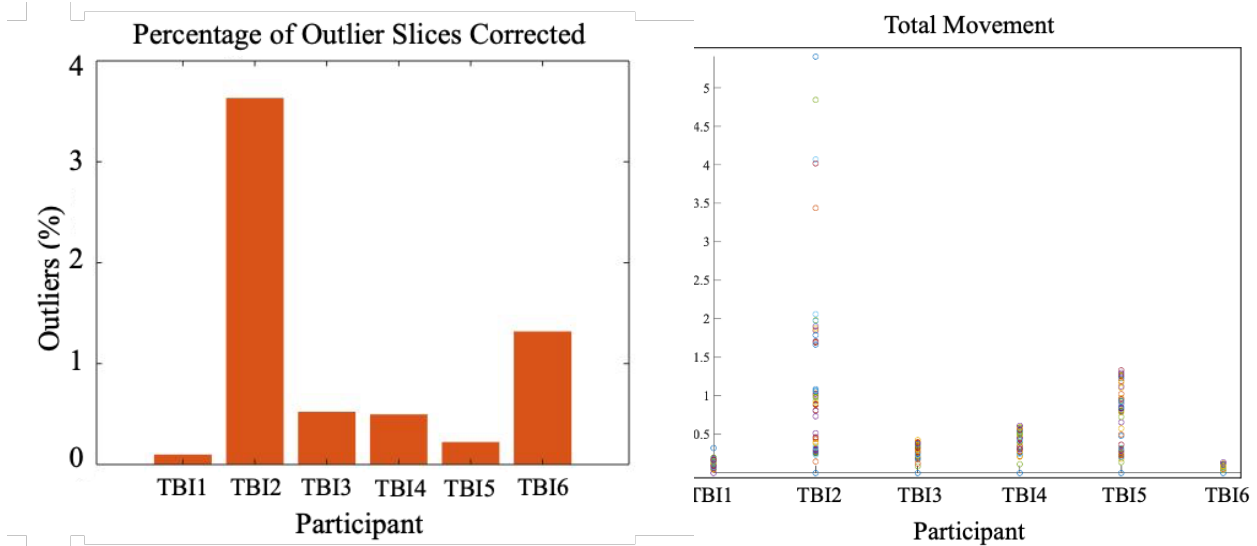
Overview of the Processing Pipeline for Connectome Construction



Note: Overview of the processing pipeline for connectome construction. (A) Raw diffusion images are preprocessed to remove artefacts (noise, Gibbs-ringing, motion correction, distortion correction). (B) Concurrently, T₁ images are registered to diffusion images for (i) 5tgen, to create images for anatomically constrained tractography (ACT), and (ii) Freesurfer, to parcellate the nodes for the connectome analysis. (C) Lesion maps of subjects who failed the quality assessment after Freesurfer parcellation are provided along with the T₁ image (in diffusion space) to VBG for improved anatomical segmentation. (D) Fibre orientation distributions (FODs) are estimated from the group average response functions on upsampled images, and intensity normalised. (E) Anatomically Constrained Tractography (ACT) is performed using the FODs from (D) and the 5tgen images from (B(ii)), before Spherically Informed Filtering of Tractograms (SIFT2) is applied to filter the streamlines and to make the weight of the streamlines proportional to the underlying fibre orientation distribution. (F) The connectome is created using the Freesurfer parcellation and the sifted tractogram.

Figure 2

Head Motion Summary for Six TBI Patients



Note: Outlier slices are corrected by eddy motion correct, by removing and replacing with corrected slices; Data points in the Total Movement plot represent the root mean square movement for each volume ($n=67$).

Edge reconstruction: Pre-processed data were up-sampled to a voxel size of 1.3mm^3 to improve spatial resolution for image registration before binary masks were created. To estimate the white matter fibre orientation distributions (FODs) in each voxel, single-shell 3-tissue constrained spherical deconvolution (SS3T-CSD) was performed on the upsampled data (Dhollander & Connelly, 2016). SS3T-CSD preserves the angular information of the GM- and CSF-like signal, removing contributions from these components to increase the specificity of the WM FODs, while avoiding over estimation into GM and CSF signal from the lesioned area (Khan et al., 2020). Finally, the resulting FODs were corrected for intensity inhomogeneity and global intensity level differences (Raffelt et al., 2017).

The advanced normalisation tools package (ANTs; Avants et al., 2009) was used to remove non-brain structures from the T1 weighted images for white matter extraction (Zhang

et al., 2011). Next, FSL FLIRT (Jenkinson et al., 2002; Jenkinson & Smith, 2001) was used to perform the boundary-based registration between brain-extracted anatomical and diffusion images. MRtrix's 5 tissue-type segmentation script was then used on the T₁ images in dMRI space to create the relevant masks for tractography (Smith et al., 2012).

Next, we performed whole brain anatomically constrained tractography (Smith et al., 2012). The FOD cut-off threshold, step size, and angle were carefully determined to attain a reasonable trade-off between false negatives and false positives (seed points=dynamic; maximum length=250mm; minimum length=5mm; step size=1.25; angle=45°; FOD amplitude cut-off threshold = 0.08). Twenty-two million streamlines were generated to keep connectome variability low enough for SIFT2 to be relatively stable (Yeh et al., 2018). Next, the SIFT2 algorithm was applied to match the density of the reconstructed streamlines to that of the underlying white matter structures (Smith et al., 2015a; Smith et al., 2015b; Yeh et al., 2018). A proportionality coefficient μ was also calculated for each participant to be later applied to the connectome edge weights to ensure these are proportional to the apparent fibre density.

Node reconstruction: Anatomical images were parcellated using Freesurfer's *recon-all* function (v6.0; <http://surfer.nmr.mgh.harvard.edu/>), as described in previous publications (e.g., Fischl & Dale, 2000). In brief, for all anatomical images subcortical grey-matter structures were segmented (Fischl et al., 2002); image intensity normalised (Sled et al., 1998); pial surfaces and the grey-white matter boundaries estimated (Dale et al., 1999); and the entire brain “inflated” to smooth the gyri and sulci (Fischl et al., 1999). On this surface model the automated cortical and subcortical parcellation of 84 regions was generated using the Desikan-Killiany atlas (Desikan et al., 2006). Quality control was performed by inspecting output of the Freesurfer pipeline at each stage using stringent ENIGMA guidelines

(<http://enigma.usc.edu/>). Two patients (TBI3 and TBI4) did not pass the ENIGMA Freesurfer quality checks, due to significant segmentation failures in the presence of pathology. These patients were therefore run utilising the new virtual brain grafting (VBG v0.37) image processing pipeline to improve segmentation (Radwan et al., 2021). In brief, lesions are filled with healthy tissue from synthetic ‘donor brain’ images – either leveraging tissue from the native non-lesioned hemisphere for unilateral lesions, or a healthy synthetic donor brain for bilateral lesions. The resulting lesion free patient image is then passed through the Freesurfer *recon-all* pipeline, enabling improved segmentation in the absence of any structural pathology. VBG Freesurfer output for these three patients was again checked against ENIGMA quality control guidelines and any remaining errors were then corrected using control points in Freesurfer (Fischl, 2012). Finally, connectivity matrices were generated using the streamline weights from SIFT2, and area size normalisation occurred by scaling weights to the inverse of the volumes of the nodes they connect (Hagmann et al., 2008).

5.2.4.7 Graph Theoretical Analysis

We quantified the network architecture in terms of *strength*, *global efficiency*, *characteristic path length*, *navigation efficiency*, *local efficiency*, *clustering coefficient*, *normalised clustering coefficient*, and *betweenness centrality* (Table 3), using the Brain Connectivity Toolbox (Rubinov & Sporns, 2010). We selected these graph metrics, as they have previously been found to be significantly altered in moderate-severe TBI populations (Imms et al., 2019). Graph normalisation occurred by 1) normalising edge weights between 0 and 1, and 2) weight-to-length remapping using -log transformation (for global efficiency, characteristic path length, local efficiency, and navigation efficiency only). Graph metrics were calculated for each TBI patient individually. Graph metrics were also computed from the group connectivity matrix of the 12 healthy control subjects; and 95% confidence

intervals for the healthy control graph metrics was used as an estimation of variability in the absence of injury.

Table 3

Graph Metric Descriptions, Interpretations, and Evidence from Previous TBI Studies

Graph Metric	Description	Higher values mean...	Previous studies (Adult moderate-severe TBI)
<i>Integration</i>			
<i>Characteristic Path Length</i>	The shortest path is the fastest and most direct communication pathway between two network nodes. Characteristic path length is defined as the average shortest path length between all node pairs in a network (Watts & Strogatz, 1998).	A higher characteristic path length indicates that the fastest communication pathways between regions are, on average, longer and less efficient.	Higher CPL (Caeyenberghs et al., 2014; Hellyer et al., 2015; Kim et al., 2014)
<i>Global Efficiency</i>	The inverse average shortest path efficiency between all possible pairs of nodes in a network, where efficiency is computed as the inverse of shortest the path length (Latora & Marchiori, 2001).	A higher global efficiency will indicate a greater capacity for efficient integration of information (in parallel) across the network.	Lower global efficiency (Caeyenberghs et al., 2014)
<i>Navigation Efficiency</i>	Navigation paths are use a decentralised and geometrically greedy heuristic (Bogunã et al., 2009). Navigation efficiency is defined as the average navigation path efficiency between all possible pairs of nodes in a network (Seguin et al., 2018).	Higher navigation efficiency indicates greater capacity for efficient integration of information across the network.	Not yet investigated, but lower navigation efficiency observed in stroke patients (Wang et al., 2019)
<i>Segregation</i>			

Graph Metric	Description	Higher values mean...	Previous studies (<i>Adult moderate-severe TBI</i>)
<i>Clustering Coefficient</i>	The number of existing connections between the neighbours of a node, divided by all the possible connections, calculated for each node individually and averaged across the entire network (Watts & Strogatz, 1998).	A higher average clustering coefficient means that a greater proportion of connections are made between nodes neighbours, compared to the connections possible, and indicates more clustered connectivity around individual nodes.	Lower clustering coefficient (Hellyer et al., 2015; Raizman et al., 2020).
<i>Normalised Clustering Coefficient</i>	Clustering coefficient of the network normalised to a random network.	Higher normalised clustering indicates higher local specialisation, with a value of 1 being equivalent to a random network. If greater than 1, the network has greater than random clustering. There may be a point of diminishing returns, where greater local specialisation comes at the cost of communication efficiency.	Higher normalised clustering (Caeyenberghs et al., 2012; Verhelst et al., 2018)*
<i>Local Efficiency</i>	The local efficiency is the average of inverse shortest path length in a local area. Mean local efficiency is taken as the efficiency of each node in the network averaged over the total number of nodes (Latora & Marchiori, 2001).	A higher local efficiency means greater capacity for integration between the immediate neighbours of a given node.	Higher local efficiency (Jolly et al., 2020); AND/OR lower local efficiency (Caeyenberghs et al., 2012)*
Centrality			
<i>Strength</i>	The strength of a node is the sum of the weights of its edges. Mean strength is the average of all the normalised strength values across each node of the network.	A higher strength indicates a greater average edge weight for each node.	Lower strength (Raizman et al., 2019)

Graph Metric	Description	Higher values mean...	Previous studies (<i>Adult moderate-severe TBI</i>)
<i>Betweenness Centrality</i>	The proportion of shortest paths that pass-through node i between its neighboring nodes, calculated for each node and averaged across the network (Freeman, 1978).	Higher betweenness centrality means that node lies on more shortest paths in the network pass through it, and this that node is more central and important to the network. A high network/average betweenness centrality indicates a high number of nodes that are central to shortest paths.	Higher betweenness centrality (Caeyenberghs et al., 2012)*

* Note: this study is of young adults and children with TBI – no adult TBI study found significant alterations or examined this metric.

5.2.4.8 Cognitive and Network Profiles

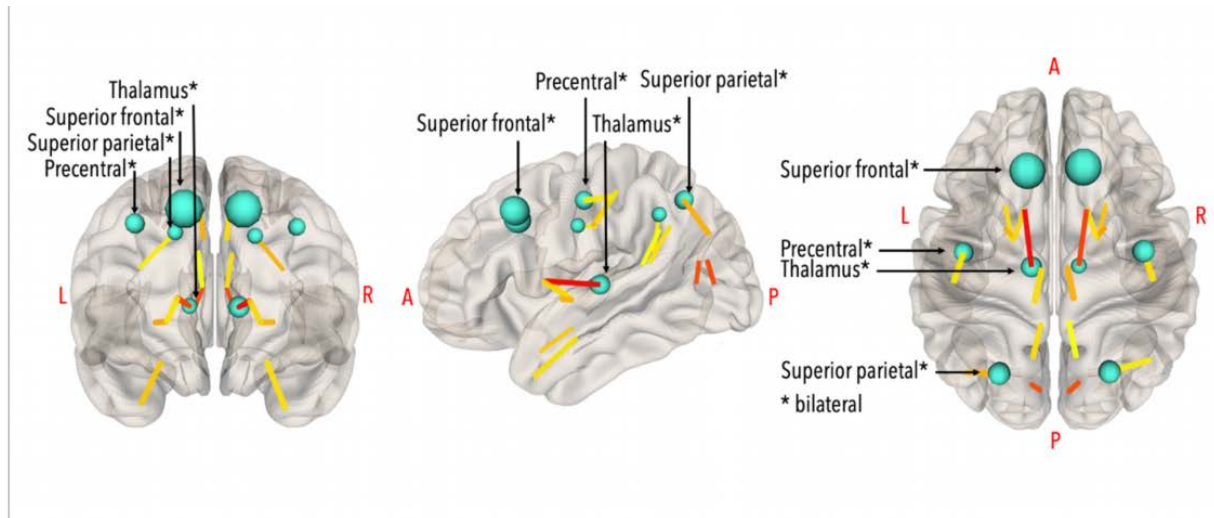
Two Spiderplots were used to efficiently represent TBI patients' results: one for cognitive performance and another one for brain network metrics (GraphMe plots). Each axis of the plot represents a cognitive task or a graph metric. Response averages from the healthy controls are represented on the Spiderplot as a 95% confidence interval for visual comparison. Importantly, measures are recoded so that *lower* scores on any measure indicate *worse* performance or brain structure, by using the inverse of the scores (for cognitive performance: Tower of London, Letter Digit Substitution, and Vigilance; for graph metrics: characteristic path length, normalised clustering coefficient, and betweenness centrality – see Table 3). This facilitates rapid comprehension of the Spiderplot, where the smaller area of the TBI patient scores compared to the healthy cohort is indicative of worse cognitive performance or brain network structure. Scores were categorised as *normal* (within the 95% confidence interval); *supra-normal* (higher than the 95% confidence interval); or *infra-normal* (lower than the 95% confidence interval) (Lv et al., 2020).

5.2.4.9 Regional analyses

Alongside the graph analysis, we compared the ‘hub’ nodes identified in the TBI patients vs. in the healthy controls, using steps outlined in Fagerholm et al. (2015) and Raizman et al. (2020). We used *betweenness centrality* to identify the brain regions that are most crucial for communication within the brain network (Freeman, 1978; Rubinov & Sporns, 2010). Betweenness centrality was calculated for each of the 84 nodes, and the top 10% ($n=8$) highest scoring nodes were identified as ‘hubs’. Hubs were visualised using NeuroMARVL (<https://immersive.erc.monash.edu/neuromarvl/>). The healthy control comparison hubs are shown in Figure 3.

Figure 3

Healthy Control Hub Regions



Note: Healthy control hub regions (top 10% of nodes with highest betweenness centrality), in light blue. Larger nodes represent higher betweenness centrality values. The strongest edges are also shown (0.5th percentile, 0.002% of edges, 18 edges shown), coloured by strength (yellow=weaker; red=stronger).

Edge analysis was performed to examine in greater detail the specific connections that were driving overall differences in the network properties. A z -score matrix $Z_{i,j}$ was derived, which describes the distance from the healthy control mean, divided by the healthy control

standard deviation, between each subject's connectivity matrix $T_{i,j}$ and the controls $H_{i,j}$ according to equations given for an edgewise analysis in Wills and Meyer (2020):

$$Z_{i,j} = \frac{T_{i,j} - \mu(H_{i,j})}{\sigma(H_{i,j})}$$

Positive scores represent stronger edges in the TBI patient compared to controls, while negative scores represent weaker edges. To visualise the z -score matrix, only edges with a score >4 (i.e., edges 4 standard deviations from the healthy control mean, representing a highly stringent 99.99% confidence interval) remain while all other edges are discarded. These edges are shown as a visual representation of graph differences between healthy controls and the TBI case.

5.2.5 Results

Presented below are the personalised profiles for six TBI patients as follows: (A) Cognitive profiles of planning, processing speed, memory, and attention domains, and NFI and IQ scores (see Table 1 for relevant scales). (B) Lesion maps drawn in mrMicroGL by ED, resulting lesion load and DAI score. (C) Quality assessment of the connectome pipeline including segmentation of cortical and subcortical parcels in Freesurfer (6.0; Fischl, 2012), fibre orientation distributions from single-shell 3 tissue constrained spherical deconvolution (mrtrix3tissue; Dhollander et al., 2019) and 5 tissue-type image for streamline generation, and registration of anatomically constrained tractography (Smith et al., 2012) with labelled subcortical and cortical parcels of the Desikan-Killianey atlas (Desikan et al., 2006). (D) GraphMe plot including healthy average with 95% confidence interval (blue), and TBI patient (red). (E) Regional and hub analyses including (i) healthy control hub nodes in pink

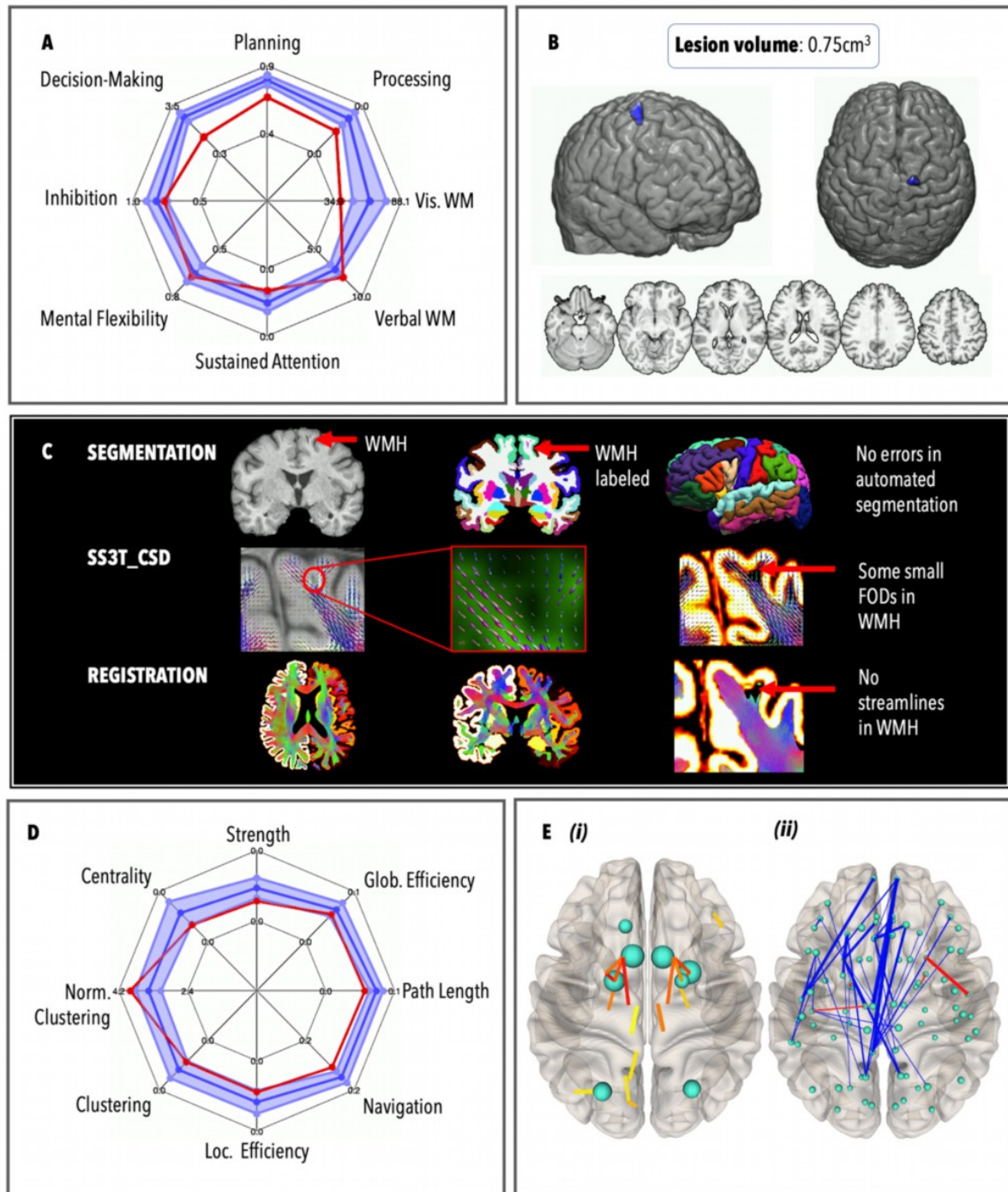
and TBI patient hub nodes in green, with strongest 0.5th percentile of edges represented (yellow = weaker edges; red = stronger edges), and (ii) comparison of edge weights from the z-score matrix (blue = edges lower than the healthy control average; red = edges stronger than the healthy control average; and thicker edges = larger number of standard deviations away from the healthy mean).

5.2.5.1 TBI1

Summary: TBI1 (45yo, TSI=21y) self-reported a normal level of cognitive complaints (NFI=133); and had intelligence score within the normal range (IQ=101). However, their cognitive profile demonstrates slow decision-making and processing speed, poor planning, and short visuospatial working memory capacity compared to healthy controls (see Figure 4a). This patient has a small lesion load and a DAI grade of 0. The GraphMe plot indicates that TBI1 has slightly weaker integration than healthy controls, in particular longer path lengths and lower navigation efficiency. Interestingly, the right superior frontal gyrus (perilesional) was a hub node in the healthy controls but was not a hub node in TBI1. We also observed many weaker edges in TBI1 compared to the healthy controls, in particular connecting the bilateral frontal poles and left temporal regions (especially the left temporal pole).

Figure 4a

Personalised Connectome Profile for TBI1



Note: **Cognitive profile:** Infra-normal performance on four cognitive tests, including *processing speed*, *planning* and *memory* (panel A); **Lesion profile:** Small lesion (load=0.75cm³) in the right precentral gyrus (panel B); **Quality Assessment:** There were no failures in the Freesurfer pipeline, no manual edits were made and there was no need for virtual brain grafting (panel C). FODs were generated at the site of the lesion (see red arrow) but did not meet streamline criteria for ACT. Registration between structural and diffusion images was unaffected by this lesion; **Personalised connectome profile:** The GraphMe plot (panel D) shows very similar global graph metric properties compared to the healthy cohort. Navigation efficiency and path length were infra-

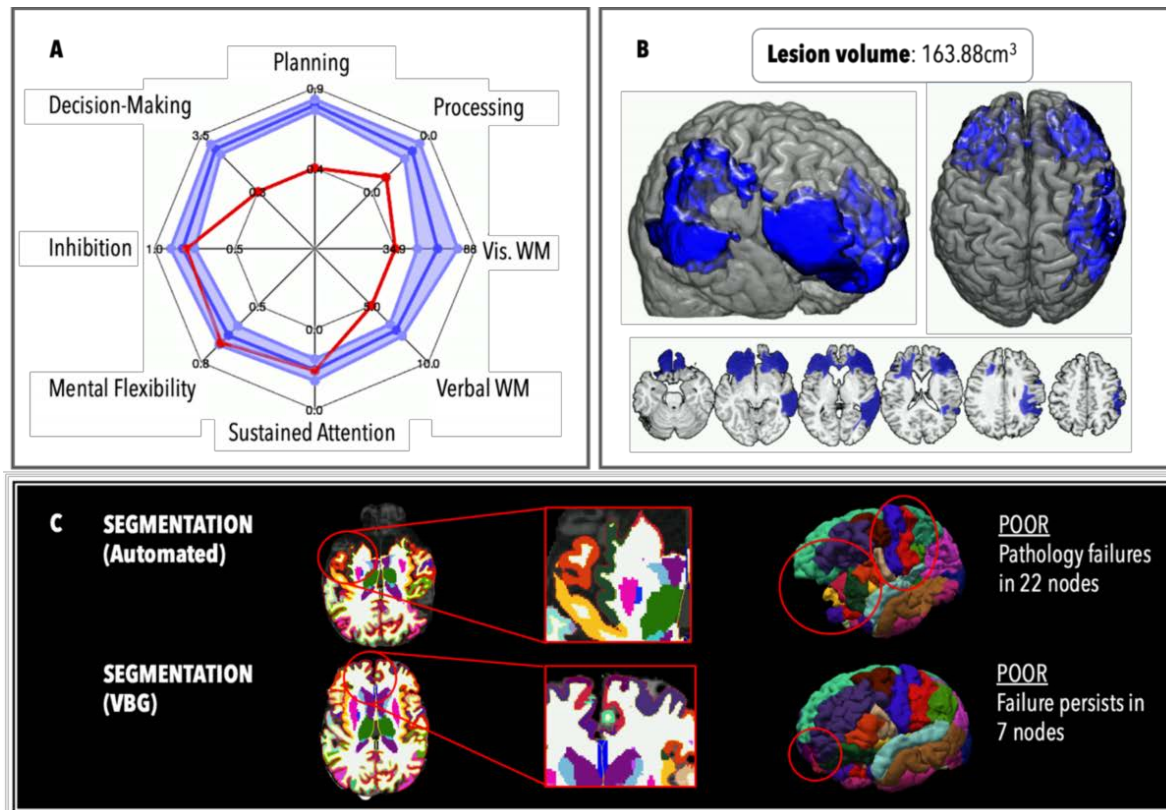
normal; **Regional analysis:** Four alterations in the hub arrangement for TBI1 were observed (panel E(i)), whereby the bilateral accumbens ($BC_{\text{left}}=1570$; $BC_{\text{right}}=1546$), palladium ($BC_{\text{left}}=1382$; $BC_{\text{right}}=978$) and right putamen were hubs ($BC_{\text{right}}=1578$), and the bilateral precentral gyri, thalamic, and right superior frontal gyrus did not meet the hub threshold. Weaker edges ($n=43$; panel E(ii)) were observed projecting across frontal, parietal, temporal, and subcortical areas, in particular the edges left posterior cingulate to right frontal pole ($z=-8.32$), the left superior temporal to left frontal pole ($z=-6.66$), the left lateral orbitofrontal to left temporal pole ($z=-7.98$) and the left medial frontal to left temporal pole ($z=-6.90$; panel E(ii)). Some stronger edges ($n=4$) were also observed, including the connection between the right superior temporal to right temporal pole ($z=5.92$).

5.2.5.2 TBI2

Summary: TBI2 (49yo, TSI=15y) self-reported a normal level of cognitive complaints (NFI=102) and had intelligence scores within the normal range (IQ=106). However, this patient showed severe cognitive deficits in processing speed, planning, and working memory (see Figure 4b). Demonstrating a clear lack of insight, this patient had the lowest self-reported level of cognitive complaints on the NFI, well below the healthy control cohort average. TBI2 also had a very large lesion load and a DAI grade of 2. Quality assessment of VBG performance demonstrated that VBG repaired 15 nodes for parcellation/segmentation. Note: personalised connectome analysis not performed due to excessive head motion.

Figure 4b

Personalised Cognitive Profile for TBI2.



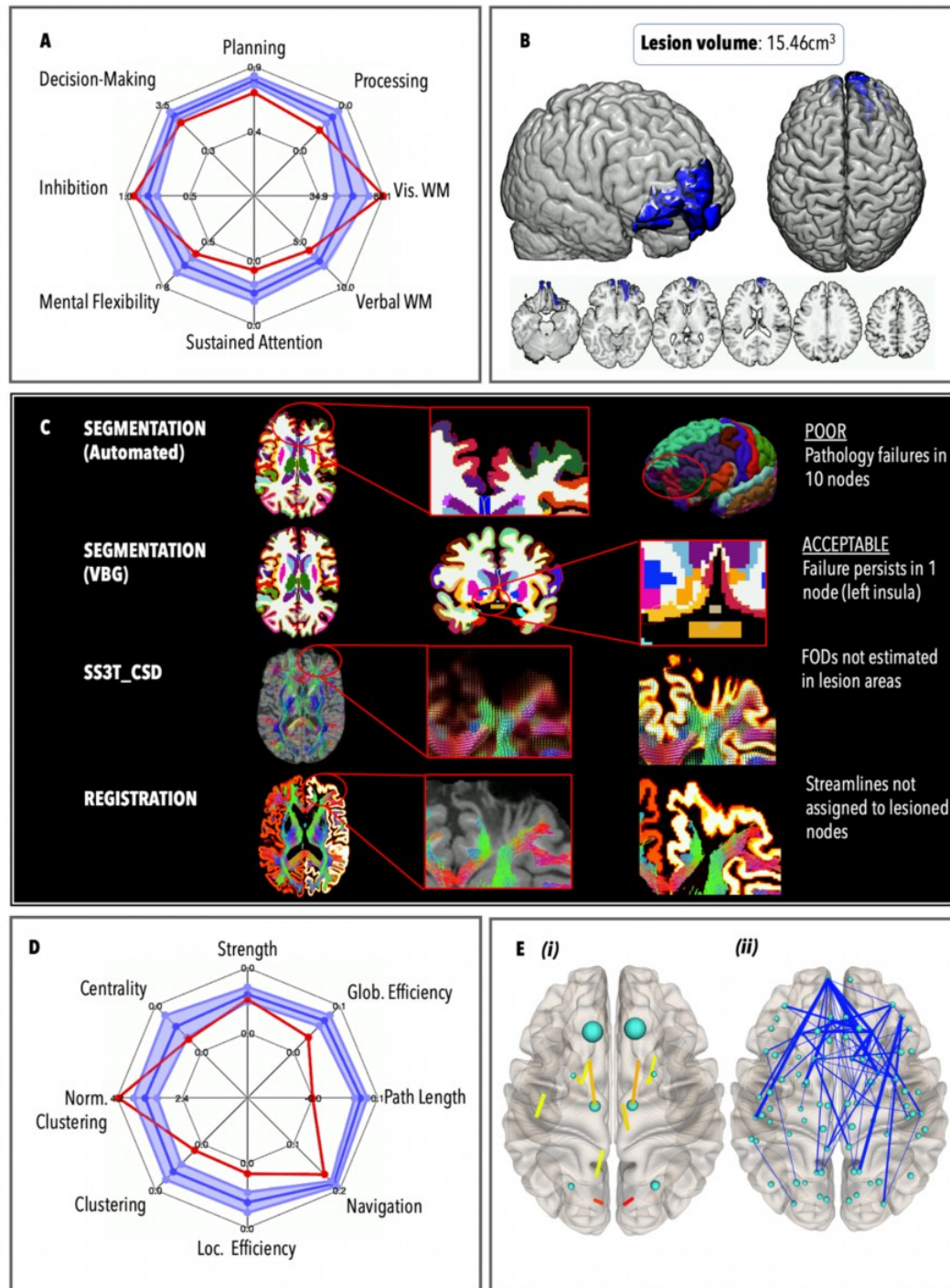
Note: **Cognitive profile:** Infra-normal performance on five cognitive tests, including *processing speed*, *planning* and *memory* domains (panel A); **Lesion profile:** Extensive bilateral frontal, and right parietal and temporal lesions (load=163cm³; panel B), as well as focal hypointensities in the left thalamus and body and genu of the corpus callosum; **Quality Assessment:** Prior to VBG, 22 nodes failed the quality assessment (panel C). VBG improved segmentation in 15 nodes. The remaining 7 nodes are located predominantly in lesioned areas. Constrained spherical deconvolution based on the single-shell 3 tissue FODs was not generated at the site of the lesions (see red arrow in panel C), and registration between VBG reconstructed nodes and streamlines show that streamlines were not assigned to lesioned nodes.

5.2.5.3 TBI3

Summary: TBI3 (49yo, TSI=3y) had intelligence scores within the normal range (IQ=95) but self-reported a high level of cognitive complaints (NFI=234). Accordingly, this patient demonstrated poor performance in all cognitive domains (processing speed, planning, memory, and attention; see Figure 4c). This patient had moderate-large lesion load involving frontal and anterior temporal regions predominantly, and a DAI grade of 2. VBG improved parcellation and segmentation from ‘poor’ to ‘acceptable’, allowing the inclusion of this patient with moderate-large lesion load in the connectome pipeline. TBI3 showed reductions in all network domains, with the exception of normalised clustering (supra-normal); and centrality and strength (normal). Finally, this patient showed 62 weaker edges, in particular projecting bilaterally from the frontal cortex to the subcortical regions such as the accumbens, caudate, and amygdala.

Figure 4c

Personalised Connectome Profile for TBI3.



Note: **Cognitive profile:** Infra-normal performance on five cognitive tests including *processing speed*, *planning*, *memory*, and *attention* domains (panel A); **Lesion profile:** Moderate-large lesion load (load=17.59cm³) including bilateral frontal and right temporal lesions (panel B), white matter hyperintensities in the medial right parietal lobe and the corpus callosum; **Quality Assessment:** Prior to VBG, 10 nodes failed the quality assessment (panel C). VBG repaired 9 nodes for parcellation. Registration between VBG reconstructed nodes and streamlines show that streamlines were not assigned to lesioned nodes; **Personalised connectome profile:** The GraphMe plot (panel D) demonstrates a mixed graph metric profile, with infra-normal integration and both

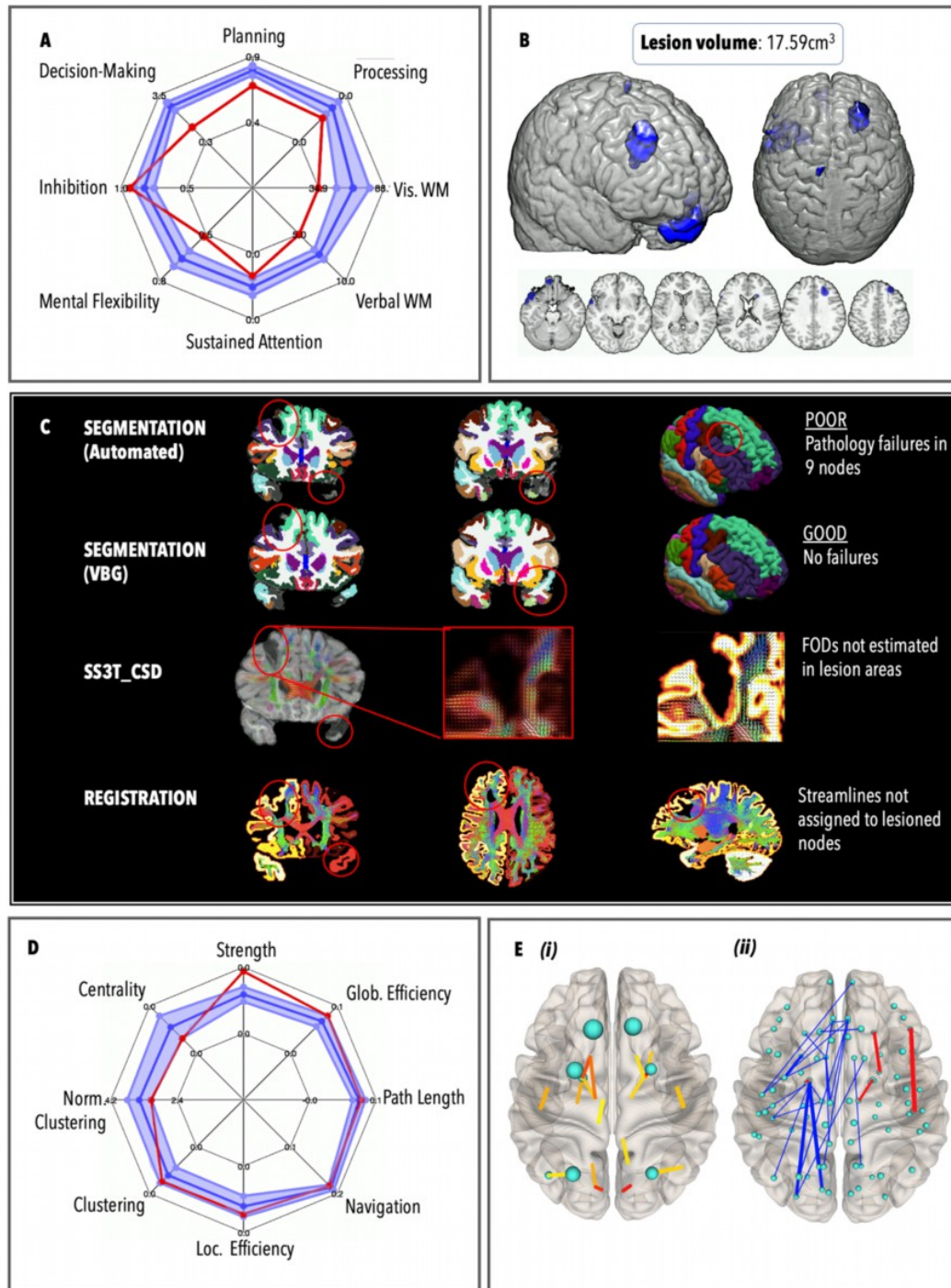
infra- and supra-normal segregation measures. Specifically, less efficient network communication as measured by both path length and navigation routing models; poorer segregation as indicated by lower clustering, but also lower normalised clustering; **Regional analysis:** Two hub alterations were observed (panel E(i)), whereby the bilateral putamen ($BC_{\text{left}}=871$; $BC_{\text{right}}=932$) were hubs, and the bilateral precentral gyri were not hubs. Weaker edges ($n=62$; panel E(ii)) projected across the whole brain, in particular in the frontal regions including the left frontal pole to the left middle temporal ($z=8.45$), right superior frontal ($z=8.12$), right lateral orbitofrontal ($z=8.17$), and right putamen ($z=8.41$); left medial orbitofrontal to left amygdala ($z=8.67$); right lateral orbitofrontal to the right accumbens ($z=8.03$) and right caudate ($z=8.33$); and the right pars orbitalis to right lingual ($z=8.10$). No stronger edges were observed.

5.2.5.4 TBI4

Summary: TBI4 (29yo, TSI=15y) had intelligence scores within the normal range (IQ=91) but self-reported a high level of cognitive complaints (NFI=218). Accordingly, this patient was infra-normal in the processing speed, planning, and memory domains (see Figure 4d). They had moderate-large lesion load involving frontal and anterior temporal regions predominantly, though their DAI grade was low (0/1). This patient showed minimal deviation from the healthy control network profile, in fact showing supra-normal strength indicating stronger edge weights relative to node size. Overall, the network analysis portrays a relatively good neurological outcome for TBI4, despite their cognitive complaints. They had only 26 weaker edges in left temporal and parietal regions, coinciding with the location of the lesions in the left anterior temporal lobe and left inferior and superior frontal gyrus.

Figure 4d

Personalised Connectome Profile for TBI4



Note: **Cognitive profile:** Infra-normal performance on six cognitive tests, including *processing speed*, *planning* and *memory* domains (panel A); **Lesion profile:** Moderate-large lesion load (load=17.59cm³), including bilateral lesions in the superior frontal, the left temporal pole and inferior temporal regions, as well as a smaller lesion in the left precentral gyrus (panel B); **Quality Assessment:** Prior to VBG, 9 nodes failed the quality assessment (panel C). VBG repaired all nodes for parcellation. Constrained spherical deconvolution based on the single-shell 3 tissue generated no FODs at the site of the lesions, and streamlines were not assigned to lesioned nodes. **Personalised connectome profile:** The GraphMe plot (panel D) demonstrates normal global graph metric

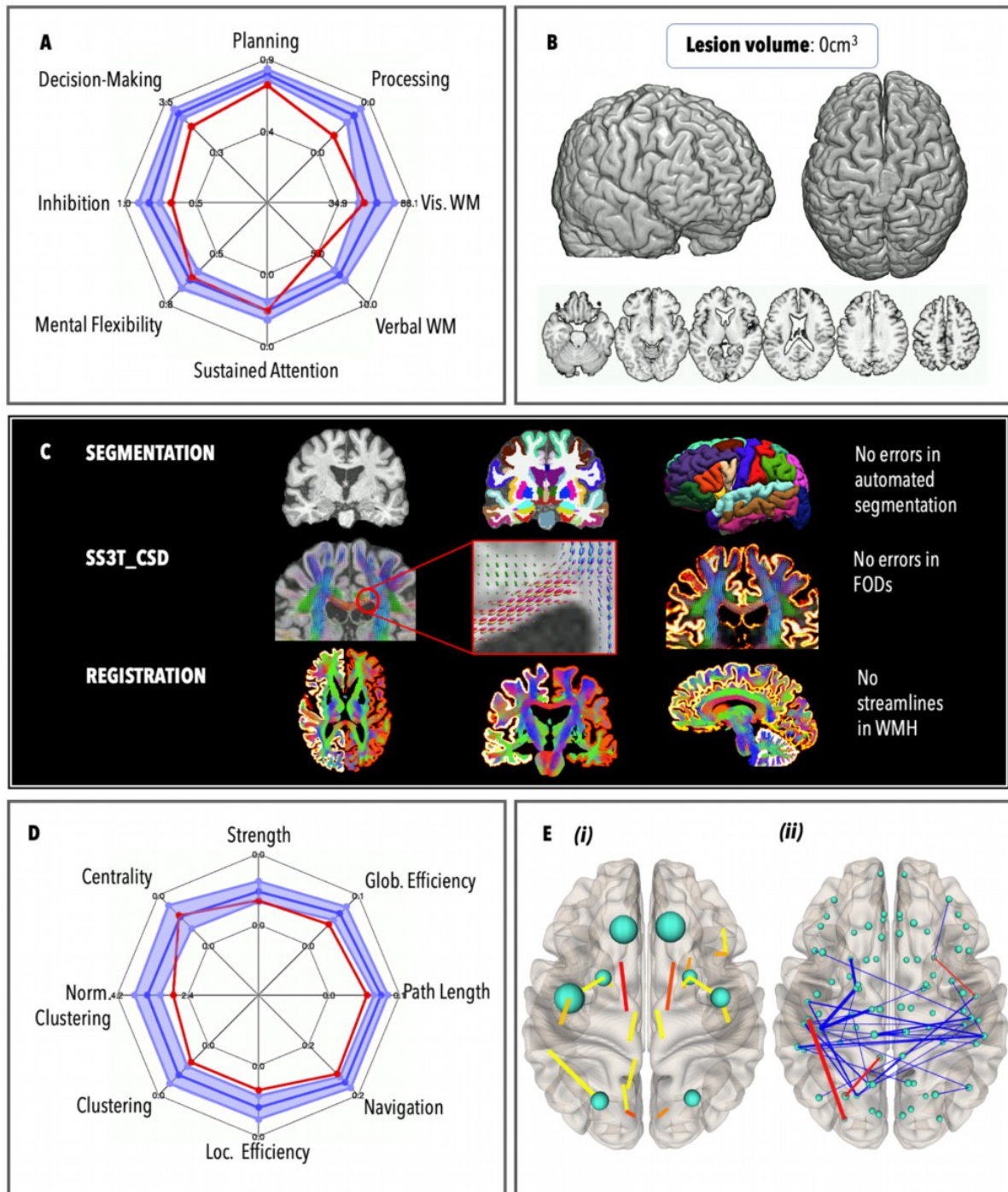
properties, although strength was supra-normal; **Regional analysis:** Four alterations in the hub arrangement were observed (panel E(i)), whereby the bilateral putamen ($BC_{\text{left}}=2246$; $BC_{\text{right}}=1550$), left palladium ($BC_{\text{left}}=1210$) and left inferior parietal ($BC_{\text{right}}=902$) were hubs, and the bilateral precentral gyri and thalamic regions were not hubs. Weaker edges ($n=26$; panel E(ii)) projected across the left hemisphere, in particular the entorhinal to the lingual gyrus ($z=10.87$), pericalcarine ($z=9.55$), superior parietal ($z=9.46$), and lateral occipital regions ($z=9.33$); the temporal pole to the insula ($z=9.37$); and the accumbens to the posterior cingulate ($z=6.71$), insula ($z=6.30$), and rostral anterior cingulate ($z=5.98$). Some stronger edges ($n=4$) were also observed in the right hemisphere, including the pars triangularis to post central ($z=5.92$), putamen to lateral orbitofrontal ($z=4.86$), pallidum to thalamus ($z=4.24$); and the left pallidum to amygdala ($z=4.55$).

5.2.5.5 TBI5

Summary: TBI5 self-reported a normal level of cognitive complaints ($NFI=123$) and had intelligence scores within the normal range ($IQ=104$). This patient also showed no lesion load and DAI grade of 0. However, cognitive testing revealed reduced processing speed, poor response inhibition, and short verbal working memory (see Figure 4e). While their hub arrangement was largely similar to the healthy controls, TBI5 demonstrated a wide array of weaker edges connecting the parietal, temporal, and subcortical hemispheres. Accordingly, they showed deviation from the healthy cohort in terms of integration, as these longer distance connections are important for efficient communication. However, their weakest edges (compared to healthy controls) were short-distance connections contained in the left hemisphere, connecting subcortical regions such as the amygdala and hippocampus with temporal regions such as the inferior temporal gyrus and the temporal pole.

Figure 4e

Personalised Connectome Profile for TBI5



Note: **Cognitive profile:** Infra-normal performance on five cognitive tests, in the *processing speed*, *planning*, *attention*, and *memory* domains (panel A); **Lesion profile:** No masked lesion load on the T1 image (load=0cm³; panel B); **Quality Assessment:** there were no failures in the Freesurfer pipeline, and no manual edits were made (panel C). FODs were generated correctly and registration between segmentation and tractography was clean; **Personalised connectome profile:** The GraphMe plot (panel D) demonstrates infra-normal global connectivity properties, with the exception of centrality and strength. Global efficiency, navigation efficiency and path length are infra-normal, indicating less efficient network communication; and local efficiency, clustering, and

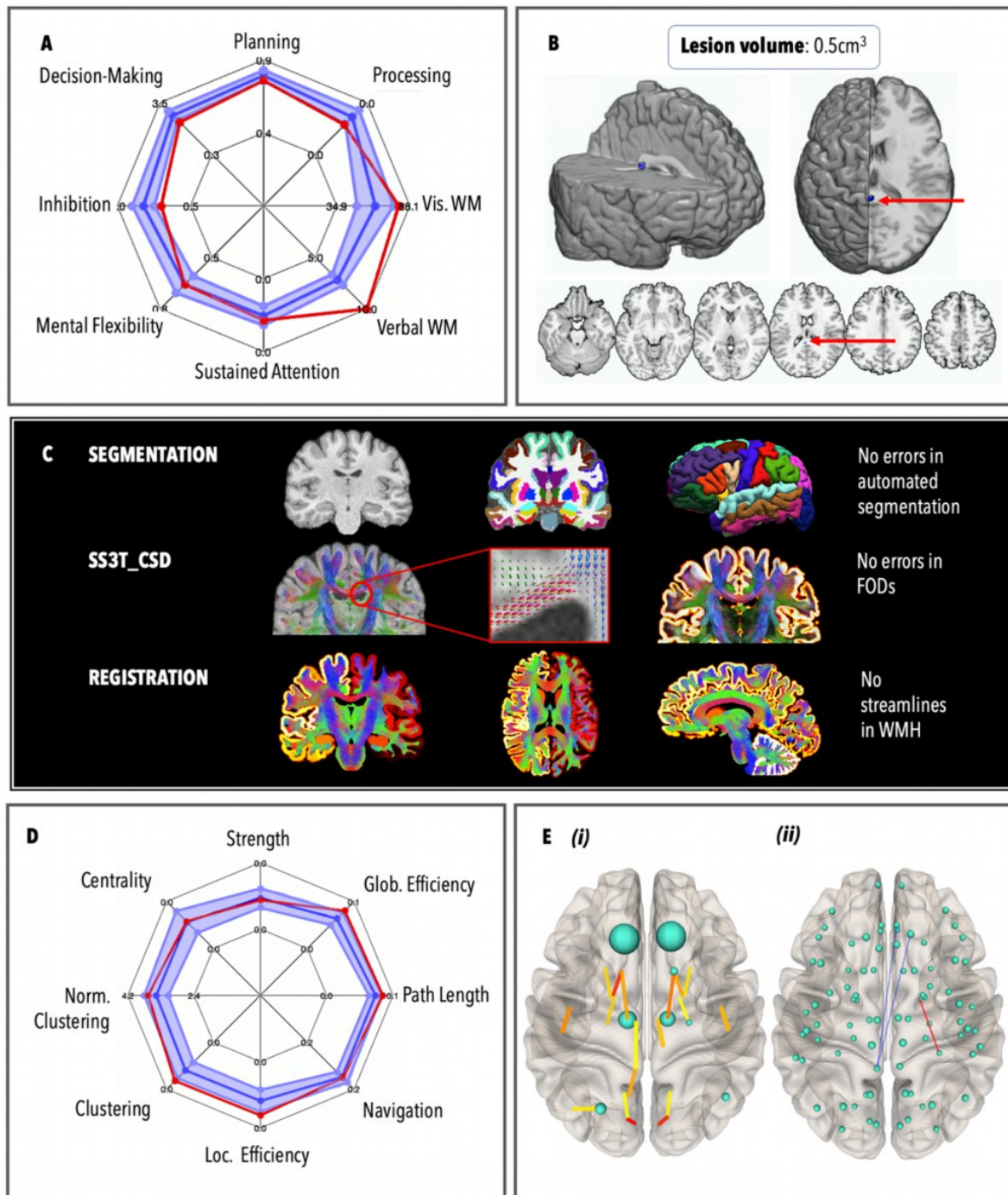
normalised clustering are also infra-normal indicating altered segregation; **Regional analysis:** Two alterations in the hub arrangement were observed (panel E(i)), whereby the bilateral putamen were hubs ($BC_{\text{left}}=1182$; $BC_{\text{right}}=1110$), while the bilateral thalamic regions were not hubs. Weaker edges ($n=33$; panel E(ii)) projected inter-hemispherically in parietal, temporal, and subcortical areas. The weakest edges (compared to healthy controls) were in the left hemisphere, from the amygdala to the temporal pole ($z=-7.19$); the amygdala to the inferior temporal gyrus ($z=-7.80$); the inferior temporal gyrus to the hippocampus ($z=-6.11$); and the inferior temporal gyrus to the thalamus ($z=-6.40$). Some stronger edges ($n=3$) were also observed, including the connection from the left post central gyrus to the left lateral occipital gyrus ($z=5.87$).

5.2.5.6 TBI6

Summary: TBI6 (29yo, TSI=5y) self-reported a normal level of cognitive complaints (NFI=120); and had a ‘very high’ intelligence score (IQ=120). They had a small lesion in the splenium of the corpus callosum, which is one of the most common locations for DAI (Park et al., 2017; Uchino et al., 2006) – symptoms are often relatively mild in lesions of this type (Park et al., 2014) – and a DAI grade of 2. Quality assessment revealed no parcellation errors (see Figure 4f). This patient showed only slightly reduced response inhibition and very strong memory scores, a normal GraphMe plot, and no weaker edges than the healthy controls.

Figure 4f

Personalised Connectome Profile for TBI6



Note: **Cognitive profile:** Infra-normal performance on only one cognitive test, in the *attention* domain (panel A); **Lesion profile:** TBI6 had a lesion (load=0.5cm³) in the splenium of the corpus callosum (panel B); **Quality Assessment:** There were no failures in the Freesurfer pipeline, and no manual edits were made (panel C). FODs were generated at the site of the lesion but did not meet streamline criteria for ACT; **Personalised connectome profile:** The GraphMe plot (panel D) shows no significant alteration in the graph metric profile – global connectivity properties of TBI6 are normal except for global efficiency, local efficiency and clustering which are marginally supra-normal. **Regional analysis:** Three hub alterations were observed (panel E(i)), whereby the

right caudate ($BC_{\text{right}}=722$), right hippocampus ($BC_{\text{right}}=606$) and right inferior parietal gyrus ($BC_{\text{right}}=680$) were hubs, and the bilateral precentral and right superior parietal regions were not hubs. No edges met the stringent threshold of being ± 4 standard deviations from the healthy control mean (panel E(ii)).

5.2.6 Discussion

In this paper, we present a novel approach to connectomics and cognitive profiling illustrated in six adult patients with chronic moderate-severe TBI. Here, we discuss the benefits of personalised connectomics, and how examination of individual TBI patients facilitates interpretation of unique disconnectivity profiles. First, we detail observations from our single-subject profiles; next, we examine how our single-subject profiling approach adds to the field of personalised connectomics in the care of chronic TBI patients; and finally, we explore the next steps in improving our methods for personalised structural connectome analyses in individuals with TBI.

5.2.6.1 Single-subject cognitive and network profiling observations

Our observations highlight an important caveat in the search for a single graph metric ‘biomarker’ that can represent alterations in the structural network of all TBI patients. Like Lv et al. (2020) in their study of FA and CT in Schizophrenia patients, the pattern of alterations we observed was not homologous. As expected, due to the heterogeneity of moderate-severe TBI patients, we observed that each TBI patient had a unique *pattern* of cognitive and graph metric alterations. This observation is underscored by the fact that patients with relatively similar lesion loads, and severities show clearly distinct profiles of network alterations. For example, TBI1 and TBI6 both have small lesion loads, but TBI1 shows slowed processing speed and planning, and less efficient network communication measures. Meanwhile, TBI6 shows minimal deviation from the normal range for both cognitive and brain network measures. Similarly, TBI3 and TBI4 both have moderate-large

lesion loads and infra-normal cognitive performance, but TBI3's brain network profile shows infra-normal integration and segregation measures while TBI4's brain network was normal. This indicates that there may not be a single graph metric that can capture the range of changes caused by TBI – highlighting the importance of this individual *profiling* approach.

This study also broaches an often discussed but rarely addressed problem – that TBI patients are neurologically and cognitively heterogeneous. Many earlier studies using a graph theoretical analysis deal with this heterogeneity by separating TBI patients according to their diagnosed severity (mild, or moderate-severe; for review, see Imms et al., 2019). Grouping by injury severity in this way is common in graph theoretical studies (e.g., Hellyer et al., 2015; Königs et al., 2017; Raizman et al., 2020; Watson et al., 2019). These studies then purport to have found a graph metric that may serve as a 'biomarker' of a particular severity of TBI. However, the examples outlined above demonstrate that separating by diagnosed severity or even lesion load may not be sufficient to control for heterogeneity in this population. In contrast, our single-subject network profiles suggest that TBI patients of similar severities can exhibit vastly different patterns in hub and edge arrangements due to other injury and personal characteristics.

Another interesting case is TBI5, who had only two small age-appropriate hyperintensities in the right parietal lobe, and a lesion load of 0mm³. This patient, however, shows impairments in processing speed, planning, verbal working memory, and inhibition, as well as infra-normal integration and segregation properties. This supports the *disconnectivity* theory of TBI – where executive functions are impaired due to disruptions to the axonal pathways they rely on (Catani & Ffytche, 2005) – and thus the presence or absence of focal grey-matter lesions does not always explain ongoing cognitive deficits. This patient exemplifies the fact that using diffusion-based graph metric analysis can reveal brain network

alterations where T₁ anatomical scans do not (for review, see Hulkower et al., 2013). Overall, these five TBI patients reinforce the benefits of using network profiling to characterise TBI patients in the years following their injury – revealing individual differences in cognition and brain network topology that may otherwise have been overlooked.

Finally, our six chronic patients all showed ongoing but different cognitive impairments across core cognitive domains. This raises the importance of continued cognitive assessment and intervention for patients with TBI, even years post-injury. While most patients demonstrated good insight into the extent of their injuries and their impact, some (i.e., TBI2) rated their neurobehavioral functioning as better than normal despite showing poorer cognitive performance on almost the entire cognitive testing battery. This patient had extensive areas of encephalomalacia in the frontal regions, which may explain this lack of insight and poor cognition (Milner, 1982; Owen et al., 1990). This reiterates the need to not rely on self-report in TBI patients (for a review of evidence-based cognitive rehabilitation practices for TBI patients, see Stephens et al., 2015).

5.2.6.2 Informing clinical assessment and rehabilitation programs using personalised connectomics

We illustrate that a personalised connectomics approach has a role for assessing TBI patients in three main ways: First, connectome maps can be used as a profile of the patient's brain network topography, providing researchers and clinicians a quick visual summary of network disruption, asymmetry, hub alterations, and overall reductions in strength. Second, by comparing the brain network of an individual patient to healthy control data, we can observe areas of the network that are topologically altered beyond the site of the focal lesion. For example, although TBI1 had focal lesions in the right precentral gyrus, their connectome also revealed weaker edges in left frontal and temporal regions in comparison to healthy

controls. Finally, we can observe these alterations longitudinally to assess network-based alterations over the time course of the injury and in response to treatment regimens, as the brain undergoes progressive secondary damage and structural and functional reorganisation (e.g., Meninger et al., 2020; Osmanlıoğlu et al., 2019). Examination of GraphMe plots over the course of the acute to chronic period could be used to examine whether dedicated customised neurorehabilitation improves network connectivity longitudinally, akin to the longitudinal assessment of white matter atrophy performed by Irimia, Chambers, et al. (2012). This exploratory work enables us to progress towards a personalised medicine approach, which, alongside group-based comparisons of patients against controls, is essential for translating structural MRI to evidence-based practice.

The current study builds on the work of Irimia, Chambers, et al. (2012), who introduced the idea of personalised structural connectomics to create personalised rehabilitation programs. There is evidence that individual network- and connectivity-based profiles can inform neuroimaging-guided rehabilitation (Dichter et al., 2012; Stoeckel et al., 2014; Wing et al., 2017), and assist health professionals to design personalised cognitive training and rehabilitation programs. The ultimate goal is to help clinicians better understand individual patients and potentially lead to personalised therapies to help improve chronic outcomes. For example, TBI1 (45yo male, TSI=21y, IQ=101, NFI=133) presented with a 0.75cm³ lesion in the right precentral gyrus, and showed (i) reduced processing speed, planning, and working memory, in the presence of (ii) longer path lengths and lower navigation efficiency; weaker edges projecting from frontal regions to parietal, temporal, and subcortical regions; and loss of frontal and thalamic hubs (Figure 4a). With further validation (see below), this assessment profile could indicate that TBI1 may benefit from an attention,

planning, and working memory neurorehabilitation program targeting white matter projections from the right superior frontal regions to the precentral gyrus and thalamus.

5.2.6.3 Improving methods for personalised connectomics

Our cognitive- and network-based approach demonstrates structural connectivity alterations in TBI patients and provides an assessment of individual profiles of graph metrics. Before the graph metric profiling approach can be considered for clinical application, the GraphMe plots require validation and assessment of test-retest reliability. Indeed, we emphasise that any comparison between an individual TBI patient and the healthy control reference group ($N=12$) is done as a proof of concept, as was done in a similar design by Attyé et al. (2020) with $N=20$ healthy controls. As a preliminary step, normative analysis with large sample sizes of healthy individuals would allow for stronger statistical inferences to be made using techniques like quartile regression, as seen in Lv et al. (2020) and Jolly et al. (2021).

We also highlight the need for statistical methods for individual-level analyses that do not violate assumptions of statistical models (Mycroft et al., 2002). We used 95% confidence intervals to determine if cognitive performance or graph metrics were infra- or supra-normal. However, this method only models variation in the healthy cohort but *not* in the TBI patients. Keeping in mind that the purpose of this study is to demonstrate the use of personalised connectomics in a handful of cases, improvements to this technique will involve reference intervals (the range of values deemed ‘normal’) designed to perform individual comparisons to group-level normative datasets (approximately $N>100$; Hansen et al., 2007) – a technique that has recently been used and does not violate statistical assumptions (Lv et al., 2020).

The use of VBG should be encouraged in the efforts to advance personalised connectomics, as it avoids the exclusion of cases with large focal lesions that fail Freesurfer

segmentation (e.g., TBI3 and TBI4). Often, studies will use lesion masks and manual edits of the white matter volume mid-way through the Freesurfer pipeline (e.g., Siegel et al., 2017), to re-align the segmentation and labelling of nodes. However, these methods are time-consuming and not reproducible across labs (Beelen et al., 2020). Instead, the implemented approach proposed by Radwan et al. (2021) utilises a novel method for automatic filling of uni- and bilaterally lesioned brains using healthy synthetic donor tissue, to improve segmentation without manual edits. Our implementation of the personalised connectomics approach therefore represents an important step in developing a framework for retaining TBI cases that are otherwise being excluded. Further steps towards improving this approach include incorporating other imaging modalities for lesion identification such as FLAIR or susceptibility weighted imaging (we used only T₁ images, thus it is possible we missed some WM pathology); and validating VBG using the healthy donor image against true bilateral lesions (Radwan et al., 2021).

Finally, we observed that the single-shell 3 tissue model for CSD (SS3T-CSD) (Dhollander et al., 2020; Dhollander et al., 2019) was suitable for constructing connectomes in the presence of lesions with TBI lesions. SS3T-CSD preserves the angular information of the GM- and CSF-like signal, removing contributions from these components to increase the specificity of the WM FODs, while avoiding over-estimation into GM and CSF signal from the lesioned area (Khan et al., 2020). Combined with anatomically constrained tractography (Smith et al., 2012), streamlines were not generated in lesioned areas, meaning anatomically disconnected regions were not removed from the connectivity matrix. This allows us to calculate graph metrics from connectivity matrices that are the same size (84x84) as those of the healthy controls, making comparisons more interpretable.

5.2.6.4 Conclusions

Observations from these six cases reinforce the need for single-subject analyses to be re-evaluated in the context of network alterations following brain injury. Profiling individual patients based on their unique injury presentation provides insights into the heterogeneity of network-based alterations in moderate-severe TBI patients. This can help identify patterns or subgroups (otherwise obscured by group-level approaches) that can then be further explored in group-level studies. Finally, this study provides clinicians with a novel framework for using graph metrics to characterise cognitive performance and brain network structure. Future development of GraphMe plots can augment assessment and planning of cognitive training programs in conjunction with conventional approaches, by providing clinicians with personalised structural network alteration profiles for individual TBI patients.

5.2.7 Supplementary Materials

Supplementary Table 2

Detailed Description of the PEBL Test Battery

Name	Task Description	Cognitive Ability	Variables	Reference/link to Wiki
Go/No-Go	A simple continuous performance task. For the first part of the test, the participant must respond to P's (Go trials), but not R's (No-Go trials). There are more P's than R's. In the second part, responses to R's (Go trials), not P's (No-Go trials) must be made. There are less R's than P's.	<i>Attention</i> Response inhibition	Number and average reaction time (RT) of correct and incorrect responses, for go and no-go trials.	Go/No-go Task Bezdjian, S. Baker, L. A., Lozano, D. I & Raine, A. (2009). Assessing inattention and impulsivity in children during the Go/NoGo task. <i>Br J Dev Psychol.</i> 2009 June 1; 27(2): 365–383
Tower of London	Traditional problem solving/planning task. Tests ability to make and follow plans in problem solving task. Participants must match the pattern of stacked discs in as few moves as possible. The pattern must be matched on colour, stack, and position of the disc within the stack.	<i>Planning</i> Problem solving	Total movements and RT for overall task, mean movements and RT per trail.	Tower of London Shallice T. (1982), <i>Philosophical Transactions of the Royal Society of London, B</i> , 298, 199-209.
Corsi Blocks	An implementation of the classic spatial working memory test. The participant must reproduce the sequence of blocks after they light up by clicking on the box, in the correct order. Number of locations to reproduce increases with success.	<i>Memory</i> Visuospatial working memory span	Longest sequence correctly remembered.	Corsi Blocks Corsi, P. M. (1972). Human memory and the medial temporal region of the brain. <i>Dissertation Abstracts International</i> , 34, 819B.
Digit Span	The task is to reproduce the sequence of numbers heard, in the correct order. If the participant completes two correct trials of a particular length, sequence length increases by one digit.	<i>Memory</i> Verbal working memory span	Longest sequence correctly remembered.	Digit Span Croschere, J., Dupey, L., Hilliard, M., Koehn, H., & Mayra, K. (2012). The effects of time of day and practice on cognitive abilities: Forward and backward Corsi block test and digit span. <i>PEBL Technical Report</i>

Name	Task Description	Cognitive Ability	Variables	Reference/link to Wiki
				Series [On-line], #2012-03.
Letter-Digit Substitution	A 9-option version of the 'code substitution' task. Participants are asked to match the letter that appears on the screen with its corresponding number, according to the code.	<i>Processing speed</i>	Number and RT of correctly identified codes.	Letter-Digit Task Perez, W. A., Masline, P. J., Ramsey, E. G. and Urban, K. E. (1987). Unified Tri-services cognitive performance assessment battery: Review and methodology, DTIC Document ADA181697
Connections	A trail-making test based on Salthouse et al. (2000), originally based on Zahlen Verbindungs Test. In the control trials, the participant has 20 seconds to create as large a trail as possible by connecting letters or digits (as directed). In the switch trials, the trials alternate between letters and digits (e.g., A-1-B-2).	<i>Processing speed</i> Mental flexibility	Mean length and accuracy of sequences.	Connections Salthouse, T. A., Toth, J., Daniels, K., Parks, C., Pak, R., Wolbrette, M., et al. (2000). Effects of aging on the efficiency of task switching in a variant of the Trail Making Test. Neuropsychology, 14, 102–111.
Global Local Task	A basic version of Navon's (1977) global-local task. The participant must respond to either the large (global) or small (local) stimuli, an 'S' or 'H', as directed. Stimuli are both congruent (e.g., a large 'S' made of small 's's) or incongruent (e.g., a large 'S' made of small 'h's).	<i>Processing speed</i> Decision-making time	Number of correct/incorrect stimuli, and RT of neutral, congruent, and incongruent trials.	Global Local Navon, D. (1977). Forest before trees: The precedence of global features in visual perception. Cognitive Psychology, 9(3), 353-383.

Name	Task Description	Cognitive Ability	Variables	Reference/link to Wiki
Vigilance	A novel vigilance task requiring both rest and vigilance periods (similar to standard Test of Attentional Vigilance). The participant must wait for an X to appear in the circle. A cross appears before each trial, to alert the participant that a response will be required soon. When the X appears in the circle, the participant must respond as fast as possible. If the letter is not an X, the participant must not respond.	<i>Attention</i> Sustained attention	RT to X trials.	PEBL Vigilance Task Forbes, G. B. (1998). Clinical Utility of the Test of Variables of Attention (TOVA) in the Diagnosis of Attention-Deficit/Hyperactivity Disorder. <i>Journal of Clinical Psychology</i> , 54 (4), 461-476.

Chapter 6: General Discussion and Conclusions

6.1 Restatement of the Research Aims and Main Findings

6.1.1 Summary by chapter

The purpose of this dissertation was to investigate the relationship between brain injury with cognitive symptoms and disruptions in the brain network using graph theory. First, a systematic review and meta-analysis of studies of adults with moderate-severe injuries was conducted. Next, the behavioural relevance of graph metrics was explored in a proof-of-concept study in healthy adults, where the relationship between measures of network communication and processing speed was used to evaluate whether graph metrics can be interpreted in terms of cognitive performance. Finally, a novel visualisation approach was developed to analyse the profile of graph metric alterations in single-subject TBI patients compared to healthy controls.

In Study 1 (Chapter 2), a systematic review and meta-analysis assessed the consistency of recent graph theoretical studies of TBI (Imms et al., 2019). Findings suggested that normalized clustering coefficient and characteristic path length are altered in TBI patients compared to healthy controls: characteristic path length was also robust across studies and subgroups. The meta-analysis revealed evidence that the TBI brain network is closer to a regular lattice structure than healthy controls and that graph metrics have potential as diagnostic and prognostic biomarkers. Study 1 also raised pertinent issues prevalent in the TBI graph theory literature that became the focus of the remaining empirical chapters. These issues included over-interpretation of the relationship between graph metrics such as characteristic path-length and the ‘efficiency’ of cognitive processes – leading to an empirical report studying this relationship in more detail (Study 2). Finally, limitations of the group-level analyses that combine heterogeneous patient samples and discard patients with large lesions were discussed, forming the rationale for Study 3.

In Study 2 the relationship between graph metrics and cognitive performance was explored, by examining whether inter-individual differences in decision-making time are related to network communication in healthy adults. Communication efficiency was measured using traditional path length-based metrics as well as a novel routing strategy (navigation efficiency; Seguin et al., 2018), across both the whole-brain and the fronto-parietal subnetwork. Results support the idea that poor communication efficiency is related to slowed processing speed. Higher navigation efficiency of the whole brain network, and both higher navigation efficiency and shorter characteristic path length of the fronto-parietal subnetwork, were related to faster decision-making time on a global-local task (Wiecki et al., 2013). Interestingly, navigation efficiency and characteristic path length were differentially related to decision-making time for controlled and automatic processes respectively. These findings infer those measures of network communication may reflect behaviour – however, this relationship is dependent on the specificity of the cognitive process being observed; the model of communication routing used to measure network efficiency; and the connectome methodology employed.

Study 3 (Chapter 5) demonstrated unique profiles of graph metric alterations among moderate-severe TBI patients. The ‘GraphMe’ plots were used to represent alterations in segregation, integration, and centrality, facilitating interpretation of individual disconnectivity profiles. This study also employed a new technique Virtual Brain Grafting (VBG) that allowed the inclusion of patients with extensive focal lesions (Radwan et al., 2021); and newly available methods that improve the estimation of edges (single-shell 3 tissue constrained spherical deconvolution SS3T_CSD; Dhollander et al., 2019). As expected, the profile of graph metric alterations was different across the five individuals. Patients who might normally have been grouped together on the basis of age, severity of injury, and lesion

size showed very different network alterations in the GraphMe plots. The renewed emphasis on single-subject profiling of patients is discussed in relation to providing a patient-specific perspective to the question of whether graph metrics can be used as biomarkers. Finally, future directions are suggested for implementing GraphMe plots as a novel method for clinicians to characterise individual patient's network alterations following brain injury.

6.1.2 Collective summary of results

Overall, evidence from this thesis indicates that graph metrics display potential for quantifying structural brain network alterations in TBI patients. First, measures of segregation and integration are sensitive to brain injury (Imms et al., 2019); and second, communication metrics can be related to individual differences in processing speed (Imms et al., 2021), demonstrating that graph metrics may have interpretive value. Study 3 suggests, however, that a single-subject profiling approach may better capture the 'fingerprint' of graph metric alterations, allowing characterisation of TBI patients based on their unique structural brain network profile. The following sections highlight the novel and original contributions this thesis provides to the field and details the potential implications of results for future research.

6.2 Discussion

6.2.1 Implications for the structural network topology of patients with TBI

6.2.1.1 A regular lattice structure

In Study 1 it is suggested that TBI patients display a brain network that has shifted towards a lattice structure, compared to healthy controls. The healthy connectome represents the ideal state of the cellular wiring of a brain, which sits between the highly clustered/poorly integrated regular lattice and the poorly clustered/highly integrated random graph (Fornito et al., 2016). Thus, the healthy connectome has a high level of clustering *and* shorter than expected path length, facilitating segregation of discrete brain functions in clusters, and integration of information across spatially distant regions (Watts & Strogatz, 1998). In contrast, the meta-analysis showed that characteristic path length and normalised clustering coefficient were both higher across TBI subtypes. This pattern is thought to be caused by loss of long-distance connections, which are particularly vulnerable in TBI (e.g., the corpus callosum; Kim et al., 2014a). Damage or loss of long-distance connections leads to longer paths and inflated measures of clustering. Other articles have made similar observations in TBI patients: for example, Sharp et al. (2014) also observed a shift in the TBI network, in particular within the default-mode network and the salience network. Also, a similar pattern of increased segregation and decreased integration has been observed in Alzheimer's disease and Schizophrenia patients (for review, see Griffa et al., 2013). Thus, the findings of Study 1 insinuate that traumatic injury may lead to a more costly network architecture of the brain.

The impact of this less 'efficient' network structure is thought to underly the broad range of impairments in executive function and cognition (Bullmore & Sporns, 2012). Because the brain is metabolically expensive, its topological organisation is thought to be driven by the need to minimise these costs (Sporns, 2011). Thus, loss of important

connections between important hubs of the brain can disrupt this cost-efficiency trade-off (van den Heuvel & Sporns, 2011) and cause disorders of higher-order cognitive functioning (Bassett & Bullmore, 2009; Fornito & Bullmore, 2010). Accordingly, topology may be related to cognitive performance – for example Kim et al. (2014a) found that increased path length was correlated with poorer executive functioning and slower verbal learning. Thus, Study 2 presents an in-depth investigation into the relationship between communication measures and processing speed, to explore whether network topology has implications for cognition – albeit in healthy adults. Study 2 supports findings from Seguin et al. (2020), who note that communication measures that summarise capacity for integration are relevant to behavioural measures. However, there remains an absence of literature specifically investigating the relationship between topology and cognition in TBI patients. Nevertheless, results from Study 1 and Study 2 imply that communication measures (i.e., characteristic path length, global efficiency, and navigation efficiency) are important measures of topology to examine in TBI patients with regards to cognitive outcome.

In the single-subject profiles of Study 3, it was noted that the topology of two patients shifted towards regular lattice structure (TBI1 and TBI3), while the others showed a different pattern of alterations: some patients remained economically balanced (i.e., TBI4 and TBI6) and others were closer to a random graph (TBI5). Thus, these highly variable patterns of alterations in each individual TBI patient were observed across all network properties. In support of Study 1 that purports characteristic path length to be the most robust metric across studies, it was observed that measures of integration (i.e., path length, global efficiency, and navigation efficiency) were most often affected: infra-normal in three of the five GraphMe plots, and normal in the remaining two. However, measures of segregation (i.e., normalised clustering coefficient, clustering coefficient, and local efficiency) showed mixed results –

infra-normal in one, normal in two, and supra-normal and infra-normal in the remaining two patients. This implies that, while at the group level TBI patients display a regular lattice structure, this does not necessarily translate to individual TBI patients. Similar findings were reported by Lv et al. (2020) who found that the brain structure of Schizophrenia patients deviated from healthy controls, but the exact topology of the differences was highly variable among individuals. Instead of the shift to a regular lattice structure being homogenously attributable to all TBI patients, results of Study 3 suggest that it will be necessary to stratify different ‘subgroups’ of personalised connectome profiles. With test-retest validation, the GraphMe plots show promise as a tool in this process of characterisation.

6.2.1.2 Advanced theoretical reasoning and hypothesis generation

The hypotheses of previous studies, described in detail in Study 1, reflect the exploratory nature of graph theoretical analysis in TBI – they lack clear rationales regarding the specific choice of graph metrics. Furthermore, the expected direction of effect was omitted in most of the studies analysed – only Yuan et al. (2015) and Königs et al. (2017) justified their choice of each graph metric. A clear rationale concerning the selection of graph metrics was required: to advance theoretical reasoning in the field, and to minimise unnecessary multiple comparisons thus reducing chance findings that inflate the false positive rate. Accordingly, a key outcome from this dissertation can be observed in the formulation of the GraphMe plots in Study 3. Each graph metric was chosen based on the results of previous literature – only those metrics that were significantly altered in TBI populations compared to healthy controls according to the meta-analysis were included in the GraphMe plots. Furthermore, whether these altered metrics were generally higher or lower than the healthy controls further informed the visualisation, with graph metrics recoded such that lower values indicated poorer topological structure (see Table 2 in Chapter 5). In this way, the GraphMe

plots provide a literature driven guide for investigating topological reorganisation in TBI patients, to aid in the development of hypotheses for future studies.

6.2.2 Implications for the interpretive value of graph metrics

6.2.2.1 Biomarkers of TBI?

Biomarkers are a key outcome for the field of translational neuroscience. In their review, Griffa et al. (2013) state that graph metrics hold potential as neuroimaging biomarkers of brain disorders, in particular those that demonstrate disconnectivity (including TBI). However, questions remain around the biological validity of graph metrics, and their relationships with biological substrates, existing diagnostic criteria, and cognitive performance. Biomarkers must be able to 1) diagnose a particular brain disorder, and 2) predict cognitive or other outcomes (Woo et al., 2017). The ultimate goal of biomarkers is to then engage their use at 3) an individual level, to provide clinicians with tools to diagnose, prognose, and treat patients.

With regards to the first criteria, the meta-analysis in Study 1 revealed that longer path lengths are the most robust diagnostic biomarker of TBI across all published studies (see section 6.2.1.2). With regards to the second criteria, Study 2 found that that communication measures such as path length and navigation efficiency (not previously studied in this regard) are related to cognitive outcomes. This study was one of the first ever to look at the direct interpretive value of communication measures, especially of the novel graph metric navigation efficiency (Seguin et al., 2018). There is currently no robust, widely used model of how structural network metrics relate to cognitive performance or capacity. Study 2 therefore provides a starting point for future studies to build mechanistic models of how network summary measures relate to cognition; grounds for an evidence-based interpretation of graph measures; and a framework for forming *a priori* hypotheses.

For the third criteria, Study 3 provides a framework for examining individual TBI patients with cognitive sequela using a profile of graph metrics. This shift away from searching for one ‘biomarker’ towards a profile of graph metrics enables examination of heterogeneity in the TBI population, which underscored the lack of robust findings in the meta-analysis (Imms et al., 2019). As expected, a diverse range of network alterations in the five moderate-severe participants was observed, which suggests there may not be a global change caused by TBI that can be robustly captured by a single graph metric. These observations highlight the importance of looking beyond a single global graph metric as a ‘biomarker’, towards an individual profiling approach. Using the GraphMe plots, these profiles can be treated as a representation of an individual’s connectome that considers all network properties (integration, segregation, centrality) – not just one. This type of profiling approach provides an avenue for future research into graph metric biomarkers of TBI.

In summary, this thesis demonstrates that 1) some graph metrics are robustly linked to TBI across studies; and 2) communication metrics are related to behaviour. However, this thesis does not validate this metric as a biomarker – for this, large scale studies testing the diagnostic and prognostic validity of this metric would be required (see Limitations section, Woo et al., 2017). Instead, it is argued that a profile of graph metrics might inform clinical practice by using a single-subject profiling approach.

6.2.2.2 Specific measures of cognition and network structure

Previously, studies that investigated whether graph metrics are biomarkers of TBI aimed to uncover relationships between network structure and cognition, with various levels of success. For example, Caeyenberghs et al. (2014) revealed that slower processing speeds on the GLT corresponded with lower global efficiency in adults with traumatic brain injury. Kim et al. (2014a) found that the increase in path length in TBI patients was related to poorer

executive functioning and slower verbal learning. However, they note that given characteristic path length is a measure of communication efficiency, they expected to see a relationship with processing speed – which was not significant. In Study 2 it was observed that these relationships may be improved by using specific measures of cognitive performance and network structure. By investigating the fronto-parietal subnetwork more specifically, this thesis found that navigation efficiency and characteristic path length are differentially related to controlled and automatic processing speeds respectively. This is in support of work by Román et al. (2017), who state that investigating task-relevant subnetworks improved their observed relationship with working memory and engagement. Furthermore, extracting task-relevant subnetworks and evaluating their relationship with cognitive performance may better reveal cognition-graph metric relationships.

Equally as essential to linking graph metrics with cognition is the use of specific measures of cognitive performance. The HDDM was used to extract a specific measure of decision-making time from the Global-Local task (Wiecki et al., 2013). Importantly, relationships between communication measures and conditions on the Global-Local task were then found using these specific measures, which may not have been observed had basic reaction time been used to measure processing speed (e.g., Kim et al., 2014a). In other words, results of Study 2 suggest that it may be necessary to examine graph metrics of task-relevant subnetworks to uncover specific relationships with cognitive outcome.

6.2.3 What can be gained from the use of Personalised Connectomics?

6.2.3.1 Representation of the TBI population

Importantly, understanding the link between cognition and affected neurological organisation has implications for the management of chronic TBI cases with persistent cognitive impairments. However, most research examining this link has done so using group-

level analyses, which average TBI patient neuroimaging and cognitive data to compare to healthy controls (Imms et al., 2019). While group-level analysis is essential for statistical evaluation, TBI patients are notoriously heterogeneous in terms of their lesion characteristics and cognitive outcomes (Rabinowitz & Levin, 2014); meaning important individual differences are ‘left on the cutting room floor’, and group-level results are not necessarily applicable to individual patients (Mant, 1999). Instead, there is incentive for the use of individual-level approaches to investigate the cognitive and neurological facets of brain injuries in general (e.g., Irimia, Chambers, et al., 2012; Irimia, Wang, et al., 2012; Jolly et al., 2021; Lv et al., 2020). The single-subject profiles of Study 3 constitute a timely response to the push for individual-level approaches – they provide a framework for future studies to examine a profile of cognitive and neurological alterations without averaging individual differences in TBI patients.

In previous connectome studies of TBI it is common to exclude cases with large focal lesions that fail Freesurfer segmentation – which was not designed for brain images with structural pathology. Consequently, results are not representative of the broader TBI population, and the models based on this data are less likely to be generalisable to real-life clinical settings (Woo et al., 2017). However, if these patients are discarded, our understanding of TBI is limited only to patients with smaller lesions. New techniques for improving image processing of patients with large lesions are currently being developed, that will allow inclusion of these patients (see section 6.2.4.3). In Study 3 one such technique is successfully employed (Radwan et al., 2021), enabling the demonstration of the individual profiling approach in moderate-severe TBI patients, including two with extensive lesions. Inclusion of these patients is essential for ensuring that the true diversity of the TBI population is represented in the literature.

6.2.3.2 A framework for clinical application

Irimia, Wang, et al. (2012) introduced the idea of personalised structural connectomics for TBI patients, to visualise trauma-related white matter atrophy. In particular, they assert the need for techniques that allow clinicians to rapidly compare changes in structural connectivity profiles in order to create personalised rehabilitation programs (Irimia, Chambers, et al., 2012). There is evidence that individual network- and connectivity-based profiles are promising in this regard (e.g., Bonilha et al., 2015; Kottaram et al., 2020). However, few studies have examined personalised connectome approaches in TBI patients (Irimia, Chambers, et al., 2012). Study 3 demonstrates the usefulness of personalised structural connectomics in three ways: First, connectome maps can be used as a profile of the TBI patient's brain topography, giving researchers and clinicians a quick visual summary of network asymmetry, hub alterations, and overall reductions in connectivity strength. Second, by comparing an individual to normative data, areas of the network that are topologically damaged beyond the site of the focal lesion can be observed. Finally, cognitive symptoms can be compared to changes in summary network metrics such as path length, navigation efficiency, and normalised clustering coefficient. Thus, the novel visual representation 'GraphMe' plot opens avenues for employing graph metrics in the clinical care of TBI patients.

Moving forward, this revaluing of single-subject profiling can be used alongside group-level analyses to inform clinical practice. This approach could be useful longitudinally to assess network-based alterations over the time course of the injury. There is evidence that structural connectivity changes over time according to time since injury (e.g., Meninger et al., 2020; Osmanlioğlu et al., 2019). For example, Osmanlioğlu et al. (2019) found that moderate-severe TBI patients were identical to healthy controls immediately after the injury

and showed greater dissimilarity by three months post injury. Meninger et al. (2020) found that clustering coefficient dropped in the first week post injury then returned to baseline within a month in mice, while global efficiency increased in the first week then decreased over the following month. These fluctuations are likely to be a result of neurobiological responses to the injury which may continue for up to 6 months post-injury (e.g., Bramlett & Dietrich, 2015). Examination of multiple GraphMe plots over the course of the acute-chronic period could provide insights into how these fluctuations occur 1) in comparison to a healthy cohort, and 2) in comparison to the initial brain network at injury.

Finally, there is evidence that individual network- and connectivity-based profiles are promising for informing personalised rehabilitation programs (Irimia, Wang, et al., 2012). Individual profiling approaches can inform neuroimaging-guided rehabilitation (Dichter et al., 2012; Stoeckel et al., 2014; Wing et al., 2017), and assist health professionals to design personalized cognitive training and rehabilitation programs. For example, clinicians can relate the single-subject brain profiles to the cognitive profiles, to design personalized therapies that take into account damaged connections. Assessment of cognitive and structural network alterations in comparison to a normative cohort provides essential information to deliver a compensatory training program that targets specific white matter tracts and cognitive domains.

6.2.4 Methodological considerations of diffusion-based graph analysis in TBI

6.2.4.1 Overview

Although recent advances in computational neuroscience and image processing have been provided that ameliorate the challenges of connectome reconstruction, they are not always widely used (Yeh et al., 2020). It is important to judiciously select tools and approaches that minimise biases, as connectome analyses can be heavily influenced by

methodological choices in the processing pipeline (for reviews, see Sotiropoulos & Zalesky, 2019; Yeh et al., 2020; Zalesky et al., 2010). This is especially true for brain injured cohorts – as such, the current research program utilised a meticulously crafted connectome pipeline. Here, the approach to the three major domains of the connectome pipeline is described: 1) tractography and generation of streamline edge weights; 2) creation of the connectome matrices and node choice; and 3) performance of the graph analysis.

6.2.4.2 Edges

According to a recent methodological review by Yeh et al. (2020), there are two main areas in which the generation of streamlines can bias the connectome analysis: 1) the streamline termination bias, and 2) the streamline quantification bias. The streamline termination bias infers that a streamline seed and termination point essentially defines which node that streamline belongs to. These termination criteria are (conventionally) that a streamline will begin at a randomly generated seed point, and end when the streamline passes through an area of low FOD amplitude or high curvature (Jeurissen et al., 2019; Tournier et al., 2011). However, the resulting streamlines are often biologically implausible, ending in white matter or the CSF. Instead, Smith et al. (2012) propose Anatomically Constrained Tractography (ACT) which were employed in the current research program. The streamlines generated were initiated and terminated in the grey matter boundary, using anatomical priors derived from T₁ images, which better reflects the true biological nature of white matter tracts. In support of this, a recent study by Schilling et al. (2020) found that the best-case scenario for the accuracy of streamline generation occurred using anatomical priors, which improved both the sensitivity and specificity to the ground truth.

One concern regarding the use of ACT in the presence of pathology was that streamlines may incorrectly be terminated and removed as implausible in cases where the

streamline ends in the lesion. However, recent work by Horbruegger et al. (2019) found that ACT improved the tractography of patients with Multiple Sclerosis lesions by preventing implausible tracts. Similarly, in Study 3, the combined effect of ACT and VBG (to improve image segmentation) produced connectomes that quite accurately reflected the underlying pathology. Nevertheless, new techniques are currently being crafted to improve the registration between streamline end-point and anatomy by using more accurate anatomical constraints (Yeh et al., 2017).

Second, the streamline quantification bias (also referred to as the reconstruction bias) signifies that streamlines themselves do not actually represent the underlying fibre density and thus are not biologically relevant (Jones, 2010a; Jones et al., 2013; Smith et al., 2013). Accordingly, longer pathways are underestimated as there are more opportunities for the streamline to terminate (Jones, 2010a). Length correction and representation of the fibre density have been addressed using advances in streamline filtering algorithms, including COMMIT2 (Schiavi, 2020), LiFE (Pestilli et al., 2014), and SIFT2 (Smith et al., 2015a). In this thesis SIFT2 was utilised, which alters the streamline count to represent the underlying tissue microstructural properties inherent in the FODs. This avoids the streamline quantification bias and has been shown to result in connectomes that have stronger relationships with cognitive performance (McColgan et al., 2018). SIFT2 may provide greater confidence in the biological relevance of structural connectomes – however, of note, it also resulted in a heavy-tailed distribution of edge weights. A recent study by Frigo et al. (2020) found that filtering techniques such as SIFT2 alter the topology of TBI brain networks and can thus influence the measurement of network metrics – while thresholding based on density has negligible effects on network topology. However, density-based thresholding does not

fully overcome the streamline quantification bias, as it does not make the streamlines proportional to the underlying FOD amplitudes.

It has also been suggested that SIFT2 is not appropriate for brain images where pathology is present, as the cross-sectional area of an individual fibre bundle may not be consistent along the length of the bundle in cases of neurodegeneration and lesions (Sarwar et al., 2019; Smith, Calamante, & Connelly, 2020; Zalesky et al., 2020). Zalesky et al. (2020, p. 793) provide the metaphor a chain is only as strong as its weakest link, and that SIFT2 (by taking the sum of the weights of the cross-sectional area along the entire bundle, regardless of the weakest point), does not account for this. In response, Smith, Calamante, Gajamante, et al. (2020) propose a modification to the SIFT2 method where axonal truncation pathologies (such as lesions) are taken into account, by ensuring that the streamline density does not exceed the fibre density estimated by the diffusion model. Unfortunately, this proposed amendment was not available at the time of analysis; however, this technique shows promise for mitigating the effects of lesions on the quantification of streamlines in future studies.

Finally, it was observed that the single-shell 3 tissue model for CSD (SS3T-CSD) inherently dealt well with TBI lesions (Dhollander et al., 2020; Dhollander et al., 2019). CSD provides an improvement to the tensor model of generating tractography, as it is able to represent multiple fibre directions in a single voxel, allowing for estimation of crossing fibres (Jeurissen et al., 2013). Even though CSD is probabilistic, graph metrics calculated from CSD show excellent reproducibility across iterations (Roine et al., 2019). SS3T-CSD reserves the angular information of the GM- and CSF-like signal, removing contributions from these components to increase the specificity of the WM FODs, while avoiding over estimation into GM and CSF signal from the lesioned area (Khan et al., 2020). Combined with anatomically constrained tractography (Smith et al., 2012), streamlines were not generated in lesioned

areas, meaning anatomically disconnected regions were represented as such in the TBI connectivity matrices.

6.2.4.3 Nodes

The manner in which the ‘nodes’ of the graph analysis are selected have an undeniable impact on the resulting metrics (Zalesky et al., 2010). While there is no consensus on the optimal choice of parcellation scheme (Sotiropoulos & Zalesky, 2019; Yeh et al., 2020; Zalesky et al., 2010) the Desikan-Killiany atlas was used in Study 2 and 3 (Desikan et al., 2006), as it is one of the most commonly used parcellation schemes and shows good test-retest reliability in structural connectome analysis (e.g., Buchanan et al., 2014; further reasons are outlined in Study 2, section 4.2.4.3). The interpretation of results are therefore mitigated by the specific choice of parcellation scheme (i.e., the Desikan-Killianey atlas has 82 relatively large nodes, thus results are relevant for a more macro-scale understanding of the structural connectome). Zalesky et al. (2010) found that network parameters such as path length vary as spatial scale of the parcellation scheme increases, and thus findings should be reported with reference to the scale of the parcellation used. Therefore, other parcellation granularities may lead to different results - for instance, in Study 2, significant correlations using the higher-resolution Destrieux atlas were not observed (164 regions; Destrieux et al., 2010).

Node definition in patients with large lesions is both problematic and largely ignored – leading to a biased representation of the TBI population (see section 6.2.3.1). TBI patients often have lesions that do not cope well with standard segmentation procedures from which atlases like the Desikan-Killianey and the Destrieux are derived (Fischl et al., 2002). In cases where large regions of the brain are structurally damaged (e.g., TBI2, TBI3, TBI4), it is logical to presume that these nodes are disconnected (thus, the weight of the corresponding

row/column in the connectivity matrix should be set to 0). However, these disconnected nodes must still be generated to run the connectome analysis. Unsurprisingly, in cases of severe lesions, automated Freesurfer segmentation was problematic, resulting in inaccurate streamline assignment – at which point these patients are often excluded. The use of manual edits to the white matter volume to re-align the segmentation is not feasible for patients with extensive regions of encephalomalacia, and these methods are time-consuming and unreproducible across labs (Beelen et al., 2020).

Automated lesion filling or ‘virtual repair’ methods instead aim to ‘fill in’ structural pathologies to aid in segmentation processes. Significant advances have been made for automatic identification (e.g., Lesion Identification using Neighbourhood Data Analysis; Pustina et al., 2016) and filling of large unilateral lesions such as those commonly seen in stroke. Unfortunately, these methods are not suitable for use in all TBI patients as they rely on leveraging healthy tissue from the contralateral hemisphere to fill a lesion (i.e., enantiomorphic normalisation; Nachev et al., 2008), and TBI lesions often occupy homologous regions of both hemispheres of the brain. This is the first time the approach proposed by (Radwan et al., 2021), which utilises a novel method for automatic filling of bilaterally lesioned brains using healthy synthetic donor tissue, has been applied in TBI research. Study 3 demonstrates that VBG improved segmentation accuracy in TBI patients with extensive bilateral lesions. As such, this single-subject approach has been beneficial for piloting approaches for rare TBI cases which may otherwise have been excluded. However, it is also noted that VBG using the healthy donor image has not yet been validated against a ground truth – though, this work is currently underway.

6.2.4.4 Graph analysis

There are many ‘decision points’ within the graph theoretical analysis, including: 1) binary or weighted, 2) thresholding (or not), and 3) weight-length remapping. All studies in the meta-analysis (Study 1), and empirical Study 2 and 3 used the BCT to run the graph analysis, which is designed to provide a consistent methodology (Rubinov & Sporns, 2010). However, the three decisions described above are not prescribed by the BCT, such that every step taken will alter the outcome of the analysis. The benefits of each decision are laid out in Yeh et al. (2020) – here, justification is provided for the methodology used in this thesis.

First, a weighted connectome was used, as this has been shown to provide a stronger representation of the properties of the brain network (Bassett & Bullmore, 2017). Given the use of SIFT2 to ensure the generated streamlines represented the underlying fibre orientation density, the edge weights were as biologically representative as possible (Smith et al., 2015a). This choice is also recommended for connectomes of patients with neurological pathology such as Alzheimer’s disease (Mito et al., 2018) and by extension TBI, where reduced but not absent connectivity is important to the interpretation of altered network properties. Second, the use of SIFT2 also meant that no thresholding was necessary, as very weak edges were given an extremely low edge weight – meaning their impact on resulting metrics was almost non-existent (Civier et al., 2019). However, the third decision (weight-length remapping) was more contentious. In Study 2, a series of control analyses were performed, changing the method of remapping between $-\log(10)$ and $1/W$. The resulting communication measures and subsequent correlations with processing speed changed depending on the procedure used. There is no best practice method prescribed for this step in the BCT – however, this step needs to be synchronised, as this study (and others: e.g., Avena-Koenigsberger et al., 2018) found that this step can impact the distribution of edge weights.

6.2.4.5 Summary

In summary, up-to-date processing techniques were utilised to ensure the biological validity and replicability of the connectome pipeline. While the application of some methods to patients with structural pathology are still being debated (e.g., SIFT2 and ACT), advances are being made relatively quickly in these areas. Furthermore, the use of new methods that allow better representation of neurodiversity in the TBI literature are demonstrated (i.e., VBG; Radwan et al., 2021). Finally, currently accepted and standardised methods for graph theoretical analysis were employed wherever possible (Rubinov & Sporns, 2010), and methods that require further investigation (i.e., weight-length remapping) were highlighted to improve the robustness and reproducibility of graph analyses.

6.3 Strengths, Limitations and Future Directions

6.3.1 Limitations and future directions

6.3.1.1 Correlational analysis

It is important that biomarkers are able to predict cognitive outcome (Woo et al., 2017) – which was not examined by the correlational study in Chapter 4. Instead, Study 2 provides insights into the potential mechanisms of graph metric-cognition relationships. It is noted that while communication metrics are related to processing speed, this relationship is highly dependent on the measures being used (see section 6.2.2.2). There is now a subsequent, ongoing investigation using a previously published dataset with a sample size of N=92 TBI patients (Jolly et al., 2020). Using a machine-learning approach, an algorithm will be trained on a subset of the TBI cohort to determine if slow processing speed can be predicted using navigation efficiency and path length measures. This would enable the predictive validity of navigation efficiency to be more directly examined in TBI patients. This

next step in biomarker development is essential to establish which injury-related changes in the brain network are behaviourally relevant.

6.3.1.2 Structural versus functional connectivity

The scope of this research program was limited to the use of structural connectivity to investigate TBI related alterations in patients with cognitive sequelae. Structural connectivity represents the network architecture, the circuitry and wiring that brain function relies upon (Sporns et al., 2005). There is strong evidence that brain structural connectivity is related to functional connectivity (Straathof et al., 2019), in both healthy adults (Honey et al., 2009) and TBI patients (for review in preprint, see Parsons et al., 2020, December 3). Utilising multimodal measures of connectivity (i.e., pairing structural and functional connectivity) may improve the capacity to observe the relationship between properties of the brain network and cognitive performance (Dhamala et al., 2020; Seguin et al., 2020). For example, Seguin et al. (2020) found that communication measures calculated on functional connectomes are better indicators of cognitive performance than structural measures alone. The idea of coupling structural-functional connectivity for connectome analysis is rising in popularity (Sarwar et al., 2020). Future iterations of the GraphMe plots could include functional plots alongside the structural, to examine 1) whether the pattern of alterations is similar across domains in an individual patient, and 2) whether the combination of modalities provides a more informed perspective of the patient's brain network that better reflects their unique cognitive outcome.

6.3.1.3 Normative data

Individual level analyses require a comparison of 1 subject to N controls. This individual approach to neuroimaging biomarker studies has flourished in recent months (e.g., Attyé et al., 2020; Garcia-Rudolph et al., 2020; Jolly et al., 2021; Lv et al., 2020). Compared

to Study 3 the sample size of the healthy cohort in these attribution studies is much larger – minimum N=103 (Jolly et al., 2021). Normative analysis with large sample sizes of healthy individuals allows for stronger statistical inferences to be made using such techniques as quartile regression, as was done by Lv et al. (2020) and Jolly et al. (2021). Normative data approaches are limited by access to substantial healthy control cohorts scanned with the same sequence at the same site – as results from tractography and connectome analyses are not robust to differences in image acquisition and processing (Sotiropoulos & Zalesky, 2019; Yeh et al., 2020). However, with the use of data harmonisation techniques (for review, see Pinto et al., 2020) this limitation could potentially be overcome in the near future, allowing larger normative datasets to be more easily created.

6.3.2 Strengths

One of the main strengths of this research program is its inclusivity – no patients were discarded for having large lesions. As such, this thesis constitutes an important step towards addressing the problems of heterogeneity in the TBI population, made possible by the up-to-date connectome pipeline that was employed (see section 6.2.4) (Radwan et al., 2021; Smith et al., 2015a; Smith et al., 2012). Specific measures of cognition (Wiecki et al., 2013) and network communication (Seguin et al., 2018) were also used to uncover relationships between graph metrics and cognition (see section 6.2.2.2). An ongoing area of investigation before graph metrics can be considered as ‘biomarkers’ is whether they have interpretive value, and specific measures such as those utilised in Study 2 may provide opportunities for a more mechanistic understanding of this link. Finally, this research provides new, clinician targeted output for assessing TBI patients, particularly those with chronic, ongoing disability who are often under-represented and unable to access ongoing rehabilitation.

6.4 Conclusions

This thesis provides a substantive critical evaluation of the use of graph metrics in the study of patients with TBI. The three empirical studies form a body of work that examines the robustness (Study 1), behavioural relevance (Study 2), and applicability at the single-subject level (Study 3) of graph theoretical approaches to studying brain injury. It was found that brain network communication is often altered across different TBI groups (Imms et al., 2019); which may also be related to cognitive processing speed (Imms et al., 2021). However, the pattern of graph metric alterations varies extensively in individual patients, depending on their age, lesion size, and lesion location. Therefore, future graph theoretical studies of TBI must adopt a profiling approach to better characterise network alterations that consider the unique ‘disconnectivity’ of each patient. In this way, graph theoretical analysis holds promise as a means of characterising and informing treatment decisions for patients with TBI.

Reference List

- Access Economics Pty Limited. (2009). *The economic cost of spinal cord injury and traumatic brain injury in Australia*. <http://www.spinalcure.org.au/pdf/Economic-cost-of-SCI-and-TBI-in-Au-2009.pdf>
- Adams, J. H., Graham, D. I., Murray, L. S., & Scott, G. (1982). Diffuse axonal injury due to nonmissile head injury in humans: An analysis of 45 cases. *Annals of Neurology*, 12(6), 557–563. <https://doi.org/10.1002/ana.410120610>
- Andersson, J. L. R., Graham, M. S., Zsoldos, E., & Sotiropoulos, S. N. (2016). Incorporating outlier detection and replacement into a non-parametric framework for movement and distortion correction of diffusion MR images. *Neuroimage*, 141, 556-572. <https://doi.org/10.1016/j.neuroimage.2016.06.058>
- Andersson, J. L. R., Skare, S., & Ashburner, J. (2003). How to correct susceptibility distortions in spin-echo echo-planar images: Application to diffusion tensor imaging. *Neuroimage*, 20(2), 870-888. [https://doi.org/10.1016/S1053-8119\(03\)00336-7](https://doi.org/10.1016/S1053-8119(03)00336-7)
- Andersson, J. L. R., & Sotiropoulos, S. N. (2016). An integrated approach to correction for off-resonance effects and subject movement in diffusion MR imaging. *Neuroimage*, 125, 1063-1078. <https://doi.org/10.1016/j.neuroimage.2015.10.019>
- Aoki, Y., & Inokuchi, R. (2016). A voxel-based meta-analysis of diffusion tensor imaging in mild traumatic brain injury. *Neuroscience & Biobehavioral Reviews*, 66, 119-126. <https://doi.org/10.1016/j.neubiorev.2016.04.021>
- Arfanakis, K., Haughton, V. M., Carew, J. D., Rogers, B. P., Dempsey, R. J., & Meyerand, M. E. (2002). Diffusion tensor MR imaging in diffuse axonal injury. *American Journal of Neuroradiology*, 23(5), 794-802. <http://www.ajnr.org/content/ajnr/23/5/794.full.pdf>
- Assaf, Y., Freidlin, R. Z., Rohde, G. K., & Basser, P. J. (2004). New modeling and experimental framework to characterize hindered and restricted water diffusion in brain white matter. *Magnetic resonance in Medicine*, 52(5), 965-978. <https://doi.org/10.1002/mrm.20274>
- Attyé, A., Renard, F., Baciú, M., Roger, E., Lamalle, L., Dehail, P., . . . Calamante, F. (2020). TractLearn: A geodesic learning framework for quantitative analysis of brain bundles [preprint]. *medRxiv*. <https://doi.org/10.1101/2020.05.27.20113027.this>
- Avants, B. B., Tustison, N., & Song, G. (2009). Advanced normalization tools (ANTS). *Insight Journal*, 2(365), 1-35.

- Avena-Koenigsberger, A., Misic, B., & Sporns, O. (2018). Communication dynamics in complex brain networks. *Nature Reviews Neuroscience*, 19(1), 17.
<https://doi.org/10.1038/nrn.2017.149>
- Avena-Koenigsberger, A., Yan, X., Kolchinsky, A., van den Heuvel, M., Hagmann, P., & Sporns, O. (2019). A spectrum of routing strategies for brain networks. *Plos Computational Biology*, 15(3), e1006833. <https://doi.org/10.1371/journal.pcbi.1006833>
- Baiano, M., David, A., Versace, A., Churchill, R., Balestrieri, M., & Brambilla, P. (2007). Anterior cingulate volumes in schizophrenia: A systematic review and a meta-analysis of MRI studies. *Schizophrenia Research*, 93(1-3), 1-12. <https://doi.org/10.1016/j.schres.2007.02.012>
- Banich, M. T. (2009). Executive function: The search for an integrated account. *Current directions in psychological science*, 18(2), 89-94. <https://doi.org/10.1111/j.1467-8721.2009.01615.x>
- Banich, M. T., Milham, M. P., Atchley, R., Cohen, N. J., Webb, A., Wszalek, T., . . . Shenker, J. (2000). fMRI studies of Stroop tasks reveal unique roles of anterior and posterior brain systems in attentional selection. *Journal of Cognitive Neuroscience*, 12(6), 988-1000.
<https://doi.org/10.1162/08989290051137521>
- Basser, P. J., & Jones, D. K. (2002). Diffusion-tensor MRI: Theory, experimental design and data analysis—a technical review. *Nuclear Magnetic Resonance in Biomedicine*, 15(7-8), 456-467.
<https://doi.org/10.1002/nbm.783>
- Basser, P. J., Mattiello, J., & LeBihan, D. (1994). MR diffusion tensor spectroscopy and imaging. *Biophysical journal*, 66(1), 259-267. [https://doi.org/10.1016/S0006-3495\(94\)80775-1](https://doi.org/10.1016/S0006-3495(94)80775-1)
- Bassett, D. S., Brown, J. A., Deshpande, V., Carlson, J. M., & Grafton, S. T. (2011). Conserved and variable architecture of human white matter connectivity. *Neuroimage*, 54(2), 1262-1279. <https://doi.org/10.1016/j.neuroimage.2010.09.006>
- Bassett, D. S., & Bullmore, E. T. (2009). Human brain networks in health and disease. *Current Opinion In Neurology*, 22(4), 340-347. <https://doi.org/10.1097/WCO.0b013e32832d93dd>
- Bassett, D. S., & Bullmore, E. T. (2017). Small-world brain networks revisited. *The Neuroscientist*, 23(5), 499-516. <https://doi.org/10.1177/1073858416667720>
- Bassett, D. S., & Sporns, O. (2017). Network neuroscience. *Nature Neuroscience*, 20(3), 353-364.
<https://doi.org/10.1038/nn.4502>
- Battistone, M., Woltz, D., & Clark, E. (2008). Processing speed deficits associated with traumatic brain injury: Processing inefficiency or cautiousness? *Applied neuropsychology*, 15(1), 69-78.
<https://doi.org/10.1080/09084280801917863>

- Baxter, D., & Wilson, M. H. (2012). The fundamentals of head injury. *Neurosurgery*, 30(3), 116-121. <https://doi.org/10.1016/B978-0-444-52892-6.00004-0>.
- Bazarian, J. J., Zhong, J., Blyth, B., Zhu, T., Kavcic, V., & Peterson, D. (2007). Diffusion tensor imaging detects clinically important axonal damage after mild traumatic brain injury: A pilot study. *Journal Of Neurotrauma*, 24(9), 1447-1459. <https://doi.org/10.1089/neu.2007.0241>
- Beelen, C., Phan, T. V., Wouters, J., Ghesquière, P., & Vandermosten, M. (2020). Investigating the added value of FreeSurfer's manual editing procedure for the study of the reading network in a pediatric population. *Front Hum Neurosci*, 14, 143-143. <https://doi.org/10.3389/fnhum.2020.00143>
- Belanger, H. G., & Vanderploeg, R. D. (2005). The neuropsychological impact of sports-related concussion: A meta-analysis. *Journal of the International Neuropsychological Society*, 11, 345–357. <https://doi.org/10.1017/s1355617705050411>
- Bendlin, B. B., Ries, M. L., Lazar, M., Alexander, A. L., Dempsey, R. J., Rowley, H. A., . . . Johnson, S. C. (2008). Longitudinal changes in patients with traumatic brain injury assessed with diffusion-tensor and volumetric imaging. *Neuroimage*, 42(2), 503-514. <https://doi.org/10.1016/j.neuroimage.2008.04.254>
- Benjamini, Y., & Yekutieli, D. (2001). The control of the false discovery rate in multiple testing under dependency. *The Annals of Statistics*, 29(4), 1165-1188. <https://doi.org/10.1214/aos/1013699998>
- Benson, R. R., Meda, S. A., Vasudevan, S., Kou, Z., Govindarajan, K. A., Hanks, R. A., . . . Coplin, W. (2007). Global white matter analysis of diffusion tensor images is predictive of injury severity in traumatic brain injury. *Journal Of Neurotrauma*, 24(3), 446-459. <https://doi.org/10.1089/neu.2006.0153>
- Betz, R. F. (2020). Network neuroscience and the connectomics revolution. *arXiv*, 2010.01591. <https://doi.org/arXiv:2010.01591>
- Biesbroek, J. M., Leemans, A., den Bakker, H., Duering, M., Gesierich, B., Koek, H. L., . . . Biessels, G. J. (2017). Microstructure of strategic white matter tracts and cognition in memory clinic patients with vascular brain injury. *Dementia & Geriatric Cognitive Disorders*, 44(5-6), 268-282. <https://doi.org/10.1159/000485376>
- Bigler, E. D. (2013). Traumatic brain injury, neuroimaging, and neurodegeneration [Review]. *Front Hum Neurosci*, 7, 395. <https://doi.org/10.3389/fnhum.2013.00395>

- Binder, J. R. (2015). The Wernicke area: Modern evidence and a reinterpretation. *Neurology*, 85(24), 2170-2175. <https://doi.org/10.1212/WNL.0000000000002219>
- Boguna, M., Krioukov, D., & Claffy, K. C. (2009). Navigability of complex networks. *Nature Physics*, 5(1), 74-80. <https://doi.org/10.1038/NPHYS1130>
- Bonilha, L., Jensen, J. H., Baker, N., Breedlove, J., Nesland, T., Lin, J. J., . . . Kuzniecky, R. I. (2015). The brain connectome as a personalized biomarker of seizure outcomes after temporal lobectomy. *Neurology*, 84(18), 1846-1853. <https://doi.org/10.1212/WNL.0000000000001548>
- Bonnelle, V., Leech, R., Kinnunen, K. M., Ham, T. E., Beckmann, C. F., De Boissezon, X., . . . Sharp, D. J. (2011). Default mode network connectivity predicts sustained attention deficits after traumatic brain injury. *Journal of Neuroscience*, 31(38), 13442-13451. <https://doi.org/10.1523/JNEUROSCI.1163-11.2011>
- Bramlett, H. M., & Dietrich, W. D. (2015). Long-term consequences of traumatic brain injury: Current status of potential mechanisms of injury and neurological outcomes. *Journal Of Neurotrauma*, 32(23), 1834-1848. <https://doi.org/10.1089/neu.2014.3352>
- Brenner, E. K., Grossner, E. C., Johnson, B. N., Bernier, R. A., Soto, J., & Hillary, F. G. (2020). Race and ethnicity considerations in traumatic brain injury research: Incidence, reporting, and outcome. *Brain Injury*, 34(6), 801-810. <https://doi.org/10.1080/02699052.2020.1741033>
- Bressler, S. L., & Menon, V. (2010). Large-scale brain networks in cognition: Emerging methods and principles. *Trends in Cognitive Sciences*, 14(6), 277-290. <https://doi.org/10.1016/j.tics.2010.04.004>
- Buchanan, C. R., Pernet, C. R., Gorgolewski, K. J., Storkey, A. J., & Bastin, M. E. (2014). Test-retest reliability of structural brain networks from diffusion MRI. *Neuroimage*, 86, 231-243. <https://doi.org/10.1016/j.neuroimage.2013.09.054>
- Buckner, R. L., Head, D., Parker, J., Fotenos, A. F., Marcus, D., Morris, J. C., & Snyder, A. Z. (2004). A unified approach for morphometric and functional data analysis in young, old, and demented adults using automated atlas-based head size normalization: Reliability and validation against manual measurement of total intracranial volume. *Neuroimage*, 23(2), 724-738. <https://doi.org/10.1016/j.neuroimage.2004.06.018>
- Bullmore, E. T., & Bassett, D. S. (2011). Brain graphs: Graphical models of the human brain connectome. *Annual Review in Clinical Psychology*, 7, 113-140. <https://doi.org/10.1146/annurev-clinpsy-040510-143934>

- Bullmore, E. T., & Sporns, O. (2009). Complex brain networks: Graph theoretical analysis of structural and functional systems. *Nature Reviews Neuroscience*, 10(3), 186-198.
<https://doi.org/10.1038/nrn2575>
- Bullmore, E. T., & Sporns, O. (2012). The economy of brain network organization. *Nature Reviews Neuroscience*, 13(5), 336-349. <https://doi.org/10.1038/nrn3214>
- Bulmer, M. G. (1979). *Principles of Statistics*. Courier Corporation.
- Caeyenberghs, K., Clemente, A., Imms, P., Egan, G., Hocking, D., Leemans, A., . . . Wilson, P. (2018). Evidence for training-dependent structural neuroplasticity in brain-injured patients: Can structural MRI help us to improve rehabilitation? *Neurorehabilitation & Neural Repair*, 32(2), 99-114. <https://doi.org/10.1177/1545968317753076>
- Caeyenberghs, K., & Leemans, A. (2014). Hemispheric lateralization of topological organization in structural brain networks [Article]. *Human Brain Mapping*, 35(9), 4944-4957.
<https://doi.org/10.1002/hbm.22524>
- Caeyenberghs, K., Leemans, A., Coxon, J., Leunissen, I., Drikkoningen, D., Geurts, M., . . . Swinnen, S. P. (2011). Bimanual coordination and corpus callosum microstructure in young adults with traumatic brain injury: A diffusion tensor imaging study. *Journal Of Neurotrauma*, 28(6), 897-913. <https://doi.org/10.1089/neu.2010.1721>
- Caeyenberghs, K., Leemans, A., De Decker, C., Heitger, M., Drikkoningen, D., Linden, C. V., . . . Swinnen, S. P. (2012). Brain connectivity and postural control in young traumatic brain injury patients: A diffusion MRI based network analysis. *NeuroImage: Clinical*, 1(1), 106-115. <https://doi.org/10.1016/j.nicl.2012.09.011>
- Caeyenberghs, K., Leemans, A., Geurts, M., Linden, C. V., Smits-Engelsman, B. C., Sunaert, S., & Swinnen, S. P. (2011). Correlations between white matter integrity and motor function in traumatic brain injury patients. *Neurorehabilitation & Neural Repair*, 25(6), 492-502.
<https://doi.org/10.1177/1545968310394870>
- Caeyenberghs, K., Leemans, A., Geurts, M., Taymans, T., Vander Linden, C., Smits-Engelsman, B. C., . . . Swinnen, S. P. (2010). Brain-behavior relationships in young traumatic brain injury patients: Fractional anisotropy measures are highly correlated with dynamic visuomotor tracking performance. *Neuropsychologia*, 48(5), 1472-1482.
<https://doi.org/10.1016/j.neuropsychologia.2010.01.017>
- Caeyenberghs, K., Leemans, A., Heitger, M. H., Leunissen, I., Dhollander, T., Sunaert, S., . . . Swinnen, S. P. (2012). Graph analysis of functional brain networks for cognitive control

- of action in traumatic brain injury. *Brain*, 135(Pt 4), 1293-1307.
<https://doi.org/10.1093/brain/aws048>
- Caeyenberghs, K., Leemans, A., Leunissen, I., Gooijers, J., Michiels, K., Sunaert, S., & Swinnen, S. P. (2014). Altered structural networks and executive deficits in traumatic brain injury patients. *Brain Struct Funct*, 219(1), 193-209. <https://doi.org/10.1007/s00429-012-0494-2>
- Caeyenberghs, K., Leemans, A., Leunissen, I., Michiels, K., & Swinnen, S. P. (2013). Topological correlations of structural and functional networks in patients with traumatic brain injury. *Front Hum Neurosci*, 7, 726. <https://doi.org/10.3389/fnhum.2013.00726>
- Caeyenberghs, K., Metzler-Baddeley, C., Foley, S., & Jones, D. K. (2016). Dynamics of the human structural connectome underlying working memory training. *Journal of Neuroscience*, 36(14), 4056-4066. <https://doi.org/10.1523/JNEUROSCI.1973-15.2016>
- Cao, Q., Shu, N., An, L., Wang, P., Sun, L., Xia, M.-R., . . . He, Y. (2013). Probabilistic diffusion tractography and graph theory analysis reveal abnormal white matter structural connectivity networks in drug-naïve boys with attention deficit/hyperactivity disorder. *The Journal of Neuroscience*, 33(26), 10676. <https://doi.org/10.1523/JNEUROSCI.4793-12.2013>
- Capruso, D. X., & Levin, H. S. (1992). Cognitive impairment following closed head injury. *Neurologic clinics*, 10(4), 879-893. [https://doi.org/10.1016/S0733-8619\(18\)30185-3](https://doi.org/10.1016/S0733-8619(18)30185-3)
- Carmichael, S. T. (2003). Gene expression changes after focal stroke, traumatic brain and spinal cord injuries. *Current Opinion In Neurology*, 16(6), 699-704.
<https://doi.org/10.1097/01.wco.0000102621.38669.77>
- Carroll, L., Cassidy, D. J., Peloso, P., Borg, J., von Holst, H., Holm, L., . . . Pépin, M. (2004). Prognosis for mild traumatic brain injury: Results of the WHO collaborating centre task force on mild traumatic brain injury. *Journal of Rehabilitation Medicine*, 36(0), 84-105.
<https://doi.org/10.1080/16501960410023859>
- Catani, M., & Ffytche, D. H. (2005). The rises and falls of disconnection syndromes. *Brain*, 128(10), 2224-2239. <https://doi.org/10.1093/brain/awh622>
- Civier, O., Smith, R. E., Yeh, C.-H., Connelly, A., & Calamante, F. (2019). Is removal of weak connections necessary for graph-theoretical analysis of dense weighted structural connectomes from diffusion MRI? *Neuroimage*, 194, 68-81.
<https://doi.org/10.1016/j.neuroimage.2019.02.039>
- Cohen, J. (1988). *Statistical power analysis for the behavioral sciences* (2 ed.). Lawrence Earlbaum Associates.

- Cordero-Grande, L., Christiaens, D., Hutter, J., Price, A. N., & Hajnal, J. V. (2019). Complex diffusion-weighted image estimation via matrix recovery under general noise models. *Neuroimage*, 200, 391-404. <https://doi.org/10.1016/j.neuroimage.2019.06.039>
- Currie, S., Saleem, N., Straiton, J. A., Macmullen-Price, J., Warren, D. J., & Craven, I. J. (2016). Imaging assessment of traumatic brain injury. *Postgraduate Medical Journal*, 92(1083), 41-50. <https://doi.org/10.1136/postgradmedj-2014-133211>
- D'souza, M. M., Trivedi, R., Singh, K., Grover, H., Choudhury, A., Kaur, P., . . . Tripathi, R. P. (2015). Traumatic brain injury and the post-concussion syndrome: A diffusion tensor tractography study. *The Indian journal of radiology & imaging*, 25(4), 404. <https://doi.org/10.4103/0971-3026.169445>
- Dale, A. M., Fischl, B., & Sereno, M. I. (1999). Cortical Surface-Based Analysis: I. Segmentation and Surface Reconstruction. *Neuroimage*, 9(2), 179-194. <https://doi.org/10.1006/nimg.1998.0395>
- Dall'Acqua, P., Johannes, S., Mica, L., Simmen, H. P., Glaab, R., Fandino, J., . . . Hanggi, J. (2016). Connectomic and surface-based morphometric correlates of acute mild traumatic brain injury. *Front Hum Neurosci*, 10, 127. <https://doi.org/10.3389/fnhum.2016.00127>
- Dashnaw, M. L., Petraglia, A. L., & Bailes, J. E. (2012). An overview of the basic science of concussion and subconcussion: Where we are and where we are going. *Neurosurgical focus*, 33(6), E5. <https://doi.org/10.3171/2012.10.FOCUS12284>
- Delouche, A., Attie, A., Heck, O., Grand, S., Kastler, A., Lamalle, L., . . . Krainik, A. (2016). Diffusion MRI: Pitfalls, literature review and future directions of research in mild traumatic brain injury. *European Journal of Radiology*, 85(1), 25-30. <https://doi.org/10.1016/j.ejrad.2015.11.004>
- Desikan, R. S., Ségonne, F., Fischl, B., Quinn, B. T., Dickerson, B. C., Blacker, D., . . . Killiany, R. J. (2006). An automated labeling system for subdividing the human cerebral cortex on MRI scans into gyral based regions of interest. *Neuroimage*, 31(3), 968-980. <https://doi.org/10.1016/j.neuroimage.2006.01.021>
- Destrieux, C., Fischl, B., Dale, A., & Halgren, E. (2010). Automatic parcellation of human cortical gyri and sulci using standard anatomical nomenclature. *Neuroimage*, 53(1), 1-15. <https://doi.org/10.1016/j.neuroimage.2010.06.010>
- Dhamala, E., Jamison, K. W., Jaywant, A., Dennis, S., & Kuceyeski, A. (2020). Integrating multimodal connectivity improves prediction of individual cognitive abilities [preprint]. *bioRxiv*. <https://doi.org/10.1101/2020.06.25.172387>

- Dhollander, T., Clemente, A., Singh, M., Boonstra, F., Civier, O., Egorova, N., . . . Caeyenberghs, K. (2020). Fixel-based analysis of diffusion MRI: Methods, applications, challenges and opportunities. *OSF Preprints*. <https://doi.org/10.31219/osf.io/zu8fv>
- Dhollander, T., & Connelly, A. (2016). *A novel iterative approach to reap the benefits of multi-tissue CSD from just single-shell (+b=0) diffusion MRI data* International Society for Magnetic Resonance in Medicine, Singapore.
- Dhollander, T., Mito, R., Raffelt, D., & Connelly, A. (2019). *Improved white matter response function estimation for 3-tissue constrained spherical deconvolution* International Society of Magnetic Resonance in Medicine, Montréal, Québec, Canada.
- Dhollander, T., Raffelt, D., & Connelly, A. (2016). *Unsupervised 3-tissue response function estimation from single-shell or multi-shell diffusion MR data without a co-registered T1 image* ISMRM Workshop on Breaking the Barriers of Diffusion MRI Lisbon, Portugal.
- Dichter, G. S., Sikich, L., Song, A., Voyvodic, J., & Bodfish, J. W. (2012). Functional neuroimaging of treatment effects in psychiatry: Methodological challenges and recommendations. *International Journal of Neuroscience*, 122(9), 483-493. <https://doi.org/10.3109/00207454.2012.678446>
- Dikmen, S. S., Corrigan, J. D., Levin, H. S., Machamer, J., Stiers, W., & Weisskopf, M. G. (2009). Cognitive outcome following traumatic brain injury. *Journal of Head Trauma Rehabilitation*, 24(6), 430-438. <https://doi.org/10.1097/HTR.0b013e3181c133e9>
- Donders, J., & Stout, J. (2019). The influence of cognitive reserve on recovery from traumatic brain injury. *Archives of Clinical Neuropsychology*, 34(2), 206-213. <https://doi.org/10.1093/arclin/acy035>
- Drakesmith, M., Harms, R., Rudrapatna, S. U., Parker, G. D., Evans, C. J., & Jones, D. K. (2019). Estimating axon conduction velocity in vivo from microstructural MRI. *Neuroimage*, 203, 116186. <https://doi.org/10.1016/j.neuroimage.2019.116186>
- Drew, L. B., & Drew, W. E. (2004). The contrecoup-coup phenomenon: A new understanding of the mechanism of closed head injury. *Neurocritical care*, 1(3), 385-390. <https://doi.org/10.1385/NCC:1:3:385>
- Egger, M., Smith, G. D., Schneider, M., & Minder, C. (1997). Bias in meta-analysis detected by a simple, graphical test. *British Medical Journal*, 315, 629 - 634. <https://doi.org/10.1136/bmj.315.7109.629>

- Fagerholm, E. D., Hellyer, P. J., Scott, G., Leech, R., & Sharp, D. J. (2015). Disconnection of network hubs and cognitive impairment after traumatic brain injury. *Brain*, *138*(6), 1696-1709. <https://doi.org/10.1093/brain/awv075>
- Farbota, K. D., Bendlin, B. B., Alexander, A. L., Rowley, H. A., Dempsey, R. J., & Johnson, S. C. (2012). Longitudinal diffusion tensor imaging and neuropsychological correlates in traumatic brain injury patients. *Front Hum Neurosci*, *6*, 160. <https://doi.org/10.3389/fnhum.2012.00160>
- Finn, E. S., Shen, X., Scheinost, D., Rosenberg, M. D., Huang, J., Chun, M. M., . . . Constable, R. T. (2015). Functional connectome fingerprinting: Identifying individuals using patterns of brain connectivity. *Nature Neuroscience*, *18*(11), 1664-1671. <https://doi.org/10.1038/nn.4135>
- Fischl, B. (2012). FreeSurfer. *Neuroimage*, *62*(2), 774-781. <https://doi.org/10.1016/j.neuroimage.2012.01.021>
- Fischl, B., & Dale, A. (2000). Measuring the thickness of the human cerebral cortex from magnetic resonance images. *Proceedings of the National Academy of Sciences*, *97*(20), 11050-11055. <https://doi.org/10.1073/pnas.200033797>
- Fischl, B., Salat, D. H., Busa, E., Albert, M., Dieterich, M., Haselgrove, C., . . . Dale, A. M. (2002). Whole brain segmentation: Automated labeling of neuroanatomical structures in the human brain. *Neuron*, *33*(3), 341-355. [https://doi.org/10.1016/s0896-6273\(02\)00569-x](https://doi.org/10.1016/s0896-6273(02)00569-x)
- Fischl, B., Sereno, M. I., & Dale, A. M. (1999). Cortical surface-based analysis. II: Inflation, flattening, and a surface-based coordinate system. *Neuroimage*, *9*(2), 195-207. <https://doi.org/10.1006/nimg.1998.0396>
- Floyd, R. W. (1962). Algorithm 97: Shortest path. *Communications of the Association for Computing Machinery*, *5*(6), 345. <https://doi.org/10.1145/367766.368168>
- Fornito, A., & Bullmore, E. T. (2010). What can spontaneous fluctuations of the blood oxygenation-level-dependent signal tell us about psychiatric disorders? *Current opinion in psychiatry*, *23*(3), 239-249. <https://doi.org/10.1097/YCO.0b013e328337d78d>
- Fornito, A., Zalesky, A., & Breakspear, M. (2013). Graph analysis of the human connectome: Promise, progress, and pitfalls. *Neuroimage*, *80*, 426-444. <https://doi.org/10.1016/j.neuroimage.2013.04.087>
- Fornito, A., Zalesky, A., & Breakspear, M. (2015). The connectomics of brain disorders. *Nature Reviews Neuroscience*, *16*(3), 159-172. <https://doi.org/10.1038/nrn3901>

- Fornito, A., Zalesky, A., & Bullmore, E. T. (2016). *Fundamentals of Brain Network Analysis*. Academic Press.
- Fornito, A., Zalesky, A., Pantelis, C., & Bullmore, E. T. (2012). Schizophrenia, neuroimaging and connectomics. *Neuroimage*, 62(4), 2296-2314.
<https://doi.org/10.1016/j.neuroimage.2011.12.090>
- Forstmann, B. U., Ratcliff, R., & Wagenmakers, E.-J. (2016). Sequential sampling models in cognitive neuroscience: Advantages, applications, and extensions. *Annual review of psychology*, 67, 641-666. <https://doi.org/10.1146/annurev-psych-122414-033645>
- Fraser, E. E., Downing, M. G., Biernacki, K., McKenzie, D. P., & Ponsford, J. L. (2019). Cognitive reserve and age predict cognitive recovery after mild to severe traumatic brain injury. *Journal Of Neurotrauma*, 36(19), 2753-2761. <https://doi.org/10.1089/neu.2019.6430>
- Freeman, L. C. (1978). Centrality in social networks conceptual clarification. *Social Networks*, 1(3), 215-239. [https://doi.org/10.1016/0378-8733\(78\)90021-7](https://doi.org/10.1016/0378-8733(78)90021-7)
- Fridriksson, J., Fillmore, P., Guo, D., & Rorden, C. (2015). Chronic Broca's aphasia is caused by damage to Broca's and Wernicke's areas. *Cerebral Cortex*, 25(12), 4689-4696.
<https://doi.org/10.1093/cercor/bhu152>
- Frigo, M., Deslauriers-Gauthier, S., Parker, D., Aziz Ould Ismail, A., John Kim, J., Verma, R., & Deriche, R. (2020). Diffusion MRI tractography filtering techniques change the topology of structural connectomes. *Journal of Neural Engineering*, 17(6), 065002.
<https://doi.org/10.1088/1741-2552/abc29b>
- Fujiwara, E., Schwartz, M. L., Gao, F., Black, S. E., & Levine, B. (2008). Ventral frontal cortex functions and quantified MRI in traumatic brain injury. *Neuropsychologia*, 46(2), 461-474.
<https://doi.org/10.1016/j.neuropsychologia.2007.08.027>
- Gadgil, M., Peterson, E., Tregellas, J., Hepburn, S., & Rojas, D. C. (2013). Differences in global and local level information processing in autism: An fMRI investigation. *Psychiatry Research: Neuroimaging*, 213(2), 115-121.
<https://doi.org/10.1016/j.psychresns.2013.02.005>
- Garcia-Rudolph, A., Garcia-Molina, A., Opisso, E., & Tormos Muñoz, J. (2020). Personalized web-based cognitive rehabilitation treatments for patients with traumatic brain injury: Cluster analysis. *Journal of Medical Internet Research*, 8(10), e16077.
<https://doi.org/10.2196/16077>

- Gerlach, C., & Poirel, N. (2018). Navon's classical paradigm concerning local and global processing relates systematically to visual object classification performance. *Scientific Reports*, 8(1), 1-9. <https://doi.org/10.1038/s41598-017-18664-5>
- Goñi, J., Van Den Heuvel, M. P., Avena-Koenigsberger, A., De Mendizabal, N. V., Betzel, R. F., Griffa, A., . . . Sporns, O. (2014). Resting-brain functional connectivity predicted by analytic measures of network communication. *Proceedings of the National Academy of Sciences*, 111(2), 833-838. <https://doi.org/10.1073/pnas.1315529111>
- Gratton, C., Laumann, T. O., Nielsen, A. N., Greene, D. J., Gordon, E. M., Gilmore, A. W., . . . Petersen, S. E. (2018). Functional brain networks are dominated by stable group and individual factors, not cognitive or daily variation. *Neuron*, 98(2), 439-452.e435. <https://doi.org/10.1016/j.neuron.2018.03.035>
- Green, R. E. (2016). Brain injury as a neurodegenerative disorder. *Front Hum Neurosci*, 9, 615. <https://doi.org/10.3389/fnhum.2015.00615>
- Griffa, A., Baumann, P. S., Thiran, J. P., & Hagmann, P. (2013). Structural connectomics in brain diseases. *Neuroimage*, 80, 515-526. <https://doi.org/10.1016/j.neuroimage.2013.04.056>
- Grimes, D. A., & Schulz, K. F. (2002). Descriptive studies: What they can and cannot do. *The Lancet*, 359(9301), 145-149. [https://doi.org/10.1016/s0140-6736\(02\)07373-7](https://doi.org/10.1016/s0140-6736(02)07373-7)
- Gronwall, D., & Sampson, H. (1974). *The psychological effects of concussion*. Auckland U Press.
- Håberg, A. K., Olsen, A., Moen, K. G., Schirmer-Mikalsen, K., Visser, E., Finnanger, T. G., . . . Eikenes, L. (2015). White matter microstructure in chronic moderate-to-severe traumatic brain injury: Impact of acute-phase injury-related variables and associations with outcome measures. *Journal of Neuroscience Research*, 93(7), 1109-1126. <https://doi.org/10.1002/jnr.23534>
- Hagmann, P., Cammoun, L., Gigandet, X., Meuli, R., Honey, C. J., Wedeen, V. J., & Sporns, O. (2008). Mapping the structural core of human cerebral cortex. *PLoS Biology*, 6(7), e159. <https://doi.org/10.1371/>
- Hammoud, D. A., & Wasserman, B. A. (2002). Diffuse axonal injuries: Pathophysiology and imaging. *Neuroimaging Clinics of North America*, 12(2), 205-216. [https://doi.org/10.1016/s1052-5149\(02\)00011-4](https://doi.org/10.1016/s1052-5149(02)00011-4)
- Hampshire, A., Hellyer, P. J., Parkin, B., Hiebert, N., MacDonald, P., Owen, A. M., . . . Rowe, J. (2016). Network mechanisms of intentional learning. *Neuroimage*, 127, 123-134. <https://doi.org/10.1016/j.neuroimage.2015.11.060>

- Han, S., Jiang, Y., & Gu, H. (2004). Neural substrates differentiating global/local processing of bilateral visual inputs. *Human Brain Mapping*, 22(4), 321-328.
<https://doi.org/10.1002/hbm.20044>
- Hannawi, Y., & Stevens, R. D. (2016). Mapping the connectome following traumatic brain injury [Article]. *Current Neurology & Neuroscience Reports*, 16(5), Article 44.
<https://doi.org/10.1007/s11910-016-0642-9>
- Hansen, A. M., Garde, A. H., & Eller, N. H. (2007). Estimation of individual reference intervals in small sample sizes. *International Journal of Hygiene & Environmental Health*, 210(3-4), 471-478. <https://doi.org/10.1016/j.ijheh.2007.01.012>
- Hedden, T., & Gabrieli, J. D. (2010). Shared and selective neural correlates of inhibition, facilitation, and shifting processes during executive control. *Neuroimage*, 51(1), 421-431.
<https://doi.org/10.1016/j.neuroimage.2010.01.089>
- Hedges, L. V., & Olkin, I. (2014). *Statistical methods for meta-analysis*. Academic press.
- Hellyer, P. J., Scott, G., Shanahan, M., Sharp, D. J., & Leech, R. (2015). Cognitive flexibility through metastable neural dynamics is disrupted by damage to the structural connectome. *Journal of Neuroscience*, 35(24), 9050-9063.
<https://doi.org/10.1523/JNEUROSCI.4648-14.2015>
- Higgins, J. P., Thompson, S. G., & Deeks, J. J. (2003). Measuring inconsistency in meta-analyses. *British Medical Journal*, 327(7414), 557-560. <https://doi.org/10.1136/bmj.327.7414.557>
- Hikosaka, O., & Isoda, M. (2010). Switching from automatic to controlled behavior: Cortico-basal ganglia mechanisms. *Trends in Cognitive Sciences*, 14(4), 154-161.
<https://doi.org/10.1016/j.tics.2010.01.006>
- Holdnack, J. A., Prifitera, A., Weiss, L. G., & Saklofske, D. H. (2015). WISC-V and the personalized assessment approach. *WISC-V assessment and interpretation: Scientist-practitioner perspectives*, 373. <https://doi.org/10.1016/B978-0-12-404697-9.00012-1>
- Honey, C. J., Sporns, O., Cammoun, L., Gigandet, X., Thiran, J.-P., Meuli, R., & Hagmann, P. (2009). Predicting human resting-state functional connectivity from structural connectivity. *Proceedings of the National Academy of Sciences*, 106(6), 2035-2040.
<https://doi.org/10.1073/pnas.0811168106>
- Horbruegger, M., Loewe, K., Kaufmann, J., Wagner, M., Schippling, S., Pawlitzki, M., & Schoenfeld, M. A. (2019). Anatomically constrained tractography facilitates biologically plausible fiber reconstruction of the optic radiation in multiple sclerosis. *NeuroImage: Clinical*, 22, 101740. <https://doi.org/10.1016/j.nicl.2019.101740>

- Hsu, Y. C., Lo, Y. C., Chen, Y. J., Wedeen, V. J., & Isaac Tseng, W. Y. (2015). NTU-DSI-122: A diffusion spectrum imaging template with high anatomical matching to the ICBM-152 space. *Human Brain Mapping*, 36(9), 3528-3541. <https://doi.org/10.1002/hbm.22860>
- Hübner, R. (2014). Does attentional selectivity in global/local processing improve discretely or gradually? *Frontiers in Psychology*, 5, 61. <https://doi.org/10.3389/fpsyg.2014.00061>
- Huisman, T. A., Schwamm, L. H., Schaefer, P. W., Koroshetz, W. J., Shetty-Alva, N., Ozsunar, Y., . . . Sorensen, A. G. (2004). Diffusion tensor imaging as potential biomarker of white matter injury in diffuse axonal injury. *American Journal of Neuroradiology*, 25(3), 370-376.
- Hulkower, M. B., Poliak, D. B., Rosenbaum, S. B., Zimmerman, M. E., & Lipton, M. L. (2013). A decade of DTI in traumatic brain injury: 10 years and 100 articles later. *American Journal of Neuroradiology*, 34(11), 2064-2074. <https://doi.org/10.3174/ajnr.A3395>
- Humphreys, I., Wood, R. L., Phillips, C. J., & Macey, S. (2013). The costs of traumatic brain injury: A literature review. *ClinicoEconomics & Outcomes Research*, 5, 281-287. <https://doi.org/10.2147/CEOR.S44625>
- Hutchinson, E. B., Schwerin, S. C., Avram, A. V., Juliano, S. L., & Pierpaoli, C. (2018). Diffusion MRI and the detection of alterations following traumatic brain injury. *Journal of Neuroscience Research*, 96(4), 612-625. <https://doi.org/10.1002/jnr.24065>
- Hyder, A. A., Wunderlich, C. A., Puvanachandra, P., Gururaj, G., & Kobusingye, O. C. (2007). The impact of traumatic brain injuries: A global perspective. *NeuroRehabilitation*, 22, 341-353. <https://doi.org/10.3233/NRE-2007-22502>
- Imms, P., Clemente, A., Cook, M., D'Souza, W., Wilson, P. H., Jones, D. K., & Caeyenberghs, K. (2019). The structural connectome in traumatic brain injury: A meta-analysis of graph metrics. *Neuroscience & Biobehavioral Reviews*, 99, 128-137. <https://doi.org/10.1016/j.neubiorev.2019.01.002>
- Imms, P., Dominguez, D. J. F., Burmester, A., Seguin, C., Clemente, A., Dhollander, T., . . . Caeyenberghs, K. (2021). Navigating the link between processing speed and network communication in the human brain. *Brain Struct Funct*, 226(4), 1281-1302. <https://doi.org/10.1007/s00429-021-02241-8>
- Inglese, M., Makani, S., Johnson, G., Cohen, B. A., Silver, J. A., Gonen, O., & Grossman, R. I. (2005). Diffuse axonal injury in mild traumatic brain injury: A diffusion tensor imaging study. *Journal Of Neurosurgery*, 103(2), 298-303. <https://doi.org/10.3171/jns.2005.103.2.0298>

- Irimia, A., Chambers, M. C., Torgerson, C. M., Filippou, M., Hovda, D. A., Alger, J. R., . . . Van Horn, J. D. (2012). Patient-tailored connectomics visualization for the assessment of white matter atrophy in traumatic brain injury [Article]. *Frontiers in Neurology*, 3(1), 10, Article Article 10. <https://doi.org/10.3389/fneur.2012.00010>
- Irimia, A., Wang, B., Aylward, S. R., Prastawa, M. W., Pace, D. F., Gerig, G., . . . Van Horn, J. D. (2012). Neuroimaging of structural pathology and connectomics in traumatic brain injury: Toward personalized outcome prediction. *NeuroImage: Clinical*, 1(1), 1-17. <https://doi.org/10.1016/j.nicl.2012.08.002>
- James, S. L., Theadom, A., Ellenbogen, R. G., Bannick, M. S., Montjoy-Venning, W., Lucchesi, L. R., . . . Murray, C. J. L. (2019). Global, regional, and national burden of traumatic brain injury and spinal cord injury, 1990-2016: A systematic analysis for the Global Burden of Disease Study 2016. *The Lancet Neurology*, 18(1), 56-87. [https://doi.org/10.1016/S1474-4422\(18\)30415-0](https://doi.org/10.1016/S1474-4422(18)30415-0)
- Jelcic, N., Della Puppa, A., Mottaran, R., Cecchin, D., Manara, R., Dam, M., & Cagnin, A. (2013). Case series evidence for improvement of executive functions after late cranioplasty. *Brain Injury*, 27(13-14), 1723-1726. <https://doi.org/10.3109/02699052.2013.844857>
- Jenkinson, M., Bannister, P., Brady, M., & Smith, S. (2002). Improved optimization for the robust and accurate linear registration and motion correction of brain images. *Neuroimage*, 17(2), 825-841. [https://doi.org/10.1016/s1053-8119\(02\)91132-8](https://doi.org/10.1016/s1053-8119(02)91132-8)
- Jenkinson, M., Beckmann, C. F., Behrens, T. E., Woolrich, M. W., & Smith, S. M. (2012). FSL. *Neuroimage*, 62(2), 782-790. <https://doi.org/10.1016/j.neuroimage.2011.09.015>
- Jenkinson, M., & Smith, S. (2001). A global optimisation method for robust affine registration of brain images. *Medical Image Analysis*, 5(2), 143-156. [https://doi.org/10.1016/s1361-8415\(01\)00036-6](https://doi.org/10.1016/s1361-8415(01)00036-6)
- Jeurissen, B., Descoteaux, M., Mori, S., & Leemans, A. (2019). Diffusion MRI fiber tractography of the brain. *Nuclear Magnetic Resonance in Biomedicine*, 32(4), e3785. <https://doi.org/10.1002/nbm.3785>
- Jeurissen, B., Leemans, A., Tournier, J. D., Jones, D. K., & Sijbers, J. (2013). Investigating the prevalence of complex fiber configurations in white matter tissue with diffusion magnetic resonance imaging. *Human Brain Mapping*, 34(11), 2747-2766. <https://doi.org/10.1002/hbm.22099>

- Jeurissen, B., Tournier, J.-D., Dhollander, T., Connelly, A., & Sijbers, J. (2014). Multi-tissue constrained spherical deconvolution for improved analysis of multi-shell diffusion MRI data. *Neuroimage*, *103*, 411-426. <https://doi.org/10.1016/j.neuroimage.2014.07.061>
- Jiang, J., Zhao, Y. J., Hu, X. Y., Du, M. Y., Chen, Z. Q., Wu, M., . . . Gong, Q. Y. (2017). Microstructural brain abnormalities in medication-free patients with major depressive disorder: A systematic review and meta-analysis of diffusion tensor imaging. *Journal of Psychiatry & Neuroscience*, *42*(3), 150-163. <https://doi.org/10.1503/jpn.150341>
- Jolly, A. E., Balaet, M., Azor, A., Friedland, D., Sandrone, S., Graham, N. S. N., . . . Sharp, D. J. (2021). Detecting axonal injury in individual patients after traumatic brain injury. *Brain*, *144*(1), 92-113. <https://doi.org/10.1093/brain/awaa372>
- Jolly, A. E., Scott, G. T., Sharp, D. J., & Hampshire, A. H. (2020). Distinct patterns of structural damage underlie working memory and reasoning deficits after traumatic brain injury. *Brain*, *143*(4), 1158-1176. <https://doi.org/10.1093/brain/awaa067>
- Jones, D. K. (2010a). Challenges and limitations of quantifying brain connectivity in vivo with diffusion MRI. *Imaging in Medicine*, *2*(3), 341–355. <https://doi.org/10.2217/iim.10.21>
- Jones, D. K. (2010b). *Diffusion MRI*. Oxford University Press.
- Jones, D. K., & Cercignani, M. (2010). Twenty-five pitfalls in the analysis of diffusion MRI data. *Nuclear Magnetic Resonance in Biomedicine*, *23*(7), 803-820. <https://doi.org/10.1002/nbm.1543>
- Jones, D. K., Knosche, T. R., & Turner, R. (2013). White matter integrity, fiber count, and other fallacies: The do's and don'ts of diffusion MRI. *Neuroimage*, *73*, 239-254. <https://doi.org/10.1016/j.neuroimage.2012.06.081>
- Kail, R., & Salthouse, T. A. (1994). Processing speed as a mental capacity. *Acta Psychologica*, *86*(2-3), 199-225. [https://doi.org/10.1016/0001-6918\(94\)90003-5](https://doi.org/10.1016/0001-6918(94)90003-5)
- Karahan, E., Costigan, A. G., Graham, K. S., Lawrence, A. D., & Zhang, J. (2019). Cognitive and white-matter compartment models reveal selective relations between corticospinal tract microstructure and simple reaction time. *Journal of Neuroscience*, *39*(30), 5910-5921. <https://doi.org/10.1523/JNEUROSCI.2954-18.2019>
- Kay, T., & Lezak, M. (1990). The nature of head injury. In D. W. Corthell (Ed.), *Traumatic brain injury and vocational rehabilitation* (pp. 22-65).
- Kellner, E., Dhital, B., Kiselev, V. G., & Reiser, M. (2016). Gibbs-ringing artifact removal based on local subvoxel-shifts. *Magnetic resonance in Medicine*, *76*(5), 1574-1581. <https://doi.org/10.1002/mrm.26054>

- Kerchner, G. A., Racine, C. A., Hale, S., Wilhelm, R., Laluz, V., Miller, B. L., & Kramer, J. H. (2012). Cognitive processing speed in older adults: Relationship with white matter integrity. *PLoS One*, 7(11), e50425. <https://doi.org/10.1371/journal.pone.0050425>
- Khan, W., Egorova, N., Khlif, M. S., Mito, R., Dhollander, T., & Brodtmann, A. (2020). Three-tissue compositional analysis reveals in-vivo microstructural heterogeneity of white matter hyperintensities following stroke. *Neuroimage*, 218, 116869. <https://doi.org/10.1016/j.neuroimage.2020.116869>
- Kim, J., Parker, D., Whyte, J., Hart, T., Pluta, J., Ingallhalikar, M., . . . Verma, R. (2014a). Disrupted structural connectome is associated with both psychometric and real-world neuropsychological impairment in diffuse traumatic brain injury. *Journal of the International Neuropsychological Society*, 20(9), 887-896. <https://doi.org/10.1017/S1355617714000812>
- Kim, J., Parker, D., Whyte, J., Hart, T., Pluta, J., Ingallhalikar, M., . . . Verma, R. (2014b). Disrupted structural connectome predicts cognitive performance in people with diffuse traumatic brain injury: A graph theoretical analysis. *Brain Injury*, 28(5-6), 644-644. <Go to ISI>://WOS:000335017000312
- Kimchi, R. (2015). The perception of hierarchical structure. In J. Wagemans (Ed.), *Oxford handbook of perceptual organization* (pp. 129-149). Oxford University Press.
- Kinnunen, K. M., Greenwood, R., Powell, J. H., Leech, R., Hawkins, P. C., Bonnelle, V., . . . Sharp, D. J. (2011). White matter damage and cognitive impairment after traumatic brain injury. *Brain*, 134(Pt 2), 449-463. <https://doi.org/10.1093/brain/awq347>
- Königs, M., van Heurn, L. W. E., Bakx, R., Vermeulen, R. J., Goslings, J. C., Poll-The, B. T., . . . Pouwels, P. J. W. (2017). The structural connectome of children with traumatic brain injury [Article in Press]. *Human Brain Mapping*, 38, 3603-3614. <https://doi.org/10.1002/hbm.23614>
- Kottaram, A., Johnston, L. A., Tian, Y., Ganella, E. P., Laskaris, L., Cocchi, L., . . . Zalesky, A. (2020). Predicting individual improvement in schizophrenia symptom severity at 1-year follow-up: Comparison of connectomic, structural, and clinical predictors. *Human Brain Mapping*, 41(12), 3342-3357. <https://doi.org/10.1002/hbm.25020>
- Kou, Z. F., Iraj, A., Chen, H. B., Wiseman, N., Haacke, E. M., Welch, R., & Liiu, T. M. (2015, Jun). Connectome scale assessment of brain network connectivity in mild traumatic brain injury. Annual National Neurotrauma Symposium, New Mexico.

- Kraus, M. F., Susmaras, T., Caughlin, B. P., Walker, C. J., Sweeney, J. A., & Little, D. M. (2007). White matter integrity and cognition in chronic traumatic brain injury: A diffusion tensor imaging study. *Brain*, 130(10), 2508-2519. <https://doi.org/10.1093/brain/awm216>
- Kreutzer, J. S., Kolakowsky-Hayner, S. A., Demm, S. R., & Meade, M. A. (2002). A structured approach to family intervention after brain injury. *The Journal Of Head Trauma Rehabilitation*, 17(4), 349-367. <https://doi.org/10.1097/00001199-200208000-00008>
- Kreutzer, J. S., Marwitz, J. H., Seel, R. T., & Serio, C. D. (1996). Validation of a neurobehavioral functioning inventory for adults with traumatic brain injury *Archives of Physical Medicine & Rehabilitation*, 77, 116 - 124. [https://doi.org/10.1016/s0003-9993\(96\)90155-0](https://doi.org/10.1016/s0003-9993(96)90155-0)
- Kreutzer, J. S., Seel, R. T., & Marwitz, J. H. (1999). *Neurobehavioral Functioning Inventory: NFI*.
- Kurland, D., Hong, C., Aarabi, B., Gerzanich, V., & Simard, J. M. (2012). Hemorrhagic progression of a contusion after traumatic brain injury: A review. *Journal Of Neurotrauma*, 29(1), 19-31. <https://doi.org/10.1089/neu.2011.2122>
- Lamme, V. A. (2003). Why visual attention and awareness are different. *Trends in Cognitive Sciences*, 7(1), 12-18. [https://doi.org/10.1016/s1364-6613\(02\)00013-x](https://doi.org/10.1016/s1364-6613(02)00013-x)
- Latora, V., & Marchiori, M. (2001). Efficient behavior of small-world networks. *Physical Review Letters*, 87(19), 198701. <https://doi.org/10.1103/PhysRevLett.87.198701>
- Lazaridou, A., Astrakas, L., Mintzopoulos, D., Khanicheh, A., Singhal, A. B., Moskowitz, M. A., . . . Tzika, A. A. (2013). Diffusion tensor and volumetric magnetic resonance imaging using an MR-compatible hand-induced robotic device suggests training-induced neuroplasticity in patients with chronic stroke. *International Journal of Molecular Medicine*, 32(5), 995-1000. <https://doi.org/10.3892/ijmm.2013.1476>
- Le Bihan, D., Poupon, C., Amadon, A., & Lethimonnier, F. (2006). Artifacts and pitfalls in diffusion MRI. *Journal of Magnetic Resonance Imaging*, 24(3), 478-488. <https://doi.org/10.1002/jmri.20683>
- Leunissen, I., Coxon, J. P., Caeyenberghs, K., Michiels, K., Sunaert, S., & Swinnen, S. P. (2014). Subcortical volume analysis in traumatic brain injury: The importance of the fronto-striato-thalamic circuit in task switching. *Cortex*, 51, 67-81. <https://doi.org/10.1016/j.cortex.2013.10.009>
- Leunissen, I., Coxon, J. P., & Swinnen, S. P. (2016). A proactive task set influences how response inhibition is implemented in the basal ganglia. *Human Brain Mapping*, 37(12), 4706-4717. <https://doi.org/10.1002/hbm.23338>

- Levin, H. S., Wilde, E. A., Chu, Z., Yallampalli, R., Hanten, G. R., Li, X., . . . Hunter, J. V. (2008). Diffusion tensor imaging in relation to cognitive and functional outcome of traumatic brain injury in children. *Journal of Head Trauma Rehabilitation*, 23(4), 197-208. <https://doi.org/10.1097/01.HTR.0000327252.54128.7c>
- Levine, B., Kovacevic, N., Nica, E., Cheung, G., Gao, F., Schwartz, M., & Black, S. (2008). The Toronto traumatic brain injury study: Injury severity and quantified MRI. *Neurology*, 70(10), 771-778. <https://doi.org/10.1212/01.wnl.0000304108.32283.aa>
- Li, X. Y., & Feng, D. F. (2009). Diffuse axonal injury: Novel insights into detection and treatment. *Journal of Clinical Neuroscience*, 16(5), 614-619. <https://doi.org/10.1016/j.jocn.2008.08.005>
- Liddell, B. J., Das, P., Battaglini, E., Malhi, G. S., Felmingham, K. L., Whitford, T. J., & Bryant, R. A. (2015). Self-orientation modulates the neural correlates of global and local processing. *PLoS One*, 10(8), e0135453. <https://doi.org/10.1371/journal.pone.0135453>
- Lipton, M. L., Gellella, E., Lo, C., Gold, T., Ardekani, B. A., Shifteh, K., . . . Branch, C. A. (2008). Multifocal white matter ultrastructural abnormalities in mild traumatic brain injury with cognitive disability: A voxel-wise analysis of diffusion tensor imaging. *Journal Of Neurotrauma*, 25(11), 1335-1342. <https://doi.org/10.1089/neu.2008.0547>
- Lo, C.-Y., Wang, P.-N., Chou, K.-H., Wang, J., He, Y., & Lin, C.-P. (2010). Diffusion tensor tractography reveals abnormal topological organization in structural cortical networks in Alzheimer's disease. *The Journal of Neuroscience*, 30(50), 16876-16885. <https://doi.org/10.1523/JNEUROSCI.4136-10.2010>
- Lv, J., Di Biase, M., Cash, R. F. H., Cocchi, L., Cropley, V. L., Klauser, P., . . . Zalesky, A. (2020). Individual deviations from normative models of brain structure in a large cross-sectional schizophrenia cohort. *Molecular Psychiatry*. <https://doi.org/10.1038/s41380-020-00882-5>
- Lynn, C. W., & Bassett, D. S. (2019). The physics of brain network structure, function and control. *Nature Reviews Physics*, 1(5), 318-332. <https://doi.org/10.1038/s42254-019-0040-8>
- Maas, A. (2016). Traumatic brain injury: Changing concepts and approaches. *Chinese journal of traumatology*, 19(1), 3-6. <https://doi.org/10.1016/j.cjtee.2016.01.001>
- Maas, A. I. R., Stocchetti, N., & Bullock, R. (2008). Moderate and severe traumatic brain injury in adults. *Lancet Neurology*, 7, 728-741. [https://doi.org/10.1016/S1474-4422\(08\)70164-9](https://doi.org/10.1016/S1474-4422(08)70164-9)
- Madigan, N. K., DeLuca, J., Diamond, B. J., Tramontano, G., & Averill, A. (2000). Speed of information processing in traumatic brain injury: Modality-specific factors. *The Journal Of*

- Head Trauma Rehabilitation*, 15(3), 943-956. <https://doi.org/10.1097/00001199-200006000-00007>
- Maier-Hein, K. H., Neher, P. F., Houde, J. C., Côté, M. A., Garyfallidis, E., Zhong, J., . . . Descoteaux, M. (2017). The challenge of mapping the human connectome based on diffusion tractography. *Nature communications*, 8(1), 1-13. <https://doi.org/10.1038/s41467-017-01285-x>
- Majdan, M., Mauritz, W., Brazinova, A., Rusnak, M., Leitgeb, J., Janciak, I., & Wilbacher, I. (2011). Severity and outcome of traumatic brain injuries (TBI) with different causes of injury. *Brain Injury*, 25(9), 797-805. <https://doi.org/10.3109/02699052.2011.581642>
- Makowski, C., Lepage, M., & Evans, A. C. (2019). Head motion: The dirty little secret of neuroimaging in psychiatry. *Journal of Psychiatry & Neuroscience*, 44(1), 62. <https://doi.org/10.1503/jpn.180022>
- Mancini, M., Giulietti, G., Dowell, N., Spanò, B., Harrison, N., Bozzali, M., & Cercignani, M. . (2017). Introducing axonal myelination in connectomics: A preliminary analysis of g-ratio distribution in healthy subjects. *Neuroimage*, 17, 30766-30768. <https://doi.org/10.1016/j.neuroimage.2017.09.018>
- Mant, D. (1999). Can randomised trials inform clinical decisions about individual patients? *The Lancet*, 353(9154), 743-746. [https://doi.org/10.1016/S0140-6736\(98\)09102-8](https://doi.org/10.1016/S0140-6736(98)09102-8)
- Mason, P. H., Dominguez, D. J., Winter, B., & Grignolio, A. (2015). Hidden in plain view: Degeneracy in complex systems. *Biosystems*, 128, 1-8. <https://doi.org/10.1016/j.biosystems.2014.12.003>
- Mayer, A. R., Ling, J., Mannell, M., Gasparovic, C., Phillips, J., Doezenia, D., . . . Yeo, R. (2010). A prospective diffusion tensor imaging study in mild traumatic brain injury. *Neurology*, 74(8), 643-650. <https://doi.org/10.1212/WNL.0b013e3181d0ccdd>
- McColgan, P., Blom, T., Rees, G., Seunarine, K. K., Gregory, S., Johnson, E., . . . Clark, C. A. (2018). Stability and sensitivity of structural connectomes: Effect of thresholding and filtering and demonstration in neurodegeneration. *bioRxiv*, 416826. <https://doi.org/10.1101/416826>
- Meningher, I., Bernstein-Eliav, M., Rubovitch, V., Pick, C. G., & Tavor, I. (2020). Alterations in network connectivity after traumatic brain injury in mice. *Journal Of Neurotrauma*, 37(20). <https://doi.org/10.1089/neu.2020.7063>
- Metzler-Baddeley, C., Caeyenberghs, K., Foley, S., & Jones, D. K. (2016). Task complexity and location specific changes of cortical thickness in executive and salience networks after

- working memory training. *Neuroimage*, 130, 48-62.
<https://doi.org/10.1016/j.neuroimage.2016.01.007>
- Meythaler, J. M., Peduzzi, J. D., Eleftheriou, E., & Novack, T. A. (2001). Current concepts: Diffuse axonal injury–associated traumatic brain injury. *Archives of Physical Medicine and Rehabilitation*, 82(10), 1461-1471. <https://doi.org/10.1053/apmr.2001.25137>
- Milner, B. (1982). Some cognitive effects of frontal-lobe lesions in man. *Philosophical transactions of the Royal Society of London. Series B, Biological sciences*, 298(1089), 211-226.
<https://doi.org/10.1098/rstb.1982.0083>
- Miranda-Dominguez, O., Mills, B. D., Carpenter, S. D., Grant, K. A., Kroenke, C. D., Nigg, J. T., & Fair, D. A. (2014). Connectotyping: Model based fingerprinting of the functional connectome. *PLoS One*, 9(11), e111048. <https://doi.org/10.1371/journal.pone.0111048>
- Mito, R., Raffelt, D., Dhollander, T., Vaughan, D. N., Tournier, J.-D., Salvado, O., . . . Connelly, A. (2018). Fibre-specific white matter reductions in Alzheimer’s disease and mild cognitive impairment. *Brain*, 141(3), 888-902. <https://doi.org/10.1093/brain/awx355>
- Mitra, J., Shen, K. K., Ghose, S., Bourgeat, P., Fripp, J., Salvado, O., . . . Rose, S. (2016). Statistical machine learning to identify traumatic brain injury (TBI) from structural disconnections of white matter networks. *Neuroimage*, 129, 247-259.
<https://doi.org/10.1016/j.neuroimage.2016.01.056>
- Mueller, S. T., & Piper, B. J. (2014). The Psychology Experiment Building Language (PEBL) and PEBL Test Battery. *Journal of Neuroscience Methods*, 222, 250-259.
<https://doi.org/10.1016/j.jneumeth.2013.10.024>
- Murray, C. J., Lopez, A. D., & Organization, W. H. (1996). *The global burden of disease: A comprehensive assessment of mortality and disability from diseases, injuries, and risk factors in 1990 and projected to 2020: summary* (0965546608).
- Myburgh, J. A., Cooper, D. J., Finfer, S. R., Venkatesh, B., Jones, D., Higgins, A., . . . Hignett, T. (2008). Epidemiology and 12-month outcomes from traumatic brain injury in Australia and New Zealand. *Journal of Trauma*, 64(4), 854-862.
<https://doi.org/10.1097/TA.0b013e3180340e77>
- Mycroft, R. H., Mitchell, D. C., & Kay, J. (2002). An evaluation of statistical procedures for comparing an individual's performance with that of a group of controls. *Cognitive Neuropsychology*, 19(4), 291-299. <https://doi.org/10.1080/02643290143000150>

- Nachev, P., Coulthard, E., Jäger, H. R., Kennard, C., & Husain, M. (2008). Enantiomorphic normalization of focally lesioned brains. *Neuroimage*, 39(3), 1215-1226.
<https://doi.org/10.1016/j.neuroimage.2007.10.002>
- Navon, D. (1977). Forest before trees: The precedence of global features in visual perception. *Cognitive psychology*, 9(3), 353-383. [https://doi.org/10.1016/0010-0285\(77\)90012-3](https://doi.org/10.1016/0010-0285(77)90012-3)
- Niogi, S. N., Mukherjee, P., Ghajar, J., Johnson, C., Kolster, R. A., Sarkar, R., . . . McCandliss, B. D. (2008). Extent of microstructural white matter injury in postconcussive syndrome correlates with impaired cognitive reaction time: A 3T diffusion tensor imaging study of mild traumatic brain injury. *American Journal of Neuroradiology*, 29(5), 967-973.
<https://doi.org/10.3174/ajnr.A0970>
- Nortje, J., & Menon, D. K. (2004). Traumatic brain injury: Physiology, mechanisms, and outcome. *Current Opinion In Neurology*, 17(6), 711-718.
<https://doi.org/10.1097/00019052-200412000-00011>
- Novack, T. A., Bush, B. A., Meythaler, J. M., & Canupp, K. (2001). Outcome after traumatic brain injury: Pathway analysis of contributions from premorbid, injury severity, and recovery variables. *Archives of Physical Medicine and Rehabilitation*, 82(3), 300-305.
<https://doi.org/10.1053/apmr.2001.18222>
- Oldfield, R. C. (1971). The assessment and analysis of handedness: The Edinburgh inventory. *Neuropsychologia*, 9(1), 97-113. [https://doi.org/10.1016/0028-3932\(71\)90067-4](https://doi.org/10.1016/0028-3932(71)90067-4)
- Olsen, A., Babikian, T., Bigler, E. D., Caeyenberghs, K., Conde, V., Dams-O'Connor, K., . . . Hillary, F. G. (2020). Toward a global and reproducible science for brain imaging in neurotrauma: The ENIGMA adult moderate/severe traumatic brain injury working group. *Brain Imaging & Behavior*. <https://doi.org/10.1007/s11682-020-00313-7>
- Oni, M. B., Wilde, E. A., Bigler, E. D., McCauley, S. R., Wu, T. C., Yallampalli, R., . . . Levin, H. S. (2010). Diffusion tensor imaging analysis of frontal lobes in pediatric traumatic brain injury. *Journal of Child Neurology*, 25(8), 976-984.
<https://doi.org/10.1177/0883073809356034>
- Osmanlıoğlu, Y., Alappatt, J. A., Parker, D., Kim, J., & Verma, R. (2019). *A graph based similarity measure for assessing altered connectivity in traumatic brain injury* International MICCAI Brainlesion Workshop, Granada, Spain.
- Owen, A. M., Downes, J. J., Sahakian, B. J., Polkey, C. E., & Robbins, T. W. (1990). Planning and spatial working memory following frontal lobe lesions in man. *Neuropsychologia*, 28(10), 1021-1034. [https://doi.org/10.1016/0028-3932\(90\)90137-d](https://doi.org/10.1016/0028-3932(90)90137-d)

- Papo, D., Zanin, M., Martinez, J. H., & Buldu, J. M. (2016). Beware of the small-world neuroscientist! *Front Hum Neurosci*, 10, 96. <https://doi.org/10.3389/fnhum.2016.00096>
- Park, E., Bell, J. D., & Baker, A. J. (2008). Traumatic brain injury: Can the consequences be stopped? *Canadian Medical Association Journal*, 178(9), 1163-1170. <https://doi.org/10.1503/cmaj.080282>
- Park, M. K., Hwang, S. H., Jung, S., Hong, S. S., & Kwon, S. B. (2014). Lesions in the splenium of the corpus callosum: Clinical and radiological implications [Article]. *Neurology Asia*, 19(1), 79-88. <http://ezproxy.acu.edu.au/login?url=https://search.ebscohost.com/login.aspx?direct=true&db=a9h&AN=95405170&site=ehost-live&scope=site>
- Park, S. E., Choi, D. S., Shin, H. S., Baek, H. J., Choi, H. C., Kim, J. E., . . . Park, M. J. (2017). Splenial lesions of the corpus callosum: Disease spectrum and MRI findings. *Korean journal of radiology*, 18(4), 710-721. <https://doi.org/10.3348/kjr.2017.18.4.710>
- Parsons, N., Hughes, M., Poudel, G. R., Dominguez, D. J. F., & Caeyenberghs, K. (2020, December 3). *Structure-function relationships in brain-injured patients: A scoping review*.
- Pekna, M., & Pekny, M. (2012). The neurobiology of brain injury. *Cerebrum: The Dana Forum on Brain Science*, Jul-Aug, 9.
- Pekna, M., Pekny, M., & Nilsson, M. (2012). Modulation of neural plasticity as a basis for stroke rehabilitation. *Stroke*, 43(10), 2819-2828. <https://doi.org/10.1161/STROKEAHA.112.654228>
- Pestilli, F., Yeatman, J. D., Rokem, A., Kay, K. N., & Wandell, B. A. (2014). Evaluation and statistical inference for human connectomes. *Nature methods*, 11(10), 1058-1063. <https://doi.org/10.1038/nmeth.3098>
- Pinto, M. S., Paolella, R., Billiet, T., Van Dyck, P., Guns, P.-J., Jeurissen, B., . . . Sijbers, J. (2020). Harmonization of brain diffusion MRI: Concepts and methods. *Frontiers in Neuroscience*, 14, 396-396. <https://doi.org/10.3389/fnins.2020.00396>
- Ponsford, J., & Kinsella, G. (1992). Attentional deficits following closed-head injury. *Journal of Clinical & Experimental Neuropsychology*, 14(5), 822-838. <https://doi.org/10.1080/01688639208402865>
- Posner, M. I., & Boies, S. J. (1971). Components of attention. *Psychological review*, 78(5), 391. <https://doi.org/10.1037/h0031333>

- Posner, M. I., & DiGirolamo, G. J. (1998). Executive attention: Conflict, target detection, and cognitive control. In R. Parasuraman (Ed.), *The Attentive Brain* (pp. 401-423). The MIT Press.
- Poudel, G. R., Bhattarai, A., Dickinson, D. L., & Drummond, S. (2017). Neural correlates of decision-making during a Bayesian choice task. *Neuroreport*, 28(4), 193-199.
<https://doi.org/0.1097/WNR.0000000000000730>
- Poudel, G. R., Dominguez, D. J., Verhelst, H., Vander Linden, C., Deblaere, K., Jones, D. K., . . . Caeyenberghs, K. (2020). Network diffusion modeling predicts neurodegeneration in traumatic brain injury. *Annals of Clinical & Translational Neurology*, 7(3), 270-279.
<https://doi.org/10.1002/acn3.50984>
- Poudel, G. R., Harding, I. H., Egan, G. F., & Georgiou-Karistianis, N. (2019). Network spread determines severity of degeneration and disconnection in Huntington's disease. *Human Brain Mapping*, 40(14), 4192-4201. <https://doi.org/10.1002/hbm.24695>
- Powell, G., Jones, C. R. G., Hedge, C., Charman, T., Happé, F., Simonoff, E., & Sumner, P. (2019). Face processing in autism spectrum disorder re-evaluated through diffusion models. *Neuropsychology*, 33(4), 445-461. <https://doi.org/10.1037/neu0000524>
- Price, C. J., & Friston, K. J. (2002). Degeneracy and cognitive anatomy. *Trends in Cognitive Sciences*, 6(10), 416-421. [https://doi.org/10.1016/s1364-6613\(02\)01976-9](https://doi.org/10.1016/s1364-6613(02)01976-9)
- Pustina, D., Coslett, H. B., Turkeltaub, P. E., Tustison, N., Schwartz, M. F., & Avants, B. (2016). Automated segmentation of chronic stroke lesions using LINDA: Lesion identification with neighborhood data analysis. *Human Brain Mapping*, 37(4), 1405-1421.
<https://doi.org/10.1002/hbm.23110>
- Qi, S., Meesters, S., Nicolay, K., Romeny, B. M., & Ossenblok, P. (2015). The influence of construction methodology on structural brain network measures: A review. *Journal of Neuroscience Methods*, 253, 170-182. <https://doi.org/10.1016/j.jneumeth.2015.06.016>
- Rabinowitz, A. R., & Levin, H. S. (2014). Cognitive sequelae of traumatic brain injury. *Psychiatric Clinics of North America*, 37(1), 1-11. <https://doi.org/10.1016/j.psc.2013.11.004>
- Radwan, A. M., Emsell, L., Blommaert, J., Zhylka, A., Kovacs, S., Theys, T., . . . Sunaert, S. (2021). Virtual brain grafting: Enabling whole brain parcellation in the presence of large lesions. *Neuroimage*, 229, 117731. <https://doi.org/10.1016/j.neuroimage.2021.117731>
- Raffelt, D., Dhollander, T., Tournier, J.-D., Tabbara, R., Smith, R. E., Pierre, E., & Connelly, A. (2017). *Bias field correction and intensity normalisation for quantitative analysis of apparent fibre density* International Society of Magnetic Resonance in Medicine, Honolulu.

- Raizman, R., Tavor, I., Biegon, A., Harnof, S., Hoffmann, C., Tsarfaty, G., . . . Livny, A. (2020). Traumatic brain injury severity in a network perspective: A diffusion MRI based connectome study. *Scientific Reports*, 10(1), 9121. <https://doi.org/10.1038/s41598-020-65948-4>
- Rapoport, M., McCauley, S., Levin, H., Song, J., & Feinstein, A. (2002). The role of injury severity in neurobehavioral outcome 3 months after traumatic brain injury. *Neuropsychiatry, Neuropsychology, & Behavioral Neurology*, 15(2), 123-132.
- Rassovsky, Y., Levi, Y., Agranov, E., Sela-Kaufman, M., Sverdlik, A., & Vakil, E. (2015). Predicting long-term outcome following traumatic brain injury (TBI). *Journal of Clinical & Experimental Neuropsychology*, 37(4), 354-366. <https://doi.org/10.1080/13803395.2015.1015498>
- Ratcliff, R., & McKoon, G. (2008). The diffusion decision model: Theory and data for two-choice decision tasks. *Neural computation*, 20(4), 873-922. <https://doi.org/10.1162/neco.2008.12-06-420>
- Reijmer, Y. D., Leemans, A., Brundel, M., Kappelle, L. J., & Biessels, G. J. (2013). Disruption of the cerebral white matter network is related to slowing of information processing speed in patients with type 2 diabetes. *Diabetes*, 62(6), 2112-2115. <https://doi.org/10.2337/db12-1644>
- Reijmer, Y. D., Leemans, A., Caeyenberghs, K., Heringa, S. M., Koek, H. L., Biessels, G. J., & Utrecht Vasc Cognitive, I. (2013). Disruption of cerebral networks and cognitive impairment in Alzheimer disease [Article]. *Neurology*, 80(15), 1370-1377. <https://doi.org/10.1212/WNL.0b013e31828c2ee5>
- Roine, T., Jurissen, B., Perrone, D., Alterman, J., Philips, W., Sijbers, J., & Leemans, A. (2019). Reproducibility and intercorrelation of graph theoretical measures in structural brain connectivity networks. *Medical Image Analysis*, 52, 56-67. <https://doi.org/10.1016/j.media.2018.10.009>
- Román, F. J., Iturria-Medina, Y., Martínez, K., Karama, S., Burgaleta, M., Evans, A. C., . . . Colom, R. (2017). Enhanced structural connectivity within a brain sub-network supporting working memory and engagement processes after cognitive training. *Neurobiology of Learning & Memory*, 141, 33-43. <https://doi.org/10.1016/j.nlm.2017.03.010>
- Romo, R., & Salinas, E. (1999). Sensing and deciding in the somatosensory system. *Current opinion in neurobiology*, 9(4), 487-493. [https://doi.org/10.1016/S0959-4388\(99\)80073-7](https://doi.org/10.1016/S0959-4388(99)80073-7)

- Roozenbeek, B., Lingsma, H. F., & Maas, A. I. (2012). New considerations in the design of clinical trials for traumatic brain injury. *Clinical investigation*, 2(2), 153.
<https://doi.org/10.4155/cli.11.179>
- Rossi, C., & Sullivan, J. (1996). Motor fitness in children and adolescents with traumatic brain injury. *Archives of Physical Medicine & Rehabilitation*, 77, 1062-1065.
[https://doi.org/10.1016/s0003-9993\(96\)90069-6](https://doi.org/10.1016/s0003-9993(96)90069-6)
- Rubinov, M., & Sporns, O. (2010). Complex network measures of brain connectivity: Uses and interpretations. *Neuroimage*, 52(3), 1059-1069.
<https://doi.org/10.1016/j.neuroimage.2009.10.003>
- Ruff, R. M., Cullum, C. M., & Luerksen, T. G. (1989). Brain imaging and neuropsychological outcome in traumatic brain injury. In R. A. Yeo, Bigler E.D., & T. E. (Eds.), *Neuropsychological Function and Brain Imaging. Critical Issues in Neuropsychology*. (pp. 161-183). Springer.
- Ruff, R. M., Marshall, L. F., Crouch, J., Klauber, M. R., Levin, H. S., Barth, J., . . . Marmarou, A. (1993). Predictors of outcome following severe head trauma: Follow-up data from the Traumatic Coma Data Bank. *Brain Injury*, 7(2), 101-111.
<https://doi.org/10.3109/02699059309008164>
- Russell, W. R., & Smith, A. (1961). Post-traumatic amnesia in closed head injury. *Archives of Neurology*, 5(1), 4-17. <https://doi.org/10.1001/archneur.1961.00450130006002>
- Rutgers, D. R., Toulgoat, F., Cazejust, J., Fillard, P., Lasjaunias, P., & Ducreux, D. (2008). White matter abnormalities in mild traumatic brain injury: A diffusion tensor imaging study. *American Journal of Neuroradiology*, 29(3), 514-519. <https://doi.org/10.3174/ajnr.A0856>
- Sairanen, V., Leemans, A., & Tax, C. (2018). Robust estimation of diffusion MRI metrics based on slice-wise outlier detection (SOLID). International Society for Magnetic Resonance in Medicine, Paris.
- Sambunjak, D., Cumpston, M., & Watts, C. (2017). *Module 6: Analysing the data*. . Cochrane Interactive Learning: Conducting an intervention review. .
<https://training.cochrane.org/interactivelarning/module-6-analysing-data>.
- Sandberg, M. A. (2011). Neurobehavioral Functioning Inventory. In J. S. Kreutzer, J. DeLuca, & B. Caplan (Eds.), *Encyclopedia of Clinical Neuropsychology* (pp. 1739-1740). Springer New York. https://doi.org/10.1007/978-0-387-79948-3_202

- Sanz Leon, P., Knock, S., Woodman, M., Domide, L., Mersmann, J., McIntosh, A., & Jirsa, V. (2013). The Virtual Brain: A simulator of primate brain network dynamics [Methods]. *Frontiers In Neuroinformatics*, 7(10). <https://doi.org/10.3389/fninf.2013.00010>
- Sarwar, T., Ramamohanarao, K., & Zalesky, A. (2019). Mapping connectomes with diffusion MRI: Deterministic or probabilistic tractography? *Magnetic resonance in Medicine*, 81(2), 1368-1384. <https://doi.org/10.1002/mrm.27471>
- Sarwar, T., Tian, Y., Yeo, B., Ramamohanarao, K., & Zalesky, A. (2020). Structure-function coupling in the human connectome: A machine learning approach. *Neuroimage*, 117609. <https://doi.org/10.1016/j.neuroimage.2020.117609>
- Satterthwaite, T. D., Xia, C. H., & Bassett, D. S. (2018). Personalized neuroscience: Common and individual-specific features in functional brain networks. *Neuron*, 98(2), 243-245. <https://doi.org/10.1016/j.neuron.2018.04.007>
- Schall, J. D. (2001). Neural basis of deciding, choosing and acting. *Nature Reviews Neuroscience*, 2(1), 33-42. <https://doi.org/10.1038/35049054>
- Schiavi, S. O.-P., M.; Barakovic, M.; Petit, L.; Descoteaux, M.; Thiran, J.-P.; Daducci, A. (2020). A new method for accurate in vivo mapping of human brain connections using microstructural and anatomical information. *Science Advances*, 6(31), eaba8245. <https://doi.org/10.1126/sciadv.aba8245>
- Schilling, K. G., Petit, L., Rheault, F., Remedios, S., Pierpaoli, C., Anderson, A. W., . . . Descoteaux, M. (2020). Brain connections derived from diffusion MRI tractography can be highly anatomically accurate-if we know where white matter pathways start, where they end, and where they do not go. *Brain Structure and Function*, 225(8). <https://doi.org/10.1007/s00429-020-02129-z>
- Schirner, M., Rothmeier, S., Jirsa, V. K., McIntosh, A. R., & Ritter, P. (2015). An automated pipeline for constructing personalized virtual brains from multimodal neuroimaging data. *Neuroimage*, 117, 343-357. <https://doi.org/10.1016/j.neuroimage.2015.03.055>
- Schlaug, G., Forgeard, M., Zhu, L., Norton, A., Norton, A., & Winner, E. (2009). Training-induced neuroplasticity in young children. *Annals of the New York Academy of Sciences*, 1169, 205-208. <https://doi.org/10.1111/j.1749-6632.2009.04842.x>
- Schneider, W., & Chein, J. M. (2003). Controlled & automatic processing: Behavior, theory, and biological mechanisms. *Cognitive science*, 27(3), 525-559. [https://doi.org/10.1016/S0364-0213\(03\)00011-9](https://doi.org/10.1016/S0364-0213(03)00011-9)

- Schneider, W., & Shiffrin, R. M. (1977). Controlled and automatic human information processing: I. Detection, search, and attention. *Psychological review*, 84(1), 1.
<https://doi.org/10.1037/0033-295X.84.1.1>
- Schönberger, M., Ponsford, J., Reutens, D., Beare, R., & O'Sullivan, R. (2009). The relationship between age, injury severity, and MRI findings after traumatic brain injury. *Journal Of Neurotrauma*, 26(12), 2157-2167. <https://doi.org/10.1089/neu.2009.0939>
- Schopp, L. H., Shigaki, C. L., Bounds, T. A., Johnstone, B., Stucky, R. C., & Conway, D. L. (2006). Outcomes in TBI with violent versus nonviolent etiology in a predominantly rural setting. *The Journal Of Head Trauma Rehabilitation*, 21(3), 213-225.
<https://doi.org/10.1097/00001199-200605000-00002>
- Schretlen, D. J., & Shapiro, A. M. (2003). A quantitative review of the effects of traumatic brain injury on cognitive functioning. *International Review of Psychiatry*, 15(4), 341-349.
<https://doi.org/10.1080/09540260310001606728>
- Seguin, C., Tian, Y., & Zalesky, A. (2020). Network communication models improve the behavioral and functional predictive utility of the human structural connectome [preprint]. *Network Neuroscience*, 4(4), 980-1006. https://doi.org/10.1162/netn_a_00161
- Seguin, C., van den Heuvel, M. P., & Zalesky, A. (2018). Navigation of brain networks. *Proceedings of the National Academy of Sciences*, 115(24), 6297-6302.
<https://doi.org/10.1073/pnas.1801351115>
- Selassie, A. W., Zaloshnja, E., Langlois, J. A., Miller, T., Jones, P., & Steiner, C. (2008). Incidence of long-term disability following traumatic brain injury hospitalization. *Journal of Head Trauma Rehabilitation*, 23(2), 123-131.
<https://doi.org/10.1097/01.HTR.0000314531.30401.39>
- Sharp, D. J., Scott, G., & Leech, R. (2014). Network dysfunction after traumatic brain injury. *Nature Reviews Neurology*, 10, 156-166. <https://doi.org/10.1038/nrneurol.2014.15>
- Shenton, M. E., Hamoda, H. M., Schneiderman, J. S., Bouix, S., Pasternak, O., Rath, Y., . . . Zafonte, R. (2012). A review of magnetic resonance imaging and diffusion tensor imaging findings in mild traumatic brain injury. *Brain Imaging & Behaviour*, 6(2), 137-192.
<https://doi.org/10.1007/s11682-012-9156-5>
- Shepherd, A. M., Matheson, S. L., Laurens, K. R., Carr, V. J., & Green, M. J. (2012). Systematic meta-analysis of insula volume in schizophrenia. *Biological Psychiatry*, 72(9), 775-784.
<https://doi.org/10.1016/j.biopsych.2012.04.020>

- Sheppard, L. D., & Vernon, P. A. (2008). Intelligence and speed of information-processing: A review of 50 years of research. *Personality & Individual Differences*, 44(3), 535-551. <https://doi.org/10.1016/j.paid.2007.09.015>
- Shu, N., Liu, Y., Li, K., Duan, Y., Wang, J., Yu, C., . . . He, Y. (2011). Diffusion tensor tractography reveals disrupted topological efficiency in white matter structural networks in multiple sclerosis. *Cerebral Cortex*, 21(11), 2565-2577. <https://doi.org/10.1093/cercor/bhr039>
- Shum, D., Fleming, J., Gill, H., Gullo, M. J., & Strong, J. (2011). A randomized controlled trial of prospective memory rehabilitation in adults with traumatic brain injury. *Journal of Rehabilitation Medicine*, 43(3), 216-223. <https://doi.org/10.2340/16501977-0647>
- Shum, D., Gill, H., Banks, M., Maujean, A., Griffin, J., & Ward, H. (2009). Planning ability following moderate to severe traumatic brain injury: Performance on a 4-Disk version of the tower of london. *Brain Impairment*, 10(3), 320-324. <https://doi.org/10.1375/brim.10.3.320>
- Siegel, J. S., Shulman, G. L., & Corbetta, M. (2017). Measuring functional connectivity in stroke: Approaches and considerations. *Journal of Cerebral Blood Flow & Metabolism*, 37(8), 2665-2678. <https://doi.org/10.1177/0271678X17709198>
- Sivanandam, T. M., & Thakur, M. K. (2012). Traumatic brain injury: A risk factor for Alzheimer's disease. *Neuroscience & Biobehavioral Reviews*, 36(5), 1376-1381. <https://doi.org/10.1016/j.neubiorev.2012.02.013>
- Skare, S., & Bammer, R. (2010). Jacobian weighting of distortion corrected EPI data. International Society for Magnetic Resonance in Medicine, Stockholm, Sweden.
- Sled, J. G., Zijdenbos, A. P., & Evans, A. C. (1998). A nonparametric method for automatic correction of intensity nonuniformity in MRI data. *Institute of Electrical & Electronics Engineers Transactions on Medical Imaging*, 17(1), 87-97. <https://doi.org/10.1109/42.668698>
- Smith, D. H., Chen, X.-H., Xu, B.-N., McIntosh, T. K., Gennarelli, T. A., & Meaney, D. E. (1997). Characterization of diffuse axonal pathology and selective hippocampal damage following inertial brain trauma in the pig. *Journal of Neuropathology & Experimental Neurology*, 56(7), 822-834. <https://doi.org/10.1097/00005072-199756070-00009>
- Smith, R. E., Calamante, F., & Connelly, A. (2020). Mapping connectomes with diffusion MRI: Deterministic or probabilistic tractography? *Magnetic resonance in Medicine*, 83(3), 787-790. <https://doi.org/10.1002/mrm.27471>

- Smith, R. E., Calamante, F., Gajamante, F., Kolbe, S., & Connelly, A. (2020). Modulation of white matter bundle connectivity in the presence of axonal truncation pathologies [preprint]. *bioRxiv*. <https://doi.org/10.1101/2020.01.14.903559>
- Smith, R. E., Raffelt, D., Tournier, J.-D., & Connelly, A. (2020). Quantitative streamlines tractography: Methods and inter-subject normalisation. *OSF Preprints*. <https://doi.org/10.31219/osf.io/c67kn>
- Smith, R. E., Tournier, J., Calamante, F., & Connelly, A. (2015a). SIFT2: Enabling dense quantitative assessment of brain white matter connectivity using streamlines tractography. *Neuroimage*, 119, 338-351. <https://doi.org/10.1016/j.neuroimage.2015.06.092>
- Smith, R. E., Tournier, J.-D., Calamante, F., & Connelly, A. (2012). Anatomically-constrained tractography: Improved diffusion MRI streamlines tractography through effective use of anatomical information. *Neuroimage*, 62(3), 1924-1938. <https://doi.org/10.1016/j.neuroimage.2012.06.005>
- Smith, R. E., Tournier, J.-D., Calamante, F., & Connelly, A. (2013). SIFT: Spherical-deconvolution informed filtering of tractograms. *Neuroimage*, 67, 298-312. <https://doi.org/10.1016/j.neuroimage.2012.11.049>
- Smith, R. E., Tournier, J.-D., Calamante, F., & Connelly, A. (2015b). The effects of SIFT on the reproducibility and biological accuracy of the structural connectome. *Neuroimage*, 104, 253-265. <https://doi.org/10.1016/j.neuroimage.2014.10.004>
- Solmaz, B., Tunç, B., Parker, D., Whyte, J., Hart, T., Rabinowitz, A., . . . Verma, R. (2017). Assessing connectivity related injury burden in diffuse traumatic brain injury [Article]. *Human Brain Mapping*, 38(6), 2913-2922. <https://doi.org/10.1002/hbm.23561>
- Soloveva, M. V., Jamadar, S. D., Poudel, G., & Georgiou-Karistianis, N. (2018). A critical review of brain and cognitive reserve in Huntington's disease. *Neuroscience & Biobehavioral Reviews*, 88, 155-169. <https://doi.org/10.1016/j.neubiorev.2018.03.003>
- Sotiropoulos, S. N., & Zalesky, A. (2019). Building connectomes using diffusion MRI: Why, how and but. *Nuclear Magnetic Resonance in Biomedicine*, 32(4), e3752. <https://doi.org/10.1002/nbm.3752>
- Spikman, J. M., Timmerman, M. E., Milders, M. V., Veenstra, W. S., & van der Naalt, J. (2012). Social cognition impairments in relation to general cognitive deficits, injury severity, and prefrontal lesions in traumatic brain injury patients. *Journal Of Neurotrauma*, 29(1), 101-111. <https://doi.org/10.1089/neu.2011.2084>

- Spitz, G., Bigler, E. D., Abildskov, T., Maller, J. J., O'Sullivan, R., & Ponsford, J. L. (2013). Regional cortical volume and cognitive functioning following traumatic brain injury. *Brain & Cognition*, 83(1), 34-44. <https://doi.org/10.1016/j.bandc.2013.06.007>
- Spitz, G., Maller, J. J., O'Sullivan, R., & Ponsford, J. L. (2013). White matter integrity following traumatic brain injury: The association with severity of injury and cognitive functioning. *Brain Topography*, 26(4), 648-660. <https://doi.org/10.1007/s10548-013-0283-0>
- Sporns, O. (2010). *Networks of the brain*. MIT press.
- Sporns, O. (2011). The human connectome: A complex network. *Annals of the New York Academy of Sciences*, 1224(1), 109-125. <https://doi.org/10.1111/j.1749-6632.2010.05888.x>
- Sporns, O. (2012). *Discovering the human connectome*. MIT press.
- Sporns, O. (2013). Network attributes for segregation and integration in the human brain. *Current opinion in neurobiology*, 23(2), 162-171. <https://doi.org/10.1016/j.conb.2012.11.015>
- Sporns, O., Tononi, G., & Kotter, R. (2005). The human connectome: A structural description of the human brain. *Plos Computational Biology*, 1(4), 42. <https://doi.org/10.1371/journal.pcbi.0010042>
- Stephens, J. A., Williamson, K.-N. C., & Berryhill, M. E. (2015). Cognitive rehabilitation after traumatic brain injury: A reference for occupational therapists. *Occupational Therapy Journal of Research: Occupation, Participation and Health*, 35(1), 5-22. <https://doi.org/10.1177/1539449214561765>
- Stoeckel, L. E., Garrison, K. A., Ghosh, S. S., Wighton, P., Hanlon, C. A., Gilman, J. M., . . . Scheinost, D. (2014). Optimizing real time fMRI neurofeedback for therapeutic discovery and development. *NeuroImage: Clinical*, 5, 245-255. <https://doi.org/10.1016/j.nicl.2014.07.002>
- Straathof, M., Sinke, M. R., Dijkhuizen, R. M., & Otte, W. M. (2019). A systematic review on the quantitative relationship between structural and functional network connectivity strength in mammalian brains. *Journal of Cerebral Blood Flow & Metabolism*, 39(2), 189-209. <https://doi.org/10.1177/0271678X18809547>
- Strakowski, S. M., DelBello, M. P., Adler, C., Cecil, K. M., & Sax, K. W. (2000). Neuroimaging in bipolar disorder. *Bipolar Disorders*, 2, 148-164. <https://doi.org/10.1034/j.1399-5618.2000.020302.x>
- Tate, R. L., McDonald, S., & Lulham, J. M. (1998). Incidence of hospital-treated traumatic brain injury in an Australian community. *Australian & New Zealand Journal of Public Health*, 22(4), 419 - 423. <https://doi.org/10.1111/j.1467-842x.1998.tb01406.x>

- Teasdale, G., & Jennett, B. (1974). Assessment of coma and impaired consciousness: A practical scale. *The Lancet*, 304(7872), 81-84. [https://doi.org/10.1016/s0140-6736\(74\)91639-0](https://doi.org/10.1016/s0140-6736(74)91639-0)
- Thomas, C., Frank, Q. Y., Irfanoglu, M. O., Modi, P., Saleem, K. S., Leopold, D. A., & Pierpaoli, C. (2014). Anatomical accuracy of brain connections derived from diffusion MRI tractography is inherently limited. *Proceedings of the National Academy of Sciences*, 111(46), 16574-16579. <https://doi.org/10.1073/pnas.1405672111>
- Till, C., Colella, B., Verwegen, J., & Green, R. E. (2008). Postrecovery cognitive decline in adults with traumatic brain injury. *Archives of Physical Medicine & Rehabilitation*, 89(12), S25-34. <https://doi.org/10.1016/j.apmr.2008.07.004>
- Tolhurst, D., & Lewis, P. (1992). Effect of myelination on the conduction velocity of optic nerve fibres. *Ophthalmic & Physiological Optics*, 12(2), 241-243. <https://doi.org/10.1111/j.1475-1313.1992.tb00298.x>
- Tournier, J.-D., Calamante, F., & Connelly, A. (2007). Robust determination of the fibre orientation distribution in diffusion MRI: Non-negativity constrained super-resolved spherical deconvolution. *Neuroimage*, 35(4), 1459-1472. <https://doi.org/10.1034/j.1399-5618.2000.020302.x>
- Tournier, J.-D., Calamante, F., Gadian, D. G., & Connelly, A. (2004). Direct estimation of the fiber orientation density function from diffusion-weighted MRI data using spherical deconvolution. *Neuroimage*, 23(3), 1176-1185. <https://doi.org/10.1016/j.neuroimage.2004.07.037>
- Tournier, J. D., Mori, S., & Leemans, A. (2011). Diffusion tensor imaging and beyond. *Magnetic resonance in Medicine*, 65(6), 1532-1556. <https://doi.org/10.1002/mrm.22924>
- Tournier, J. D., Smith, R., Raffelt, D., Tabbara, R., Dhollander, T., Pietsch, M., . . . Connelly, A. (2019). MRtrix3: A fast, flexible and open software framework for medical image processing and visualisation. *Neuroimage*, 202, 116137. <https://doi.org/10.1016/j.neuroimage.2019.116137>
- Treble, A., Hasan, K. M., Iftikhar, A., Stuebing, K. K., Kramer, L. A., Cox Jr, C. S., . . . Ewing-Cobbs, L. (2013). Working memory and corpus callosum microstructural integrity after pediatric traumatic brain injury: A diffusion tensor tractography study. *Journal Of Neurotrauma*, 30(19), 1609-1619. <https://doi.org/10.1089/neu.2013.2934>
- Tuch, D. S. (2004). Q-ball imaging. *Magnetic resonance in Medicine*, 52(6), 1358-1372. <https://doi.org/10.1002/mrm.20279>

- Turken, U., Whitfield-Gabrieli, S., Bammer, R., Baldo, J. V., Dronkers, N. F., & Gabrieli, J. D. (2008). Cognitive processing speed and the structure of white matter pathways: Convergent evidence from normal variation and lesion studies. *Neuroimage*, 42(2), 1032-1044. <https://doi.org/10.1016/j.neuroimage.2008.03.057>
- Uchino, A., Takase, Y., Nomiyama, K., Egashira, R., & Kudo, S. (2006). Acquired lesions of the corpus callosum: MR imaging. *European Radiology*, 16(4), 905-914. <https://doi.org/10.1007/s00330-005-0037-9>
- Vaessen, M. J., Hofman, P. A., Tijssen, H. N., Aldenkamp, A. P., Jansen, J. F., & Backes, W. H. (2010). The effect and reproducibility of different clinical DTI gradient sets on small world brain connectivity measures. *Neuroimage*, 51(3), 1106-1116. <https://doi.org/10.1016/j.neuroimage.2010.03.011>
- van den Heuvel, M. P., & Sporns, O. (2011). Rich-club organization of the human connectome [Article]. *Journal of Neuroscience*, 31(44), 15775-15786. <https://doi.org/10.1523/JNEUROSCI.3539-11.2011>
- van der Horn, H. J., Kok, J. G., de Koning, M. E., Scheenen, M. E., Leemans, A., Spikman, J. M., & van der Naalt, J. (2017). Altered wiring of the human structural connectome in adults with mild traumatic brain injury. *Journal Of Neurotrauma*, 34(5), 1035-1044. <https://doi.org/10.1089/neu.2016.4659>
- van Wijk, B. C., Stam, C. J., & Daffertshofer, A. (2010). Comparing brain networks of different size and connectivity density using graph theory. *PLoS One*, 5(10), e13701. <https://doi.org/10.1371/journal.pone.0013701>
- Veraart, J., Novikov, D. S., Christiaens, D., Ades-aron, B., Sijbers, J., & Fieremans, E. (2016). Denoising of diffusion MRI using random matrix theory. *Neuroimage*, 142, 394-406. <https://doi.org/10.1016/j.neuroimage.2016.08.016>
- Verhelst, H., Vander Linden, C., De Pauw, T., Vingerhoets, G., & Caeyenberghs, K. (2018). Impaired rich club and increased local connectivity in children with traumatic brain injury: Local support for the rich? *Human Brain Mapping*, 39(7), 2800-2811. <https://doi.org/10.1002/hbm.24041>
- Voss, A., Rothermund, K., & Voss, J. (2004). Interpreting the parameters of the diffusion model: An empirical validation. *Memory & Cognition*, 32(7), 1206-1220. <https://doi.org/10.3758/BF03196893>
- Wagner, A. K., Sasser, H. C., Hammond, F. M., Wiercisiewski, D., & Alexander, J. (2000). Intentional traumatic brain injury: Epidemiology, risk factors, and associations with

- injury severity and mortality. *Journal of Trauma & Acute Care Surgery*, 49(3), 404-410.
<https://doi.org/10.1097/00005373-200009000-00004>
- Wallace, E. J., Mathias, J. L., & Ward, L. (2018). The relationship between diffusion tensor imaging findings and cognitive outcomes following adult traumatic brain injury: A meta-analysis. *Neuroscience & Biobehavioral Reviews*, 92, 93-103.
<https://doi.org/10.1016/j.neubiorev.2018.05.023>
- Wang, R., & Ware, J. H. (2013). Detecting moderator effects using subgroup analyses. *Prevention Science*, 14(2), 111-120. <https://doi.org/10.1007/s11121-011-0221-x>
- Wang, X., Seguin, C., Zalesky, A., Wong, W.-w., Chu, W. C.-w., & Tong, R. K.-y. (2019). Synchronization lag in post stroke: Relation to motor function and structural connectivity. *Network Neuroscience*, 3(4), 1121-1140.
https://doi.org/10.1162/netn_a_00105
- Warshall, S. (1962). A theorem on boolean matrices. *Journal of the Association for Computing Machinery*, 9(1), 11-12. <https://doi.org/10.1145/321105.321107>
- Watson, C. G., DeMaster, D., & Ewing-Cobbs, L. (2019). Graph theory analysis of DTI tractography in children with traumatic injury. *NeuroImage: Clinical*, 21, 101673.
<https://doi.org/10.1016/j.nicl.2019.101673>
- Watts, D. J., & Strogatz, S. H. (1998). Collective dynamics of 'small-world' networks. *Nature*, 393, 440 - 442. <https://doi.org/10.1038/30918>
- Wechsler, D. (2011). *Wechsler Abbreviated Scale of Intelligence Second Edition (WASI-II)* TX: Pearson.
- Wefel, J. S., Vardy, J., Ahles, T., & Schagen, S. B. (2011). International cognition and cancer task force recommendations to harmonise studies of cognitive function in patients with cancer. *The Lancet Oncology*, 12(7), 703-708. [https://doi.org/10.1016/s1470-2045\(10\)70294-1](https://doi.org/10.1016/s1470-2045(10)70294-1)
- Weissman, D., & Woldorff, M. (2005). Hemispheric asymmetries for different components of global/local attention occur in distinct temporo-parietal loci. *Cerebral Cortex*, 15(6), 870-876. <https://doi.org/10.1093/cercor/bhh187>
- Weissman, D. H., Roberts, K., Visscher, K., & Woldorff, M. (2006). The neural bases of momentary lapses in attention. *Nature Neuroscience*, 9(7), 971-978.
<https://doi.org/10.1038/nn1727>
- Wen, W., Zhu, W., He, Y., Kochan, N. A., Reppermund, S., Slavin, M. J., . . . Sachdev, P. (2011). Discrete neuroanatomical networks are associated with specific cognitive abilities in old

- age [Article]. *Journal of Neuroscience*, 31(4), 1204-1212.
<https://doi.org/10.1523/JNEUROSCI.4085-10.2011>
- Whiteneck, G. G., Gerhart, K. A., & Cusick, C. P. (2004). Identifying environmental factors that influence the outcomes of people with traumatic brain injury. *Journal of Head Trauma Rehabilitation*, 19(3), 191–204. <https://doi.org/10.1097/00001199-200405000-00001>
- Wiecki, T., Sofer, I., & Frank, M. (2013). HDDM: Hierarchical bayesian estimation of the drift-diffusion model in python [Methods]. *Frontiers In Neuroinformatics*, 7(14).
<https://doi.org/10.3389/fninf.2013.00014>
- Wilde, E. A., Chu, Z., E.D., B., Hunter, J. V., Fearing, M. A., Hanten, G. R., . . . Levin, H. (2006). Diffusion tensor imaging in the corpus callosum in children after moderate to severe traumatic brain injury. *Journal Of Neurotrauma*, 23(10), 1412–1426.
<https://doi.org/10.1089/neu.2006.23.1412>
- Wills, P., & Meyer, F. G. (2020). Metrics for graph comparison: A practitioner's guide. *PLoS One*, 15(2), e0228728-e0228728. <https://doi.org/10.1371/journal.pone.0228728>
- Wing, B. H., Tucker, B. J., Fong, A. K., & Allen, M. D. (2017). Developing the standard of care for post-concussion treatment: Neuroimaging-guided rehabilitation of neurovascular coupling. *The open neuroimaging journal*, 11, 58.
<https://doi.org/10.2174/1874440001711010058>
- Woo, C. W., Chang, L. J., Lindquist, M. A., & Wager, T. D. (2017). Building better biomarkers: Brain models in translational neuroimaging. *Nature Neuroscience*, 20(3), 365-377.
<https://doi.org/10.1038/nn.4478>
- Xiong, K. L., Zhu, Y. S., & Zhang, W. G. (2014). Diffusion tensor imaging and magnetic resonance spectroscopy in traumatic brain injury: A review of recent literature. *Brain Imaging & Behavior*, 8(4), 487-496. <https://doi.org/10.1007/s11682-013-9288-2>
- Yeh, C., Smith, R., Liang, X., Calamante, F., & A, C. (2018). *Investigating the streamline count required for reproducible structural connectome construction across a range of brain parcellation resolutions* International Society for Magnetic Resonance in Medicine, Paris.
- Yeh, C., Smith, R. E., Dhollander, T., & Connelly, A. (2017). Mesh-based anatomically-constrained tractography for effective tracking termination and structural connectome construction. International Society of Magnetic Resonance in Medicine, Honolulu.
- Yeh, C.-H., Smith, R. E., Liang, X., Calamante, F., & Connelly, A. (2016). Correction for diffusion MRI fibre tracking biases: The consequences for structural connectomic metrics. *Neuroimage*, 142, 150-162. <https://doi.org/10.1016/j.neuroimage.2016.05.047>

- Yeh, C. H., Jones, D. K., Liang, X., Descoteaux, M., & Connelly, A. (2020). Mapping structural connectivity using diffusion MRI: Challenges and opportunities. *Journal of Magnetic Resonance Imaging*. <https://doi.org/10.1002/jmri.27188>
- Yuan, W., Treble-Barna, A., Sohlberg, M. M., Harn, B., & Wade, S. L. (2017). Changes in structural connectivity following a cognitive intervention in children with traumatic brain injury. *Neurorehabilitation & Neural Repair*, 31(2), 190-201. <https://doi.org/10.1177/1545968316675430>
- Yuan, W., Wade, S. L., & Babcock, L. (2015). Structural connectivity abnormality in children with acute mild traumatic brain injury using graph theoretical analysis. *Human Brain Mapping*, 36(2), 779-792. <https://doi.org/10.1002/hbm.22664>
- Yuan, W., Wade, S. L., Quatman-Yates, C., Hugentobler, J. A., Gubanich, P. J., & Kurowski, B. G. (2017). Structural connectivity related to persistent symptoms after mild TBI in adolescents and response to aerobic training: Preliminary investigation. *Journal of Head Trauma Rehabilitation*, 32(6). <https://doi.org/10.1097/HTR.0000000000000318>
- Zalesky, A., Fornito, A., Harding, I. H., Cocchi, L., Yucel, M., Pantelis, C., & Bullmore, E. T. (2010). Whole-brain anatomical networks: Does the choice of nodes matter? *Neuroimage*, 50(3), 970-983. <https://doi.org/10.1016/j.neuroimage.2009.12.027>
- Zalesky, A., Sarwar, T., & Ramamohanarao, K. (2020). A cautionary note on the use of SIFT in pathological connectomes. *Magnetic resonance in Medicine*, 83(3), 791-794. <https://doi.org/10.1002/mrm.28037>
- Zhang, H., Liu, J., Zhu, Z., & Li, H. (2011). An automated and simple method for brain MR image extraction. *BioMedical Engineering OnLine*, 10(1), 81. <https://doi.org/10.1186/1475-925X-10-81>
- Zhang, J., Rittman, T., Nombela, C., Fois, A., Coyle-Gilchrist, I., Barker, R. A., . . . Rowe, J. B. (2016). Different decision deficits impair response inhibition in progressive supranuclear palsy and Parkinson's disease. *Brain*, 139(1), 161-173. <https://doi.org/10.1093/brain/awv331>
- Zhang, Y., Brady, M., & Smith, S. (2001). Segmentation of brain MR images through a hidden Markov random field model and the expectation-maximization algorithm. *Institute of Electrical & Electronics Engineers Transactions on Medical Imaging*, 20(1), 45-57. <https://doi.org/10.1109/42.906424>

Appendices

Appendix A. Proof of Publication and Publishing Rights for Study 1

Imms, P., Clemente, A., Cook, M., D'Souza, W., Wilson, P. H., Jones, D. K., & Caeyenberghs, K. (2019). The structural connectome in traumatic brain injury: A meta-analysis of graph metrics. *Neuroscience & Biobehavioral Reviews*, 99, 128-137.

Your manuscript NEUBIOREV_2018_601_R1 has been accepted

Samuel Chamberlain (Neuroscience & Biobehavioral Reviews) <EvisSupport@elsevier.com>

Thu 3/01/2019 6:58 PM

To: Phoebe Imms <phoebe.imms@myacu.edu.au>

Ref: NEUBIOREV_2018_601_R1

Title: The structural connectome in traumatic brain injury: A meta-analysis of graph metrics

Journal: Neuroscience & Biobehavioral Reviews

Dear Ms. Imms,

I am pleased to inform you that your paper has been accepted for publication. My own comments as well as any reviewer comments are appended to the end of this letter.

Your accepted manuscript will now be transferred to our production department. We will create a proof which you will be asked to check. You can read more about this [here](#). Meanwhile, you will be asked to complete a number of online forms required for publication. If we need additional information from you during the production process, we will contact.

Thank you for submitting your work to Neuroscience & Biobehavioral Reviews. We hope you consider us again for future submissions.

Kind regards,

Samuel Chamberlain

Associate Editor

Neuroscience & Biobehavioral Reviews

Comments from the editors and reviewers:

- Reviewer 1

- No further concerns.

- Reviewer 2

- All comments have been addressed. I have no further comments, and I strongly believe this manuscript should be accepted for publication.

Appendix B. Statement of Contribution for Study 1

Statement of Contribution

PhD Candidate: Phoebe Imms

Supervisors: Karen Caeyenberghs, Govinda Poudel, Peter Wilson

Published Thesis Chapter 2

Publication Reference: Imms, P., Clemente, A., Cook, M., D'Souza, W., Wilson, P. H., Jones, D. K., & Caeyenberghs, K. (2019). The structural connectome in traumatic brain injury: A meta-analysis of graph metrics. *Neuroscience & Biobehavioral Reviews*, 99, 128-137.

Title of Paper: The structural connectome in traumatic brain injury: A meta-analysis of graph metrics.

Authors: Phoebe Imms¹, Adam Clemente¹, Mark Cook², Wendyl D'Souza², Peter Wilson¹, Derek Jones³, Karen Caeyenberghs⁴.

Author Institutions:

¹ Mary MacKillop Institute for Health Research, ACU, Melbourne VIC, Australia

² Department of Medicine, St. Vincent's Hospital, University of Melbourne.

³ Cardiff University, Cardiff, UK

⁴ Cognitive Neuroscience Unit, School of Psychology, Faculty of Health, Deakin University, Melbourne VIC, Australia


Phoebe Imms

I, Phoebe Imms, acknowledge that my contribution to the above paper is 55 percent.

Signature:  Date: 29/04/2020

Adam Clemente

I, Adam Clemente, acknowledge that my contribution to the above paper is 5 percent.

Signature:  Date: 28/04/2020

Mark Cook

I, Mark Cook, acknowledge that my contribution to the above paper is 5 percent.

Signature: _____ Date: _____

Wendyl D'Souza

I, Wendyl D'Souza, acknowledge that my contribution to the above paper is 5 percent.

Signature:  Date: 28/04/2020

Peter H. Wilson

I, Peter H. Wilson, acknowledge that my contribution to the above paper is 5 percent.

Signature:  Date: 29/04/2020

Derek K. Jones

I, Derek K Jones, acknowledge that my contribution to the above paper is 10 percent.

Signature:  Date: 28.4.2020

Karen Caeyenberghs

I, Karen Caeyenberghs, acknowledge that my contribution to the above paper is 15 percent.

Signature:  Date: 29/04/2020

Appendix C. Statement of Contribution for Study 2 and Proof of Acceptance

Statement of Contribution

PhD Candidate: Phoebe Imms

Supervisors: Govinda Poudel, Karen Caeyenberghs, Peter Wilson

Published Thesis Chapter 4

Title of Paper: Navigating the link between processing speed and network communication in the human brain

Authors: Phoebe Imms^{a,1}, Juan F Dominguez D^b, Alex Burmester^b, Caio Seguin^c, Adam Clemente^a, Thijs Dhollander^d, Peter H Wilson^e, Govinda Poudel^{a,*} & Karen Caeyenberghs^{b,*}

Affiliations:

^a Mary MacKillop Institute for Health Research, Australian Catholic University; 5/215 Spring Street, Melbourne VIC, Australia 3000

^b Cognitive Neuroscience Unit, School of Psychology, Faculty of Health, Deakin University; 221 Burwood Highway, Burwood VIC, Australia 3125

^c Melbourne Neuropsychiatry Centre, The University of Melbourne and Melbourne Health; 3/161 Barry Street, Carlton VIC, Australia 3053

^d Developmental Imaging, Murdoch Children's Research Institute; 50 Flemington Road, Parkville VIC, Australia 3052

^e Healthy Brain and Mind Research Centre, School of Behavioural, Health and Human Sciences, Faculty of Health Sciences, Australian Catholic University; 115 Victoria Parade, Fitzroy VIC, Australia 3065

* Shared senior authors

PhD Candidate statement

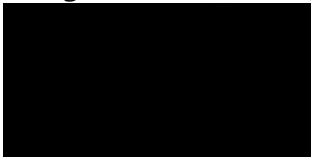
Phoebe Imms

I, Phoebe Imms, acknowledge that my contribution to the above paper is 51 percent.

Signature:  Date: 21/01/2021

Juan F Dominguez D

I, Juan F Dominguez D, acknowledge that my contribution to the above paper is 5 percent.

Signature:  Date: 22/01/2021

Alex Burmester

I, Alex Burmester, acknowledge that my contribution to the above paper is 5 percent.

Signature:  Date: 21/01/2021

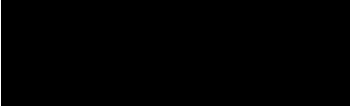
Caio Seguin

I, Caio Seguin, acknowledge that my contribution to the above paper is 5 percent.

Signature:  Date: 22/01/2021

Adam Clemente

I, Adam Clemente, acknowledge that my contribution to the above paper is 4 percent.

Signature:  Date: 21/01/2021

Thijs Dhollander

I, Thijs Dhollander, acknowledge that my contribution to the above paper is 5 percent.

Signature:  Date: 21/01/2021


Peter Wilson

I, Peter Wilson, acknowledge that my contribution to the above paper is 5 percent.

Signature:  Date: 21/1/2021

Govinda Poudel

I, Govinda Poudel, acknowledge that my contribution to the above paper is 10 percent.

Signature:  Date: 21/01/2021

Karen Caeyenberghs

I, Karen Caeyenberghs, acknowledge that my contribution to the above paper is 10 percent.

Signature: [REDACTED] Date: 22/01/2021

Fw: Your Submission - [EMID:22d8c511c685f9d1]

① Flag for follow up. Completed on 23/02/2021.



em.bsaf.0.718354.82a1f861@editorialmanager.com on behalf
of
Brain Structure & Function (BSAF) <em@editorialmanager.com>



Tue 23/02/2021 3:58 AM
To: Phoebe Imms

Ref.:
Ms. No. BSAF-D-21-00047
Navigating the link between processing speed and network communication in the human brain
Brain Structure and Function

Dear Dr Imms,

I am pleased to tell you that your work has now been accepted for publication in Brain Structure and Function. Sorry, it took so long; I made the decision in my office and I caught up in too many works. Best, lz

Thank you for submitting your work to this journal.

With kind regards,

Prof. Laszlo Zaborszky
Editor-in-Chief
Brain Structure and Function

Appendix D. Statement of Contribution for Study 3

Statement of Contribution

PhD Candidate: Phoebe Imms

Supervisors: Govinda Poudel, Karen Caeyenberghs, Peter Wilson

Published Thesis Chapter 5

Title of Paper: Personalised structural connectome mapping in Traumatic Brain Injury

Authors: Phoebe Imms^{a,1}, Adam Clemente^a, Evelyn Deutscher^b, Ahmed Radwan^c, Hamed Akhlaghi^d, Paul Beech^e, Peter H Wilson^f, Govinda Poudel^a, Juan F Domínguez D^{b*} & Karen Caeyenberghs^{b*}

Affiliations:

^a Mary MacKillop Institute for Health Research, Australian Catholic University; 5/215 Spring Street, Melbourne, VIC 3000, AUSTRALIA.

^b Cognitive Neuroscience Unit, School of Psychology, Faculty of Health, Deakin University; 221 Burwood Highway, Burwood, VIC 3125, AUSTRALIA.

^c Department of Imaging and Pathology, Katholieke Universiteit Leuven. Oude Markt 13, Leuven, Vlaams Brabant 3000, BELGIUM.

^d Department of Medicine, St. Vincent's Hospital, University of Melbourne. 41 Victoria Parade, Melbourne, VIC 3065, AUSTRALIA.

^e Department of Radiology and Nuclear Medicine, The Alfred Hospital. 55 Commercial Road, Melbourne, VIC 3004, AUSTRALIA.

^f Healthy Brain and Mind Research Centre, School of Behavioural, Health and Human Sciences, Faculty of Health Sciences, Australian Catholic University; 115 Victoria Parade, Fitzroy, VIC 3065, AUSTRALIA.

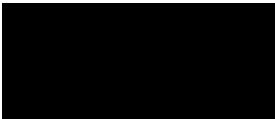
¹ Corresponding author: Phoebe Imms – phoebe.imms@myacu.edu.au. ORCID identification: 0000-0002-7205-4177

* Joint senior authors

PhD Candidate statement

Phoebe Imms

I, Phoebe Imms, acknowledge that my contribution to the above paper is 51 percent.

Signature:  Date: 21/01/2021

Adam Clemente

I, Adam Clemente, acknowledge that my contribution to the above paper is 4 percent.

Signature:  Date: 21/01/2021

Evelyn Deutscher

I, Evelyn Deutscher, acknowledge that my contribution to the above paper is 4 percent.

Signature:  Date: 01/02/2021

Ahmed Radwan

I, Ahmed Radwan, acknowledge that my contribution to the above paper is 4 percent.

Signature:  Date: 22/01/2021

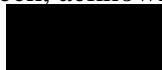
Hamed Akhlaghi

I, Hamed Akhlaghi, acknowledge that my contribution to the above paper is 4 percent.

Signature:  Date: 04/02/2021

Paul Beech

I, Paul Beech, acknowledge that my contribution to the above paper is 4 percent.

Signature:  Date: 9/2/2021

Peter Wilson

I, Peter Wilson, acknowledge that my contribution to the above paper is 4 percent.

Signature:  Date: 01/02/2021


Govinda Poudel

I, Govinda Poudel, acknowledge that my contribution to the above paper is 6 percent.

Signature:  Date: 01/02/2021

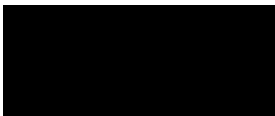
Juan F Dominguez D

I, Juan F Dominguez D, acknowledge that my contribution to the above paper is 7.5 percent.

Signature:  Date: 04/02/2021

Karen Caeyenberghs

I, Karen Caeyenberghs, acknowledge that my contribution to the above paper is 7.5 percent.

Signature:  Date: 04/02/2021

HEALTHY CONTROLS NEEDED FOR A COGNITIVE TRAINING & MRI STUDY

WE NEED HEALTHY CONTROLS TO PARTICIPATE IN COGNITIVE TESTING AND A STRUCTURAL MRI SCAN

Patients may be eligible if they,

- are 18-65 years
- are right-handed
- have no history of serious head injuries
- are currently not taking medications for psychotic/psychiatric illness
- have no contra-indications for MRI (such as metal implants)

Participation involves taking part in

- neuropsychological testing (1 hour), brain scan (1 hour), and surveys (25 minutes) at Monash Biomedical Imaging lab (Clayton)


There is no cost to the participants for any of the testing or scanning procedures.

FOR INFORMATION, PLEASE CONTACT ADAM (e: adam.clemente@myacu.edu.au), PHOEBE (e: phoebe.imms@myacu.edu.au) OR HANNAH (e: hanny.r93@gmail.com)

Principal Investigator: Karen Caeyenberghs, Ph.D.
School of Psychology | Faculty of Health Sciences
Australian Catholic University
115 Victoria Pde., Melbourne VIC 3065



ACU
AUSTRALIAN CATHOLIC UNIVERSITY



ACU HREC: 2017-222R

Appendix F. Screening form for healthy adults (MBI)

Healthy Control Screening Questionnaire – Please do via the phone

Date:

Check with participant that they have 10-15 minutes to spend with you on the phone.

Name: _____ Gender: _____

DOB: _____ First MRI: Y / N

Right handed: Y / N

Fluent in English: Y / N Details: _____

Pregnant: Y / N

Braces/Orthodontics: Y / N Details: _____

Piercings: Y / N Details: _____

Tattoos: Y / N Details: _____

Head Injury: Y / N Details: _____

Psychotic Illness: Y / N Details: _____

Psychiatric Disorder: Y / N Details: _____

History of epilepsy: Y / N Details: _____

Recent Surgeries: Y / N Details: _____

Any implants (not just metal): Y / N Details: _____

Injuries caused by metal (esp. eye): Y / N Details: _____

Ear, eye, heart, or brain surgeries: Y / N Details: _____

Electronic or wire implants including...

Pacemakers: Y / N Details: _____

Implanted Contraceptive Devices: Y / N Details: _____

Anything in your body: wires, clips, stents, sutures, screws, rods, cochlear implants, valves, prosthetics? Y / N Details: _____

If N to everything, book scanner session with participant using the Arin system.

OK to participate: Y / N

Date and Time of Session: _____

MRI and testing room booked: Y / N MRI time: _____

Healthy Control Screening Questionnaire – Please do via the phone

If Y to something, use screening form on the next page to clarify, then check with Karen and the team, or email Richard, and call back.

Have you ever had any eye injury caused by metal?..... NO / YES

If yes, did you see a doctor at the time?..... NO / YES

Did they remove the foreign body?..... NO / YES

Did they tell you that they got it all out?..... NO / YES

Was this the last injury involving metal?..... NO / YES

Are you pregnant, suspect you may be pregnant or breastfeeding?..... NO / YES

Do You Have (Or Have You Ever Had):

A Cardiac Pacemaker/stent/defibrillator/wire..... NO / YES

Any heart operation or valve replacement..... NO / YES

Any Brain operationNO / YES

Abdominal Aneurysm repair or IVC filter NO / YES

Brain Aneurysm Clips..... NO / YES

Deep Brain Stimulator..... NO / YES

Brain Shunt Tube..... NO / YES

If YES, is it programmable NO / YES

Any Ear operations /cochlear or stapes implants..... NO / YES

Implanted drug infusion devices..... NO / YES

Neuro or Bone growth stimulator..... NO / YES

Shrapnel, bullet, gunshot..... NO / YES

Any stents, vascular, oesophageal or biliary..... NO / YES

Any Surgical clips/wire sutures/screws/mesh/prosthesis..... NO / YES

Joint Replacement or Prosthesis..... NO / YES

Do You Have: Ocular prosthesis (eye implants) NO / YES

A Swan-Ganz Catheter..... NO / YES

Skin patches..... NO / YES

Intrauterine device (IUD)..... NO / YES

A penile prosthesis..... NO / YES

Any other implant, or breast tissue expander..... NO / YES

Tattooed eyelids or tattoos..... NO / YES

Hearing Aid..... NO / YES

Removable dentures..... NO / YES

Have You:

Had an operation or procedure within the last 8 weeks NO / YES

What? / When?.....

Had a history of seizures or epilepsy NO / YES

What? / When?.....

OK to participate: Y / N

Date and Time of Session: _____

MRI and testing room booked: Y / N MRI time: _____

Appendix G. MRI screening form (MBI)



Phone: 03 9905 0100 manager.mbi@monash.edu

MRI Screening & Information Form

Please complete BEFORE scan and bring with you to MBI on the day of the scan

PQMS3-MBI-FRM-C001-V1

Surname: Given Names:

SEX: M / F Address:

..... Post Code: Date of Birth: / /

Age: Phone:

Your MRI appointment has been scheduled for: Date: / /

Arrival time: am/pm Scan time: am/pm

Your Contact Person /Researcher's Name (if known):

MBI Project ID (if known): MRH.....

WASLEIGH HOSPITAL RADIOLOGY

WHAT IS MRI? ARE THERE ANY RISKS?

Magnetic Resonance Imaging (MRI) uses radio waves and very strong magnetic fields to make detailed pictures of the inside of your body.

There are no known harmful effects, from either the radio waves or the magnetic field, on your body.

However, some people have electronic devices (such as cardiac pacemakers), metal fragments in the eye, or surgically implanted metal objects, which could be badly affected by the strong magnetic field. Attached is a detailed safety questionnaire about such objects, to help us decide if there would be any risk to you during an MRI scan.

WASLEIGH HOSPITAL RADIOLOGY

PREPARATION

No special preparation is necessary – please eat, drink and take usual medications normally.

Please do not use makeup or hairspray if you are having a scan of the head, face, or neck.

WHAT WILL HAPPEN?

We will review the questionnaire sheet with you, to double-check any possible risks.

We will then explain the scanning procedure to you, and will be happy to answer any questions you may have.

You can also ring us in advance – 9905 0100

Before you enter the MRI scan room, you will be asked to take off your watch and any metallic jewellery. Occasionally you may be asked to change into a hospital-style gown. Items such as CREDIT CARDS, PAGERS, and MOBILE PHONES MUST NOT be brought into the scan room – they may be severely damaged, and may also be hazardous to other persons in the room. A locker will be provided for safekeeping of such objects, other valuables, and clothing.

The MRI machine looks like a large metal doughnut. The table on which you lie passes through the middle of the doughnut; the part of the body being scanned must be positioned at the centre of the doughnut. Cushions and pillows will be provided to make you comfortable on the table, and mirrors will allow you to see out of the "doughnut".

During the scan, it is important that you keep as still as possible – particularly when the scanner is making noises. You will hear various clicking, tapping, buzzing and banging noises during the scan – these are quite normal. They are sometimes quite loud, and headphones or earplugs will be provided to protect your ears. If you wish, music of your choice can be played through the headphones during some scans. The scan will take between 15 and 45 minutes. At all times, you will be able to talk to us through an intercom system built into the MRI machine. We will speak to you periodically, through this system, throughout the scan.

AFTER THE TEST

Once the scan is completed, you will be free to get dressed and go. There will be no after-effects from the scan. Although the MRI scans are setup for the individual research projects and not chosen to show clinical information, they will be viewed and reported by an MRI radiologist.

Name: Age:

Weight Kg Height : Date of Birth: / /

DARIS Number (to be filled in by researcher on the day of scan)

TO ENSURE YOUR SAFETY & COMFORT PLEASE ANSWER THE FOLLOWING:

Have you ever had any eye injury caused by metal? NO / YES
If yes, did you see a doctor at the time? NO / YES
Did they remove the foreign body? NO / YES
Did they tell you that they got it all out? NO / YES
Was this the last injury involving metal? NO / YES
Are you pregnant, suspect you may be pregnant or breastfeeding? NO / YES

Do You Have (Or Have You Ever Had):

A Cardiac Pacemaker/stent/defibrillator/wire NO / YES
Any heart operation or valve replacement NO / YES
Any Brain operation NO / YES
Abdominal Aneurysm repair or IVC filter NO / YES
Brain Aneurysm Clips NO / YES
Deep Brain Stimulator NO / YES
Brain Shunt Tube, NO / YES
If YES, is it programmable NO / YES
Any Ear operations / cochlear or stapes implants NO / YES
Implanted drug infusion devices NO / YES
Neuro or Bone growth stimulator NO / YES
Shrapnel, bullet, gunshot NO / YES
Any stents, vascular, oesophageal or biliary NO / YES
Any Surgical clips/wire sutures/screws/mesh/prosthesis NO / YES
Joint Replacement or Prosthesis NO / YES

Do You Have:

Ocular prosthesis (eye implants) NO / YES
A Swan-Ganz Catheter NO / YES
Skin patches NO / YES
Intrauterine device (IUD) NO / YES
A penile prosthesis NO / YES
Any other implant, or breast tissue expander NO / YES
Tattooed eyelids or tattoos NO / YES
Hearing Aid NO / YES
Removable dentures NO / YES

Have You:

What? / When?

Had an operation or procedure within the last 8 weeks NO / YES
Had a history of seizures or epilepsy NO / YES

IF YOU ANSWERED YES TO ANY OF THE ABOVE QUESTIONS PLEASE PHONE MRI RECEPTION ON 99050100 BEFORE ATTENDING

Have you had a previous MRI NO / YES

Print Name.....

Signature Date / /

If not completed by Subject, the name of the person completing the form

Relationship to the Subject

Contact number (mobile)

MBI / MRI Staff

Print name..... Signature Date / /

Appendix H. Outline of what to expect on the testing day (MBI)

Cognitive Training and Brain Structure

Cognitive function and brain structure: A longitudinal MRI study

Healthy controls are needed for one time point, as a basis of comparison to our clinical population (patients with Traumatic Brain Injury, "TBI")

If you are interested in participating, please respond to the experimenter with your **phone number** so we can go through a screening questionnaire with you, to ensure your eligibility.

Participants who are **Right Handed** only. Please let your experimenter know if you are left handed.

Please also let your experimenter know if you have ever had a **head injury, psychotic illness or psychiatric disorder**; or if you have any possible contraindications for MRI scanning such as **metal implants, piercings, injuries caused by metal, recent surgeries, electronic or wire implants including pacemakers, implanted contraceptive devices, or metal flakes in the eye.**

If you would like, you can bring **your own movie with subtitles** on a usb - G, PG or MA only please.

TOTAL TIME FOR EXPERIMENT: approximately 3 hours.

- ☐ Surveys, screening forms, and consent forms, 25 - 30 minutes;
 - Simple surveys of your daily life functioning and participation
- ☐ Scan, 1 hour total
 - See next pages for more details
- ☐ Cognitive and Motor testing, 1 hour
 - The cognitive testing involves a number of simple computer games and manual dexterity games that are designed to test your cognitive and motor abilities - such as response inhibition and processing speed.

Cognitive Training and Brain Structure

- **MBI SCREENING FORM:** Have a read through this form, and let us know if you have any questions. You will fill this form out at MBI before the scan, so no need to bring it with you.

https://platforms.monash.edu/mbi/images/stories/Forms_policies/pqms3-mbi-form-c001%20mri%20screening%20%20information%20form.pdf

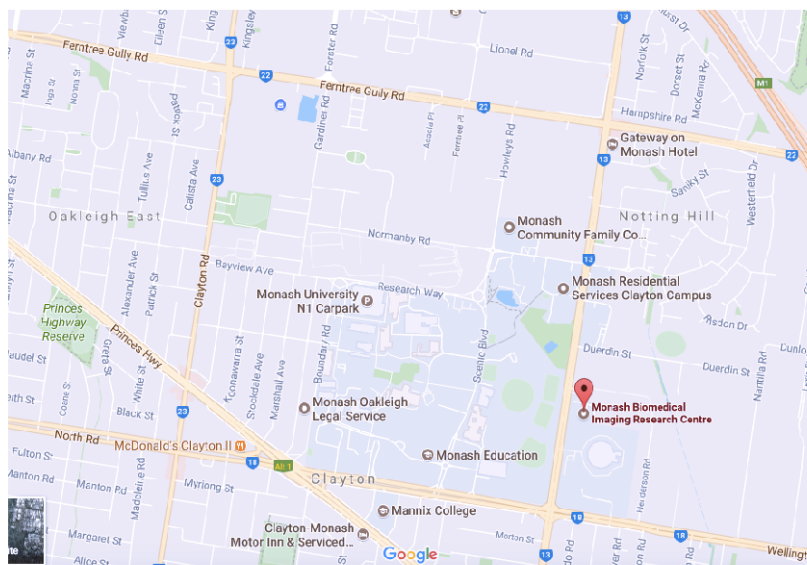
- **SCANNER WEBSITE:** For some information about the MBI and the MRI scanner

https://platforms.monash.edu/mbi/index.php?option=com_content&view=article&id=92&Itemid=205

Scanner Location: Monash University (Clayton)
Monash Biomedical Imaging
762-772 Blackburn Road
Building 220 Monash University,
Clayton, VIC 3800



Parking: Free, out front



Transport: Phoebe or Adam can pick up and drop off from Clayton train station, if transport is inconvenient for you.

MRI scan details (from MBI screening form)

WHAT IS MRI? ARE THERE ANY RISKS?

Magnetic Resonance Imaging (MRI) uses radio waves and very strong magnetic fields to make detailed pictures of the inside of your body. There are no known harmful effects, from either the radio waves or the magnetic field, on your body. However, some people have electronic devices (such as cardiac pacemakers), metal fragments in the eye, or surgically implanted metal objects, which could be badly affected by the strong magnetic field. Attached is a detailed safety questionnaire about such objects, to help us decide if there would be any risk to you during an MRI scan.

During the scan, sometimes you may feel hot or tingly in one part of your body. This may be uncomfortable but is a very normal, harmless side effect. There is no need to be alarmed if you feel this. However, if you are in discomfort or would like to stop, there will be a squeeze that you can squeeze, and the scan will stop and the radiographer will talk to you.

PREPARATION

No special preparation is necessary – please eat, drink and take usual medications normally. Please do not use makeup or hairspray if you are having a scan of the head, face, or neck. Try to avoid wearing jewellery and if necessary/possible remove piercings from the face area, and any orthodontic plates.

WHAT WILL HAPPEN?

We will review the questionnaire sheet with you, to double-check any possible risks. We will then explain the scanning procedure to you, and will be happy to answer any questions you may have. *You can also ring us in advance – 9905 0100.* Before you enter the MRI scan room, you will be asked to take off your watch and any metallic jewellery. Occasionally you may be asked to change into a hospital-style gown – normally though you can wear your own clothes into the scanner. Items such as **credit cards, pagers, and mobile phones must not** go into the scan room – they may be severely damaged, and may also be hazardous to other persons in the room. A locker will be provided for safekeeping of such objects, other valuables, and clothing.

The MRI machine looks like a large metal doughnut. The table on which you lie passes through the middle of the doughnut; the part of the body being scanned must be

Cognitive Training and Brain Structure

positioned at the centre of the doughnut. Cushions and pillows will be provided to make you comfortable on the table, and mirrors will allow you to see out of the "doughnut". During the scan, it is important that you **keep as still as possible** – particularly when the scanner is making noises. You will hear various clicking, tapping, buzzing and banging noises during the scan – these are quite normal. They are sometimes quite loud, and headphones or earplugs will be provided to protect your ears. If you wish, you can bring with you on a USB a movie of your choice (G, PG, or MA only please) with subtitles for us to play to you during your scan. The scan will take between 50 minutes to an hour. At all times, you will be able to talk to us through an intercom system built into the MRI machine. We will speak to you periodically, through this system, throughout the scan.

AFTER THE TEST

Once the scan is completed, you will complete the cognitive testing and surveys, if you haven't already done so. There will be no after-effects from the scan. Although the MRI scans are setup for the individual research projects and not chosen to show clinical information, they will be viewed and reported by an MRI radiologist.

Total scan time: 59 mins 36 secs

- **Localiser:** This scan will go for 13 seconds. The main role of this scan is to localise and plan the sequences for the rest of the MRI scans.
- **T1 scan:** This scan will go for 3 minutes and 52 seconds. This scan is used to identify differences in brain tissue and provides a clear, high resolution image of the whole brain.
- **T2 spc scan:** This scan will go for 4 minutes and 52 seconds. This scan focuses on detecting any lesions that may be present in the brain tissue.
- **SF scans:** These three scans will go for approximately 13 minutes and 22 seconds. These three scans look at the white matter of the brain. White matter is involved in carrying information between nerve cells in the brain.
- **Multi-flip, Irsprgr, Multi-flip phase 180, Multi-flip phase 0:** These four scans will go for a total of approximately 15 minutes. These four scans work together to measure the myelin in the brain. Myelin surrounds parts of neurons and is necessary for the processing of information in the brain. During this scan sequence, you may feel some sensations such as tingling or heat in your arms, legs and/or fingers. This is completely normal but if you feel uncomfortable at any time please let us know and we can stop the scan and get you out.
- **T2 swi, Gre-field, QSM, REST scans:** These three scans will go for approximately 22 minutes and 45 seconds. Together these scans look at the blood flow within the different brain regions.

Cognitive Training and Brain Structure

Scan type	Duration
Localiser	13 seconds
T1_mprgase_sag_p3_iso_1_ADNI	3 minutes 52 seconds
T2_spc_da-fi_sag_p3_iso_1.0	4 minutes 52 seconds
SF_1R-L_ep2d_diff_dir_66_inter	42 seconds
SF_1L-R_ep2d_diff_dir_66_inter	42 seconds
SF_1R-L_ep2d_diff_3000_dir_66_inter	11 minutes 49 seconds
multiflipSPGR_tr53_8fa18	4 minutes 37 seconds
lrspgr_tr53_ti450_pe96	59 seconds
multiflipSSFP_tr54_8fa55_phase180	4 minutes 42 seconds
multiflipSSFP_tr54_8fa55_phase0	4 minutes 42 seconds
T2swi3d_axial_p2_1.8mm	5 minutes 47 seconds
Gre-field_mapping_3mm	1 minute 24 seconds
QSM_p2_1x1x1mm_3echo (NEW SCAN)	9 minutes 59 seconds
REST_cmrr_mbep2d_bold_mat64	5 minutes 16 seconds

Contact Details:

PhD students, your first point of contact if you have any questions or concerns.

Adam Clemente – adam.clemente@myacu.edu.au

Phoebe Imms – phoebe.imms@myacu.edu.au

CI, lead researcher and PhD supervisor.

Dr. Karen Caeyenberghs – Karen.Caeyenberghs@acu.edu.au

Project Honours student.

Emma Lawrence - emma.lawrence@myacu.edu.au

Project research assistant.

Hannah Richards – hanny.r93@gmail.com

Appendix I. Explanatory statement provided to healthy adults (MBI)



MONASH University

EXPLANATORY STATEMENT

Control Group

Project: Cognitive function and brain structure

Chief Investigator's name:

Karen Caeyenberghs

Department of Psychological Sciences

Phone: (03) 92308067

email: Karen.caeyenberghs@acu.edu.au

Student's names:

Adam Clemente

email: adam.clemente@myacu.edu.au

Phoebe Imms

email: phoebe.imms@myacu.edu.au

Emma Lawrence

email: emma.lawrence@myacu.edu.au

You are invited to take part in this study. Please read this Explanatory Statement in full before deciding whether or not to participate in this research. If you would like further information regarding any aspect of this project, you are encouraged to contact the researchers via the phone numbers or email addresses listed above.

What does the research involve?

This research project investigates cognitive functioning. Many daily life activities are involved in acquiring information, including listening, watching, reading, searching out information, or just paying attention to things around you. In all cases, you are using your cognitive functions to gather information. Cognitive functions include attention, memory, language, perception, decision making, and problem solving. This study aims to examine the relationship between cognitive function and brain structure.

Participation involves taking part in (1) a session of tests of cognitive functioning, motor performance, and questionnaires (2) one MRI brain scan at Monash Biomedical Imaging lab. All of this is done at no cost to you. This study will take approximately 2 hours to complete (cognitive testing session: 1 hour and MRI scanning session: 1 hour).

Cognitive functioning

You will complete a series of tests of cognitive functioning. The testing will consist mainly of tests of memory, processing speed and other cognitive functions. For example, during one task you are presented with a 4x4 grid and are instructed to remember and reproduce a sequence of flashing boxes presented on the screen. This testing is not tedious and most participants find it enjoyable as the tests are in the format of computer games.

Questionnaires

You will complete 3 separate self-report questionnaires measuring subjective experience of attention/executive functioning in everyday life situations, as well as everyday life participation levels. For example, one question regarding attention experiences may be "do you often forget yesterday's events?" and one question regarding daily life participation levels may be "In a typical week, how many hours do you spend in active homemaking, including cleaning, cooking, and raising children?".

Motor Performance

You will be partaking in measures of motor performance of upper limb deficits. These measures will give an indication of both your manual and bimanual dexterity. These tests do not require rigorous physical activity, and are engaging tasks such as throwing cubes over a barrier into a box.

MRI scan

The third and final part of the study will include an MRI scan of the brain to examine the path ways between your brain regions. Scanning will take approximately 1 hour, you are encouraged to bring along your favourite movie to watch while you are being scanned.

Tests of cognitive functioning and the MRI scanning will take place at Monash Biomedical Imaging lab located in Clayton. Taxi vouchers will be provided to eliminate the possible costs of transport. After reading this explanatory statement you will be provided with a consent form so you can provide written consent for participation in this study.

Why were you chosen for this research?

Your participation in this study will assist us to obtain control data of healthy individuals, which will be compared with the cognitive function and brain structure of individuals who have sustained brain injury due to traffic accident or sport injury.

Consenting to participate in the project and withdrawing from the research

Prior to participation in the study, you will be provided with a consent form. If you are willing to participate, you need to sign the form and return it to the researcher. Participation in this study is completely voluntary. You are not under any obligation to participate. If you agree to participate, you can withdraw from the study at any time without adverse consequences. You are free to withdraw from the study without giving any reason.

Possible benefits and risks to participants

By obtaining your data and comparing it with the cognitive function and brain structure of individuals who have sustained brain injury due to traffic accident or sport injury, you will be providing us with valuable information that may assist with the rehabilitation for those with brain injuries.

The research is not expected to have any risks; however, the study does involve you undergoing magnetic resonance imaging (MRI) testing which can be anxiety provoking. MRI is a safe and non-invasive procedure used to take brain images. Before undergoing the scan, you will be thoroughly screened to ensure you are able to have the scan. Screening will involve completion of a checklist consisting of questions such as whether you have any metal implants in your body, e.g. pacemakers and/or piercings (metal disrupts the scans) or whether you experience claustrophobia (fear of confined spaces). A radiographer will be present during scanning to assist in the administration of the scans. The scanner requires you to be in a confined space for approximately 1 hour and can be quite loud. However, you will be provided with ear plugs and a rubber ball containing a buzzer that you can squeeze at any time during the scan if you are feeling anxious. If you squeeze the rubber ball the scan will be stopped immediately and a staff member will come and get you out.

Research involving diagnostic testing or possible incidental findings

As the study involves an MRI brain scan, the scan will be examined by a neuroradiologist. Before testing begins, you will be asked to indicate whether you wish to be informed of i) any diagnostic findings, ii) all incidental findings (any finding that may require treatment, or have implications on your future health), iii) only those adverse findings (findings that would normally lead to prompt) in relation to the MRI brain scan. You will be asked whether you would like any diagnostic/incidental/adverse findings to be discussed with them by their usual General Practitioner (GP), another doctor of their choice, or by a member of the research team. After reading this explanatory statement you will be provided with a consent form so you can provide written consent for potential incidental findings during the MRI brain scan.

Services on offer if adversely affected

Currently there are no known adverse effects of MRI magnetic fields and radio waves on humans. Some people (approximately 3-5%) find lying in the MRI scanner causes claustrophobia. If you are aware that you suffer from claustrophobia, you can choose not to participate in this study. While participating, if you do experience discomfort during your scan, you will be able to communicate immediately with radiographer or researcher to ask to be removed from the scanner. Some people may notice warmth and/or minor tingling during some scans. This is nothing to worry about, and is caused by the magnetic fields generated by the scanner. Once again, if you feel uncomfortable, you can ask to be removed from the scanner.

MRI scans performed at Monash Biomedical Imaging are formally reported by a Radiologist, in order to identify any unexpected abnormalities that might affect either your health, or the results of the research study. These reports are held securely at Monash Biomedical Imaging. In general, we will not contact you about the scan results unless there is an abnormality ('no news is good news'). Very occasionally (in approximately 2% of cases), the images of normal participants may show anatomical abnormalities. It may be necessary to do further tests to establish whether an abnormality is truly present. Some findings may have no negative implications for your health, and are called incidental. However, in about 1% of scans, the imaging abnormality may represent a risk to your health, and is called an adverse finding. In many cases, there are effective treatments available for adverse findings, but sometimes there are adverse findings for which no effective treatment is currently available. Therefore, if any abnormalities are found as a result of the MRI brain scan, you will be contacted, if you consent to do so.

Confidentiality / Use of data for other purposes

All individual results will remain confidential, and anything that you say or do during the session will not be communicated to anyone in a way that could identify you. Personal identifying data such as names will not be connected to the results obtained. The results of this study will be published in the form of an honours thesis and may be published in an academic journal and/or conference proceedings. Again, individual participants will not be able to be identified as being part of the study.

Storage of data

All records will be kept for 7 years within the locked office of the leading chief investigator located at Australian Catholic University. The data will be accessed by the chief investigator if required.

Results

Following the completion of your participation, you can register your interest in the results of the study with the researcher. You will be sent a summary of the de-identified group results approximately 12 months later.

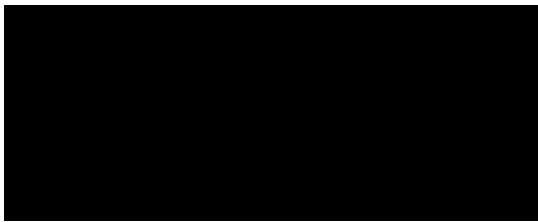
Complaints

Should you have any concerns or complaints about the conduct of the project, you are welcome to contact the Executive Officer, Monash University Human Research Ethics (MUHREC):

Executive Officer
Monash University Human Research Ethics Committee (MUHREC)
Room 111, Chancellery Building E,
24 Sports Walk, Clayton Campus
Research Office
Monash University VIC 3800

Tel: +61 3 9905 2052 Email: muhrec@monash.edu Fax: +61 3 9905 3831

Thank you,



Karen Caeyenberghs

Appendix J. Consent form provided to healthy adults (MBI)



MONASH University

--	--	--

Appendix K. Letter of invitation to TBI participants (RCH)

Associate Professor Wendyl D'Souza

MBChB, MPH, FRACP, PhD
Neurologist, Epilepsy & Epidemiology
Provider No. 211773GJ

Suite 8, Level 6,
55 Victoria Parade
Fitzroy 3065

Ph: 9419 1007

Fax: 9486 0017

(For all appointments & referrals)

Dear [individuals name],

I am inviting you to participate in a research project to improve recovery from past head injury. We are resending this information as a reminder, as you may have overlooked our last letter in your busy live and might want to reconsider.

Specifically, we have started a trial on patients with a brain injury, as a result of a trauma to the head. Some people unlucky enough to have a traumatic brain injury (TBI) can have problems that continue even years after their injury. For example, problems with thinking, difficulty concentrating, processing things slowly, and trouble with hand and arm movements. These sorts of problems restrict someone's ability to have a normal life, to cook meals, drive a car, or to be able to function normally at work.

Our research is in helping people who have had a TBI to recover and repair from these problems. Our team have found new ways to deliver therapy by combining brain training and physical exercises in a meaningful, fun and intensive form, on a tablet (e.g., iPad) that can be used at home. This therapy is called CogMo. We would like to investigate whether this new brain training program can improve your daily life functioning, memory, concentration and hand/arm function. While we do this, we would also like to analyse the brain to see whether it changes as well. This is called brain plasticity, which is basically the brain's ability to repair with training. Ultimately, we hope if successful it may be possible to implement positive results in future rehabilitation programs for patients with a brain injury.

If you are interested or would like more information, please read the enclosed Participant Information Sheet and other information provided. You will be reimbursed for travel expenses and for your time participating with us. The collected data will be treated strictly confidentially. If you have any questions about the research or if you would like to participate in our research project, you can contact the research team by phone (03 9230 8426). You can also contact the lead researcher (Karen Caeyenberghs) or the research assistant (Hannah Richards) via email (details on the Participant Information Sheet). Or, you can fill in the short form below and mail this letter using the envelope provided; we will contact you for more information and to make an appointment.

We wish you all the best and
hope to hear from you soon,

Kind regards,

Wendyl D'Souza

**Yes, I would like to hear
from the research team
about this study**

Full Name

Phone Number

Email

Appendix L. Participant information form for TBI participants (RCH)



Participant Information Sheet/Consent Form

Interventional Study - Adult providing own consent

Title	The effects of tablet-based home interventions on brain structure, cognitive functioning, motor performance, and daily life participation in patients with Traumatic Brain Injury.
Short Title	Home-based interventions for brain-injured patients
Principal Investigators	A/Prof Karen Caeyenberghs Prof Mark Cook A/Prof Wendy D'Souza
Associate Investigator(s)	Mr Adam Clemente, Ms Phoebe Imms, Ms Evelyn Deutscher, Ms Annalee Cobden, Mr Nicholas Parsons, Dr Hamed Akhlaghi, Mr Rakesh Patibanda, Dr Jonathan Duckworth, and Prof Peter H. Wilson
Research Assistants	Ms Hannah Richards, Ms Alexandra Armstrong and Ms Honey Baseri
Location	St. Vincent's Hospital, Melbourne

Part 1 What does my participation involve?

1 Introduction

You are invited to take part in this research project because you have acquired a Traumatic Brain Injury (TBI) in the past. The research project is testing rehabilitation interventions for TBI.

This Participant Information Sheet/Consent Form tells you about the research project. It explains the tests and treatments involved. Knowing what is involved will help you decide if you want to take part in the research.

Please read this information carefully. Ask a member of the research team questions about anything that you don't understand or want to know more about. Before deciding whether or not to take part, you might want to talk about it with a relative, friend, your local doctor, or a member of the research team.

Participation in this research is voluntary. If you don't wish to take part, you don't have to. You will receive the best possible care whether or not you take part.

If you decide you want to take part in the research project, you will be asked to sign the consent section. By signing it you are telling us that you:

- Understand what you have read
- Consent to take part in the research project
- Consent to have the tests and treatments that are described

- Consent to use your personal and health (medical files) information as described.

You will be given a copy of this Participant Information and Consent Form to keep.

2 What is the purpose of this research?

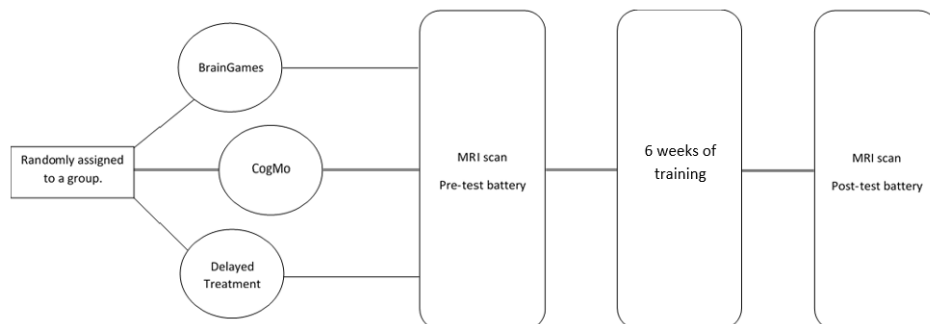
This research project investigates the effect of home-based rehabilitation interventions for various symptoms experienced by patients with Traumatic Brain Injury (TBI). This study aims to examine whether a home-based tablet intervention can promote improvements across the many symptoms of TBI. This includes deficits of cognitive functions (e.g., forgetting tasks to do, or problems concentrating for long periods of time), motor problems (e.g., problems with hand grip, or writing), and daily functional behaviours (e.g., lack of social life since brain injury). You will have 2 MRI scans of your brain. One at the start of the study and the other at the end. This is to see if the home-based rehabilitation has made any changes to the structure of your brain.

This research has been initiated by researcher, Associate Professor Karen Caeyenberghs, from the School of Psychology at Australian Catholic University (ACU). The research has been funded by internal ACU research funding. The results will be used by the associate researchers Mr Adam Clemente and Ms Phoebe Imms to obtain a PhD degree. Further, your data obtained for this study may also be shared with other researchers for the purpose of future research through online databases that are available to the public. This data will not contain identifiable information such as your name and address, which will remain confidential.

3 What does participation in this research involve?

You will be participating in a randomised controlled research project. To find out the effects of tablet-based training programs, we need to compare the effects of them compared to no training. We will assign participants into groups, and provide the training groups with one of the two available training programs. The Delayed Treatment group will continue their daily routine as normal. The results are compared to identify the benefits of the treatment. To try to make sure the groups are the same, each participant is put into a group by chance (random).

As a participant in this study, you will be taking part in a rehabilitation program using a novel tablet-based (e.g., iPad) application BrainGames or CogMo, or be part of the Delayed Treatment group. You will be randomly assigned to one of these three groups. In addition, we will administer pre- and post-rehabilitation intervention measures of cognitive functioning, motor control, daily life functional behaviours, and a brain MRI scan. All groups will undergo these two testing sessions (i.e., pre- and post- intervention testing) at Murdoch Children's Research Institute (MCRI) in Parkville, Melbourne. These two sessions will occur six weeks apart from each other. This will accompany the training rehabilitation if you are in one of the training groups. You will be randomly assigned into one of the groups during your first round of testing and MRI scans.



Intervention:

Immediate Treatment

For the Immediate Treatment groups (BrainGames and CogMo), participation involves taking part in one of two rehabilitation programs at home for 6 weeks immediately after your first test session. Following the 6 weeks of training you will undergo your second test session.

Delayed Treatment

For the Delayed Treatment group, you will undergo two rounds of cognitive testing and MRI scans six weeks apart. Following these two rounds, you will then be able to take part in a training rehabilitation program at home for six weeks.

Training Interventions

Training interventions will involve the use of an electronic touch screen tablet that can be used at home. Training will take approximately 30-40 minutes and will need to be done 4 times a week for 6 weeks. Dependant on the training intervention assigned, we will provide an iPad (mini 2) or Microsoft Surface Pro which will have the brain training program installed, allowing you to complete the training in the comfort of your own home situation. During training, researchers will contact with you via phone call or email to ask how your training is going.

“BrainGames” is an iPad application comprising eight games designed to train different aspects of attention and working memory. For example, one game involves moles popping-up successively at different locations in a four-by-four grid and you will be asked to reproduce the same sequence. In another game, you have to prepare ice cream cones according to the orders they receive. You have to keep track of multiple ice cream stations at the same time and need to react quickly so the ice cream does not melt. Difficulty level of the games will increase with better performance over the training period.

“CogMo” is a multimodal tool comprising five games to train different aspects of cognition and motor control. For example, in one game you will be asked to place objects as accurate and timely as possible, depending on the colour or shape of the targets. In another game, you will see shapes with laser beams coming from them, and you will need to move the shapes so that the beams fit through tunnels and shine out the other end. As with BrainGames, difficulty levels of the games will also increase with better performance over the training period.

Testing:

Cognitive testing

Pre- and post- training intervention, you will complete a series of tests of cognitive functioning. Testing will take approximately 1 hour and will consist mainly of tests of memory, processing speed and other cognitive functions. For example, during one task participants are presented with a set of circles that are labelled with numbers and/ or letters. In different trials of the task, you will connect them by clicking the mouse based on a sequence of numbers (1-2-3-4), letters (A-B-C-D) or an alternating sequence (1-A-2-B). You will have 30 seconds to respond to as many stimuli in the sequence as possible. During another task nine blue squares will appear on the screen. On each trial, the squares will light up one at a time. Once the sequence is finished, you will then respond to each square and reproduce the sequence in the same order they were presented. This testing is not tedious and most participants find it enjoyable as the tests are in the format of computer games. You will be provided with breaks in between each of the tests (if necessary). You will also complete a brief task-based IQ test prior to the commencement of your training.

Motor performance tests

There will be three measures of bimanual (i.e., tasks involving the use of both hands) and unimanual (i.e., tasks involving the use of a single hand) dexterity. For example, you will be asked to twist a screw into a nut as fast as you can. Also, you will be asked to move as many cubes as possible over a vertical wooden barrier in 60 seconds, one at a time, using one hand. These measures are not intensive or rigorous forms of physical activity and will provide beneficial information of any potential improvements in upper limb deficits as a result of the training interventions.

Measures of daily life functioning

A self-report questionnaire measuring subjective experience of attention/executive functioning in everyday life situations will also be administered. For example, one question may be 'do you often forget yesterday's events?' Two other questionnaires measuring the extent to which your lifestyle (e.g., time spent socialising) may have changed as a result of brain injury and also to investigate any improvements as a result of the training intervention.

Tablet-based application experience

During and following your participation in one of the tablet-based applications, you will be given some questionnaires on your experience with the application to measure your motivations to take part in the training and your experience with the games setting. For example, one question may be "I enjoyed this activity very much".

MRI scan

Before and after the training, we will administer a non-invasive Magnetic Resonance Imaging (MRI) scan to examine the effects of the training on the patient's brain. MRI is a scan used for a medical imaging procedure. It uses a magnetic field and radio waves to take pictures inside the body. It is especially helpful to collect pictures of soft tissue, including the brain, which does not show up on x-ray examinations. Scanning will take approximately 50 minutes. Participants will be encouraged to bring along their favourite movie to watch while they are being scanned.

Time commitment:

Training:

This study will take 6 weeks to complete. This includes 6 weeks of cognitive training which you will do at home (30-40 minutes each session, four times a week for six weeks). Before your first day of training and after your final day of training, you will undergo a session of cognitive and motor testing (approximately 60 minutes each session), daily functional behaviour surveys (approximately 20-30 minutes each session) and an MRI scanning session (50 minutes each session). Both the cognitive testing and MRI scanning will be completed on the same day at MCRI which will take approximately three to four hours to complete including breaks. If you believe that completing the MRI scan and testing on the same day is too long, it can be organised to do this over two days. The researchers can come to the comfort of your own home to complete the cognitive testing and you can come to MCRI to do the scans on a separate day. If you feel like this may be more beneficial to you, please let the researchers know to organise this.

To summarise, your overall time commitment is a three hour session of cognitive testing, surveys, and MRI scanning prior to the beginning of your training. Following this, you will undergo approximately 12-14 hours of training across the 6 weeks. Once training is completed, you will finish off with a final three hour session of cognitive testing, surveys, and MRI scanning. Overall, the study will take approximately 18-20 hours of your time over an 6 week period.

If you decide to take part in the research project, you will first be given a questionnaire via telephone to determine if you are able to have an MRI. If the screening questionnaire shows

that you may have an MRI safely, then you will be able to start the research project. If the screening questionnaire shows that you cannot be in the research project, the research coordinator will discuss other options with you.

For participating in this research, you will be reimbursed \$50 per scan/testing session (\$100 in total for the pre- and post-training scan and testing sessions) to cover your travel costs and time, and \$150 for the 6 weeks of training. In total, you will be reimbursed \$250.

Baseline only: If you feel that completing the training intervention would not be feasible, there is an option to complete a single baseline assessment only. The baseline assessment requires you to complete measures of cognitive functioning, motor control, daily life functional behaviours, and undergo a brain MRI scan. The details are the same as listed above. This testing session will be conducted at Murdoch Children's Research Institute (MCRI) in Parkville, Melbourne. You will be reimbursed \$50 for your travel costs and time.

4 What do I have to do?

To participate in this study, you are still able to go about your daily routines and take your usual medications. However, if you are taking part in any cognitive training interventions (e.g., the Lumosity application), these need to be stopped during the 6 weeks of your participation.

5 Other relevant information about the research project

Approximately 45 other people will be taking part in this research project, and they all, like you, have been living with TBI for at least six months. Results of all measures will be compared between the different rehabilitation programs to provide an assessment of different rehabilitation types that may be beneficial for patients with TBI. Comparisons will also be made between the groups who received training and the group that didn't to evaluate the benefits of training following TBI.

6 Do I have to take part in this research project?

Participation in any research project is voluntary. If you do not wish to take part, you do not have to. If you decide to take part and later change your mind, you are free to withdraw from the project at any stage.

If you do decide to take part, you will be given this Participant Information and Consent Form to sign and you will be given a copy to keep.

Your decision whether to take part or not to take part, or to take part and then withdraw, will not affect your routine care, your relationship with professional staff or your relationship with St Vincent's Hospital and Australian Catholic University.

7 What are the alternatives to participation?

You do not have to take part in this research project to receive treatment at St Vincent's Hospital. Other options are available; these include physiotherapy. Your study doctor will discuss these options with you before you decide whether or not to take part in this research project. You can also discuss the options with your local doctor.

8 What are the possible benefits of taking part?

We cannot guarantee or promise that you will receive any benefits from this research; however, if you choose to take part in the training, possible benefits may include improved cognitive

function and upper limb motor deficits that will lead to improved daily life functioning. Though there may be no clear benefit to you from your participation in this research, results of the research may be used to improve rehabilitation services to people with TBI.

9 What are the possible risks and disadvantages of taking part?

You may feel that some of the questions in the questionnaires we ask are stressful or upsetting. If you do not wish to answer a question, you may skip it and go to the next question, or you may stop immediately. If you become upset or distressed as a result of your participation in the research project, the research team will be able to arrange for counselling or other appropriate support. Any counselling or support will be provided by qualified staff who are not members of the research team. This counselling will be provided free of charge. There are no associated risks involved with the tablet-based rehabilitation training programs.

MRI stands for magnetic resonance imaging. An MRI scanner is a machine that uses electromagnetic radiation (radio waves) in a strong magnetic field to take clear pictures of the inside of the body. Electromagnetic radiation is not the same as ionising radiation used, for example, in X-rays. The pictures taken by the machine are called MRI scans. We will ask you to lie on a table inside the MRI scanner. The scanner will record information about your brain. It is very important that you keep very still during the scanning. When you lie on the table, we will provide you with cushions to make sure you are in a comfortable position so that you can keep still. The scanner is very noisy and we can give you some earplugs to reduce the noise. Some people may experience symptoms of claustrophobia from lying in a confined space. If you do experience discomfort at any time during the scan, you will be able to alert staff by pressing on a call button provided to you.

There are no proven long-term risks related to MRI scans as used in this research project. MRI is considered to be safe when performed at a centre with appropriate procedures. However, the magnetic attraction for some metal objects can pose a safety risk, so it is important that metal objects (e.g., phone, earrings, keys) are not taken into the scanner room.

We will thoroughly examine you to make sure we are safe to proceed with the study. You must tell us if you have metal implanted in your body, such as a pacemaker or metal pins.

The scans we are taking are for research purposes. They are not intended to be used like scans taken for a full clinical examination. The scans will not be used to help diagnose, treat or manage TBI. A neuroradiologist will look at your MRI scans for features relevant to the research project.

10 What if new information arises during this research project?

Sometimes during the course of a research project, new information becomes available about the treatment that is being studied. If this happens, your study doctor will tell you about it and discuss with you whether you want to continue in the research project. If you decide to withdraw, your study doctor will make arrangements for your regular health care to continue. If you decide to continue in the research project you will be asked to sign an updated consent form.

Also, on receiving new information, your study doctor might consider it to be in your best interests to withdraw you from the research project. If this happens, he/ she will explain the reasons and arrange for your regular health care to continue.

11 Can I have other treatments during this research project?

Whilst you are participating in this research project, you may not be able to take part in other online cognitive training rehabilitation programs. You should also tell your study doctor about any changes to training programs during your participation in the research project.

12 What if I withdraw from this research project?

If you do consent to participate, you may withdraw at any time. If you decide to withdraw from the project, please notify a member of the research team before you withdraw. A member of the research team will inform you if there are any special requirements linked to withdrawing. If you do withdraw, you will be asked to complete and sign a 'Withdrawal of Consent' form; this will be provided to you by the research team.

If you decide to leave the research project, the researchers will not collect additional personal information from you, although personal information already collected will be retained to ensure that the results of the research project can be measured properly and to comply with law. You should be aware that data collected up to the time you withdraw will form part of the research project results. If you do not want your data to be included, you must tell the researchers when you withdraw from the research project.

13 Could this research project be stopped unexpectedly?

This research project may be stopped unexpectedly for a variety of reasons. These may include reasons such as:

- The rehabilitation program is being shown not to be effective.
- The rehabilitation program is being shown to work and not need further testing.
- Loss of funding.

In these events, all participants will be notified immediately and made aware of how their data will be stored before being destroyed after the 7-year duration required by HREC institutions.

14 What happens when the research project ends?

All individual results will remain confidential, and anything that you say or do during the session will not be communicated to anyone in a way that could identify you. Personal identifying data such as names will not be connected to the obtained results. De-identified results of this study will be published in the form of a PhD thesis and may be published in an academic journal and/or conference proceedings which you can access and read if you would like to do so by contacting a member of the research team. Again, individual participants will not be able to be identified as being part of the study.

There is an opportunity for you to participate in a study about neuroinflammation after TBI. The aim of this study is to determine the role that overactivity of the brain's immune system may play in the brain degeneration that occurs in TBI. This study will involve one session of ~3 hours. In this session, you will do some surveys and cognitive testing, and have blood and saliva samples taken. Then, you will have fluid tracer injected into your arm prior to 1.5 hours in the PET-MRI scanner. If you would like to be contacted in the future about participation in this study, please tick the box at the bottom of the consent form that says "I give permission for this lab to contact me in the future about participation in other ethically approved research studies". If you tick this box, we may not contact you for a few months. Ticking this box does not mean that you have to participate in any way, only that we will call you and ask if you want to participate.

Part 2 How is the research project being conducted?

15 What will happen to information about me?

By signing the consent form you consent to the research team collecting and using personal information about you for the research project. Any information obtained in connection with this research project that can identify you will remain confidential. Your information will only be used

for the purpose of this research project and it will only be disclosed with your permission, except as required by law.

All individual results will remain confidential, and anything that you say or do during the session will not be communicated to anyone in a way that could identify you. Personal identifying data such as names will not be connected to the obtained results. It is anticipated that the results of this research project will be published and/or presented in a variety of forums (e.g., academic journals, conference proceedings). In any publication and/or presentation, information will be provided in such a way that you cannot be identified, except with your express permission. Again, individual participants will not be able to be identified as being part of the study. All records will be securely stored in the locked office of the principle investigator at Australian Catholic University. These records will be kept for 7 years following publication in keeping with the hospital research and ethics procedures.

The personal information that the research team collect and use is name, age, gender, medical history and psychological history. Information about you may be obtained from your medical records held at this and other health organisations for the purpose of this research. By signing the consent form you agree to the research team accessing health records if they are relevant to your participation in this research project.

In accordance with relevant Australian and/or Victorian privacy and other relevant laws, you have the right to request access to the information about you that is collected and stored by the research team. Please inform the research team member named at the end of this document if you would like to access your information.

16 Complaints and compensation

Although there are no risks involved with participation in this research project, if you suffer any injuries or complications as a result of this research project, you should contact the study team as soon as possible and you will be assisted with arranging appropriate medical treatment. If you suffer an injury as a result of participating in this research project, hospital care and treatment will be provided by St Vincent's Hospital. Alternatively, if you are eligible for Medicare, you can receive any medical treatment required to treat the injury or complication, free of charge, as a public patient in any Australian public hospital.

17 Who is organising and funding the research?

This project is being conducted by Associate Professor Karen Caeyenberghs (Australian Catholic University) and Professor Mark Cook (St Vincent's Hospital), funded by internal ACURF grants. You will not benefit financially from your involvement in this research project. No member of the research team will receive personal financial benefit from your involvement in this project (other than ordinary wages).

18 Who has reviewed the research project?

All research in Australia involving humans is reviewed by an independent group of people called a Human Research Ethics Committee (HREC). The ethical aspects of this research project have been approved by the HREC of St Vincent's hospital.

This project will be carried out according to the *National Statement on Ethical Conduct in Human Research (2007)*. This statement has been developed to protect the interests of people who agree to participate in human research studies.

19 Further information and who to contact

The person you may need to contact will depend on the nature of your query. If you want any further information concerning this project or if you have any problems which may be related to your involvement in the project, please contact a member of the research team.

The principle investigator responsible for this project is:
Associate Professor Karen Caeyenberghs (Karen.Caeyenberghs@acu.edu.au)
03 9230 8067

You may also contact the research assistant:
Ms Hannah Richards (hannahrichards09@gmail.com)

If you have any complaints about any aspect of the project or the way in which it is being conducted you may contact the Patient Liaison Officer at St Vincent's Hospital (Melbourne) on Telephone: (03) 9288 3108. You will need to tell the Patient Liaison Officer the name of the person who is noted above as the principal investigator.

If you have any questions about your rights as a research participant, then you may contact the Executive Officer Research at St Vincent's Hospital (Melbourne) on Telephone: (03) 9288 3930



Phone Recruitment Script

for HREC250.17 titled:

“The effects of tablet-based home interventions on brain structure, cognitive functioning, motor performance, and daily life participation in patients with Traumatic Brain Injury”

Version 2

18/11/2019

“Phone Recruitment Script – HREC250.17” – Version 2, Date: 18 November 2019

Hello, I am calling on behalf of A/Prof Karen Caeyenberghs from the Australian Catholic University who does research in conjunction with St Vincent's Hospital here in Melbourne. We have received your name from St Vincent's Hospital emergency department outpatient lists because you might be eligible to take part in our study because of your head injury in [MONTH/YEAR]. We are calling to see if you might be interested in our project looking at rehabilitation after a head injury. The study involves participating in several tests about your everyday functioning as well as undergoing home-based training. We would like to tell you more about the study and ask a few questions to see if you are interested and eligible for participation. Is that okay?

[If NO, thank them for their time, and ask them if they would like to be notified about future studies. If NO, shred their contact information.]

[If YES, ...] We are currently recruiting participants for a research project that looks at the effect of home-based rehabilitation for symptoms experienced by patients with head injuries. We are interested in the effects of training in people who are more than 6 months past their time of injury.

This study looks at whether home-based tablet games, like on an iPad, can help improve the symptoms of head injuries like forgetting to do tasks, or problems concentrating for long periods of time, motor problems (e.g., problems with hand grip, or writing), and daily life (e.g., socialising).

We cannot guarantee that you will receive any benefits from this training; however, possible benefits may include improved concentration and thinking, and improved hand movement abilities that will lead to improved participation in every day tasks. The results of the research may also be used to improve rehabilitation services to people with head injuries.

There are no costs associated with participating in this research project. You will be reimbursed for your time and travel costs associated with this research project up to \$250.

Are you interested in participating? Would you like to know more about what is involved in the study?

[If NO, thank them for their time, and shred their contact information.]

[If YES,...] We are testing training-based apps, called BrainGames and CogMo that our research team have developed. This training will take place in your home at your convenience and will take about 30-40 minutes per session. We aim to complete the training 4 times per week, for 6 weeks.

We will provide tablet, like an iPad, with the training program installed, allowing you to complete the training in the comfort of your own home.

In addition, we will test your concentration and attention skills, how well you use your hands and participation in every day tasks before and after the training. This will be done at the Murdoch Children's Research Institute (MCRI) at the Royal Children's Hospital in Parkville, Melbourne.

You will also have 2 MRI scans of your brain. One at the start of the study and the other at the end. This is to see if the home-based rehabilitation has made any changes to the structure of your brain.

To find out the effects of tablet-based training programs, we need to compare the effects of training to a group of participants who do no training. Therefore, some participants will be in a control group. They will do the testing and MRI scan, and then continue their daily routine as normal for 6 weeks. After this, they will again do the testing and MRI scan, and then will be offered the training at the end of the study instead.

To try to make sure the groups are the same, each participant is put into a group by chance (random). This will be completed after consent. Is this something you may be interested in?

[If NO, thank them for their time and shred their contact information.]

[If YES, you need to screen the participant to ensure that they are eligible for the study.]

Before we send you information about the study, we need to ask you some questions to see if you are eligible to participate:

1. Are you fluent in English?
2. What is your age and date of birth?
3. What is your current home address and email address?
4. Are you or is there a chance that you may be pregnant?
5. Do you have a history of psychiatric illness (not including moderate levels of depression and anxiety)?
6. Are you currently taking any prescribed medications?
7. Have you had a diagnosed TBI before the current one?
8. Do you have a history of seizures or epilepsy?
9. [If YES to the above...] Did you have epilepsy before your TBI? What type of epilepsy is it? When was your last seizure? What was it triggered by?
10. Are you able to get around by yourself or do you require a carer?
11. Are you currently taking part in any treatments, therapies, or training for mental disorders, physical or cognitive problems?

[If THEY ANSWER YES TO ANY OF THE EXCLUSION QUESTIONS GO DIRECTLY TO THIS SECTION] Because we are looking for very specific conditions, unfortunately, you are not eligible to participate in this research study at this time. I'd like to thank you for your time. Have a great day. Goodbye.

[If THEY ANSWER NO TO ALL QUESTIONS] Okay great, it seems that you may be eligible to participate in this research study. Before we can send you the information letter for the study, we need to make sure you are MRI safe. I have some more questions regarding MRI safety.

1. Have you had an MRI before?
2. [If YES...] when was your last MRI?
3. Do you have braces/orthodontics/dentures (brace on the back teeth ok, most fillings/caps/dentures are ok - full braces are not ok)?

4. Do you have any piercings?
5. Do you have any tattoos?
6. Have you ever had any eye injury caused by metal?
7. Is there anything in your body: wires, screws, implants, prosthetics?
8. Have you ever had a brain operation?
9. Do you have any clips or wires in your brain?
10. Do you have a deep brain stimulator?
11. Do you have a brain shunt tube?
12. [If YES...] Is it programmable?
13. Have you had any ear operations/cochlear or stapes implants?
14. Do you have a hearing aid?
15. Do you have a cardiac pacemaker?
16. Have you ever had any heart operations, pacemaker, stents, defib, or wires on the heart?
17. Do you have any implanted devices in your body (metal or otherwise)?
18. Do you have any shrapnel, gunshot wounds?
19. Do you have any Surgical clips/wire sutures/screws/mesh?
20. Do you have any joint replacement or prosthesis?
21. Have you had an operation or procedure within the last 8 weeks (take note of what the surgeries were and ask if there is any chance that there are staples or wires still in the body)?
22. [If YES...] What was the operation? And when was the operation?

[If PARTICIPANT IS NOT MRI SAFE] We can only recruit participants who can undergo an MRI scan, unfortunately, you are not eligible to participate in this research study at this time due to not being able to be scanned. I'd like to thank you for your time. Have a great day. Goodbye. [Shred their contact information.]

[If PARTICIPANT IS MRI SAFE] We will send you the participant information letter, via email or to your home address. Please have a read of this and we will confirm if you are interested, if so, we can book in a time for you to come in. Final consent for participation will happen when you come in. Can you please give us your email address or home address? [record address].

[If PARTICIPANT IS NOT INTERESTED TO PARTICIPATE, thank them for their time and shred their contact information.]

[If PARTICIPANT IS INTERESTED TO PARTICIPATE. Are you available to come in at this [X date] at [Y time]?
[Continue to arrange times]

Appendix N. Screening form for TBI participants (Royal Children's Hospital)

TBI Screening - do via the phone

Date:

Exclusion criteria screening

Question	Yes	No	Details	Info
Name:				
Name of Neurologist (Wendyl D'Souza or Mark Cook)				Need this info for the MCRI screening form - scans will be sent to their neurologist
Sex/Gender:				All genders/sex ok.
DOB:				Age criteria: 18 – 65. Anyone born before 1953 is ineligible.
Date of Injury:				
Right handed:				Left-handed participants are not necessarily excluded at this moment.
Fluent in English:				Second language is ok, but they need to be fluent in English for testing/training to make sense.
Are you ambulant/independently mobile:				Due to difficulties getting in and out of the MRI. Ask about major physical disabilities.
Would you like us to also be in contact with a carer/parent/guardian/friend /relative (and grab their number)				To make sure we aren't excluding anyone who needs to know about their involvement - the RP effect.
Have you ever had a diagnosed TBI before this current one:				Check with Karen, but generally exclude those that have had a TBI before the current one.
Are you currently taking any prescribed medication:				Check the medications with Karen. Anti-depressants/anti-anxiety meds are exclusion criteria. In general, no 'brain altering drugs'.
Are you currently participating in any treatments, therapies, or training for mental disorders, physical or cognitive symptoms:				Cannot be doing cognitive training. Otherwise just take a note of their therapy programs.
What suburb do you live in:				If more than 2 hours away, maybe not possible to deliver the tablet
Are you taking medications for a psychiatric illness:				Participants with moderate levels of depression/anxiety (not taking meds) are ok to include.
Do you have a history of epilepsy or seizures:				

TBI Screening - do via the phone

Date:

If yes: Did you have epilepsy before your TBI? What type of epilepsy is it (e.g., focal or generalised)? Subtype? When was your last seizure?				Take as much detail as possible, tell them we will get back to them after discussing with our lead researchers.
OK to participate:				Move on to MRI screening

MRI screening – ANY CONCERNS check with radiographer before including the participant

Have you had an MRI before? NO / YES
 If Yes, when was your last MRI? NO / YES

Braces/Orthodontics/Dentures (brace on the back teeth ok, most fillings/caps/dentures are ok

- **full braces are not ok**: Y / N Details:
 Piercings: Y / N Details:
 Tattoos: Y / N Details:

Have you ever had any eye injury caused by metal? NO / YES

Are you pregnant, suspect you may be pregnant or breastfeeding? NO / YES

Is there anything in your body: wires, screws, implants, prosthetics? Y / N Details:

Any Brain operation NO / YES
 Brain Aneurysm Clips NO / YES
 Deep Brain Stimulator NO / YES
 Brain Shunt Tube NO / YES
 If YES, is it programmable NO / YES
 Any Ear operations/cochlear or stapes implants NO / YES
 Hearing Aid NO / YES
 A Cardiac Pacemaker/stent/defibrillator/wire NO / YES
 Any heart operation, pacemaker, stents, defib, wires on the heart NO / YES
 Implanted devices (metal or otherwise) NO / YES
 Shrapnel, gunshot wounds NO / YES
 Any Surgical clips/wire sutures/screws/mesh/prosthesis NO / YES
 Joint Replacement or Prosthesis NO / YES

Have You:

Had an operation or procedure within the last 8 weeks (take note of what the surgeries were and ask if there is any chance that there are staples or wires still in the body) NO / YES

What? / When?

Had a history of seizures or epilepsy NO / YES

When was your last seizure

What was it triggered by

TBI Screening - do via the phone

Date:

OK to participate: Y / N

The next step will be to organise a scan time and date for **both scan dates**.

Date and Time of scan: _____

MRI and testing room booked: Y / N **MRI time:** _____

Appendix O. Participant information form for Healthy Controls (Royal Children's Hospital)



Participant Information Sheet/Consent Form Non-Interventional Study - Adult providing own consent

Title	The effects of tablet-based home interventions on brain structure, cognitive functioning, motor performance, and daily life participation in healthy adults.
Short Title	Home-based interventions for brain-injured patients
Coordinating Principal Investigator/ Principal Investigator	A/Prof Karen Caeyenberghs Prof Mark Cook and A/Prof Wendy D'Souza
Associate Investigator(s)	Mr Adam Clemente, Ms Phoebe Imms, Ms Evelyn Deutscher, Ms Annalee Cobden, Mr Thomas Bowen, Ms Eva Mezei, Prof Peter H. Wilson, Dr Jonathan Duckworth, and Mr. Rakesh Patibanda.
Research Assistants	Miss Hannah Richards, Ms Alexandra Armstrong
Location	St. Vincent's Hospital, Melbourne

Part 1 What does my participation involve?

1 Introduction

You are invited to take part in this research project, *the effects of tablet-based home interventions on brain structure, cognitive functioning, motor performance, and daily life participation*. This is because we are interested in the structure and function of the human brain. The research project is aiming to investigate whether a tablet-based home intervention can improve the brain structure, cognitive functioning, motor performance, and daily life participation of healthy adults.

This Participant Information Sheet/Consent Form tells you about the research project. It explains the tests and research involved. Knowing what is involved will help you decide if you want to take part in the research.

Please read this information carefully. Ask questions about anything that you don't understand or want to know more about. Before deciding whether or not to take part, you might want to talk about it with a relative, friend or local doctor.

Participation in this research is voluntary. If you don't wish to take part, you don't have to. You will receive the best possible care whether or not you take part.

If you decide you want to take part in the research project, you will be asked to sign the consent section. By signing it you are telling us that you:

- Understand what you have read
- Consent to take part in the research project
- Consent to the tests and research that are described
- Consent to the use of your personal and health information as described.

You will be given a copy of this Participant Information and Consent Form to keep.

2 What is the purpose of this research?

This research project investigates cognitive functioning. Many daily life activities are involved in acquiring information, including listening, watching, reading, searching out information, or just paying attention to things around you. In all cases, you are using your cognitive functions to gather information. Cognitive functions include attention, memory, language, perception, decision making, and problem solving. This study aims to examine the relationship between cognitive function and brain structure.

This research has been initiated by researcher, Associate Professor Karen Caeyenberghs, from the School of Psychology at Australian Catholic University (ACU). The research has been funded by internal ACU research funding. The results will be used by the associate researchers Mr Adam Clemente and Ms Phoebe Imms to obtain a PhD degree. Further, your data obtained for this study may also be shared with other researchers for the purpose of future research through online databases that are available to the public. This data will not contain identifiable information such as your name and address, which will remain confidential.

3 What does participation in this research involve?

Baseline only: You will be participating in a research project to find out the links between cognition, motor ability, and daily-life functioning and the structure of your brain. As a participant in this study, we will administer measures of cognitive functioning, motor control, daily life

functional behaviours, and a brain MRI scan. This testing session will be conducted at Murdoch Children's Research Institute (MCRI) in Parkville, Melbourne. You will be reimbursed \$50 for your travel costs and time.

Training: If you choose to participate further, you can also complete 6 weeks of cognitive/motor training on a tablet that you can take home, to examine the effects of a tablet-based training program on structural brain changes. If you complete the training part of this study, you will take part in a program using a novel tablet-based application called CogMo. You will still do the measures and brain scan outlined above at the first session, but you will also complete these same measures at the end of the 6 weeks of training. To summarise, you will undergo baseline testing (a MRI brain scan and a testing session). Following this, you will do six weeks of CogMo training in your own home. Once completed, you will undergo a final testing session (brain scan and various tests). For this, you will be reimbursed \$50 per testing session and \$150 for the six weeks of training. In total, you will be reimbursed \$250.

Intervention:

Training Interventions – will not be completed by participants who choose to do baseline only.

If you choose to do so, training interventions will involve the use of an electronic touch screen tablet that can be used at home. Training will take approximately 30-40 minutes and will need to be done 4 times a week for 6 weeks. We will provide you with a Microsoft Surface Pro which will have the brain training program installed, allowing you to complete the training in the comfort of your own home situation. During training, researchers will contact you via phone call or email to ask how your training is going.

"CogMo" is a multimodal tool comprising five games to train different aspects of cognition and motor control. For example, in one game you will be asked to place objects as accurate and timely as possible, depending on the colour or shape of the targets. In another game, you will see shapes with laser beams coming from them, and you will need to move the shapes so that the beams fit through tunnels and shine out the other end. Difficulty levels of the games will also increase with better performance over the training period.

Testing:

Cognitive testing

In the first testing session (and at the post-training session if you so choose), you will complete a series of tests of cognitive functioning. Testing will take approximately 1 hour and will consist mainly of tests of memory, processing speed and other cognitive functions. For example, during one task participants are presented with a set of circles that are labelled with numbers and/ or letters. In different trials of the task, you will connect them by clicking the mouse based on a sequence of numbers (1-2-3-4), letters (A-B-C-D) or an alternating sequence (1-A-2-B). You will have 30 seconds to respond to as many stimuli in the sequence as possible. During another task nine blue squares will appear on the screen. On each trial, the squares will light up one at a time. Once the sequence is finished, you will then respond to each square and reproduce the sequence in the same order they were presented. This testing is not tedious and most participants find it enjoyable as the tests are in the format of computer games. You will be provided with breaks in between each of the tests (if necessary). You will also complete a brief task-based IQ test prior to the commencement of your training.

Motor performance tests

In the first testing session (and at the post-training session if you so choose), you will undertake three measures of bimanual (i.e., tasks involving the use of both hands) and unimanual (i.e.,

tasks involving the use of a single hand) dexterity. For example, you will be asked to twist a screw into a nut as fast as you can. Also, you will be asked to move as many cubes as possible over a vertical wooden barrier in 60 seconds, one at a time, using one hand. Another test involves moving pegs from hole to hole. These measures are not intensive or rigorous forms of physical activity and will provide beneficial information of any potential improvements in upper limb deficits as a result of the training interventions.

Measures of daily life functioning

A self-report questionnaire measuring subjective experience of attention/executive functioning in everyday life situations will also be administered in the first session. For example, one question may be 'do you often forget yesterday's events?' Two other questionnaires measuring the extent to which your lifestyle (e.g., time spent socialising) may have changed as a result of brain injury and also to investigate any improvements as a result of the training intervention.

MRI scan

Before or after the training, we will administer a non-invasive Magnetic Resonance Imaging (MRI) scan to examine the effects of the training on the patient's brain. MRI is a scan used for a medical imaging procedure. It uses a magnetic field and radio waves to take pictures inside the body. It is especially helpful to collect pictures of soft tissue, including the brain, which does not show up on x-ray examinations. Scanning will take approximately 50 minutes. Participants will be encouraged to bring along their favourite movie to watch while they are being scanned.

Tablet-based application experience

During and following your participation in one of the tablet-based applications, you will be given some questionnaires on your experience with the application to measure your motivations to take part in the training and your experience with the games setting. For example, one question may be "I enjoyed this activity very much".

Time commitment:

If you choose to do baseline only, your overall time commitment is a three hour session of cognitive testing, surveys, and MRI scanning.

If you choose to do the training component of this study, it will take 6-8 weeks to complete. This includes 6 weeks of cognitive training which you will do at home (30-40 minutes each session, four times a week for six weeks). Before your first day of training and after your final day of training, you will undergo a session of cognitive and motor testing (approximately 60 minutes each session), daily functional behaviour surveys (approximately 20-30 minutes each session) and an MRI scanning session (50 minutes: only before training). Both the cognitive testing and MRI scanning will be completed on the same day at MCRI which will take approximately three to four hours to complete including breaks. If you believe that completing the MRI scan and testing on the same day is too long, it can be organised to do this over two days. The researchers can come to the comfort of your own home to complete the cognitive testing and you can come to MCRI to do the scans on a separate day. If you feel like this may be more beneficial to you, please let the researchers know to organise this.

To summarise, your overall time commitment is a three hour session of cognitive testing, surveys, and MRI scanning prior to the beginning of your training. Following this, if you choose to do the training, you will undergo approximately 20 hours of training across the 6 weeks. Once training is completed, you will finish off with a final three hour session of cognitive testing and surveys. Overall, the study would then take approximately 26 hours of your time over an 8 week period.

If you decide to take part in either part of the research project, you will first be given a questionnaire via telephone to determine if you are able to have an MRI. If the screening questionnaire shows that you may have an MRI safely, then you will be able to start the research project. If the screening questionnaire shows that you cannot be in the research project, the research coordinator will discuss other options with you.

There are no costs associated with participating in this research project, nor will you be paid.

4 What do I have to do?

To participate in the training part of this study, you are still able to go about your daily routines and take your usual medications. However, if you are taking part in any cognitive training interventions (e.g., the Lumosity application), these need to be stopped during the 6 weeks of your participation.

5 Do I have to take part in this research project?

Participation in any research project is voluntary. If you do not wish to take part, you do not have to. If you decide to take part and later change your mind, you are free to withdraw from the project at any stage.

Participation in the training part of this program is entirely voluntary, and you are under no obligation to complete the training portion of the study if you choose to take part in the baseline portion of the study.

If you do decide to take part, you will be given this Participant Information and Consent Form to sign and you will be given a copy to keep.

Your decision whether to take part or not to take part, or to take part and then withdraw, will not affect your relationship with professional staff or your relationship with St Vincent's Hospital and Australian Catholic University.

6 What are the possible benefits of taking part?

We cannot guarantee or promise that you will receive any benefits from this research; however, possible benefits may include improved cognitive function and upper limb motor deficits that will lead to improved daily life functioning. Though there may be no clear benefit to you from your participation in this research, results of the research may be used to improve rehabilitation services to other people.

7 What are the possible risks and disadvantages of taking part?

You may feel that some of the questions in the questionnaires we ask are stressful or upsetting. If you do not wish to answer a question, you may skip it and go to the next question, or you may stop immediately. If you become upset or distressed as a result of your participation in the research project, the research team will be able to arrange for counselling or other appropriate support. Any counselling or support will be provided by qualified staff who are not members of the research team. This counselling will be provided free of charge. There are no associated risks involved with the tablet-based rehabilitation training programs.

MRI stands for magnetic resonance imaging. An **MRI** scanner is a machine that uses electromagnetic radiation (radio waves) in a strong magnetic field to take clear pictures of the inside of the body. Electromagnetic radiation is not the same as ionising radiation used, for example, in X-rays. The pictures taken by the machine are called **MRI** scans.

We will ask you to lie on a table inside the **MRI** scanner. The scanner will record information about your brain. It is very important that you keep very still during the scanning. When you lie on the table, we will provide you with cushions to make sure you are in a comfortable position so that you can keep still. The scanner is very noisy and we can give you some earplugs to reduce the noise. Some people may experience symptoms of claustrophobia from lying in a confined space. If you do experience discomfort at any time during the scan, you will be able to alert staff by pressing on a call button provided to you.

There are no proven long-term risks related to **MRI** scans as used in this research project. **MRI** is considered to be safe when performed at a centre with appropriate procedures. However, the magnetic attraction for some metal objects can pose a safety risk, so it is important that metal objects (e.g., phone, earrings, keys) are not taken into the scanner room.

We will thoroughly examine you to make sure we are safe to proceed with the study. You must tell us if you have metal implanted in your body, such as a pacemaker or metal pins.

The scans we are taking are for research purposes. They are not intended to be used like scans taken for a full clinical examination. A neuroradiologist will look at your **MRI** scans for features relevant to the research project.

8 What if new information arises during this research project?

Sometimes during the course of a research project, new information becomes available about the treatment that is being studied. If this happens, your study doctor will tell you about it and discuss with you whether you want to continue in the research project. If you decide to withdraw, your study doctor will make arrangements for your regular health care to continue. If you decide to continue in the research project you will be asked to sign an updated consent form.

Also, on receiving new information, your study doctor might consider it to be in your best interests to withdraw you from the research project. If this happens, he/ she will explain the reasons and arrange for your regular health care to continue.

9 Can I have other treatments during this research project?

Whilst you are participating in this research project, you may not be able to take part in other online cognitive training rehabilitation programs. You should also tell your study doctor about any changes to training programs during your participation in the research project.

10 What if I withdraw from this research project?

If you do consent to participate, you may withdraw at any time. If you decide to withdraw from the project, please notify a member of the research team before you withdraw. A member of the research team will inform you if there are any special requirements linked to withdrawing. If you do withdraw, you will be asked to complete and sign a 'Withdrawal of Consent' form; this will be provided to you by the research team.

If you decide to leave the research project, the researchers will not collect additional personal information from you, although personal information already collected will be retained to ensure that the results of the research project can be measured properly and to comply with law. You should be aware that data collected up to the time you withdraw will form part of the research

project results. If you do not want your data to be included, you must tell the researchers when you withdraw from the research project.

11 Could this research project be stopped unexpectedly?

This research project may be stopped unexpectedly for a variety of reasons. These may include reasons such as:

- The training program is being shown not to be effective.
- The training program is being shown to work and not need further testing.
- Loss of funding.

In these events, all participants will be notified immediately and made aware of how their data will be stored before being destroyed after the 7-year duration required by HREC institutions.

12 What happens when the research project ends?

All individual results will remain confidential, and anything that you say or do during the session will not be communicated to anyone in a way that could identify you. Personal identifying data such as names will not be connected to the obtained results. De-identified results of this study will be published in the form of a PhD thesis and may be published in an academic journal and/or conference proceedings which you can access and read if you would like to do so by contacting a member of the research team. Again, individual participants will not be able to be identified as being part of the study.

Part 2 How is the research project being conducted?

13 What will happen to information about me?

By signing the consent form you consent to the research team collecting and using personal information about you for the research project. Any information obtained in connection with this research project that can identify you will remain confidential. Your information will only be used for the purpose of this research project and it will only be disclosed with your permission, except as required by law.

All individual results will remain confidential, and anything that you say or do during the session will not be communicated to anyone in a way that could identify you. Personal identifying data such as names will not be connected to the obtained results. It is anticipated that the results of this research project will be published and/or presented in a variety of forums (e.g., academic journals, conference proceedings). In any publication and/or presentation, information will be provided in such a way that you cannot be identified, except with your express permission. Again, individual participants will not be able to be identified as being part of the study. All records will be securely stored in the locked office of the principle investigator at Australian Catholic University. These records will be kept for 7 years following publication in keeping with the hospital research and ethics procedures.

The personal information that the research team collect and use is name, age, gender, medical history and psychological history. Information about you may be obtained from your medical records held at this and other health organisations for the purpose of this research. By signing the consent form you agree to the research team accessing health records if they are relevant to your participation in this research project.

In accordance with relevant Australian and/or Victorian privacy and other relevant laws, you have the right to request access to the information about you that is collected and stored by the research team. Please inform the research team member named at the end of this document if you would like to access your information.

14 Complaints and compensation

Although there are no risks involved with participation in this research project, if you suffer any injuries or complications as a result of this research project, you should contact the study team as soon as possible and you will be assisted with arranging appropriate medical treatment. If you suffer an injury as a result of participating in this research project, hospital care and treatment will be provided by St Vincent's Hospital. Alternatively, if you are eligible for Medicare, you can receive any medical treatment required to treat the injury or complication, free of charge, as a public patient in any Australian public hospital.

15 Who is organising and funding the research?

This project is being conducted by Associate Professor Karen Caeyenberghs (Australian Catholic University) and Professor Mark Cook (St Vincent's Hospital), funded by internal ACURF grants. You will not benefit financially from your involvement in this research project. No member of the research team will receive personal financial benefit from your involvement in this project (other than ordinary wages).

16 Who has reviewed the research project?

All research in Australia involving humans is reviewed by an independent group of people called a Human Research Ethics Committee (HREC).

The ethical aspects of this research project have been approved by the HREC of St Vincent's hospital.

This project will be carried out according to the National Statement on Ethical Conduct in Human Research (2007). This statement has been developed to protect the interests of people who agree to participate in human research studies.

17 Further information and who to contact

The person you may need to contact will depend on the nature of your query. If you want any further information concerning this project or if you have any problems which may be related to your involvement in the project, please contact a member of the research team.

The principle investigator responsible for this project is:
Associate Professor Karen Caeyenberghs (Karen.Caeyenberghs@acu.edu.au)
03 9230 8067

You may also contact the research assistant:
Ms Hannah Richards (hannahrichards09@gmail.com)

If you have any questions about your rights as a research participant, then you may contact the Executive Officer Research at St Vincent's Hospital (Melbourne) on Telephone: (03) 9288 3930

Appendix P. Screening checklist for Healthy Controls (RCH)

HC Screening - do via the phone

Date:

Exclusion criteria screening

Question	Yes	No	Details	Info
Name:				
Sex/Gender:				All genders/sex ok.
DOB:				Age criteria: 18 – 65. Anyone born before 1953 is ineligible.
Ever had a brain injury?				Make sure participants are eligible to be healthy controls
Right handed:				Left-handed participants are not necessarily excluded at this moment.
Fluent in English:				Second language is ok, but they need to be fluent in English for testing/training to make sense.
Are you ambulant/independently mobile:				Due to difficulties getting in and out of the MRI. Ask about major physical disabilities.
Are you currently taking any prescribed medication:				Check the medications with Karen. Anti-depressants/anti-anxiety meds are exclusion criteria. In general, no 'brain altering drugs'.
Are you currently participating in any treatments, therapies, or training for mental disorders, physical or cognitive symptoms:				Cannot be doing cognitive training. Otherwise just take a note of their therapy programs.
What suburb do you live in:				If more than 2 hours away, maybe not possible to deliver the tablet
Are you taking medications for a psychiatric illness:				Participants with moderate levels of depression/anxiety (not taking meds) are ok to include.
Do you have a history of epilepsy or seizures:				
If yes: What type of epilepsy is it (e.g., focal or generalised)? Subtype? When was your last seizure?				Take as much detail as possible, tell them we will get back to them after discussing with our lead researchers – excluded as HCs if they have had epilepsy
OK to participate:				Move on to MRI screening

MRI screening – ANY CONCERNS check with radiographer before including the participant

HC Screening - do via the phone

Date:

Have you had an MRI before? NO / YES

If Yes, when was your last MRI?..... NO / YES

Braces/Orthodontics/Dentures (brace on the back teeth ok, most fillings/caps/dentures are ok

- full braces are not ok):

Y / N

Details:

Piercings:

Y / N

Details:

Tattoos:

Y / N

Details:

Have you ever had any eye injury caused by metal?..... NO / YES

Are you pregnant, suspect you may be pregnant or breastfeeding?..... NO / YES

Is there anything in your body: wires, screws, implants, prosthetics? Y / N Details:

Any Brain operation NO / YES

Brain Aneurysm Clips..... NO / YES

Deep Brain Stimulator..... NO / YES

Brain Shunt Tube..... NO / YES

If YES, is it programmable NO / YES

Any Ear operations/cochlear or stapes implants..... NO / YES

Hearing Aid..... NO / YES

A Cardiac Pacemaker/stent/defibrillator/wire..... NO / YES

Any heart operation, pacemaker, stents, defib, wires on the heart..... NO / YES

Implanted devices (metal or otherwise)..... NO / YES

Shrapnel, gunshot wounds..... NO / YES

Any Surgical clips/wire sutures/screws/mesh/prosthesis..... NO / YES

Joint Replacement or Prosthesis..... NO / YES

Have You:

Had an operation or procedure within the last 8 weeks (take note of what the surgeries were and ask if there is any chance that there are staples or wires still in the body)..... NO / YES

What? / When?.....

Had a history of seizures or epilepsy..... NO / YES

When was your last seizure.....

What was it triggered by.....

OK to participate: Y / N

The next step will be to organise a scan time and date for both scan dates.

Date and Time of scan: _____

MRI and testing room booked: Y / N MRI time: _____

Appendix Q. Consent form for TBI participants (RCH)

Consent Form - *Adult providing own consent*

Title	The effects of tablet-based home interventions on brain structure, cognitive functioning, motor performance, and daily life participation in patients with Traumatic Brain Injury.
Short Title	Home-based interventions for brain-injured patients
Protocol Number	HREC 250.17
Principal Investigators	A/Prof Karen Caeyenberghs Prof Mark Cook A/Prof Wendy D'Souza
Associate Investigator(s)	Mr. Adam Clemente, Ms. Phoebe Imms, Ms Evelyn Deutscher, Ms Annalee Cobden, Mr Nicholas Parsons, Dr Hamed Akhlaghi, Rakesh Patibanda, Dr Jonathan Duckworth, and Prof Peter H. Wilson
Research Assistants	Ms Hannah Richards, Ms Alexandra Armstrong and Ms Honey Baseri
Location	St. Vincent's Hospital, Melbourne

Declaration by Participant

I have read the Participant Information Sheet or someone has read it to me in a language that I understand.

I understand the purposes, procedures and risks of the research described in the project.

I give permission for my doctors, other health professionals, hospitals or laboratories outside this hospital to release information to Australian Catholic University concerning my disease and treatment for the purposes of this project. I understand that such information will remain confidential.

I have had an opportunity to ask questions and I am satisfied with the answers I have received.

I freely agree to participate in this research project as described and understand that I am free to withdraw at any time during the study without affecting my future health care.

I understand that I will be given a signed copy of this document to keep.

I choose to take part in the (tick one)

Baseline only study (time commitment of 3 hours) Training study (time commitment of 18-20 hours over a 6 week period)
--

Name of Participant (please print) _____

Signature _____ Date _____

☐ I give permission for this lab to contact me in the future about participation in other ethically approved research studies

Name of Witness* to
Participant's Signature (please print) _____

Signature _____ Date _____

* Witness is not to be the investigator, a member of the study team or their delegate. In the event that an interpreter is used, the interpreter may not act as a witness to the consent process. Witness must be 18 years or older.

Declaration by Study Doctor/Senior Researcher[†]

I have given a verbal explanation of the research project, its procedures and risks and I believe that the participant has understood that explanation.

Name of Study Doctor/
Senior Researcher[†] (please print) _____

Signature _____ Date _____

[†] A senior member of the research team must provide the explanation of, and information concerning, the research project.

Note: All parties signing the consent section must date their own signature.

Appendix R. Consent form for Healthy Controls (RCH)



Consent Form - Adult providing own consent

Title	The effects of tablet-based home interventions on brain structure, cognitive functioning, motor performance, and daily life participation in healthy adults.
Short Title	Home-based interventions for brain-injured patients
Protocol Number	
Coordinating Principal Investigator/ Principal Investigator	A/Prof Karen Caeyenberghs, Prof Mark Cook and A/Prof Wendy D'Souza,
Associate Investigator(s)	Mr Adam Clemente, Ms Phoebe Imms, Ms Evelyn Deutscher, Ms Annalee Cobden, Mr Thomas Bowen, Ms Eva Mezei, Prof Peter H. Wilson, Dr Jonathan Duckworth, Ross Eldridge and Rakesh Patibanda
Research Assistants	Miss Hannah Richards, Ms Alexandra Armstrong
Location	St Vincent's Hospital, Melbourne

Consent Agreement

I have read the Participant Information Sheet or someone has read it to me in a language that I understand.

I understand the purposes, procedures and risks of the research described in the project.

I have had an opportunity to ask questions and I am satisfied with the answers I have received.

I freely agree to participate in this research project as described and understand that I am free to withdraw at any time during the project.

I understand that I will be given a signed copy of this document to keep.

I choose to take part in the (circle one)

Baseline only study (time commitment of 3 hours)

Training study (time commitment of 26 hours over an 8 week period)

Declaration by Participant – for participants who have read the information

Name of Participant (please print) _____	
Signature _____	Date _____

Declaration by Study Doctor/Senior Researcher[†]

I have given a verbal explanation of the research project, its procedures and risks and I believe that the participant has understood that explanation.

Name of Study Doctor/ Senior Researcher [†] (please print) _____	
Signature _____	Date _____

[†] A senior member of the research team must provide the explanation of, and information concerning, the research project.

Note: All parties signing the consent section must date their own signature.

Appendix S. Survey of demographic information

Participant #: _____

Demographic Questionnaire

Next of Kin/Carer information:

Name: _____

Relationship: _____

Phone: _____

Email: _____

Gender: **Age and Date of Birth:** **Level of Education (Please tick one):**

☐ MALE _____ Years

☐ Less than year 12 or equivalent

☐ FEMALE _____ / _____ / 19 _____

☐ Year 12 or equivalent

☐ Diploma/Vocational qualification

☐ Bachelor Degree (Including Honours)

☐ Postgraduate Diploma

☐ Master's Degree

☐ Doctorate

What is your dominant hand:

☐ I am right handed

☐ I am left handed

Which hand do you prefer to use when:

Writing: Left ☐ ; No Preference ☐ ; Right ☐

Drawing: Left ☐ ; No Preference ☐ ; Right ☐

Throwing: Left ☐ ; No Preference ☐ ; Right ☐

Using Scissors: Left ☐ ; No Preference ☐ ; Right ☐

Using a Toothbrush: Left ☐ ; No Preference ☐ ; Right ☐

Using a Knife (without a fork): Left ☐ ; No Preference ☐ ; Right ☐

Using a Spoon: Left ☐ ; No Preference ☐ ; Right ☐

Using a Broom (upper hand): Left ☐ ; No Preference ☐ ; Right ☐

Striking a Match: Left ☐ ; No Preference ☐ ; Right ☐

Opening a Box (holding lid): Left ☐ ; No Preference ☐ ; Right ☐

Appendix T. The Neurobehavioural Functioning Inventory

Neurobehavioral Functioning Inventory

Name:

Age:

Date:

Diagnosis:

Duration of unconsciousness at time of injury/illness (if applicable):

How often do you **currently** have any of the following problems? Please circle/check the number under the label *Never*, *Rarely*, *Sometimes*, *Often*, or *Always*. If you wish to change your answer, put an X through it and fill in your new choice.

		NEVER	RARELY	SOMETIMES	OFTEN	ALWAYS
1	Blackout spells	1	2	3	4	5
2	Seizures	1	2	3	4	5
3	Threaten to hurt yourself	1	2	3	4	5
4	Cannot be left at home alone	1	2	3	4	5

		NEVER	RARELY	SOMETIMES	OFTEN	ALWAYS
5	Miss or cannot attend work/school	1	2	3	4	5
6	Double or blurred vision	1	2	3	4	5
7	Feel hopeless	1	2	3	4	5
8	Stomach hurts	1	2	3	4	5
9	Forget yesterday's events	1	2	3	4	5
10	Difficulty pronouncing words	1	2	3	4	5
11	Curse at others	1	2	3	4	5
12	Difficulty lifting heavy objects	1	2	3	4	5
13	Feel worthless	1	2	3	4	5
14	Nauseous	1	2	3	4	5
15	Forget if you have done things	1	2	3	4	5
16	Write slowly	1	2	3	4	5
17	Hit or push others	1	2	3	4	5

		NEVER	RARELY	SOMETIMES	OFTEN	ALWAYS
18	Move slowly	1	2	3	4	5
19	Sad, blue	1	2	3	4	5
20	Headaches	1	2	3	4	5
21	Forget or miss appointments	1	2	3	4	5
22	Trouble understanding conversation	1	2	3	4	5
23	Argue	1	2	3	4	5
24	Lose balance	1	2	3	4	5
25	Lonely	1	2	3	4	5
26	Dizzy	1	2	3	4	5
27	Forget people's names	1	2	3	4	5
28	Make spelling mistakes	1	2	3	4	5
29	Inappropriate comments or behaviour	1	2	3	4	5
30	Weak	1	2	3	4	5

		NEVER	RARELY	SOMETIMES	OFTEN	ALWAYS
31	No confidence	1	2	3	4	5
32	Stomach bloated	1	2	3	4	5
33	Forget what you read	1	2	3	4	5
34	Difficulty thinking of the right word	1	2	3	4	5
35	Break or throw things	1	2	3	4	5
36	Drop things	1	2	3	4	5
37	Frustrated	1	2	3	4	5
38	Nightmares	1	2	3	4	5
39	Lose track of time, day, or date	1	2	3	4	5
40	Difficulty making conversation	1	2	3	4	5
41	Scream or yell	1	2	3	4	5
42	Muscles tingle or twitch	1	2	3	4	5
43	Sit with nothing to do	1	2	3	4	5

		NEVER	RARELY	SOMETIMES	OFTEN	ALWAYS
44	Ringing in ears	1	2	3	4	5
45	Forget to do chores or work	1	2	3	4	5
46	Speech doesn't make sense	1	2	3	4	5
47	Rude to others	1	2	3	4	5
48	Difficulty performing chores	1	2	3	4	5
49	Scared or frightened	1	2	3	4	5
50	Poor appetite	1	2	3	4	5
51	Misplace things	1	2	3	4	5
52	My writing is hard to read	1	2	3	4	5
53	Threaten to hurt others	1	2	3	4	5
54	Trip over things	1	2	3	4	5
55	Concentration is poor	1	2	3	4	5
56	Lose train of thought	1	2	3	4	5

		NEVER	RARELY	SOMETIMES	OFTEN	ALWAYS
57	Forget phone numbers	1	2	3	4	5
58	Lose way, get lost	1	2	3	4	5
59	Bored	1	2	3	4	5
60	Confused	1	2	3	4	5
61	Read slowly	1	2	3	4	5
62	Easily distracted	1	2	3	4	5
63	Talk too fast or slow	1	2	3	4	5
64	Forget to turn off appliances	1	2	3	4	5
65	Difficulty enjoying activities	1	2	3	4	5
66	Trouble following instructions	1	2	3	4	5
67	Uncomfortable around others	1	2	3	4	5
68	Curse at yourself	1	2	3	4	5

		NEVER	RARELY	SOMETIMES	OFTEN	ALWAYS
69	Forget to take medication (if none prescribed, respond 'never')	1	2	3	4	5
70	Can't get mind off certain thoughts	1	2	3	4	5
71	Disorganised	1	2	3	4	5
72	Restless	1	2	3	4	5
73	Late for appointments	1	2	3	4	5
74	Trouble falling asleep	1	2	3	4	5
75	Trouble hearing	1	2	3	4	5
76	Food doesn't taste right	1	2	3	4	5

Appendix U. MRI scan running sheet

Date:

Time:

MRI Scan Running Sheet

Participant ID/First Name: _____

Last Name: ACU_TBI

1. Check with reception upon arrival at MCRI that the scan session is still going ahead on time.
2. The MCRI MRI screening form should be completed by the participant immediately after the consent form is signed in the testing room.
 - a. In the top right-hand corner, their First Name should be their participant ID (*without the time-point identifier, i.e., no 'T1' or 'T2'*) and their Last Name is 'ACU_TBI'.
 - b. Also write their full name and DOB for the radiographers' records.
 - c. You should also write the name of the neurologist to whom the report should be sent.
3. The screening form should be taken to the radiographers (ring buzzer) 5-10 minutes before the scan – not given to reception.
4. While dropping the screening form off, grab the list of movies from the wall-mount behind the radiographers' desk and bring it to the participant to choose a movie.
 - a. At this time, also ask them to remove jewellery and use the bathroom.
5. Wait with the participant in the waiting room until the radiographer comes out to get you. While you are waiting, ask the participant if they have any questions about the scan. Let them know things like a) how long the scan will take, b) what they can expect to experience while in the scanner, c) comfort and assure them, let them know you'll be just outside the room the whole time.
6. When the radiographer comes, let them take charge of the participant and putting them into the scanner.
 - a. While they are doing this, you can get the participant's movie set up (in the 'Videos' folder on the desktop), and the KSS PowerPoint minimised (in the 'ACU_TBI' folder on the desktop, called 'ACU_TBI_resting state script.pptx').
7. Sit behind the radiographer's desk and fill out this form. Write down any big movements that you notice in the notes section for each scan.

ACU team member/s present: _____

Radiographer/s name: _____

Report sent to (neurologist): _____

Fiducial marker placed on RIGHT temple: Y / N

A>>P alignment: Y / N

FOV covers full brain (cerebellum and top of brain not cut off): Y / N

Other notes:

Date:

Time:

MRI PROTOCOL – ACU TBI MR181 v2.1			
Sequence	Duration	Completed satisfactorily	Notes (e.g., repeated, significant movements, interrupted)
AAHead_Scout_32ch-head-coil	0:14	Y / N	
T1-weighted imaging (MPRAGE)			
3D MPRAGE	05:48	Y / N	
Diffusion Weighted Imaging (HARDI)			
Blip_U 2.3mm	00:50	Y / N	
Blip_D 2.3mm	00:50	Y / N	
DWIB3000 CMT 66Dir SEg	04:37	Y / N	
Free Wave Form (FWF)			
a_ep 2d_diff_fwf_STE_s1	3:00	Y / N	
a_ep 2d_diff_fwf_LTE_s1	3:00	Y / N	
Blip_U 2.3 fwf A>P	0:20	Y / N	
Blip_U fwf P>A	0:20	Y / N	
Quantitative Susceptibility Mapping (QSM)			
3D SW1Hi-res QSM	8:43	Y / N	
T2-weighted imaging (FLAIR)			
3D FLAIR SPACE	07:20	Y / N	
Field maps			
SpinEchoFieldMap_AP_flipped	00:32	Y / N	
Gre_field_mapping_2.5mm	02:01	Y / N	
Pause – display instructions for the resting state to the participant using the Powerpoint provided			
Resting State fMRI			
Trial rsfMRI – eyes open	07:48	Y / N	
Karolinska Sleepiness Scale			
1 – Extremely alert		4 – Rather alert	7 – Sleepy, but no effort to keep awake
2 – Very alert		5 – Neither alert nor sleepy	8 – Sleepy, but some effort to keep awake
3 – Alert		6 – Some signs of sleepiness	9 – Very sleepy, great effort to keep awake
Total Scan Time			

Data saving

K-space (meas) data on virus-checked NTFS USB (~7.5GB, 20 mins): Y / N

DICOM data pushed to Marc Seal's node (DFBI_DICOM): Y / N

All data burned to DVD and collected on day of scan (30 mins): Y / N

Extra Notes (e.g., participant mood, any comments made by the radiographers or participants, technical faults or improvements that can be made to the protocol):

Appendix V. MatLab script for Graph Theoretical Analysis

2/02/21 12:33 PM /Volumes/.../Graph_Analysis_Published.m 1 of 6

```
%%%%%%%%%%%%%%%%%%%%%%%%%%%%%%%%%%%%%%%%%%%%%%%%%%%%%%%%%%%%%%%%%%%%%%%% RUN GRAPH ANALYSIS ON STRUCTURAL CONNECTOMES %%%%%%%%%%
%%%%%%%%%%%%%%%%%%%%%%%%%%%%%%%%%%%%%%%%%%%%%%%%%%%%%%%%%%%%%%%%%%%%%%%% Last updated December 1st, 2020 %%%%%%%%%%
%%%%%%%%%%%%%%%%%%%%%%%%%%%%%%%%%%%%%%%%%%%%%%%%%%%%%%%%%%%%%%%%%%%%%%%% Phoebe Imms; phoebe.imms@gmail.com %%%%%%%%%%

clear all

%%% MAKE REQUIRED CHANGES HERE %%%
subjectdir='../rawData/TBI/VBG_connectomes/'; % Folder where subjects connectome *.csv
files are stored
GROUP= {'TBI_DK_84_noareaseize_VBG/'}; % name of the group being analysed
subjects={'CMT05_T1','CMT06_T1','CMT07_T1'};

%%% LEAVE EVERYTHING ELSE %%%

datamaindir='../Data/';
datadir=char(strcat(datamaindir,GROUP));
mkdir(datadir);

for i=1:length(subjects) %iterating (starting at step 1) over the length of the
vector for all the subjects

    sub=subjects{i};
    test1=load([subjectdir sub '.csv']);
    test2=load([subjectdir sub '.txt']);
    test3=test2*test1;
    test3=test3+triu(test3,1)'; %makes the conmat symmetrical
    test3(35,:)=[]; test3(83,:)=[];test3(:,35)=[];test3(:,83)=[]; %removes all rows
and columns containing the cerebellar structures
    s1=char(datadir);
    s2=sub;
    s3='_mu_sym_82.csv';
    %dest=[s1 num2str(s2) s3];
    dest=strcat(s1,s2,s3);
    writematrix(test3,dest);
end

for i=1:length(subjects) %iterating (starting at step 1) over the length of the
vector for all the subjects

    sub=subjects{i};
    test1=load([subjectdir sub '.csv']);
    test2=load([subjectdir sub '.txt']);
    test3=test2*test1;
    test3=test3+triu(test3,1)'; %makes the conmat symmetrical
    %test3(35,:)=[]; test3(83,:)=[];test3(:,35)=[];test3(:,83)=[]; %removes all rows
and columns containing the cerebellar structures
    s1=char(datadir);
    s2=sub;
    s3='_mu_sym_84.csv';
    %dest=[s1 num2str(s2) s3];
    dest=strcat(s1,s2,s3);
    writematrix(test3,dest);
end

mkdir([datadir '82/']);
mkdir([datadir '84/']);

% Create directories for anaylses
GROUP=char(GROUP);
organisedir=char(['../Results/' GROUP]);
mkdir([organisedir 'gmcorr']);
```

```

mkdir([organisedir 'indCMs']);
mkdir([organisedir 'Neuromarvl']);
mkdir([organisedir 'nodalGMs']);
mkdir([organisedir 'boxplotGMs']);
mkdir([organisedir 'savedfiles']);

clear all;
close all;
n=1; m=n+1; n=m; % set figure labelling counter
grp=['TBI']; % MBI, CON, or TBI or TB2

if grp=='MBI'
    GROUP = {'HC82/'}; % N=37
    subjects=
    {'HC02_mu_sym', 'HC04_mu_sym', 'HC05_mu_sym', 'HC06_mu_sym', 'HC07_mu_sym', 'HC08_mu_sym', 'HC09_mu_sym', 'HC10_mu_sym', 'HC11_mu_sym', 'HC12_mu_sym', 'HC13_mu_sym', 'HC14_mu_sym', 'HC16_mu_sym', 'HC17_mu_sym', 'HC20_mu_sym', 'HC21_mu_sym', 'HC22_mu_sym', 'HC23_mu_sym', 'HC24_mu_sym', 'HC25_mu_sym', 'HC27_mu_sym', 'HC28_mu_sym', 'HC29_mu_sym', 'HC30_mu_sym', 'HC31_mu_sym', 'HC32_mu_sym', 'HC33_mu_sym', 'HC34_mu_sym', 'HC35_mu_sym', 'HC36_mu_sym', 'HC37_mu_sym', 'HC38_mu_sym', 'HC40_mu_sym', 'HC41_mu_sym', 'HC42_mu_sym', 'HC43_mu_sym', 'HC45_mu_sym'};
elseif grp=='CON'
    GROUP = {'CON_DK_84_noareasize/84/'}; % N=12
    subjects=
    {'CON01_mu_sym', 'CON02_mu_sym', 'CON03_mu_sym', 'CON04_mu_sym', 'CON05_mu_sym', 'CON06_mu_sym', 'CON07_mu_sym', 'CON08_mu_sym', 'CON09_mu_sym', 'CON10_mu_sym', 'CON11_mu_sym', 'CON12_mu_sym'};
elseif grp=='TBI'
    GROUP = {'TBI_DK_84_noareasize_VBG/84/'}; % N=6
    subjects={'CMT05_T1_mu_sym', 'CMT06_T1_mu_sym', 'CMT07_T1_mu_sym'};
else grp=='TB2'
    GROUP = {'TB2/'}; % N=4 time point 2 TBI patients
    subjects={'CMT05_T2_mu_sym', 'CMT06_T2_mu_sym', 'CMT07_T2_mu_sym', 'DTC01_T2_mu_sym'};
end

datadir='../Data/';
resultsmaindir='../Results/';
subjectdir=char(strcat(datadir, GROUP));
resultsdir=char(strcat(resultsmaindir, GROUP));

conmat_all=[];
%degree_check %check the degree of each CM
%strengths_check % check the strength of each CM

for i=1:length(subjects)
    sub=subjects{i};
    conmat=load([subjectdir sub '.csv']); %load each subjects matrix into a conmat file
    n=n+1; figure(n); imagesc(conmat);
    colorbar
    savefig([resultsdir 'indCMs/' sub '.fig']);
    csvwrite([resultsdir 'indCMs/' sub '.csv'], conmat);
    conmat_all(:, :, i)=conmat; %loads the conmat files from each iteration (subject) into the group conmat file
    csvwrite([resultsdir 'indCMs/conmat_all.csv'], conmat_all);
end

%AVERAGE CONMAT
average_conmat=mean(conmat_all, 3);
m=n+1; figure(n); imagesc(average_conmat)

```

```

colorbar
savefig([resultsdir 'averageconmat.fig']);

csvwrite([resultsdir 'average_conmat.csv'], average_conmat);

%CHECK DISTRIBUTION OF WEIGHTS
wx=reshape(average_conmat, [1, 84*84]);
wx_sort=sort(wx);
m=n+1; figure(n); plot(wx_sort)
savefig([resultsdir 'distweights.fig']);

%RUN GRAPH ANALYSIS FOR EACH SUBJECT
glob_gms_all=[];
deg=[];
str=[];
BC=[];
CC=[];
Eloc=[];

load('D_euc.mat'); %euclidean distance matrix for Navigability, if using 84 nodes✓
change to D_euc.mat

for i=1:length(subjects)
    sub=subjects{i};
    W=load([subjectdir sub '.csv']);

    for k=1:10
        ITER=k;
        W_rand=W;
        W_rand(W_rand<0.0001)=0;
        [R,eff]=randmio_und(W_rand,ITER); %make sure R is different to W
    end

    %PRELIMINARY SETTINGS FOR BRAIN CONNECTIVITY TOOLBOX
    %W = threshold_proportional(W, 0.3);
    n = length(W);
    W_norm = W./(max(W(:)) + min(W(W>0))); %normalise for everything but navigation
    R_norm = R./(max(R(:)) + min(R(R>0)));
    L_norm = 1./W_norm;
    L_R = 1./R_norm;
    L_log = -log10(W./(max(W(:)) + 1)); %log transform and normalise (set between ~0✓
    and 1, by dividing by maximum plus small minimum to avoid 0s) from Caio for✓
    navigability
    L_log(L_log == Inf) = 0; %set diagonals Inf to 0

    % RUN BCT SCRIPTS
    % Basics (raw connectivity matrices)
    % Degree - deg_ave(stat) and deg(vector)
    [deg] = degrees_und(W);
    deg=deg';
    deg_ave = mean(deg);
    % Strength - str_ave(stat) and str(vector)
    str = sum(W);
    str=str';
    str_ave = mean(str);

    % Integration - weight-length remapping is within the script and is
    % 1./W
    % Characteristic Path Length - lambda(stat)
    % Global Efficiency - efficiency(stat)
    [D] = distance_wei_floyd(L_norm);

```

```

    [lambda,efficiency] = charpath(D);
    % Normalised characteristic path length - L_norm(stat)
    [D_R] = distance_wei_floyd(L_R);
    [lambda_R] = charpath(D_R);
    lambda_norm=lambda/lambda_R;
    % Local efficiency - Eloc(vector)
    Eloc = efficiency_wei(W_norm,2);
    Eloc_ave=mean(Eloc);
    % Navigation - Nav(stat) and er_wei(stat) and sr(stat)
    [D_log, hops_log] = distance_wei_floyd(L_log);
    [sr, ~, PL_wei_log] = navigation_wu(L_log, D_euc);
    PL_wei_log(1:n+1:end) = NaN;
    Nav = nanmean(1./PL_wei_log(:));
    er_wei = nanmean(nanmean(hops_log./PL_wei_log));

    % Segregation
    % Clustering coefficient - CC_ave(stat) and CC_W(vector)
    CC=clustering_coef_wu(W_norm);
    CC_ave=mean(CC);
    % Normalised clustering coefficient - CC_norm(stat)
    C_R=clustering_coef_wu(R_norm);
    CC_R=mean(C_R);
    CC_norm=CC_ave/CC_R;
    % Transitivity - T(stat)
    T=transitivity_wu(W_norm);

    % Modularity - Q(stat)
    gamma=1;
    [Ci,Q]=modularity_und(W,gamma);

    % Centrality Betweenness Centrality) - BC_ave(stat) and BC(vector)
    BC = betweenness_wei(L_norm);
    BC_ave = mean(BC);

    % Resilience - Assortativity - A(stat)
    r = assortativity_wei(W_norm,0);

    % Small-worldness (if greater than 1, network is small world)
    sw=lambda_norm/CC_norm;

    %STORE GLOBAL METRICS IN A TABLE FOR ALL SUBJECTS
    sub_str=string(sub);
    gms=table(sub_str, deg_ave, str_ave, efficiency, lambda, lambda_norm, Nav, er_wei, sr, Eloc_ave, CC_ave, CC_norm, sw, T, Q, BC_ave, r);
    glob_gms_all=vertcat(glob_gms_all,gms);
    nodal=table(deg, str, CC, BC, Eloc, Ci);
    writetable(nodal,[resultsdir 'nodalGMS/nodal_gms_' sub '.xls']);

end

%SAVE GLOBAL METRICS TABLE IN DATA FOLDER
writetable(glob_gms_all,[resultsdir 'global_graph_analysis_84.xls']);

%%%GLOBAL METRICS INTER-RELATIONSHIPS%%%
efficiency_all=glob_gms_all.efficiency;
lambda_all=glob_gms_all.lambda;
Nav_all=glob_gms_all.Nav;
CCave_all=glob_gms_all.CC_ave;
CCnorm_all=glob_gms_all.CC_norm;
erwei_all=glob_gms_all.er_wei;
T_all=glob_gms_all.T;

```

```

Q_all=glob_gms_all.Q;
sw_all=glob_gms_all.sw;
BCave_all=glob_gms_all.BC_ave;
r_all=glob_gms_all.r;
lambdanorm_all=glob_gms_all.lambda_norm;

% All correlations between all variables, and P values
% from FDR (benjamini H dependent) crit p is 0.000058)
glob_gms_new = removevars(glob_gms_all, {'sub_str','sr','er_wei','sw'});
globgmsarray=table2array(glob_gms_new);
[X,P]=corrcoef(globgmsarray);
[h, crit_p, adj_ci_cvrg, adj_p]=fdr_bh(P,0.05,'dep');
clims=[crit_p crit_p+0.0000000001];
n=n+1; figure(n); imagesc(X); xticks(1:1:12); yticks(1:1:12); xticklabels({'deg',↵
'str', 'eglob', 'CPL', 'CPLnorm', 'Nav', 'CC', 'CCnorm', 'T', 'Q', 'BC', 'r'});↵
yticklabels({'deg', 'str', 'eglob', 'CPL', 'CPLnorm', 'Nav', 'CC', 'CCnorm', 'T', 'Q',↵
'BC', 'r'});
colorbar; savefig([resultsdire 'gmcorr/corrcoeffs.fig']);
n=n+1; figure(n); imagesc(P,clims);
xticks(1:1:12); yticks(1:1:12); xticklabels({'deg', 'str', 'eglob', 'CPL', 'CPLnorm',↵
'Nav', 'CC', 'CCnorm', 'T', 'Q', 'BC', 'r'}); yticklabels({'deg', 'str', 'eglob',↵
'CPL', 'CPLnorm', 'Nav', 'CC', 'CCnorm', 'T', 'Q', 'BC', 'r'});
colorbar; savefig([resultsdire 'gmcorr/corrvpvals.fig']);
writematrix(X,[resultsdire 'gmcorr/correlation_coefficients.xls']);
writematrix(P,[resultsdire 'gmcorr/correlation_pvalues.xls']);
%key={'deg_ave', 'str_ave', 'efficiency', 'lambda', 'lambda_norm', 'Nav', 'er_wei',↵
'sr', 'CC_ave', 'CC_norm', 'sw', 'T', 'Q', 'BC_ave', 'r'};

% Scatterplots
m=n+1; figure(n)
scatter(Nav_all, efficiency_all);
[r p]=corr(Nav_all, efficiency_all);
lsline
xlabel('Navigation Efficiency', 'FontSize', 18);
ylabel('Global Efficiency', 'FontSize', 18);
title(['r=', num2str(round(r,3)) ' ', p=' num2str(round(p,10))]);
set(gca,'FontSize',14)
savefig([resultsdire 'gmcorr/E_efficiency_corr.fig']);

m=n+1; figure(n)
scatter(Nav_all, lambda_all);
[r p]=corr(Nav_all, lambda_all);
lsline
xlabel('Navigation Efficiency', 'FontSize', 18);
ylabel('Characteristic Path Length', 'FontSize', 18);
title(['r=', num2str(round(r,3)) ' ', p=' num2str(round(p,10))]);
set(gca,'FontSize',14)
savefig([resultsdire 'gmcorr/E_lambda.fig']);

m=n+1; figure(n)
scatter(efficiency_all, lambda_all);
[r p]=corr(efficiency_all, lambda_all);
lsline
xlabel('Global Efficiency', 'FontSize', 18);
ylabel('Characteristic Path Length', 'FontSize', 18);
title(['r=', num2str(round(r,3)) ' ', p=' num2str(round(p,10))]);
set(gca,'FontSize',14)
savefig([resultsdire 'gmcorr/efficiency_lambda.fig']);

%BOXPLOTS
m=n+1; figure(n); boxplot(efficiency_all,'label','Global Efficiency'); savefig↵

```

```

([resultsdirend 'boxplotGMs/boxplot_efficiency.fig']);
m=n+1; figure(n); boxplot(lambda_all,'label','Characteristic Path Length');savefig(
([resultsdirend 'boxplotGMs/boxplot_lambda.fig']);
m=n+1; figure(n); boxplot(Nav_all,'label','Navigation Efficiency');savefig([resultsdirend
'boxplotGMs/boxplot_E_log.fig']);
m=n+1; figure(n); boxplot(CCave_all,'label','Clustering Coefficient');savefig(
([resultsdirend 'boxplotGMs/boxplot_CCave.fig']);
m=n+1; figure(n); boxplot(CCnorm_all,'label','Normalised Clustering Coefficient');
savefig([resultsdirend 'boxplotGMs/boxplot_CCnorm.fig']);
m=n+1; figure(n); boxplot(lambdanorm_all,'label','Normalised Characteristic Path
Length');savefig([resultsdirend 'boxplotGMs/boxplot_lambdanorm.fig']);
m=n+1; figure(n); boxplot(erwei_all,'label','Efficiency Ratio');savefig([resultsdirend
'boxplotGMs/boxplot_erwei.fig']);
m=n+1; figure(n); boxplot(T_all,'label','Transitivity');savefig([resultsdirend
'boxplotGMs/boxplot_T.fig']);
m=n+1; figure(n); boxplot(Q_all,'label','Modularity');savefig([resultsdirend
'boxplotGMs/boxplot_Q.fig']);
m=n+1; figure(n); boxplot(sw_all,'label','Small-Worldness');savefig([resultsdirend
'boxplotGMs/boxplot_sw.fig']);
m=n+1; figure(n); boxplot(BCave_all,'label','Betweenness Centrality');savefig(
([resultsdirend 'boxplotGMs/boxplot_BCave.fig']);
m=n+1; figure(n); boxplot(r_all,'label','Resilience (Assortativity)');savefig(
([resultsdirend 'boxplotGMs/boxplot_r.fig']);

% SMALLWORLD - if greater than 1, network is small world
% smallworld

% SPIDERPLOT
% Set variables
% phoebspider
% phoebspider_selectedgms

```